DEVELOPING ADVANCED MODEL SYSTEMS TO ASSESS THE IMPACT OF ENVIRONMENTAL EXPOSURES ON MALE REPRODUCTIVE HEALTH: FOCUS ON ALCOHOL, SARS-COV-2, AND THE BLOOD-TESTIS BARRIER

By

Robert Clayton Edenfield II

(Under the Direction of Charles A. Easley IV)

ABSTRACT

In recent decades, a concerning worldwide decline in male fertility has been observed. While the exact cause remains unclear, this decline is most likely attributable to environmental exposures. Viruses and alcohol have both played a large role throughout human history and on male reproductive health. The COVID-19 pandemic has resulted in hundreds of millions of men infected with SARS-CoV-2. Additionally, alcohol use increased during the pandemic. These two exposures were chosen because of their immediate relevance.

Two models were developed to explore how environmental exposures impact male reproductive health. The first is a blood-testis barrier model. It is made from primary Sertoli cells cultured on transwells creating a cell-formed barrier with culture medium on the top and bottom sides. The second is an advanced stem cell-based spermatogenesis model. It mimics the spatiotemporal aspects of the testis.

Using the blood-testis barrier model our research demonstrates that SARS-CoV-2 variants of concern can differentially impact the blood-testis barrier in multiple species. Furthermore, we show that clinically relevant levels of alcohol can reversibly disrupt the blood-testis barrier. Additionally, we propose diverse experimental frameworks to assess the impact of alcohol and SARS-CoV-2 infection in the blood-testis barrier and spermatogenesis models. These findings offer crucial insights and pave the way for future investigations into male reproductive health.

INDEX WORDS: male reproductive health; Sertoli cells; stem cells; blood-testis barrier; spermatogenesis; alcohol; SARS-CoV-2

DEVELOPING ADVANCED MODEL SYSTEMS TO ASSESS THE IMPACT OF ENVIRONMENTAL EXPOSURES ON MALE REPRODUCTIVE HEALTH: FOCUS ON ALCOHOL, SARS-COV-2, AND THE BLOOD-TESTIS BARRIER

By

Robert Clayton Edenfield II

BS, University of Georgia, 2018

A Dissertation Submitted to the Graduate Faculty of the University of Georgia in Partial Fulfillment of the Requirement for the Degree

DOCTOR OF PHILOSOPHY

ATHENS, GEORGIA

2023

DEVELOPING ADVANCED MODEL SYSTEMS TO ASSESS THE IMPACT OF ENVIRONMENTAL EXPOSURES ON MALE REPRODUCTIVE HEALTH: FOCUS ON ALCOHOL, SARS-COV-2, AND THE BLOOD-TESTIS BARRIER

By

Robert Clayton Edenfield II

Major Professor: Charles A. Easley IV

Committee: Michael Koval
Luke Naeher
Xiaoqin Ye

Electronic Version Approved:

Ron Walcott

Vice Provost for Graduate Education and Dean of the Graduate School

The University of Georgia

December 2023

ACKNOWLEDGEMENTS

I am extremely grateful to my family, friends, and mentors for their support in reaching my goals. Your belief in me provided the foundation for my achievements.

Thank you, Chas, for allowing me the opportunity to research in your lab. Thank you for your guidance, mentorship, and invaluable insights. Your expertise has been instrumental in shaping my research and academic growth.

To my committee, Dr. Koval, Dr. Naeher, and Dr. Ye, thank you so much for your support. Your guidance steered my research in meaningful directions, and I am honored to have benefited from your wisdom.

For your support, friendship, and good times, I would like to thank my cohort Megan Lott, Megan Beaudry, and Julia Frederick. In appreciation of your support and camaraderie during the tribulations of grad school, I would like to thank Jacob Siracusa and Elizabeth Hughes.

I extend my gratitude to the Easley Lab, past and present. Your collaboration and friendship have made my research endeavors enjoyable and (sometimes) more productive. Your teamwork and enthusiasm inspired me daily. Thank you, Katherine and Krista, for your training while I was in undergrad and your acceptance when I joined the lab. Thank you In Ki, Beth, Ian, Kylie, Kristen, and Arina. Your friendship provided an essential network of support and understanding. Thank you to the talented and dedicated undergraduate

researchers, especially Sam. Thank you to everyone making up the EHS department. I have greatly appreciated being a part of it for the past seven years.

Special thanks to the Tompkins and Ross Lab and their help in performing BSL3 experiments, especially Cheryl.

Lastly, I would like to thank my family. Thank you, Mom, Dad, David, Elizabeth, and Meemee for all your love and support. Thank you, to my infinitely supportive wife, Ashton, your love and encouragement have sustained me throughout this journey.

TABLE OF CONTENTS

LIST OF FIGURES

LIST OF TABLES

CHAPTER 1

1 EXPLANATION OF DISSERTATION STRUCTURE

This introductory chapter serves to fulfill the requirements set in the University of Georgia's Student Guide to Preparation and Processing Theses and Dissertations published by the Graduate School for using manuscript-style chapters. The specific requirement fulfilled by this chapter is to inform the reader of the structure of this dissertation.

Excluding the current chapter, the chapters included in this dissertation are written in the style of manuscripts published or to be submitted to scholarly scientific Journals. Chapter 2, Introduction (Literature Review), is primarily from "Implications of testicular ACE2 and the renin-angiotensin system for SARS-CoV-2 on testis function" published in *Nature Reviews Urology* on November 26th, 2021. This article is licensed under the Creative Commons 4.0 License (http://creativecommons.org/licenses/by/4.0/), permitting unrestricted use, sharing, adaptation, distribution, and reproduction with due credit given to the authors and source. At the time of writing (October 2023) this article is in the 99th percentile (ranked 3,666th) of the 512,948 articles of a similar age in all journals and the 99th percentile (ranked 1st) of the 24 tracked articles of a similar age in *Nature Reviews Urology*. Changes were made to include the breadth of information covered in this manuscript. Sections 2.2 – 2.4 are completely new and 2.1 was heavily edited to reflect the chapter better. Additionally, total COVID-19 cases were updated, as that number has changed drastically in the two years

since publication. Furthermore, changes were made to the titled subsections to better fit the chapter.

Chapter 3, “Impact of SARS-CoV-2 infection on the blood-testis barrier in humans and nonhuman primates,” is being prepared for submission and publication in the near future. Changes expected to be made in this preparation process, include removing unnecessary information, revising the figures for succinctness, and adding new data as it is still being processed (importantly, cytokine analysis and RNA sequencing).

Chapter 4, “Impact of alcohol use disorder on the blood-testis barrier,” is prepared for submission for publication in the journal *Scientific Reports Collection*: “Barrier function and the immune system.” It will be adapted for use in this dissertation by adding further introductory information to better contextualize.

Chapter 5, “Improving *in vitro* spermatogenesis,” will be a subsection of a manuscript prepared and submitted to *Nature.* Currently, we are in talks with the editor about the nature of this publication.

Chapter 6, “Conclusion: Predicting how multiple insults could damage the blood-testis barrier and spermatogenesis” is a forward-looking chapter addressing how alcohol use disorder in conjunction with SARS-CoV-2 infection impacts male fertility. It discusses how this could be tested and what role the two models considered in this manuscript play. Furthermore, the chapter works to tie together the previous chapters and point to their findings as well as provide a conceptual framework for future experiments and publications.

Chapter 7, “Epilogue: Chronic alcohol use primes bronchial cells for barrier dysfunction and altered inflammatory response during SARS-CoV-2 infection,” was published on October 3, 2023, in the *American Journal of Physiology, Lung and Molecular Physiology*. This publication was prepared in collaboration with Dr. Koval and Dr. K. Easley. Dr. K. Easley wrote and analyzed the data while I performed BSL3 experiments and aided in BSL2 experiments. For this reason, I have included the publication as an epilogue to highlight how SARS-CoV-2 and alcohol can disrupt barriers and highlight data that I have played an integral role in gathering.

In summary, among the chapters in this dissertation, Chapter 2 has been previously published and was adapted for this format. Chapter 3 is undergoing further revisions for future publication, while Chapter 4 is being prepared for submission with minor modifications. Chapter 5 will be included in a broader publication and is also undergoing further revisions for future submission. Chapter 6 lays out a conceptual framework for upcoming studies, and Chapter 7 has already been published.

CHAPTER 2

2 INTRODUCTION (LITERATURE REVIEW)[1]

[1] Edenfield, R.C., Easley, C.A. Implications of testicular ACE2 and the renin–angiotensin system for SARS-CoV-2 on testis function. *Nat Rev Urol* **19**, 116–127 (2022). https://doi.org/10.1038/s41585-021-00542-5. Reprinted here with permission of the publisher under Creative Commons license CC BY 4.0 http://creativecommons.org/licenses/by/4.0/.

2.1 ABSTRACT

In the last fifty years, there has been a significant decrease in semen parameters, such as sperm counts, among men globally. While the cause of this decline remains largely unknown, lifestyle factors might offer a potential explanation. This chapter focuses on novel environmental insults to biological male fertility and how that may be an underlying cause of the observed demographic fertility. There are several known environmental factors that impact male fertility. 2020 added another possible agent to the list, SARS-CoV-2. Although many studies have focused on SARS-CoV-2 infection in the lungs, comparatively little is known about the potential effects of the virus on male fertility. SARS-CoV-2 infection of target cells requires the presence of furin, angiotensin-converting enzyme 2 (ACE2) receptors, and transmembrane protease serine 2 (TMPRSS2). Thus, cells in the body that express these proteins might be highly susceptible to viral entry and downstream effects. Currently, reports regarding the expression of the viral entry proteins in the testes are conflicting; however, other members of the SARS-CoV family of viruses — such as SARS-CoV — have been suspected to cause testicular dysfunction and/or orchitis. SARS-CoV-2, which displays many similarities to SARS-CoV, could potentially cause similar adverse effects. Commonalities between SARS family members, taken in combination with sparse reports of testicular discomfort and altered hormone levels in patients with SARS-CoV-2, might indicate possible testicular dysfunction. Thus, SARS-CoV-2 infection has the potential for effects

on testis somatic and germline cells. Experimental approaches might be required to help identify potential short-term and long-term effects of SARS-CoV-2 on male fertility.

2.2 POPULATION CRISIS

In 2022, the world population surpassed 8 billion people, doubling in just 50 years, with a sustained fertility rate of over 2.1. The consequences of human overpopulation are apparent, ranging from climate change to environmental pollution. Ironically, the rapid human population growth may negatively impact human reproduction. There are now growing fears of an underpopulation crisis, with two-thirds of the world population living in areas with sub-replacement fertility. Fertility has steadily fallen from 5 births per woman in 1950 to 2.3 in 2021 and is expected to reach the replacement rate of 2.1 by 2050 [1]. Importantly, fertility has two primary meanings in the literature: Demographically, fertility refers to the number of children; biologically fertility refers to the ability to reproduce. Multiple reasons for the observed drop-in birth rate include socioeconomics, education, culture, health styles, and environmental toxicants.

Social factors have a very powerful impact on fertility. Industrialization has allowed the human population to forgo previous evolutionary strategies.[2] In industrialized society, 99% of infants will reach puberty, negating the need to have many children to counteract high childhood mortality.[3] Additionally, urbanization creates downward pressure on fertility as space decreases, the cost of children increases, and access to contraception and family planning services increases.[4,5] The education of women has also had a profound impact on

reducing fertility.[6] This association is complex and requires more consideration than is allowed in this dissertation. Low marriage rates and reduced total fertility may also have a relationship.[7] While socioeconomic, educational, and cultural causes partially explain the drop in demographic fertility they provide little explanation for the drop in biological fertility.

In parallel, a variety of environmental and lifestyle factors endanger reproductive health for men and women. Currently, 1 in 7 couples in North America experience difficulty conceiving.[8] In the United States about 9% of men and 11% of women have experienced fertility problems.[9,10] The increasing accumulation of environmental toxins in both men and women is a prominent contributor to the ongoing decline in fertility.[11] Furthermore, habits like smoking, frequent alcohol consumption, drug use, sleep hygiene, sedentation, infection control, and stress can jeopardize reproductive function.[12] While these toxins and lifestyles can damage the female reproductive system and cause loss of fetal viability, this review will primarily focus on damage to the male reproductive system.

2.3 THE ENVIRONMENT AND MALE FERTILITY

Various lifestyle and environmental factors are contributing to the decline in human fertility. This is most evident in males. Current evidence suggests that semen quality has been declining and that sperm concentration has been decreasing since 1938.[13] Meta-analyses by Swan et al. have supported these results.[14,15] Systematic review and meta-regression analyses by Levine et al. demonstrate a 52% reduction in sperm concentration in western world men from

1973 to 2011, 1.4% a year.[16] Male infertility as an increasingly prevalent condition has also been shown in industrialized non-western countries.[17-19] In addition to decreasing sperm count and quality, many groups have observed a parallel decline in circulating testosterone levels since the 1970s.[20-22] This decline in testosterone may be one of the causes of declining sperm counts and may be driven by endocrine disrupters. While genetic conditions certainly play a role in regulating male fertility, the universal and rapid changes indicate an environmental role.[3]

While various pollutants can impact male fertility, endocrine disrupting chemicals (EDCs) are one of the most prominent pollutants that effect fertility. EDCs are chemicals that can alter hormone levels, distribution, metabolism, or clearance by their interaction with hormone-producing or hormone-responsive cells or precursor cells through receptor agonism and antagonism, signal transduction, and epigenetic means.[23] Broadly, EDCs are generated by human industrial activities and are present ubiquitously in the environment.[24] Common examples of EDCs include bisphenol A, phthalates, pesticides, perfluorinated compounds, dioxins, polychlorinated biphenyls, parabens, and flame retardants.[25] Human exposure occurs through food, water, inhalation, and skin contact.[26] EDCs can cause cryptorchidism, hypospadias, alterations to male puberty, and negatively impact semen quality. Importantly, a myriad of other human exposures function as endocrine disrupters such as diet and lifestyle.

Our modern lifestyles play a major role in controlling male fertility.[27] Smoking has been linked to negative effects on semen quality.[28] Alcohol use is

another prevalent lifestyle factor linked to alcohologenic reversible azoospermia and adverse effects on semen volume and morphology.[29] Diet has been linked to male fertility with the intake of sugar-sweetened beverages being negatively associated with fecundity.[30] Obesity is a well-established risk factor for multiple health outcomes and both underweight and overweight patients are associated with increased risk of oligozoospermia or azoospermia and reduced semen quality.[31,32] Furthermore, physical activity has been shown to have a positive effect on male fertility, while a sedentary lifestyle has a negative one.[33-35]

While these studies provide insights into how the paternal environment and lifestyle can negatively impact male fertility outcomes like semen quality, much less has been done to investigate how these effects come about. For these investigations to be thoroughly carried out, alternative and improved *in vitro* models will need to be created using human cells or model organisms that most closely mimic human spermatogenesis. This manuscript will address two novel *in vitro* models to assess known and emerging threats to male fertility.

2.4 THE ROLE OF SERTOLI CELLS IN MALE FERTILITY

For spermatogenesis to properly occur in the adult male, numerous cells will have to work together to provide the proper microenvironment for spermatogenic differentiation. The most important cell for maintaining the spermatogenic microenvironment is the Sertoli cell. The Sertoli cell plays two vital roles in the testis: creating and preserving the blood testis-barrier and nursing spermatogenic cells. In order to maintain the microenvironment, the Sertoli cell is incredibly complex, able to continually change its shape and

function to orchestrate spermatogenesis.[36] Due to the challenges in isolating adult Sertoli cells for in vitro studies, research on Sertoli cell function primarily emphasizes endocrine and paracrine factors. Additionally, the focus extends to the examination of easily assayable proteins such as transferrin, aromatase, androgen receptor, and lactate dehydrogenase.[37]

The blood-testis barrier (BTB) is located near the base of the seminiferous tubule and divides the epithelium into two distinct compartments: the basal and adluminal. The basal compartment resides outside the BTB, butting up against the basement membrane, and contains spermatogonial stem cells (SSCs), spermatogonia, and preleptotene spermatocytes. This stem cell containing compartment is often referred to as the 'stem cell niche'.[38] The adluminal compartment faces the lumen inside of the seminiferous tubule and contains the primary and secondary spermatocytes, round spermatids, and elongating/elongated spermatids. The BTB functions as barrier to sequester adluminal germ cells away from the circulatory and lymphatic system. This barrier along with local immune suppression creates an immunoprivileged microenvironment in which meiosis can be completed without interference from the paternal immune system, which would target and attack germ cells.[39,40] Importantly, there is a third transient compartment that works as an interlocking system so that there always remains a barrier between the basal and adluminal compartments. A barrier will form behind a leptotene spermatocyte creating the intermediate compartment and as the spermatocyte transits toward the lumen, junction disassembly ahead of the spermatocyte is coordinated with junction

disassembly behind the germ cells.[41] The dynamic nature of this barrier allows the passage of spermatogenic cells through the barrier while restricting access to non-spermatogenic cells and toxicants.

The blood-testis barrier is often referred to as “one of the tightest junctions” of the body.[42] The BTB was discovered from early biochemical studies investigating testicular fluid for proteins, amino acids, and ions; subsequent rodent iv-injected dye studies showed brain and the seminiferous tubule infiltrations were not possible.[43-45] Importantly, the blood-testis barrier does not separate blood from testicular tissue but rather creates a boundary between diploid and haploid germ cells. Besides its dynamic nature the BTB is set apart from other barriers in that it is composed of four different cell junctions that are present between Sertoli cells: tight junction (TJs), ectoplasmic specializations, desmosomes, and gap junctions.[41] These junctions work together to prevent the flow of water, solutes, and large molecules between the paracellular space and restrict the passage of proteins and lipids between the compartments.

Tight junctions form a unique microdomain consisting of interconnected fibrils that encircle cells in a belt-like fashion. Adjacent cells will periodically connect via fibrils to form the barrier. These fibrils are comprised of an integral membrane protein that establishes direct or indirect connections with scaffolding and signaling proteins, in addition to cytoskeletal proteins. The key structural proteins of TJ fibrils are: occludin, claudin, and tricellulin. Occludin is not found in the human and probably not the primate testis and is therefore not discussed in detail in this manuscript.[46] Zona occludens, however are present. Tricellulin

localizes at bicellular and tricellular contacts.[47] At tight junctions, tricellulin can reduce strand discontinuities, increase electrical resistance, decrease ion and large solute permeability, seal epithelial sheets, and exclude the passage of macromolecules.[48] Claudins are better studied in the testis and will therefore make up a larger discussion in this manuscript.

Claudins are cell-cell adhesion molecules located at TJs between cells in epithelial sheets. Currently, there are 27 mammalian claudins that are classified into classical (claudins 1-10, 14, 15, 17, and 19) and nonclassical (claudins 11-13, 16, 18, and 20-24), according to their sequence similarities.[41,49] In general, claudins 4, 5, 6, 11, 14, and 18 increase paracellular electrical resistance while claudins 2, 7, 10, 15, and 16 increase paracellular cation permeability.[50] Claudins also play a large role intracellular signaling. In the lung, claudin-18 interacts with a signaling molecule that regulates progenitor cell proliferation, organ size, and tumorigenesis.[51] Claudins can integrate the paracellular barrier and signaling functions of tight junctions to create diverse biological systems within various tissue and organ environments.[49] Claudins are also known to participate in epithelial-mesenchymal cell transition, invasion, and migration. The mechanism by which claudins can participate may be through the indirect regulation of extracellular matrix degradation via matrix metalloprotease flow.[52] These occurrences likely initiate cytokine production that can lead to extracellular matrix degradation and/or the disassembly of cell junctions. Cytokines are recognized for their role in regulating tight junction function in epithelial cells, including Sertoli cells.[53] Furthermore, claudin function and cell

motility are directly linked by neuronal Wiskott-Aldrich protein and Ras homolog associated protein kinase.[54] Protein kinases also play a critical role in TJ function through claudin phosphorylation by protecting it from rapid internalization and degradation.[55-57] To what extent these tight junction signaling occur in the testis is currently unknown.[41] Claudins 1, 3, 4, 5, 7, 8, and 11 are expressed in the testis. Claudins 3 and 11 appear to be particularly important as their expression peaks preceding the movement of spermatocytes across the blood-testis barrier.[58] In conditional androgen sensitivity and azoospermia presenting mice, claudin 3 decreases illustrating androgen regulation of tight junctions.[59] In the BTB, androgens are shown to promote barrier integrity.[60-62] In addition to androgen regulation, hormones, cytokines, and germ cells also regulate claudin expression in Sertoli cells.[63-68] Little has been done to study these functions in primates as much of this research has been performed in rodents.

In addition to forming the blood-testis barrier, Sertoli cells play the important role of supporting spermatogenesis. Because Sertoli cells make up the BTB, they are the only somatic cells within the seminiferous epithelium. The Sertoli cells provide constant morphogenic support through cell-cell interactions and biochemical secretions like lactate, cytokines, and hormones.[69,70] Therefore, Sertoli cells are referred to as nurse cells.[71] Through Sertoli-germ cell apical junctions, Sertoli cells can morphologically shape spermatids through elongated spermatid cytoplasm endocytosis. [72] Numerous signaling pathways have been described in Sertoli cells including: the androgen-signaling pathway[73,74], AMP-activated protein kinase signaling pathway (AMPK)[75], follicle stimulating

hormone/adenylate cyclase/cyclic adenosine monophosphate/protein kinase signaling pathway[76], mitogen-activated protein kinases signaling pathway (MAPK)[77,78], the transforming growth factor-β/Smad signaling pathway (TGF-β)[79], and the Wnt signaling pathway[80]. TGF-β/Smad, AMPK, and MAPK are the most well studied pathways in Sertoli cells. The TGF-β superfamily contains activin, inhibin, bone morphogenic proteins, and growth and differentiation factors.[81] Smad 1, 3, 4, 5, 6, 7, and 8 are expressed throughout the testis. Smad4 however is distributed throughout the Sertoli cell at all ages in multiple species.[82-84] Furthermore, its deletion impairs fertility.[85] Together, it appears that the TGF-β/Smad signaling pathway occupies a continuous vital position for Sertoli cell functioning during spermatogenesis while other members of the TGF-β superfamily may perform more intermediate functions like Sertoli cell proliferation and tight junction dynamics.[71] AMPK regulates Sertoli cell energy metabolism, junctional complex stability, and proliferation.[86] α1AMPK KO mouse spermatozoa have abnormal heads, curved sheaths, impaired mobility, reduced expression of junctional proteins, and deregulation of energy homeostasis highlighting the importance of the Sertoli cell AMPK signaling pathway during spermatogenesis.[87,88] AMPK signaling also plays a role in lactate production (the primary energy source of spermatocytes and spermatids), tight junction dynamics, and Sertoli cell proliferation.[71] MAPKs are kinases that are made up of three subfamilies: c-Jun N-terminal kinase (JNK), ERK, and p38 MAPK. They are all present in mammalian Sertoli cells, but a majority of MAPK pathway-related genes exist in immature Sertoli cells in the rodent.[89] JNK signaling contributes to

BTB function and germ cell migration; its activation will increase intercellular adhesion molecule-1, important for strengthening and regulating the BTB.[90,91] ERK signaling is involved with germ cell proliferation and meiosis by directly regulating apoptosis, mitosis, meiosis progression, and spermatogonial stem cell maintenance.[92-95] Furthermore, ERK signaling regulates Sertoli cell proliferation and lactate and iron supply.[96,97] p38 MAPK is highly involved in tight junction dynamics. Upon TNF-α activation of p38 MAPK occludin and zona occluden are downregulated to allow the relocation of spermatocytes across the barrier for differentiation to occur.[98]

In addition to serving as barrier and nurse cells, Sertoli cells also aid in the creation of an immunoprivileged microenvironment within the testis. Sertoli cells produce immunomodulatory factors like anti-inflammatory cytokines and TGFβ that allow them to modify immune response, contributing to the immunosuppressive environment.[99-101] Factors secreted by Sertoli cells may also act on testicular macrophages and other interstitial immune cells that contribute to immune privilege. These immunomodulatory Sertoli secretions can be altered by hormonal aberrations.[61] For a long time, it was believed that Sertoli cells safeguarded germ cells from immune detection by confining germ cell antigens within the seminiferous tubules.[36,100] However, recent research has indicated that Sertoli cells release numerous germ-cell specific proteins into the surrounding interstitial fluid that may might facilitate peripheral tolerance.[102,103] Consequently, Sertoli cells may release germ cell-specific proteins with the purpose of inducing

immune system tolerance to a range of antigens, potentially curtailing a broader immune response in situations where immune privilege is compromised.

Because of the important roles that Sertoli cells play in maintaining and protecting male fertility anything that affects them may have significant consequences to male fertility. Over the past decade, much research has been done to show that sperm counts and semen quality are dropping. However, more research is required to determine what is to blame for this infertility. Because of the plethora of threats posed to male fertility, it is likely there is not just one cause but rather a consortium of causes working in conjunction from personal habits to exposures. This manuscript will address two of these causes, viruses and alcohol.

2.5 HOW VIRUSES IMPACT MALE FERTILITY

Infectious diseases have been affecting humans forever, however as industrialization has grown so has globalization leading to rapidly spreading global pandemics. The past forty years have seen an influx in various viral outbreaks including: Human Immunodeficiency Virus, Severe Acute Respiratory Syndrome Coronavirus, influenza strains, Middle East Respiratory Syndrome Coronavirus, Zika, Ebola virus, and the most recent Severe Acute Respiratory Syndrome Coronavirus-2 (SARS-CoV-2) that causes the Coronavirus disease-2019 (COVID-19).[104-106] Influenza is linked to male infertility by altering sperm DNA integrity, causing chromosomal abnormalities, and damage sperm quality.[107-110] Zika has been shown to live in the male genital tract and has been observed in the semen of infected men long after infection.[111,112] The testis may

serve as reservoir as it sustains a high viral load for a prolonged period.[113,114] Zika has been shown to cause orchitis, epididymo-orchitis, and testicular atrophy and decrease sperm count and increase sperm morphological abnormalities.[115-118] A number of viruses like Ebola, parvovirus, hepatitis, human papillomavirus, herpes simplex virus, HIV, and Mumps can negatively impact male fertility.[119] These viruses may cause testosterone disruption, BTB integrity disruption, altering conventional sperm parameters, causing low sperm count, reducing sperm motility, alteration of sperm quality, impairing steroidogenesis, inducing testicular atrophy, impairing Sertoli cell function, and causing DNA damage.[119] A number of viral associated mechanism have been implicated like oxidative stress-mediated apoptosis, hyper inflammatory response, inflammation of testicular cells, oxidative damage, disruption of interferon route, germline transduction, and activation of MAPK/ERK response.[119] Because of its immediate and continuing relevance this manuscript will focus on SARS-CoV-2 and its impact on male fertility.

2.6 CHARACTERISTICS OF SARS-COV-2 AND COVID-19 INFECTION

In late December 2019, SARS-CoV-2 was discovered in Wuhan, China. The resulting disease was termed coronavirus disease 2019. The virus causes similar clinical characteristics to viral pneumonia and went on to kill >70,000 people in the first 50 days of the epidemic.[120] The novel coronavirus quickly spread: at the time of writing (October, 2023), over 750 million people have been infected, and 7 million people have died worldwide.[121] Many studies have

focused on the effects of SARS-CoV-2 infection in the lungs, and comparatively little is known about the effects of COVID-19 on male fertility.

Major risk factors for SARS-COV-2 infection include being male and aged over 65 years.[122] Comorbidities such as hypertension, obesity, hypercholesterolaemia, diabetes, cardiovascular disease and respiratory diseases seem to significantly worsen the prognosis of COVID-19.[123-126] COVID-19 is primarily characterized by fever, cough, fatigue and myalgia, which follow a standard course of four main stages: first, upper respiratory tract infection, followed by onset of dyspnoea and pneumonia, then, third, cytokine storm and hyperinflammatory state and, finally, death or recovery.[127,128] However, a range of symptoms have been reported across multiple organ systems. Gastrointestinal symptoms are reported in 40% of patients and include anorexia, nausea, vomiting and diarrhoea.[129] Neurological manifestations affect 36% of patients and 45% of those with severe infection; these include symptoms of dizziness, headache, impaired consciousness, acute cerebrovascular disease, ataxia, seizures, olfactory disorders and nerve pain.[130,131] The incidence of cardiovascular manifestations is high and diverse; early studies indicate that 7–20% of COVID-19 patients experience acute myocardial injury, 24% had heart failure and 17% displayed cardiac arrhythmia, which is probably due to a systemic inflammatory response and immune system inhibition during disease progression.[132,133]

This wide array of symptoms indicates that SARS-CoV-2 is able to access several organ systems through indirect and direct mechanisms, possibly gaining

entry to multiple organ systems that express viral entry proteins. The broad tropism of SARS-CoV-2 is also indicated by the detection of the virus in the pharynx, trachea, lungs, blood, heart, vessels, intestines, liver, male genitals, brain and kidneys.[134,135] Furthermore, many COVID-19 symptoms persist after acute infection (long COVID) suggesting possible tissue damage.[136-138]

Coronaviruses are large, enveloped, positive single-stranded RNA viruses ranging from 27 to 32 kb and are known to infect humans, other mammals and birds, causing multi-organ system disease. They are split into four types: alpha-, beta-, delta- and gamma- coronaviruses, according to their antigenic activity.[139] Seven coronaviruses have been shown to cause human disease characterized by respiratory infection; two alphacoronaviruses — H-CoV-NL63 and H-CoV-229E — and two betacoronaviruses — H-CoV-OC43 and H-CoV-HKU1 — cause mild respiratory infection, whereas three betacoronaviruses — SARS-CoV, MERS-CoV and SARS-CoV-2 — are highly pathogenic.[140,141] SARS-CoV-2 is genomically similar to SARS-CoV, with which it shares 79.5% of its sequence, and to Middle East respiratory syndrome coronavirus (MERS-CoV), sharing 50% genomic homology.[142,143] However, SARS-CoV-2 has high transmissibility and infectivity and a low mortality rate compared with both SARS-CoV and MERS-CoV.[144] Two studies have shown that the basic reproduction number of SARS-CoV-2 falls between 2 and 3, whereas the reproduction number of SARS-CoV is between 2.2 and 3.6 and that of MERS-CoV is 2.0–6.7, indicating the higher transmissibility of SARS-CoV-2.[145-148]

All coronaviruses encode proteins for viral replication and nucleocapsid and envelope formation. The viral envelope is composed of three structural proteins: the matrix and envelope proteins, which are involved in virus assembly, and the spike surface glycoprotein, which mediates viral entry.[149] These spike proteins form large protrusions on the surface, giving the appearance of a crown.

SARS-CoV-2 has the typical coronavirus structure, sharing a high degree of spike homology with SARS-CoV.[141,150-153] The spike protein of SARS-CoV-2 mediates viral entry into host cells and is the determinant factor of viral infectivity, host range, tissue tropism and immune response induction.[151] The SARS-CoV-2 spike protein consists of the S1 subunit, a clover-shaped trimer, and S2 subunits, trimeric stalks linked to the S1 trimer.[154,155] The receptor-binding domain (RBD) lies on the tip of the S1 head and is only loosely connected, enabling the infection of multiple host cells (**Figure 2.1**).[153,156] The RBDs of SARS-CoV, MERS-CoV and SARS-CoV-2 recognize exopeptidases on the host cell.[157] Angiotensin-converting enzyme 2 (ACE2) is the critical receptor for cellular entry of H-CoV-NL63, SARS-CoV and SARS-CoV-2, but not MERS-CoV.[154,157-160] The SARS-CoV RBD on the S1 unit binds to the outer surface of the host ACE2, away from its zinc-chelating enzymatic site.[161-163] Upon exopeptidase binding, entry into the cell depends on cellular proteases; transmembrane protease serine 2 (TMPRSS2) splits the spike protein enabling further penetration of SARS-CoV-2.[164,165]

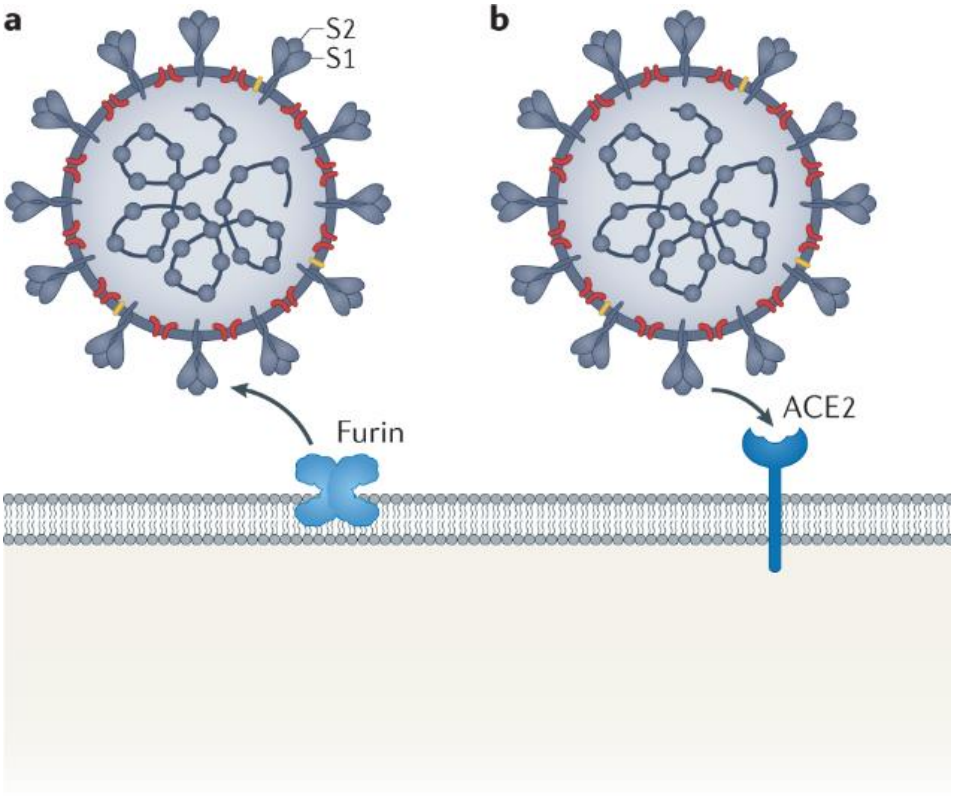
a
S2
S1
Furin
b
ACE2

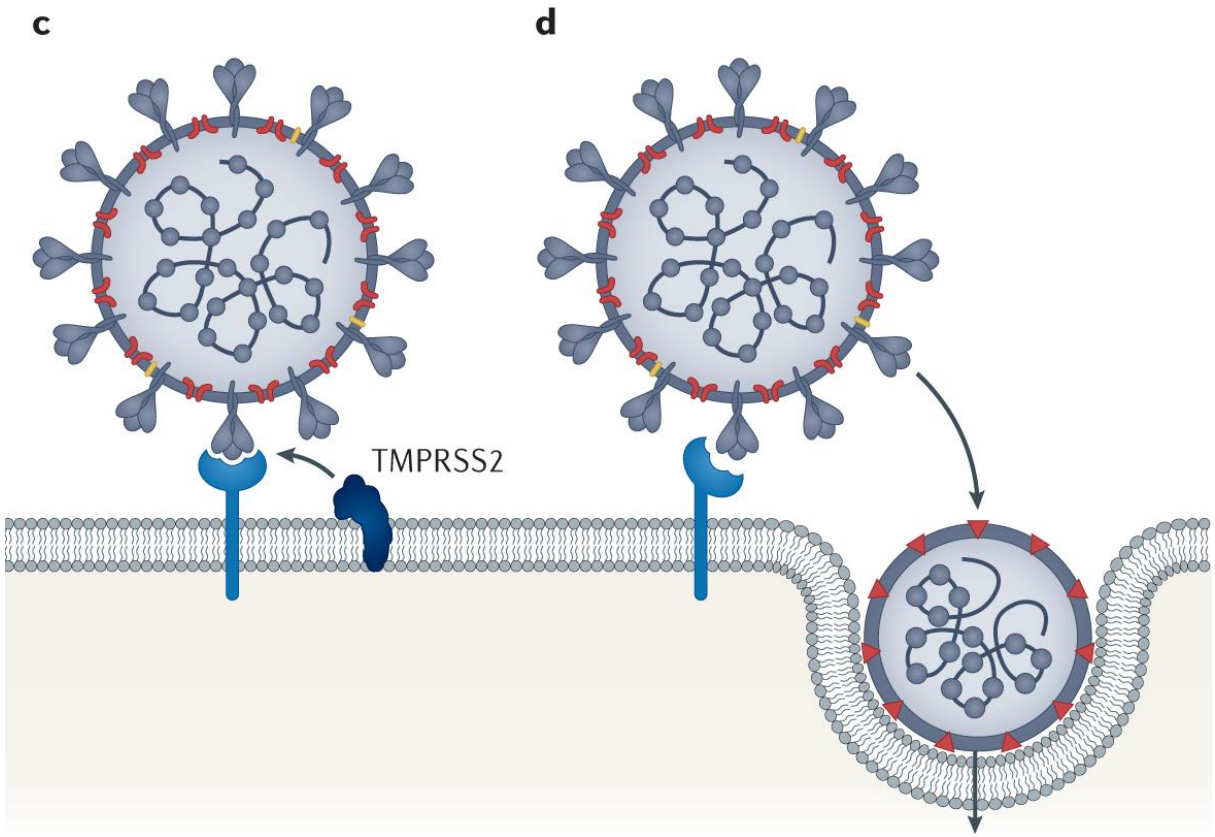
c
d
TMPRSS2

Figure 2.1 Mechanisms of SARS-CoV-2 cellular entry

a The transmembrane convertase furin cleaves and activates the S1 subunit of the SARS-CoV-2 spike glycoprotein, opening the viral receptor-binding domain (RBD).[166] **b** When the RBD is in an open conformation, it can attach to angiotensin-converting enzyme 2 (ACE2).[167-169] **c** Transmembrane protease serine 2 (TMPRSS2) is recruited to cleave the S1 subunit of the SARS-CoV-2 spike protein, enabling entry. **d** After ACE2 binding and protease cleavage, viral entry can occur.[170]

The entry mechanisms of SARS-CoV-2 have been directly demonstrated in a study showing that the virus uses ACE2 as a cellular entry receptor in multiple species, including humans, and does not use other typical coronavirus receptors such as amino peptidase N and dipeptidyl peptidase 4.[141,167,171,172] ACE2 binding is facilitated by furin, a poly-substrate convertase, which cleaves the SARS-CoV-2 polybasic cleavage site on the viral spike causing the RBD to swing out and become available for ACE2 binding.[125,173] The ubiquitous expression of furin means it has great potential for viral infiltration, and it is commonly hijacked by viruses such as Ebola, herpes and retrovirus. Additionally, furin is transactivated by cytokine stimulation, possibly allowing increased infectivity during an immune response. SARS-CoV-2 is the only coronavirus to display furin cleavage, which helps to explain its infectivity.[174,175]

RNA viruses have a high mutation rate, which results in changes to protein surface amino acids that can alter viral function and possibly lead to increased infectivity, transmissibility and mortality.[176,177] Mutations in the spike protein are of particular interest, as they can enhance viral entry and protein binding, for instance, the D614G mutation increases entrance efficiency through enhanced ACE2 binding affinity.[178] From September 2020 to June 2021, a total of 71 unique SARS-CoV-2 lineages were identified in England that contributed to SARS-CoV-2 infectivity.[179] Mutation sites have been identified, distributed across the spike protein sequence of SARS-CoV-2, with the maximum mutation density near the protease cleavage site. Additionally, the viral RBD is associated with 44 known mutation sites.[180]

The importance of furin, ACE2 and TMPRSS2 in viral entry and infection suggests that environmental factors regulating these proteins could affect SARS-CoV-2 infection and severity. Specific comorbidities — such as hormone dysregulation, increased age, obesity, diabetes and high blood pressure — can substantially increase SARS-CoV-2 risk by altering expression of ACE2, TMPRSS2 or furin.[181-189] Furthermore, other factors, such as alcohol intake, cholesterol levels, smoking and hormone-altering chemicals, can also affect COVID-19 severity by potentially dysregulating and aggregating viral entry proteins.[190-192] Furin is ubiquitous among all human cell types; thus, infection is primarily driven by ACE2 and TMPRSS2 co-expression.[193,194] ACE2 and TMPRSS2 display a broad distribution in various human organs, being co-expressed in the lung, nose, gall bladder, small intestine, large intestine, esophagus, brain, fallopian tube, testis, heart and kidney. However, SARS-CoV and SARS-CoV-2 have also been shown to enter cells through promiscuous proteases such as cathepsin B/L.[195-197] Furthermore, as TMPRSS2 has been identified in extracellular vesicles, it might be able to reach tissues distant from where it is expressed, possibly contributing to SARS-CoV-2 infection.[198] Although the necessity of TMPRSS2 for SARS-CoV-2 infection is still uncertain, ACE2 expression alongside a suitable protease clearly drives COVID-19 pathology.

2.7 ACE2 AND THE RENIN-ANGIOTENSIN-ALDOSTERONE SYSTEM

ACE2 has a vital role in regulating the renin–angiotensin–aldosterone system (RAAS) (**Figure 2.2**).[199] The RAAS is activated in response to low blood pressure, low fluid volume and specific agonists, such as salt loading and

macrophage differentiation, resulting in activation of angiotensin receptor 1 (ATR1) to cause vasoconstriction, cell proliferation, inflammation and fibrosis.[200-202] This process occurs via the angiotensin-converting enzyme–angiotensin I (ANG I)–angiotensin II (ANG II)–ATR1 axis. ACE2 is activated to mitigate these effects through its effector protein angiotensin-(1–7) (ANG-(1–7)) and major receptor mitochondrial assembly 1 (MAS1).[203-205] The ACE2–ANG-(1–7)–MAS1 axis has a protective effect, causing vasodilation, anti-inflammation, antiproliferation and antifibrosis, which mitigate the effect of ATR1.[205] Common COVID-19 comorbidities such as hypertension, diabetes and heat exhaustion are associated with RAAS overactivation or ACE2 deficiency.[206] During RAAS overactivation, ACE2 can be upregulated, providing additional entry points for SARS-CoV and SARS-CoV-2, which enter cells via ACE2 and inhibit its protective response in ACE2-expressing tissues.[207] Furthermore, in patients with deficient ACE2 expression, infection could further dysregulate the ACE–ANG I–ANG II–ATR1 and ACE2–ANG-(1–7)–MAS1 axes.[208] Several studies suggest that these viruses became highly lethal because they deregulate a lung-protective pathway.[199,209,210] Decreasing ACE2 activity through SARS-CoV-2 binding increases the acute effects of angiotensin, which are in line with many COVID-19 symptoms.[211,212]

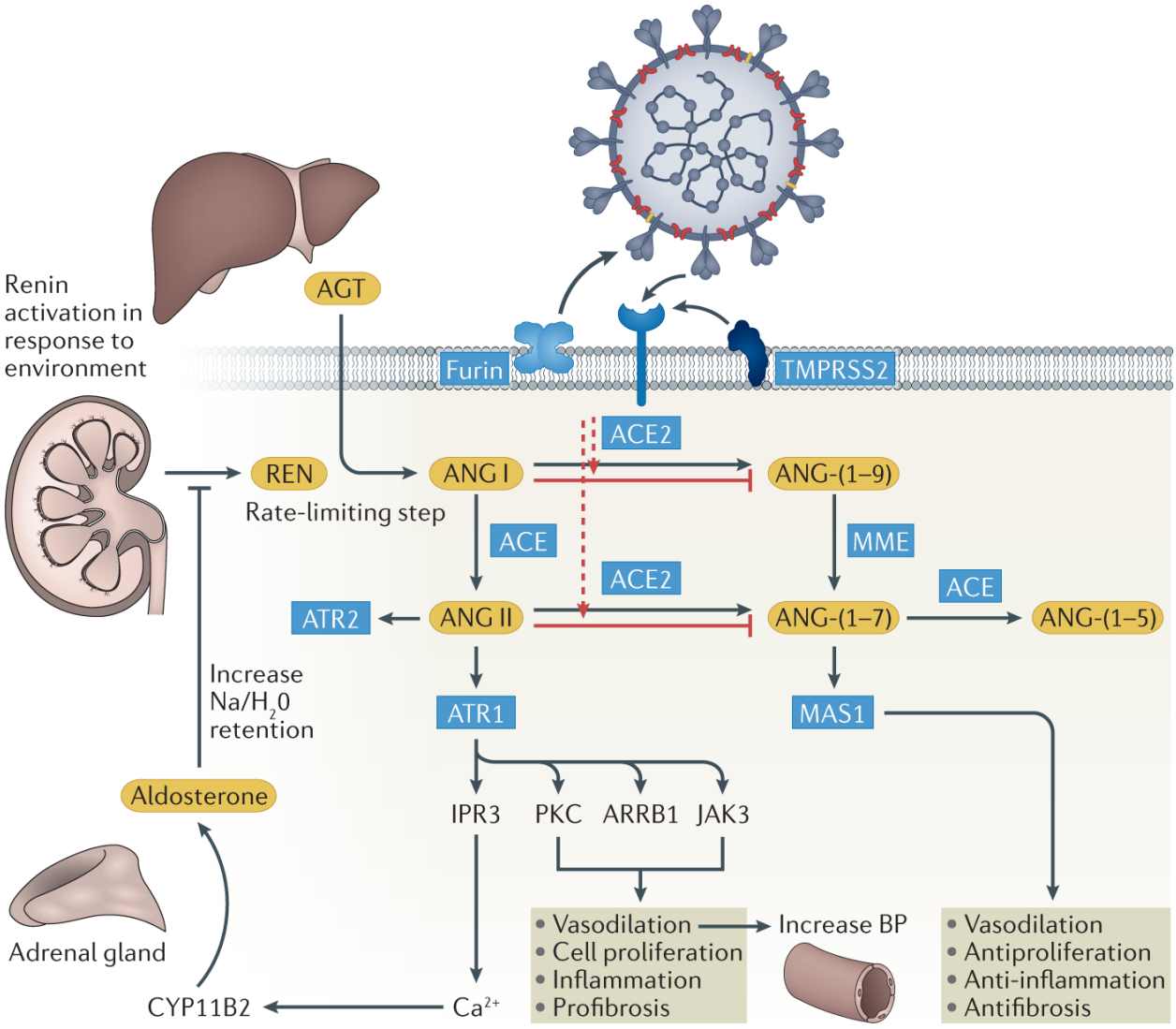
Renin activation in response to environment
AGT
Furin
TMPRSS2
ACE2
REN
ANG I
ANG-(1–9)
Rate-limiting step
ACE
MME
ACE2
ACE
ATR2
ANG II
ANG-(1–7)
ANG-(1–5)
Increase Na/H20 retention
ATR1
MAS1
Aldosterone
IPR3
PKC
ARRB1
JAK3
Adrenal gland
• Vasodilation
• Cell proliferation
• Inflammation
• Profibrosis
Increase BP
• Vasodilation
• Antiproliferation
• Anti-inflammation
• Antifibrosis
CYP11B2
Ca2+

Figure 2.2 RAAs activation mechanisms

The renin–angiotensin–aldosterone system (RAAS) activates in response to several environmental factors, including low blood pressure (BP) and fluid volume. In response to the environmental factor, the kidneys produce renin, which is quickly cleaved by angiotensinogen, which is continuously produced by the liver, into angiotensin I (ANG I). Both angiotensin-converting enzyme 2 (ACE2) and ACE can cleave ANG I, but ACE has a much higher affinity for it than ACE2. ACE will convert ANG I into ANG II, where it has many downstream effects to counteract the environmental factor, and will eventually produce aldosterone to deactivate RAAS in a negative feedback mechanism. ACE2 converts ANG II into ANG-(1–7). ANG-(1–7) binds to mitochondrial assembly 1 (MAS1), which has various protective effects in response to those caused by ATR1. When RAAS is overstimulated, ACE2, the viral entry point of SARS-CoV-2, is upregulated, providing more entry points. SARS-CoV-2 interferes with the protective function of ACE2, worsening outcomes in patients with COVID-19. This effect is particularly important in those with low ACE2, in whom the ACE–ANG I–ANG II–ATR1 axis becomes overactive. ATR1, angiotensin receptor 1; TMPRSS2, transmembrane protease serine 2.

The RAAS is activated more in men than in women, characterized by higher levels of ACE.[213] However, men display lower levels of ACE2.[214] This discrepancy might account for the worse COVID-19 outcomes observed in men than in women. The substantial involvement of ACE2 and the RAAS in vascular inflammation and remodeling illustrate the sensitivity of the vascular system to changes in blood pressure and inflammation.[215,216] Organs such as the brain, kidneys and testes are at an increased risk of viral-mediated damage.[217] In the brain, which displays similar immune-privilege, gene expression and decreased inflammatory response to foreign antigens to that seen in the testis, RAAS overactivation through ACE2 inhibition causes cognitive impairment.[218-221] Alongside the neuro-invasive potential of SARS-CoV-2, ACE2 inhibition seems to be integral to understanding SARS-CoV-2-associated neuropathology.[222,223]

The RAAS might also be relevant to male fertility — that RAAS functions in the testes is well established and various aspects of the RAAS, including renin, ACE, MAS and ANG II, are expressed in Leydig cells, germ cells, and sperm.[224-227] These components are also found in the epididymis, vesicular glands, prostate, seminal vesicles, vas deferens and seminal plasma.[228] Additionally, infertile men with impaired spermatogonia displayed lower levels of ACE2, ANG-(1–7) and MAS.[229] MAS is also found at the mRNA and protein level of matured sperm in the acrosomal and tail regions and incubation of MAS with asthenozoospermic sperm improves sperm mobility.[230] Furthermore, MAS-null rodents exhibit a reduction in testis weight and sperm production.[226]

However, the functions of local tissue-specific RAAS might operate independently of the systemic RAAS.[231] Notably, the brain, heart and testis display a local RAAS and the testes express a testicular ACE isoform that might have important roles in male fertility.[232] The involvement of the RAAS in the testis means that SARS-CoV-2 infiltration and interference with testicular ACE2 could lead to infection, loss of protective effects during inflammatory states, and coagulation and inflammation, which can disrupt spermatogenesis and testicular function.[233,234] Clinical evidence of an aetiological role of the RAAS in male infertility is currently lacking; however, many SARS-CoV-2-associated symptoms and comorbidities can affect male fertility, such as fever, hypoxia, inflammation, immune-system inhibition, obesity and cholesterol dyshomeostasis.[235] These interactions further complicate the question of whether SARS-CoV-2 can directly affect the testis via the RAAS or whether effects might be indirect through various immune responses and pre-existing pathological conditions.

2.8 COULD SARS-COV-2 AFFECT TESTICULAR FUNCTION?

The human testis is a complex multicellular system with the primary function of producing spermatozoa and androgens, the inhibition of which by viral pathogens could have severe effects on testicular function.[38] The testis comprises three major cell types: Leydig, Sertoli and germ cells. The interaction between these cells drives spermatogenesis. Sertoli and germ cells are the primary components of the seminiferous epithelium.[236] Spermatogonial stem cells (SSCs) are localized in the basal epithelium and are adjacent to the Sertoli cells, which produce various factors, such as glial-derived neurotrophic factor

and CYP26B1 to maintain SSC homeostasis.[237] Notably, Sertoli cells form junctions to create the blood–testis barrier (BTB), which divides the seminiferous epithelium into the basal and adluminal compartments. This division is crucial, as it helps to keep circulating toxicants, systemic immune components, and pathogens away from differentiating germ cells.[68]

SSCs are undifferentiated, whereas outside the BTB, up to the preleptotene stage, they remain spermatogonium, but as they progress inwards, SSCs mature towards primary and secondary spermatocytes before becoming spermatids and undergoing spermiogenesis, to ultimately become spermatozoa.[71,238] Leydig cells are interstitial and produce testosterone to maintain spermatogenesis.[239] Testicular macrophages are the most heterogeneous and abundant testicular immune cells; they are phagocytic towards cell debris, foreign particles, and invading pathogens and help to maintain the immunoprivileged state within the testis, increasing in number during inflammation. Other testicular cell types include endothelial cells, which aid in SSC renewal through the expression of glial-derived neurotrophic factor, fibroblast growth factor 2, stromal cell-derived factor 1, macrophage inflammatory protein 2 and insulin-like growth factor binding protein 2; and myoid cells, which provide ultrastructure and express leukemia inhibitory factor to help maintain SSC homeostasis.[240-242] Although all stages of spermatogenesis can be indirectly affected by viral interaction with testicular cells that provide support during proliferation, differentiation and maturation, spermatogonium — which sit outside the BTB — might be at an increased risk of direct viral interaction.

Viral infections and their induced immune response are poorly understood aetiological factors that can functionally impair male reproduction, via effects on the testis and epididymis.[243,244] Viruses can directly affect spermatozoa, resulting in sperm death, reduction in sperm counts and decreased motility, or can act indirectly by inducing inflammatory cytokine production, inhibiting hormone production and altering the function of the genital organs.[245]

Viral infection of any of the main testicular cell types can negatively affect sperm output and quality (**Figure 2.3**), via mechanisms including BTB breakdown and immune entry, hormone alteration, or a direct effect on spermatogonia.[246] Viral entry into the testis normally occurs hematogenously. The BTB provides protection and immune privilege for germ cells; however, some viruses, such as Zika and HIV, can pass through the BTB, eliciting an immune response.[247-249] The BTB is markedly different from other cell barriers, such as the blood–brain barrier and the pulmonary epithelial barrier: the BTB is much tighter than most barriers and is made up of multiple types of co-functioning junctions, unlike other barriers that are exclusively comprised of tight junctions.[41] However, the BTB also has some similarities to the epithelial barriers found in the lungs and brain. The tight junction, although not the only barrier in the BTB, is still a mainstay of the barrier; furthermore, the BTB is much more dynamic in nature than barriers found elsewhere.[41] Additionally, the BTB can be modulated by viruses, notably Zika virus.[250,251] SARS-CoV-2 has been shown to disrupt and pass through both epithelial and endothelial barriers, such as those found in the lungs and brain, demonstrating a potential means by which SARS-CoV-2 can disrupt normal BTB

function, potentially resulting in immune cell infiltration into the seminiferous tubules.[247,252-255]

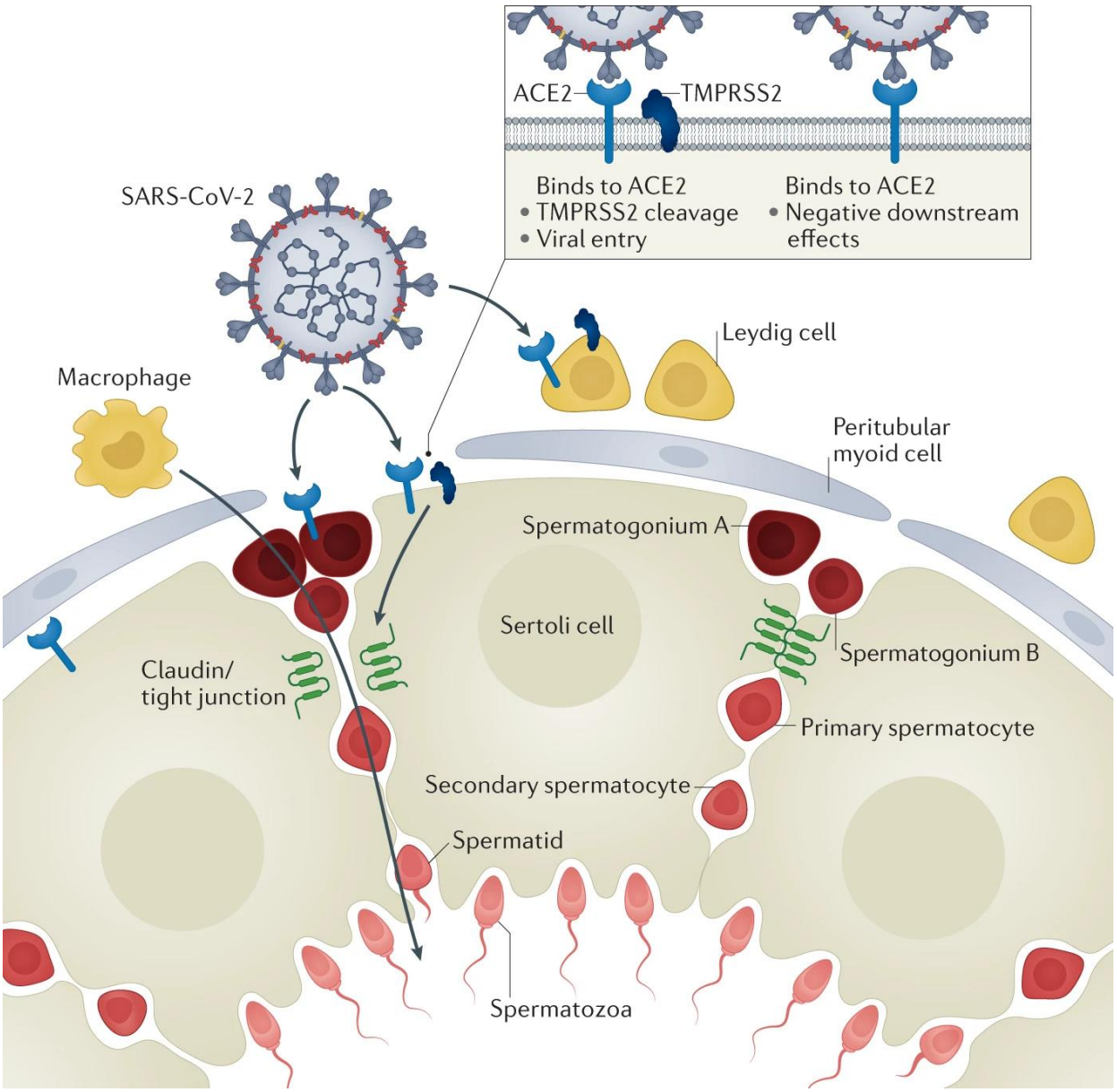
ACE2
TMPRSS2
Binds to ACE2
• TMPRSS2 cleavage
• Viral entry
Binds to ACE2
• Negative downstream effects
SARS-CoV-2
Leydig cell
Macrophage
Peritubular myoid cell
Spermatogonium A
Sertoli cell
Spermatogonium B
Claudin/ tight junction
Primary spermatocyte
Secondary spermatocyte
Spermatid
Spermatozoa

Figure 2.3 Effects of SARS-CoV-2 on the testis

Viral entry could occur in any cell type that has been shown to co-express angiotensin-converting enzyme 2 (ACE2) and transmembrane protease serine 2 (TMPRSS2) and might also be able to affect cells that only express ACE2. In the testis, every cell type except for spermatocytes and spermatids express ACE2. The spermatogonial stem cells and spermatogonia express both ACE2 and TMPRSS2, putting them at risk of SARS-CoV-2 infection. Additionally, with so many testicular cells expressing ACE2, SARS-CoV-2 could cause considerable damage, even without directly infecting testicular cells.

For SARS-CoV-2 viral entry to occur, *ACE2* and *TMPRSS2* must be co-expressed in cells. Both are primarily expressed in bronchial transient cells, especially alveolar type 2 cells; thus, the respiratory tract is often the first organ system to be affected and usually incurs the most damage. While in the lungs, SARS-CoV and SARS-CoV-2 show viral targeting of ACE2 expressive cells such as alveolar epithelial cells, vascular endothelial cells and macrophages.[256-258] Although the full mechanism for COVID-19 pathology is not understood, the destruction of infected cells, breakdown of barriers and binding of ACE2 are fundamental.[259-262]

The data are conflicting regarding the exact expression of ACE2 and TMPRSS2 in the testis (**Table 2.1**) despite both being present.[263,264] One study has suggested limited expression of ACE2 and TMPRSS2 in testis tissue and no overlapping expression of these genes in testicular cells, indicating that viral entry into testicular cells is unlikely to occur.[264,265] However, other studies have shown that ACE2 is expressed in the myoid cells, Leydig cells, Sertoli cells and spermatogonia indicating that these cell types could be highly susceptible to SARS-CoV-2 (**Table 2.1**).[195,266-271] TMPRSS2 is shown to be expressed in SSC, spermatogonia, spermatocytes and spermatid cells.[195,268] ACE2 and TMPRSS2 are both expressed in many secondary sex organs, including the prostate, seminal vesicles and adrenal glands.[182,195,208,228,264] Notably, only one study has failed to show co-expression of ACE2 and TMPRSS2 in any male reproductive tissues (Table 1).[272] Additionally, substantial inconsistencies are seen between mRNA and protein presence of ACE2 and TMPRSS2.[273] In addition, the

presence of promiscuous proteases and extracellular vesicular TMPRSS2 means that infection might not solely depend on ACE2 and TMPRSS2 co-expression, requiring only ACE2.[198] Furthermore, RAAS involvement in the testis means that direct infection of testicular cells might not be necessary for the disease to decrease testicular function.

Alongside the risk of direct infection of Leydig cells, the hypothalamic–pituitary–gonadal (HPG) axis could also be dysregulated by SARS-CoV-2 infection, resulting in altered levels of FSH, LH and testosterone, which can potentially lead to spermatogenic impairment, hypogonadism and infertility (**Figure 2.4**).[274] Many endocrine organs, including the pituitary, thyroid, hypothalamus, pancreas, adrenal glands, pancreas, ovaries and testis, express *ACE2* and *TMPRSS2*.[274-276] Although hypothalamic SARS-CoV and SARS-CoV-2 infection could theoretically result in decreased GnRH, affecting gonadal hormone levels, this hypothesis has yet to be observed.[274] FSH and LH levels increase with COVID severity, possibly indicating inflammatory activation of gonadotropin-producing cells.[274,277,278] The hypothalamic–pituitary–adrenal (HPA) and HPG axes have a reciprocal relationship, whereby they function in a tandem, flexible, and bidirectional manner and any insult to one will impact the other.[279] Additionally, the ACE2-expressive adrenal gland, which has a major role in the RAAS and HPA axis, is negatively affected by both SARS-CoV and SARS-CoV-2 infections, further implicating hormone disruption, possibly through hypothalamus and pituitary interactions.[280,281]

Cell type	ACE2	TMPRSS2
Non-testicular	✓	✓
Testis	✓	✓
Leydig	✓	×
Sertoli	✓	×
Myoid	✓	×
Stromal	✓	×
Spermatogonial stem cells	✓	✓
Spermatogonia	✓	✓
Spermatocyte	×	✓
Spermatids	×	✓

Table 2.1 Expression of ACE2 and TMPRSS2 in male reproductive cells

ACE2, angiotensin-converting enzyme 2; TMPRSS2, transmembrane protease serine 2. ACE2 is expressed in most testicular cells, notably ones outside the blood-testis barrier.

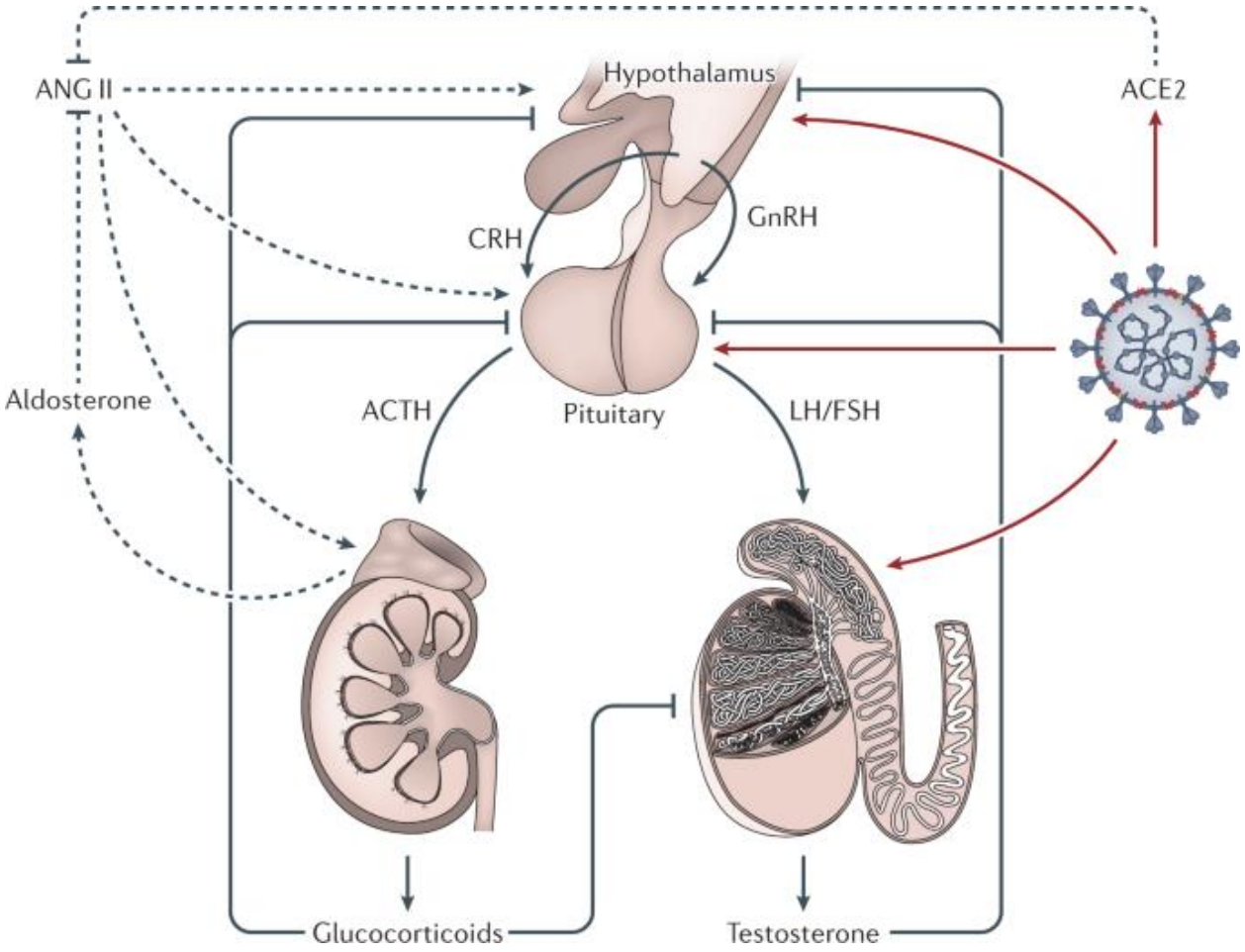
ANG II
Hypothalamus
ACE2
CRH
GnRH
Aldosterone
ACTH
Pituitary
LH/FSH
Glucocorticoids
Testosterone

Figure 2.4 Effects of SARS-CoV-2 on hormone production

Through angiotensin-converting enzyme 2 (ACE2) inhibition, SARS-CoV-2 infection might alter hormone production. SARS-CoV-2 ACE2 inhibition can cause renin–angiotensin–aldosterone system-mediated overactivation of the hypothalamic–pituitary–adrenal axis, which can interfere with the hypothalamic–pituitary–gonadal axis. SARS-CoV-2 can also directly affect the hypothalamic–pituitary–gonadal axis.

2.9 CLINICAL STUDIES IN PATIENTS WITH COVID-19

Many viruses such as HIV, hepatitis B and C, mumps, Epstein–Barr, papilloma and, notably, SARS-CoV, have been shown to cause testicular dysfunction or inflammation (orchitis).[282-284] SARS-CoV-2 displays similar pathology to SARS-CoV and could cause similar clinical effects, such as germ cell death, orchitis and immune intrusion.[283] Several case reports and studies have noted testicular pain and orchitis associated with SARS-CoV-2 infection.[285,286] Ediz et al. noted that 10.98% of 91 male patients with COVID-19 reported testicular pain, and Pan and colleagues reported that 19% of 34 male patients with COVID-19 displayed testicular discomfort suggestive of orchitis.[264,287] In addition, Kim et al. presented a clinical report of a patient with testicular and abdominal pain associated with COVID-19, whilst Bridwell and colleagues and Gagliardi et al. presented clinical cases of bilateral orchitis and orcho-epididymitis, respectively.[288-290] A report by Chen and colleagues noted that 22.5% of 142 male patients had acute orchitis, epididymitis, or epididymo-orchitis associated with COVID-19 and also observed that scrotal infection risk increased with age, with 53.3% of patients over 80 years experiencing testicular symptoms.[291] They also noted that the risk of epididymo-orchitis increased with severity of infection ($P = 0.037$). Furthermore, a study by Falahieh and co-workers, which observed 20 male patients with COVID-19 at day 14 and day 120 after infection, noted a 34.83% reduction in malondialdehyde and a 31.52% increase in total antioxidant capacity 120 days after infection. After 14 days a 33.1% increase in sperm DNA fragmentation, an increase in leukocytes, and

progressive and total sperm motility below the WHO criteria were noted, all of which had returned to normal levels 120 days after infection.[292] However, the majority of men with COVID-19 do not report testicular pain.

Testicular and epididymal autopsy sections from six patients with COVID-19 showed signs of orchitis characterized by interstitial oedema, congestion, red blood cell exudation, increased concentration of CD3/CD68^{+}, IgG within the seminiferous tubule, thinning of the seminiferous tubules and a significant increase in apoptotic cells within the seminiferous tubule ($P = 0.018$).[293] Semen collected from 23 patients with mild or ordinary cases of COVID-19 showed that 39.1% had oligozoospermia and 60.9% had increased seminal leukocytes. The patients also had decreased sperm concentration and increased IL-6, TNF and MCP1 compared with men in the control group.[293] Furthermore, assessment of 81 men with moderate-to-severe SARS-CoV-2 infection showed significantly elevated serum LH levels ($P < 0.0001$) alongside significantly decreased ratios of serum testosterone:LH ($P < 0.0001$) and FSH:LH ($P < 0.0001$).[278] Salciccia et al. and Rastrelli et al. both observed reduced total testosterone in patients with severe COVID-19 and showed a negative correlation with biochemical risk factors such as neutrophil count, lactate dehydrogenase, C-reactive protein, IL-6, D-dimer, pH and procalcitonin.[294,295] Similar effects have been brought on by SARS-CoV.[296] However, although hormonal changes were observed, none of these studies assessed the long-term effects on sperm production in the affected patients.

Reports of testicular discomfort and altered hormone levels in patients with COVID-19 indicate that SARS-CoV-2 might be able to infect testicular cells to directly affect testicular function. Viral presence in semen is a potential indicator of viral entry into the testis through the BTB, although whether SARS-CoV-2 is able to penetrate the BTB remains unclear.[297] Although presence of the SARS-CoV-2 virus in semen is debated, two groups have detected viral RNA in semen.[264,298-300] SARS-CoV-2 presence in the semen would suggest the possibility of sexual transmission of the virus and, importantly, a direct effect on the sperm itself, which are known to express and house ACE2 and TMPRSS2.[300]

Testicular origin — rather than penetration of the BTB — is one explanation for viral presence in semen. In this scenario, viral entry might originate from other sources, such as the epididymis, seminal vesicles, prostate and urethra, particularly as expression of *TMPRSS2* (and other proteases) has been shown in the seminal vesicles and prostate, as well as the kidneys.[301-303]

Notably, although viral presence in semen is concerning, it does not necessarily indicate a negative effect on fertility. Even so, semen testing should be performed in future studies to ensure that SARS-CoV-2 is not present in the semen and, at the time of writing, many reproductive clinicians have suspended fertility treatments for infertile couples until more evidence is obtained.[304]

Clinical evidence suggesting widespread infection throughout several organ systems related to reproductive function, alongside the reports of testicular pain, orchitis and hormonal changes, justify concerns of a possible effect of SARS-CoV-2 on male fertility.[275,278,291,293,298] Moreover, although the exact

testicular expression of ACE2 and TMPRSS2 is debated, their testicular presence has been observed for 20 years.[305,306] The viral modulation of ACE2 and TMPRSS2 through comorbidities and environmental factors in specific cell types, both within and outside the testis and the BTB, leads to various pathological conditions, such as changes in hormone levels, BTB breakdown, immune response, or direct effects on the germ line, all of which have the potential to affect male fertility.[307]

2.10 MODELS OF POTENTIAL TESTICULAR EFFECTS OF SARS-COV-2

The conflicting reports regarding SARS-CoV-2 entry into the testis cells mean that various informative models need to be considered for future studies in order to rigorously examine the potential effects of SARS-CoV-2 infection on male fertility. A comprehensive approach is essential as evidence of possible long-term effects of SARS-CoV-2 on many organ systems is increasing. The primary need must be to elucidate viral entry into the testis and, if this is confirmed, by what mechanism. A combination of animal, in vitro and cadaver models, guided by data from cohort and clinical studies, will be advantageous (Fig. 5). Animal models can be used to cheaply and efficiently pinpoint at-risk organ systems, whereas in vitro models can be used to investigate how specific testicular cell types might be affected by SARS-CoV-2 infection.

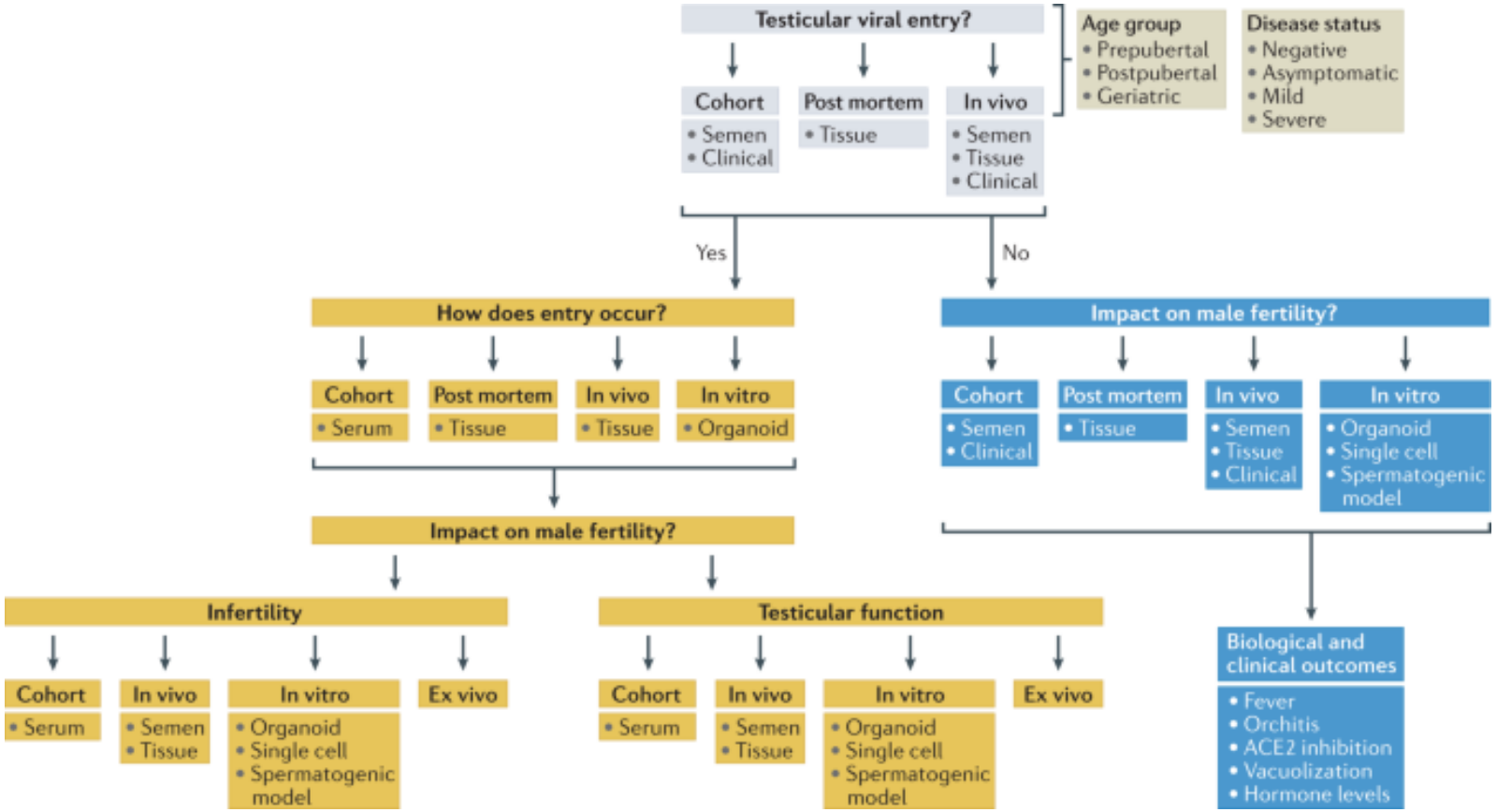
Testicular viral entry?
Age group
• Prepubertal
• Postpubertal
• Geriatric
Disease status
• Negative
• Asymptomatic
• Mild
• Severe
Cohort
• Semen
• Clinical
Post mortem
• Tissue
In vivo
• Semen
• Tissue
• Clinical
Yes
No
How does entry occur?
Cohort
• Serum
Post mortem
• Tissue
In vivo
• Tissue
In vitro
• Organoid
Impact on male fertility?
Cohort
• Semen
• Clinical
Post mortem
• Tissue
In vivo
• Semen
• Tissue
• Clinical
In vitro
• Organoid
• Single cell
• Spermatogenic model
Impact on male fertility?
Infertility
Cohort
• Serum
In vivo
• Semen
• Tissue
In vitro
• Organoid
• Single cell
• Spermatogenic model
Ex vivo
Testicular function
Cohort
• Serum
In vivo
• Semen
• Tissue
In vitro
• Organoid
• Single cell
• Spermatogenic model
Ex vivo
Biological and clinical outcomes
• Fever
• Orchitis
• ACE2 inhibition
• Vacuolization
• Hormone levels

Figure 2.5 Proposed flow chart for evaluating effects of SARS-CoV-2 on male fertility

A systematic approach is essential to guide research. To understand possible effects on male fertility, the first step is to determine viral presence in the testes or semen, using human cohort and post-mortem studies alongside in vivo animal models. In clinical studies, patient cohorts should be divided primarily by their age and disease status. If viral entry is observed, a mechanism for viral entry and possible effects on male fertility and testicular function can then be investigated. If viral entry is not observed, this does not rule out an effect on testicular function, which will still require investigation, owing to concerns raised by clinical data and viral involvement in the renin–angiotensin–aldosterone system pathway, which could have indirect effects on fertility.

For the clinical data to be useful, patients must be segregated by their age and disease status, most notably asymptomatic and symptomatic. As more information arises regarding the long-term health consequences of COVID-19, the formation of clinical cohorts will become even more important. Sperm and blood serum samples will need to be taken throughout the course of the infection and through several sperm production cycles after viral clearance. These time points will be key to observing any changes in sperm parameters and morphology, hormone levels and immune responses throughout infection, and to determine whether any of these changes persist after viral clearance.

One pilot cohort study of 69 male patients with COVID-19 noted a significant change in sperm parameters in patients with mild and moderate COVID-19: semen volume ($P < 0.001$), sperm concentration ($P = 0.008$), total sperm number ($P = 0.001$), progressive motility ($P < 0.001$), total motility ($P < 0.001$) and vitality ($P = 0.001$).[308] The conclusions drawn from this study could have been improved through the addition of more outputs such as systemic hormone levels, blood pressure, morphological analysis and characterization of immune response; however, it provides a promising springboard for further studies.

Unfortunately, these cohort studies cannot provide any mechanistic data or solid evidence of viral presence in the testis, as tissue samples, in the form of testicular biopsy samples, would be required to confirm SARS-CoV-2 in testicular tissue, but cohort data will be vital for establishing the long-term implications of SARS-CoV-2 infection for male fertility.

Post-mortem studies have a long tradition. Specifically in coronaviruses, autopsy reports for SARS and MERS were essential for elucidating their pathology and will be necessary to fully understand the reproductive pathology of SARS-CoV-2.[284,309] Only a small number of SARS-CoV-2 patient autopsy studies have been published to date, only ten have examined testicular tissue.[310-318] One of these performed post-mortem examinations on the testis of 12 men who had died with COVID-19. Of these 12 men, 1 displayed normal histology, 2 mild testicular injury, 5 moderate injury and 4 had severe injury. In the 11 patients with abnormal histology, Sertoli cells showed swelling, vacuolation and cytoplasmic rarefaction, as well as detachment from tubular basement membranes, and loss and sloughing into lumens of the intratubular cell mass. The study also illustrated substantial seminiferous tubular injury, reduced Leydig cells and mild lymphocytic inflammation. However, SARS-CoV-2 virus was not found to be present in the testes.[312]

A study of five patients aged 51–83 years who had died from COVID-19 showed germ cell sloughing into the lumen, seminiferous tubules characterized in a similar manner to Sertoli-cell-only syndrome, increased apoptotic cells, lymphocyte and macrophage infiltration, and — strikingly — SARS-CoV-2 presence in testicular cells using S1 antibody staining and the identification of coronavirus-like particles in the interstitial space of the testis providing direct evidence of testicular entry and attack by SARS-CoV-2.[317] Similarly, post-mortem examinations on 6 men who died with COVID-19 showed that 3 of them had impaired spermatogenesis.[318] In one patient, transmission electron microscopy

(TEM) showed the presence of SARS-CoV-2 in the testes and hematoxylin and eosin (H&E) staining demonstrated macrophage and leukocyte infiltrations in the same patient. Immunofluorescence studies in all six patients revealed a direct association between increased ACE2 levels ($P < 0.05$) and spermatogenic impairment.[318]

Further studies are needed to determine whether SARS-CoV-2 has direct effects on testicular dysfunction or whether the virus acts indirectly through secondary mechanisms such as elevated blood pressure, fever or inflammation triggered by SARS-CoV-2 infection.[319] However, post-mortem studies are associated with several limitations. For example, only patients who had severe infections are studied, which might not reflect accurate pathology in the majority of patients. Furthermore, many of these patients are likely to have other underlying comorbidities and risk factors that have predisposed them to severe infection as well as independent effects on fertility. Finally, death and organ collection generally occur days to weeks after acute infection and viral clearance could have occurred by the time of organ collection.

Alongside clinical and cadaver data, animal models are essential for researching disease progression, pathogenesis and immunological response. An optimal animal model of viral effects on male fertility has similar host–pathogen interactions and disease progression to humans and should enable the measurement of parameters such as clinical symptoms, viral growth and spread, and immune response.[320,321] Thus, various animal models are required to expand pathophysiological relevance and for specific research stages. The animal

models that are currently being used to research SARS-CoV-2 were vital for studying SARS and MERS biology; the best-characterized models in use are mice, ferrets, hamsters and nonhuman primates (NHPs). However, many of these animals display clinical symptoms of SARS-CoV-2 that are much milder and shorter than humans.[322]

Mice were used for studying both SARS-CoV and MERS; human ACE2 (hACE2) transgenic mice have been shown to better model SARS and MERS infection than wild-type mice.[323,324] SARS-CoV-2 infection in hACE2 transgenic mice was shown to cause weight loss, viral replication in the lungs, interstitial pneumonia, macrophage infiltration and accumulation, interstitial lymphocyte infiltration and viral antigen presence in bronchial epithelial cells, macrophages and alveolar epithelia. None of these pathological conditions was observed in wild-type mice infected with SARS-CoV-2.[325] The hACE2 transgenic model is likely to be valuable for evaluating routes of infection, barrier breakdown, therapies and vaccines of COVID-19. Additionally, the hACE2 transgenic mouse model provides a means of quickly observing the effect of ACE2 inhibition on fertility, the possible degradation of the BTB and viral impact on testicular somatic cells. Ferrets and Syrian golden hamsters are often used to study airborne viruses, particularly SARS, as they display human-like pulmonary characteristics.[326,327] One study has found viral RNA in the testes of intranasally infected hamsters up to 1 month after infection.[328] However, despite their consistent use in modelling pulmonary viral infections, including SARS-CoV-2, their use in studies of male fertility is minimal. Owing to kinetic and biological

differences in spermatogenesis between rodents, mustelids and humans, these models cannot be recommended for standalone use in the study of SARS-CoV-2 and spermatogenesis. Furthermore, animal models are burdened with ethical dilemmas as well as money and time constraints. However, as animals are able to model organs and organ systems better than in vitro models, they remain a suitable model for viral entry, BTB damage and effects on testicular somatic cells.

NHPs have a close phylogenetic and physiological relationship with humans; they are remarkably similar in their susceptibility to infectious disease, viral replication and immunological response and are, therefore, used to model viral pathogenesis, male fertility and their intersection.[329,330] Various NHP models were successfully used to uncover SARS and MERS pathogenesis and will be useful for elucidating SARS-CoV-2 infection.[331,332] Although SARS-CoV-2 infection presents with less severe symptoms in NHPs than in humans, a more relevant pathology can be replicated by repeated infections. Additionally, similarities between human and NHP SARS-CoV-2 pathology have been reported.[333] Rhesus macaques and African green monkeys were both shown to display a COVID-19-like disease, which will be useful for elucidating human pathology.[333,334] Additionally, historical use of NHPs to model viruses that are known to affect male fertility, such as Zika and mumps, suggest that NHPs will be a valuable candidate system for studying SARS-CoV-2 and male fertility.[335,336]

Although animal models are extremely useful, they do not fully recapitulate human processes such as human spermatogenesis; a human-derived in vitro

model is necessary to fill these gaps. Two-dimensional culture systems have enabled insights into germ cell, somatic cell, and extracellular matrix interactions and the effects of growth factors, hormones and viruses; however, such monolayer systems often display irrelevant physiology and cell communications that fail to mimic human biological responses.[337-339] Organoids derived from human primary or stem cells represent a more biologically relevant system than most in vivo and 2D culture systems and are useful for modelling viral infections.[340,341] Several human testicular organoids have been developed over the past few years.[337,342,343] In 2019, the generation of human testicular organoids using a microwell culture system was reported.[339] These organoids display testis-specific morphology and tight junction protein expression, and response to retinoic acid was similar to that observed in the testis in vivo. Germ cells displayed reduced levels of autophagy compared with those seen in 2D models, indicating reduced cellular stress. Overall, this model seems promising for the study of the effect of SARS-CoV-2 on male fertility.[339] Although organoids have been used to model SARS-CoV-2 infection in the brain, they have yet to be used for testicular cells.[344] However, many of these organoids cannot provide an accurate view of viral pathogenicity as they fail to reproduce the complex organization of the testis and recapitulate spermatogenesis.

Testicular explants have been used to show Zika infection of testicular tissue and germ cells, but not widely in SARS-CoV-2.[114] One study has shown viral replication in hamster testes using an ex vivo infection model.[328] However, ex vivo models have been used to model SARS-CoV-2 infection in the

lungs.[345,346] This type of model enables study of an organ's natural physiological and pathological environment, including tissue architecture, cell–cell interactions and local immune response. However, these models are best suited for short-term studies and rely on organ donors.

If SARS-CoV-2 is shown to pass through or degrade the BTB or is demonstrated to be present in patient semen, determining the effects of interactions between developing sperm cells and the virus will be essential. However, most of these spermatogenic models discussed above fail to recapitulate human in vivo effects such as germ cell death and cannot sustain chronic viral exposure, which is necessary for studying the effects of viral intrusion. An unbiased high-throughput format has been reported, which mirrored aspects of human spermatogenesis and mimicked the effects of environmental exposures in vivo.[347-349] Although this model has so far been used primarily for studying environmental toxicants, such as perfluoroalkyl and polyfluoroalkyl substances and polybrominated biphenyl , it is also well suited to observing the effects of SARS-CoV-2 and other viruses on spermatogenesis, particularly SSCs and early spermatogenic stages.[348,349] However, as this model represents only spermatogenesis and lacks the somatic cell niche, its utility is limited to studying only the direct effects of SARS-CoV-2 on spermatogenic cells. Additionally, the model is limited by low haploid generation and lacks the capability to produce fully differentiated sperm.

The focus of SARS-CoV-2 research has so far been on the lungs and immune response, as these two systems are highly engaged during infection.

Although little research has investigated effects on male fertility, several studies have reported SARS-CoV-2-induced orchitis, altered hormone levels, testicular damage and the possible presence of the virus in sperm. As increasing data indicate the long-term effects of COVID on other organ systems, long-term effects on the testis will also need to be examined.

Whether these symptoms arise from the direct effects of SARS-CoV-2 on the testis or whether they are mediated by other mechanisms, such as immune response and inflammation, remains to be determined; alternatively, underlying risk factors for SARS-CoV-2 could even be the ultimate cause. It is essential to remember that any disease state or environmental factor that dysregulates furin, ACE2 or TMPRSS2 can affect SARS-CoV-2 infection and its intersection with male fertility. The primary proteins involved in SARS-CoV-2 pathology, particularly ACE2 and TMPRSS2, are expressed throughout the body, including in the testis. Thus, their infection or negative inhibition by SARS-CoV-2 could have severe consequences for male fertility. Although the RAAS is involved in male fertility, the extent to which ACE2 and TMPRSS2 are expressed in the testes is uncertain and requires more research. Several in vivo and in vitro models show promise for studying the effects of SARS-CoV-2 on male fertility. Tandem use of a variety of models alongside clinical data will be necessary to fully elucidate the effects of SARS-CoV-2 infection on male fertility.

As long-term sequelae of SARS-CoV-2 begin to be examined, viral effects on sperm production and male fertility should be considered to guide research and to modify clinical advice for patients. Multiple justifications exist for a

potentially detrimental effect of SARS-CoV-2 on male fertility; however, a multifaceted approach is required for validation. The research laid out in this manuscript will take a step in filling in knowledge gaps of SARS-CoV-2 affects male fertility.

CHAPTER 3

IMPACT OF SARS-COV-2 INFECTION ON THE BLOOD-TESTIS BARRIER IN HUMANS AND NONHUMAN PRIMATES[2]

[2] To be submitted to *Scientific Reports*

3.1 ABSTRACT

SARS-CoV-2 has infected over 320 million men. As variants like Omicron evolve to be more infections at the cost of pathogenicity the amount of infected men will rise immensely. The effect of SARS-CoV-2 infection on male fertility is not well understood; however, there is clinical and experimental evidence that SARS-CoV-2 infection can negatively impact male reproductive health. Further evidence shows that the blood-testis barrier may be susceptible to infection. Here, we formed a blood-testis like barrier of primary human and nonhuman cells to test SARS-CoV-2 variants WA1/2020, BA.1.1.529, BA.4.6, and XBB. Barrier infection was assessed by transepithelial electrical resistance and Dye Flux assays. SARS-CoV-2 infection caused barrier disruption regardless of variant or species. Interestingly, variants that were better adapted to human viral entry proteins caused greater barrier disruption in humans than nonhuman primates. Furthermore, variants that are better suited for immune evasion cause the least amount of barrier disruption in both humans and nonhuman primates.

3.2 REINTRODUCTION TO SARS-COV-2 AND ITS IMPACT ON EPITHELIAL BARRIERS

The introduction for this chapter is brief, only covering the most recent or relevant literature as this has been extensively covered in chapter two. At the time of writing, SARS-CoV-2 has infected over 750 million people.[121] Males and females are diagnosed with COVID-19 at a similar frequency.[350] To date, 7 million people have died from this disease with a majority of them being male. Conservatively, 320 million men have been infected with SARS-CoV-2.

Furthermore, official COVID-19 case counts increasingly underestimate the number of positive tests and true infections.[351] With increased use of at home tests and reduced reporting by government agencies, COVID-19 cases will likely be perpetually underestimated.[352] Additionally, males are less likely to test at home and when they do they are more likely to have a positive test.[351] Altogether, this indicates there are more males infected with SARS-CoV-2 than previously estimated. This is particularly worrisome as men have a worse COVID-19 outcome than women.[353]

As research continues, more evidence shows that SARS-CoV-2 infection can disrupt barrier function in multiple organ systems. Wang et al. show that direct exposure of a blood-brain barrier chip to SARS-CoV-2 can cause mild changes to the *in vitro* formed barrier. Interestingly, infusion of medium from an infected alveolus chip led to more severe injuries on the BBB.[354] Song et al. have provided autopsy evidence of extensive disruption of the BBB in the brains of individuals with history of COVID-19, even though no virus was detected in the tissue sections.[355] They conclude that BBB dysfunction may play a role in neurological impairments during the disease and persistent cerebral symptoms in survivors. Proust et al. show that SARS-CoV-2 can disrupt the normal functioning of the BBB and its cellular components, contributing to the vast neurological manifestations of COVID-19.[356] They show that specific SARS-CoV-2 variants can pose a greater risk for neurological damage. Specifically, they reveal that Omicron variants may have a higher potential to damage the BBB and its cellular components, while Alpha and Beta variants appear to have a smaller impact on

neurological health and reduced ability to disrupt the BBB. Fiorito et al. propose the epithelial barrier hypothesis: that a wide array of diseases can arise from the breakdown of the skin, respiratory tract, and gastrointestinal system's epithelial barriers.[357] They link environmental exposures, epithelial damage, and altered immune response with increased susceptibility to SARS-CoV-2 infection and COVID-19 progression and outcome. Overall, they implicate barrier degradation with COVID-19 severity.

Kang et al. show that ectopic expression of SARS-CoV-2 structural proteins in primary human Sertoli cells can modulate the expression of BTB-related proteins and autophagy and increase FasL expression.[358] They induced ectopic expression by transiently transfecting primary human Sertoli cells with GFP-tagged SARS-CoV-2 structural protein plasmid DNA. Specifically, they found that SARS-CoV-2 envelope and membrane protein can induce the expression of ZO-1 and claudin 11, promote the formation of autophagosomes, and impede autophagic flux. Conversely, the spike protein decreased the expression of BTB-associated proteins ZO-1 and N-cadherin and hindered the degradation of autophagosomes. The nucleocapsid protein decreased the expression ZO-1, claudin 11 and N-cadherin. These conflicting results show the need to further study the effects of SARS-CoV-2 infection on Sertoli cells and the BTB. A mini review by Ly et al. shows that severe COVID-19 may trigger testicular inflammation and histopathological damage either through direct infection of testicular cells by SARS-CoV-2 or the immunological response elicited by SARS-CoV-2.[359]

3.3 THE OMICRON VARIANT

Since the onset of the COVID-19 pandemic, several SARS-CoV-2 variants have emerged. The Omicron variant was first identified in South Africa and Botswana in November of 2021. This notable variant is also known as B.1.1.529. It quickly spread, becoming the dominant variant in several regions and was labeled a variant of concern. The Omicron variant displays reduced virulence due to changes in cell tropism. Moreover, Omicron shows notable resistance to the neutralizing effects of vaccines, convalescent serum, and most antibody therapies.[360] Omicron is characterized by its unprecedented amount of mutations.[361] Because of Omicrons reduced pathogenicity many patients have asymptomatic cases. However, these asymptomatic individuals may have a more robust cellular immune response which may be hazardous to male fertility.[362] These asymptomatic COVID-19 cases may impact semen within 70 days of infection altering sperm concentration and semen quality.[363]

To assess what effects SARS-CoV-2 and the Omicron variants may have on the BTB, the ancestral lineage WA1/2020 and Omicron subvariants BA.1, BA.4.6, and XBB were used to infect primary human Sertoli cells. BA.1 (B.1.1.529-GA) is considered the ‘standard’ omicron, as it was the first Omicron characterized.[364] BA.4.6 contains extra spike protein mutations that allow for further reduction in neutralization by vaccines.[364] The XBB variant results from a recombination of two lineages descended from BA.2, which caused a significant outbreak in early 2022. Notably, this variant exhibits an additional spike in RBD

mutations. It may also have a greater affinity to the ACE2 receptor resulting in increased viral uptake and enhanced transmissibility.[365]

3.4 RESULTS: HUMAN AND NONHUMAN PRIMATE SERTOLI CELL ISOLATION AND CULTURE

While there is evidence showing BTB breakdown and disruptions to male fertility caused by SARS-CoV-2 infection, little has been done to interrogate its impact on the BTB in nonhuman primates and humans. To do this Sertoli cells were isolated from adult rhesus macaques' testicular biopsies and human testicular cell suspension samples. The cells were isolated from tissue as described. [366] Following tissue mincing, the cells were isolated using a Percoll gradient and plated. Purification continued by differential plating and visual analysis. After culturing to a high confluency, the cells were plated onto transwells for the rest of the experiments. The Sertoli cells were plated at a high density of 1 x 10^6 cells/cm^2 to encourage barrier formation. Additionally, testosterone was added to aid in barrier formation and help the barrier last for at least 10 days [367]. Once the barrier reached a TEER of 200 Ohm x cm^2, experiments began. This process is described in greater detail in Chapter 4.4.

3.5 RESULTS: SARS-COV-2 CAUSES BLOOD-TESTIS BARRIER BREAKDOWN IN NONHUMAN PRIMATES

SARS-CoV-2 infection is shown to alter multiple barriers including the BTB in humans.[353] SARS-CoV-2 infects species with high ACE2 homology. SARS-CoV-2 is even thought to infect most mammals.[368] Cats, ferrets, tree shrews, golden hamsters, grivets, common marmosets, and cynomolgus and rhesus

macaques have been infected with SARS-CoV-2 experimentally and can even shed the virus. These animals exhibited clinical and pathological symptoms comparable to or milder than those observed in humans.[369] SARS-CoV-1 and MERS-CoV have also been shown to infect rhesus macaques.[369] The transient, moderate disease observed in rhesus macaques aligns with the typical course of COVID-19 in most human cases.[370] However, macaques do not display severe SARS-CoV-2 infection.[353] While macaques have not yet been shown to be infected by SARS-CoV-2 from SARS-CoV-2 positive humans, it is a concern for lab populations of nonhuman primates. Captive gorillas at zoos have been infected with SARS-CoV-2 leading to COVID-19 symptoms.[371] SARS-CoV-2 infection in nonhuman primate lab populations can cause serious issues for lab studies as their susceptibility and pathology is not well understood.[372] SARS-CoV-2 infection could also impact the male's fertility, making it hard to maintain the colony.

An *in vitro* BTB model was used to assess the impact that SARS-CoV-2 infection may have on male fertility in macaques. The BTB was formed from primary rhesus macaque Sertoli cells and cultured on Matrigel coated transwells. This allowed transepithelial electrical resistance (TEER) and Dye Flux assays to be performed. The Sertoli cells were infected with different variants of SARS-CoV-2. WA1/2020 (WA1), BA.1.1.529 (BA.1), BA.4.6, and XBB were used.

TEER measures the electrical resistance of the *in vitro* formed barrier. It does so with a two-pronged probe with a node on each end, and measures the electrical resistance in ohms between the two nodes. If the barrier is altered in

any way that causes cell death or alters the cell junctions, the electrical resistance will decrease. TEER shows that SARS-CoV-2 infection, regardless of the variant, can cause BTB disruption (**Figure 3.1**). At 0 hours post-infection (hpi) and 6 hpi, there is no significant difference between the control and any of the infected; however, at 48 hpi there is a significant difference between the control and all the infected samples. Furthermore, all the infected samples display a significant decrease between the 0 hpi and the 48 hpi samples. Additionally, WA1, BA.1, and XBB have a marked decrease between 6 hpi and 48 hpi.

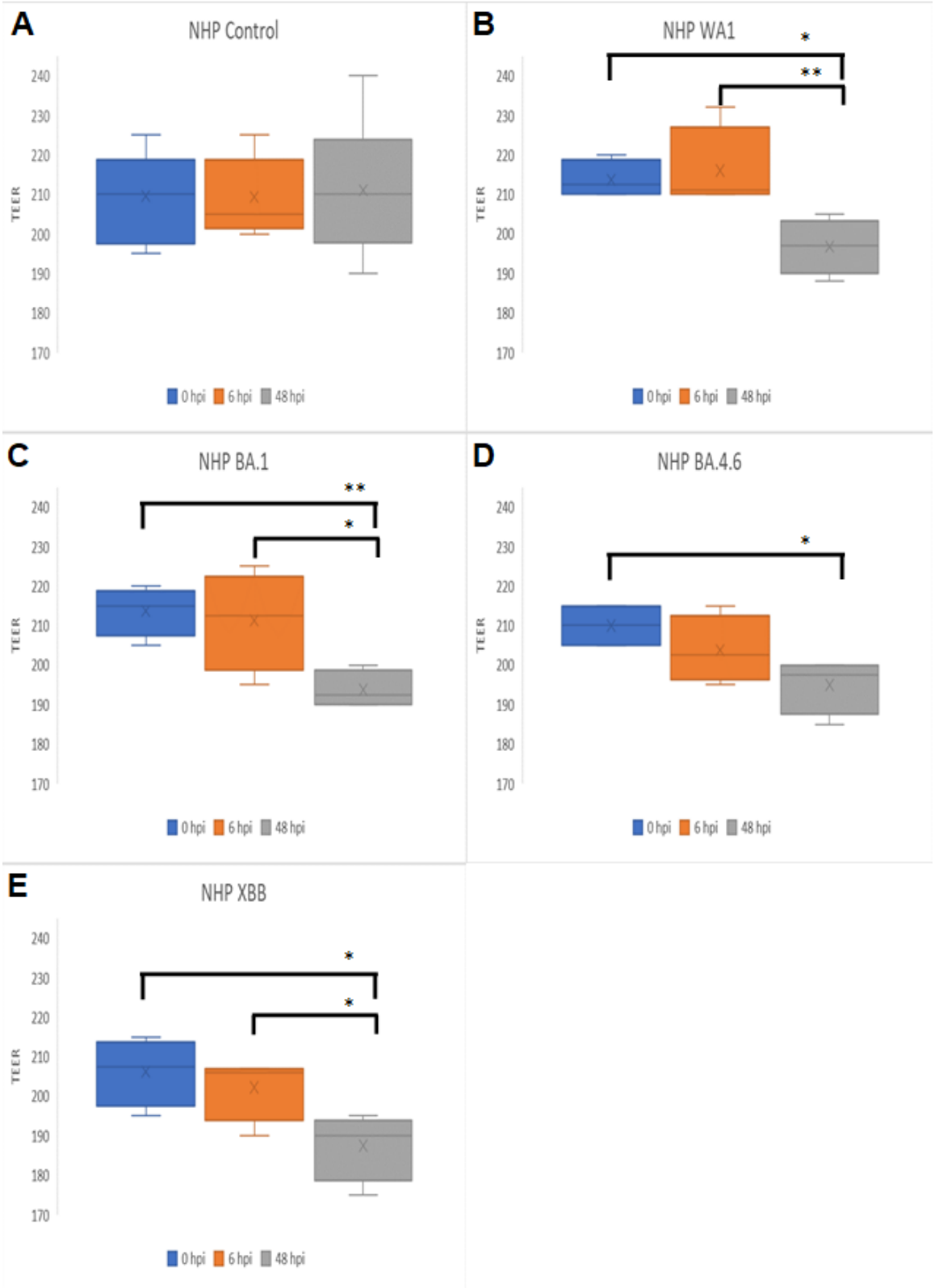
A
NHP Control
TEER
240
230
220
210
200
190
180
170
0 hpi
6 hpi
48 hpi
B
NHP WA1
*
**
C
NHP BA.1
**
*
D
NHP BA.4.6
*
E
NHP XBB
*
*

Figure 3.1 The impact of SARS-CoV-2 variants, WA1/2020, BA.1.1.529, BA.4.6, and XBB, on the blood-testis barrier as measured by transepithelial electrical resistance

Image A shows that our control maintains an appropriate and consistent TEER. Image B shows TEER in response to WA1 infection. It shows a significant decrease between the 0 hpi and 48 hpi ($p = 0.0138$) and a significant decrease from 6hpi to 48 hpi ($p = 0.0072$). Image C shows TEER response to BA.1 infection. BA.1 causes a significant decrease from 0 hpi to 48 hpi ($p = 0.0091$) and 6 hpi to 48 hpi ($p = 0.0176$). BA.4.6 (Image D) is the only variant to not have a significant difference between 6 hpi and 48 hpi; however, there is still a significant difference between 0 hpi and 48 hpi ($p = 0.0165$). Image E shows TEER response to XBB infection. It shows that there is a significant decrease in TEER from 0 hpi to 48 hpi ($p = 0.0121$) and 6 hpi to 48 hpi ($p = 0.0365$). Statistics were characterized by the student's t-test.

In addition to TEER, Dye Flux is used to assess BTB integrity. The Dye Flux assay measures the amount of calcein and dextran dye that crosses from the apical side of the barrier, where it is placed, into the basal side every thirty minutes over two hours. If the barrier is disrupted in any way this will be reflected in an increased amount of dye that is able to flow through the barrier. Calcein flow through the barrier increases significantly following BA.1 and WA1 infection (**Figure 3.2**). XBB infection however does not cause a significant increase in calcein flow through the barrier. BA.4.6 infection does cause a significant increase in calcein flow through at 60 minutes but not at any other time point. Dextran follows a similar pattern to calcein (**Figure 3.3).** BA.1 and WA1 infection both cause an increase in the flow of dextran through the barrier. However, BA.4.6 and XBB infection also cause a significant increase in dextran flow through the barrier, albeit not to the same extent as BA.1 and WA1 infection. In summary, using TEER and Dye Flux we show that SARS-CoV-2 infection can disrupt the BTB and that some variants may have a greater impact than others.

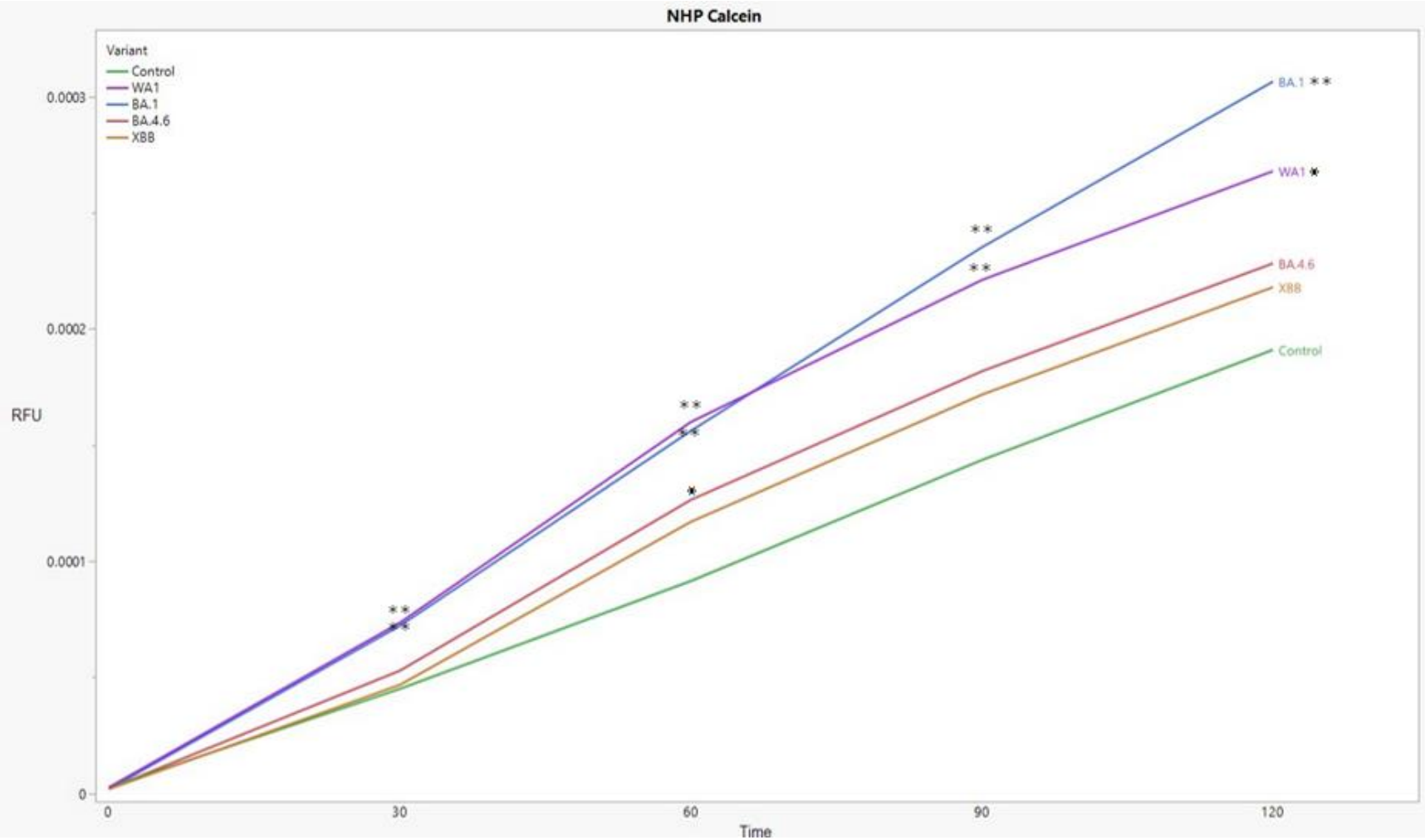
NHP Calcein
Variant
Control
WA1
BA.1
BA.4.6
XBB
RFU
0.0003
0.0002
0.0001
0
0
30
60
90
120
Time
BA.1
WA1
BA.4.6
XBB
Control

Figure 3.2: SARS-CoV-2 infection causes blood-testis barrier disruption as measured by calcein Dye Flux

At minute 30 WA1 ($p < 0.0001$) and BA.1 ($p < 0.0001$) are both significantly higher than the control. At minute 60 WA1 ($p < 0.0001$), BA.1 ($p < 0.0001$), and BA.4.6 ($p = 0.0143$) are significantly higher than the control. At 90 minutes WA1 ($p < 0.0001$) and BA.1 ($p < 0.0001$) are both significantly higher than the control. At 120 minutes BA.1 ($p < 0.0001$) and WA1 ($p = 0.0007$) are both significantly higher than the control. Interestingly, at 120 minutes BA.1 is significantly higher than both XBB ($p = 0.0002$) and BA.4.6 ($p = 0.0006$). The same is true for WA1 which is significantly higher than XBB ($p = 0.0147$) and BA.4.6 ($p = 0.0446$). BA.1 and WA1 are also both significantly higher than both XBB and BA.4.6 at 30, 60, and 90 minutes.

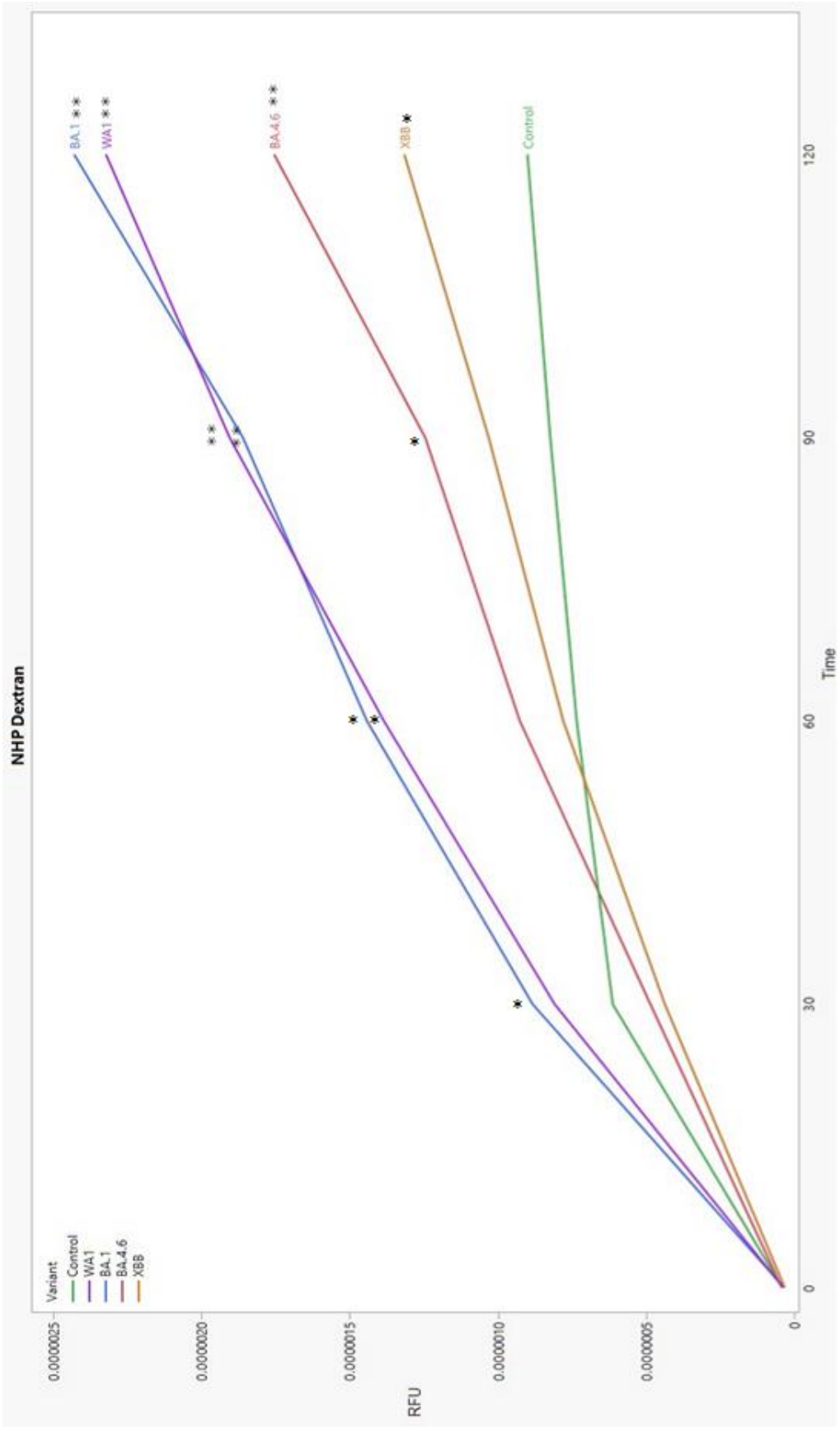
NHP Dextran
Variant
Control
WA1
BA.1
BA.4.6
XBB
BA.1 **
WA1 **
BA.4.6 **
XBB *
Control
RFU
0.0000025
0.0000020
0.0000015
0.0000010
0.0000005
0
Time
0
30
60
90
120

Figure 3.3: SARS-CoV-2 infection causes blood-testis barrier disruption as measured by dextran Dye Flux

At 30 minutes only BA.1 ($p = 0.0218$ is significantly higher than the control. At 60 minutes BA.1 ($p = 0.003$) and WA1 ($p = 0.004$) are both significantly higher than the control. At 90 minutes WA1 ($p < 0.0001$), BA.1 ($p < 0.0001$), and BA.4.6 ($p = 0.0032$) are all higher than the control. At the final time point, 120 minutes, BA.1 ($p < 0.0001$), WA1 ($p < 0.0001$), BA.4.6 ($p < 0.0001$), and XBB ($p = 0.0176$) are all significantly higher than the control. BA.1 and WA1 are also significantly higher than the XBB and BA.4.6 infected barriers. At 120 minutes BA.1 is significantly higher than XBB ($p < 0.0001$) and BA.4.6 ($p = 0.0006$). At 120 minutes WA1 is significantly higher than XBB ($p < 0.0001$) and BA.4.6 ($p < 0.0001$). Interestingly at the final time point BA.4.6 is also significantly higher than XBB ($p = 0.013$).

3.6 RESULTS: SARS-COV-2 CAUSES BLOOD-TESTIS BARRIER BREAKDOWN IN HUMANS

SARS-CoV-2 infection has been shown to alter various blood barriers and may affect the testis and semen parameters.[353] Therefore, understanding what impact SARS-CoV-2 infection has on the blood-testis barrier is vital. Kang et al. have shown that SARS-CoV-2 structural proteins can modulate proteins associated with the BTB.[358] However, they failed to show what effect SARS-CoV-2 infection has on Sertoli cells or the BTB as they used a DNA plasmid. Additionally, they did not assess any effect on the BTB directly, they only assessed BTB associated proteins. The direct effect of SARS-CoV-2 infection on the BTB is addressed here using TEER and Dye Flux assays.

TEER shows that SARS-CoV-2 infection can disrupt BTB regardless of the SARS-CoV-2 variant (**Figure 3.4**). At 6 hpi and 48 hpi, the control displays a significantly higher resistance than the infected samples. The control also stays within a tight window and does not significantly drop at 48 hpi. Using 0 hpi as the control, there is also a significant reduction in TEER at 48 hpi for each variant. Additionally, when comparing 6 hpi and 48 hpi, there is a significant reduction in TEER for the WA1, BA.4.6, and XBB infected samples but not the BA.1 infected samples.

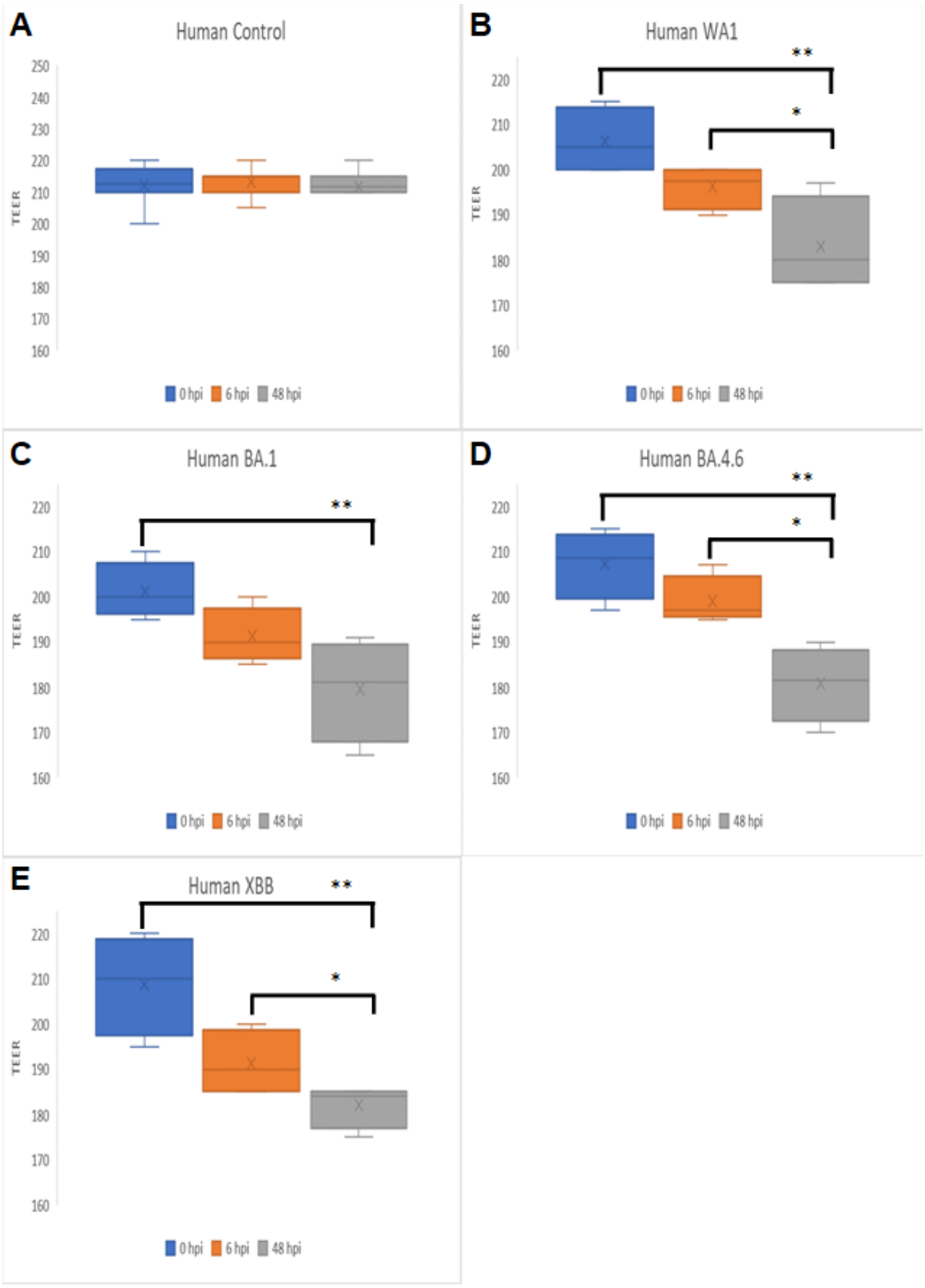
A
Human Control
B
Human WA1
C
Human BA.1
D
Human BA.4.6
E
Human XBB
TEER
0 hpi
6 hpi
48 hpi
**
*

Figure 3.4: Assessing the impact of SARS-CoV-2 infection on human blood-testis barrier integrity using transepithelial electrical resistance

Image A shows the control at 0, 6, and 48 hpi. It was cultured the same as the other groups and received medium changes at the same time but did not receive any virus. The control stays around 215 at each time point indicating a healthy barrier was formed and maintained. All infected samples display a significant drop in TEER when compared to the control at 6 hpi and 48 hpi. 6hpi: BA.1 ($p < 0.0001$), XBB ($p < 0.0001$), WA1 ($p < 0.0001$), and BA.4.6 ($p = 0.0006$). 48 hpi: BA.1 ($p < 0.0001$), XBB ($p < 0.0001$), WA1 ($p < 0.0001$), and BA.4.6 ($p < 0.0001$). Image B shows TEER in response to WA1 infection. There is a significant reduction in TEER between the 0 hpi and 48 hpi ($p = 0.0025$) and 6 hpi and 48 hpi ($p = 0.0423$). Image C shows TEER in response to BA.1 infection. There is a significant reduction in TEER between 0 hpi and 48 hpi ($p = 0.0048$), but not between 6 hpi and 48 hpi. While there is not a significant reduction, TEER does still appear to decrease between 6 hpi and 48 hpi. Image D shows TEER in response to BA.4.6 infection. There is a significant reduction in TEER between 0 hpi and 48 hpi ($p = 0.0006$) and 6 hpi and 48 hpi ($p = 0.0423$). Image E shows TEER in response to XBB infection. There is a significant reduction in TEER between 0 hpi and 48 hpi ($p = 0.0013$) and 6 hpi and 48 hpi ($p = 0.0145$).

Dye Flux shows that more dye can pass through the barrier regardless of the SARS-CoV-2 variant used to infect. This is true with both calcein and dextran. Using calcein, all four variants pass through at a significantly higher rate than the control at 60, 90, and 120 minutes (**Figure 3.5**). Interestingly, BA.1 and XBB cause the most dye to pass through while BA.4.6 is the lowest at 90 and 120 minutes. Using dextran, a similar trend appears (**Figure 3.6**). XBB, BA.1, WA1, and BA.4.6 infection all allows a significant increase in the amount of dye passing through the barrier at 90 and 120 minutes. Additionally, XBB infection causes the biggest increase in dye passing through the barrier when compared to the control. Furthermore, BA.4.6 allows the least amount of dye through the barrier when compared to the control. This is particularly interesting as XBB infection displayed the lowest alteration to the BTB in the NHP samples.

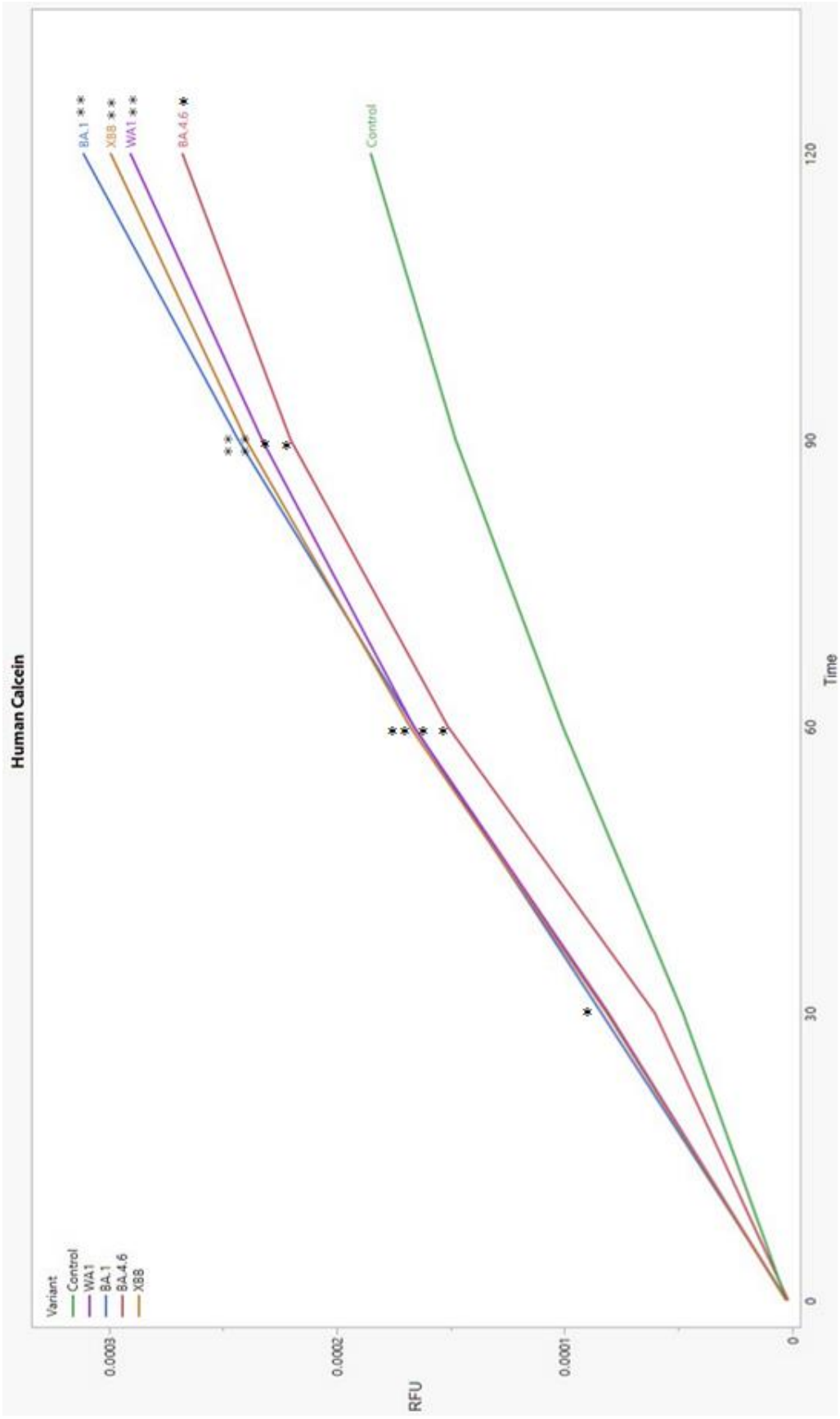
Human Calcein
Variant
Control
WA1
BA.1
BA.4.6
XBB
BA.1 **
XBB **
WA1 **
BA.4.6 *
Control
RFU
0.0003
0.0002
0.0001
0
Time
0
30
60
90
120

Figure 3.5: SARS-CoV-2 infection causes human blood-testis barrier disruption as measured by calcein Dye Flux

At 30 minutes, WA1 ($p = 0.0028$) and BA.1 ($p = 0.0123$) are both significantly higher than the control. At 60 minutes WA1 ($p = 0.0001$), BA.1 ($p = 0.0006$), XBB ($p = 0.0029$), and BA.4.6 ($p = 0.0116$) are all significantly higher than the control. At 90 minutes BA.1 ($p < 0.0001$), WA1 ($p < 0.0001$), XBB ($p = 0.0001$), and BA.4.6 ($p = 0.0006$) are all significantly higher than the control. At 120 minutes BA.1 ($p < 0.0001$), WA1 ($p < 0.0001$), XBB ($p < 0.0001$), and BA.4.6 ($p = 0.0001$) are all significantly higher than the control. Interestingly, there are differences in the variants. At 30 minutes WA1 ($p = 0.0075$) and BA.1 ($p = 0.0329$) are both significantly higher than BA.4.6. At 60 minutes only WA1 ($p = 0.0393$) is significantly higher than BA.46. At 90 minutes there is no significant difference between any of the variants. At 120 minutes BA.1 ($p = 0.0266$) and WA1 ($p = 0.0234$) are both significantly higher than the control.

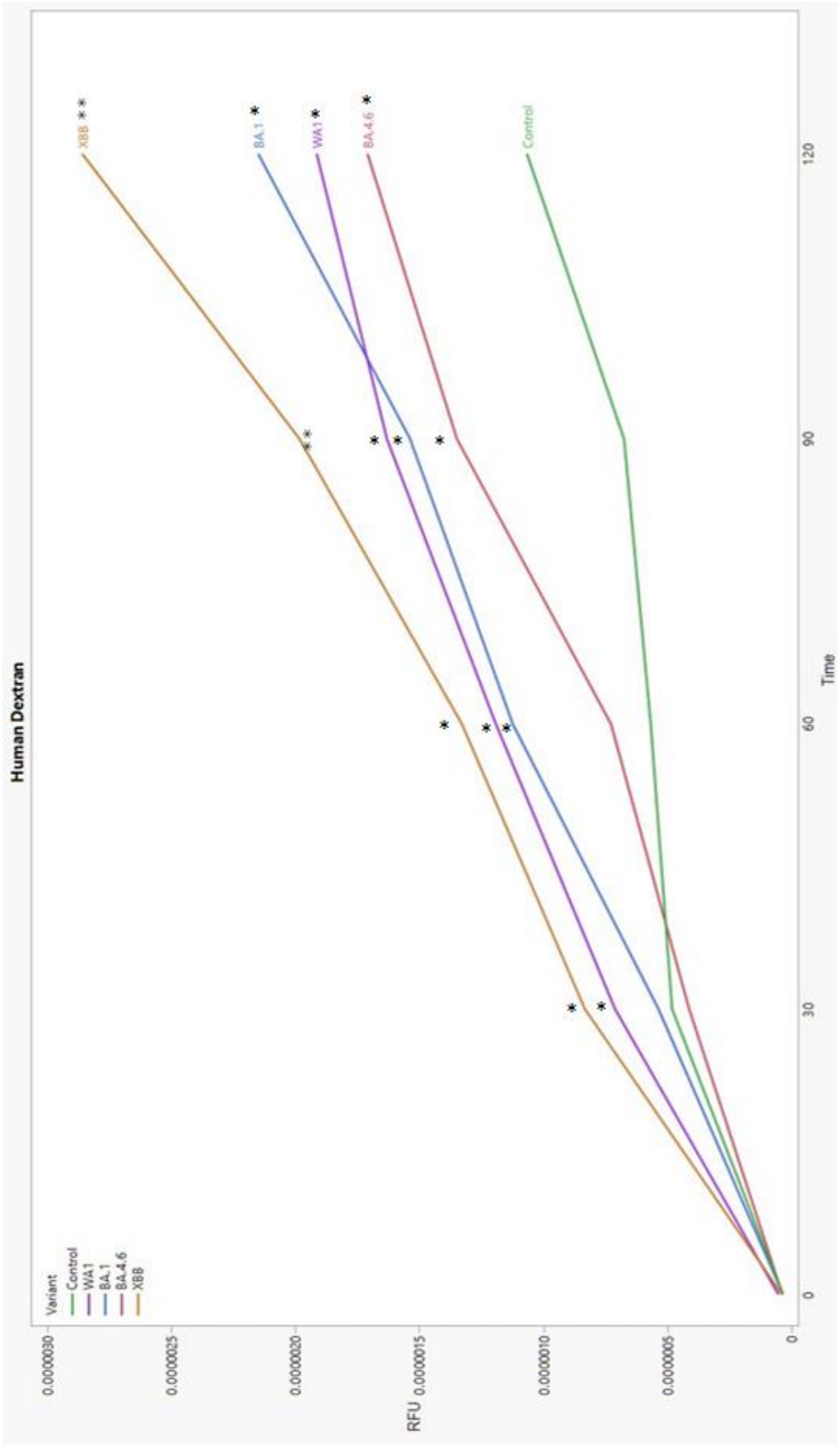
Human Dextran
Variant
Control
WA1
BA.1
BA.4.6
XBB
RFU
0.0000030
0.0000025
0.0000020
0.0000015
0.0000010
0.0000005
0
0
30
60
90
120
Time
XBB **
BA.1 *
WA1 **
BA.4.6 *
Control

Figure 3.6: SARS-CoV-2 infection causes human blood-testis barrier disruption as measured by dextran Dye Flux

At 30 minutes, XBB ($p = 0.0255$) and WA1 (0.0467) infection both cause a significant increase in dextran dye passing through the barrier than the control. At 60 minutes XBB ($p = 0.0015$), WA1 ($p = 0.01$), and BA.1 ($p = 0.0125$) infection significantly increase the flow of dye through the barrier when compared to the control. At 90 minutes XBB ($p = 0.0001$), WA1 ($p = 0.003$), BA.1 ($p = 0.0036$) and BA.4.6 ($p = 0.0164$) infection all cause a significant increase in the flow of dye passing through the barrier when compared to the control. At 120 minutes XBB ($p < 0.0001$), BA.1 ($p = 0.0007$), WA1 ($p = 0.0075$), and BA.4.6 ($p = 0.0227$) infection all cause a significant increase in the flow of dye through the barrier when compared to the control. Additionally, there is a significant difference in the flow of dye between variants. At 120 minutes XBB infection causes a significant increase in the flow of dye through the barrier than BA.4.6 ($p = 0.0004$), WA1 ($p = 0.0037$, and BA.1 ($p = 0.0136$). However, at 90 minutes XBB infection is only significantly higher than BA.4.6 ($p = 0.0224$). At 60 minutes XBB ($p = 0.0074$) and WA1 ($p = 0.0441$) are both significantly higher than BA.4.6.

3.7 DISCUSSION

SARS-CoV-2 infections will most likely continue to increase in males. Furthermore, there is growing evidence that SARS-CoV-2 infection and COVID-19 can negatively impact male reproductive health. Therefore, more research is required to assess how SARS-CoV-2 impacts male fertility. Particularly, more research into SARS-CoV-2 variants that exhibit a transmission advantage over pathology inducing one such as Omicron. These types of SARS-CoV-2 variants make up the majority of new cases.[373] Furthermore, SARS-CoV-2 appears to be evolving in that direction.

Kang et al. have already shown that SARS-CoV-2 structural proteins expressed ectopically can disrupt BTB proteins. However, their study lacked any interrogation into barrier function or actual SARS-CoV-2 infection. Additionally, various clinical and cadaver studies have implicated SARS-CoV-2 infection and COVID-19 in negatively impacting male reproductive health.[353]

Here, SARS-CoV-2 variants WA1/2020, BA.1.1.526, BA.4.6, and XBB were used to infect *in vitro* formed barriers from human and NHP primary Sertoli cells. Overall, all variants disrupt the formed barrier. This was assessed by TEER and Dye Flux. Transepithelial electrical resistance measures the electrical resistance that is put up by an *in vitro* formed barrier. The higher the TEER value, the stronger the barrier should be. Dye Flux measures the flow of dye through a barrier. The more dye that can pass through, the worse the barrier should be. Overall, SARS-CoV-2 infection will cause TEER to drop and Dye Flux to increase in both humans and NHPs indicating that the barrier is being disrupted.

Importantly, the SARS-CoV-2 variants display differential effects between each other in each species. In NHP cells WA1 and BA.1 infections have the greatest impact on barrier integrity as measured by TEER and Dye Flux. Additionally, XBB infection has the smallest impact on barrier integrity. Furthermore, WA1 and BA.1 infections cause a significant increase in barrier disruption when compared to XBB infection. Interestingly, the opposite trend appears in the human cells regarding XBB infection and barrier integrity. In humans, XBB infection causes the biggest change in BTB integrity, particularly regarding Dye Flux. BA.1 infection continues to have a significant impact on barrier integrity in human cells as it does in NHP cells. WA1 and BA.4.6 however both have the lowest impact on barrier dynamics in human cells.

The effect that SARS-CoV-2 variants have on different species is best explained by the genetic differences between the variants, in particular the genetic differences that are present in XBB and BA.4.6. XBB has a F486P substitution in the region binding domain of the spike protein. This mutation allows for better human ACE2 affinity.[374] This mutation helps to explain why XBB is so effective at causing BTB disruption in the human cells. Additionally, this mutation explains why XBB is not very effective at disrupting BTB integrity in NHP cells as the region binding domain is now better suited for human ACE2 than it is for NHP ACE2. BA.4.6 also has a region binding domain mutation of R346.[373,375] This mutation allows the BA.4.6 variant to be antibody evasive.[376] While this variant is particularly effective for causing infections in individuals, it comes with the trade of having a lower pathogenicity. This effect is well displayed

here as BA.4.6 is not very effective at disrupting the BTB in either human or NHP barriers.

Other experiments were performed, but results have not been received at the time of writing (October 2023). RNA was collected to perform RNAseq. RNAseq will allow the expression of barrier associated genes to be analyzed such as claudins and zona occludens. In addition to barrier associated genes, the expression of genes related to Sertoli cell function like *SOX9* and *AR*. In addition to RNAseq a cytokine assay will be performed to interrogate any changes in cytokines related to inflammation and spermatogenesis. Overall, it is expected that SARS-CoV-2 infection will alter the gene expression of barrier and Sertoli cell function associated proteins as well as cytokines associated with inflammation and spermatogenesis.

In summary, this study shows that SARS-CoV-2 infection can disrupt the blood-testis barrier. This is demonstrated by the drop in TEER and influx of dye across the barrier caused by infection with SARS-CoV-2. Furthermore, it is revealed that different SARS-CoV-2 variants such as WA1/2020, BA.1.1.526, BA.4.6, and XBB, will differentially disrupt the barrier based on the species of the barrier. Broadly, SARS-CoV-2 variants that are better suited for human infection do not affect NHP formed barriers to the same extent. Additionally, variants that are adapted for transmission over pathogenicity will disrupt the barrier less.

3.8 METHODS

Nonhuman Primate Sertoli Cell Isolation and Culture

All procedures were approved by the Emory University Institutional Animal Care and Use Committee and were performed in accordance with the Animal Welfare Act and the US Department of Health and Human Services "Guide for the Care and Use of Laboratory Animals" (National Research Council, 2011). The Emory National Primate Research Center is fully accredited by the Association for Assessment and Accreditation of Laboratory Animal Care (AAALAC) International. Testicular biopsies were obtained from Rhesus macaques from Dr. Chan, previously at the Emory National Primate Research Center. Biopsies were minced, and a single-cell suspension was created as previously described.[366] The suspensions were stored in liquid nitrogen until needed. Following thaw, the tissue was briefly minced further, and the germ cells were separated out by gravity sedimentation while in 80mL of HBSS and P/S. Then the remaining pellet undergoes an enzyme digestion while being shaken at 300 rpm at 37C for 15 minutes. Digestion media contains 80mL HBSS with P/S, 10 mL trypsin (2.5%), 10 mL collagenase type IV (1%), and 2 mL DNase (1 mg/mL). The digested solution was then passed through a metal sieve to remove any undigested or connective tissue. 0.1% soybean trypsin inhibitor was then added to halt digestion. The solution was then centrifuged at 200g for 5 min, the supernatant was discarded, and DMEM F12 with P/S was added in a 10:1 volume ratio. The solution then rests at room temp for 30 minutes. The pellet is enriched for tubular fragments cells and the supernatant for interstitial cells. The interstitial cells can be further isolated on a discontinuous Percoll gradient. The pellet can now be resuspended in PBS with 1M glycine and 2mM EDTA and pipetted for 10 min to

remove peritubular cells. Gravity sedimentation was then used to isolate out Sertoli cells and tubular fragments. Both were plated and cultured in DMEM F12 15% FBS with P/S. Culture media is refreshed every other day. The Sertoli cells are then purified by visual analysis and differential plating. At passage 3 the Sertoli cells were cultured at 35℃ with 10% FBS DMEM with P/S. The cells medium is changed every other day.

Human Sertoli Cell Isolation and Culture

Sertoli cells were isolated from de-identified human testis cell suspensions kindly provided by Dr. Kyle Orwig at the University of Pittsburgh. The sample number of the provided cells are Human Core – 18092304 – testis cells. The suspensions were stored in liquid nitrogen until needed at a concentration of ~20 x 10^6 cells/mL. Following thaw, the germ cells were separated out by gravity sedimentation while in 10mL of HBSS and P/S. The remaining pellet undergoes a brief enzyme digestion while being shaken at 300 rpm at 37C for 5 minutes. Digestion media contains 80mL HBSS with P/S, 10 mL trypsin (2.5%), 10 mL collagenase type IV (1%), and 2 mL DNase (1 mg/mL). 0.1% soybean trypsin inhibitor was then added to halt digestion. The solution was then centrifuged at 200g for 5 min, the supernatant was discarded, and DMEM F12 with P/S was added in a 10:1 volume ratio. The solution then rests at room temp for 30 minutes. The pellet is enriched for tubular fragments cells and the supernatant for interstitial cells. The interstitial cells can be further isolated on a discontinuous Percoll gradient. The pellet can now be resuspended in PBS with 1M glycine and 2mM EDTA and pipetted for 10 min to remove peritubular cells. Gravity

sedimentation was then used to isolate out Sertoli cells and tubular fragments. Both were plated and cultured in DMEM F12 15% FBS with P/S. Culture media is refreshed every other day. The Sertoli cells are then purified by visual analysis and differential plating. At passage 3 the Sertoli cells were cultured at 35℃ with 10% FBS DMEM12 with 5mL P/S and 5 mL Glutamax supplemented with 1:1000 FSH and 1:2000 EGF.[377] The cells medium is changed every other day.

Culture of SARS-CoV-2 Variants

SARS-CoV-2 variants WA1/2020, BA.1.1.529, BA.4.6, and XBB all were obtained from Dr. Mark Tompkins from the University of Georgia. They were expanded on Vero E6 cells transfected with human ACE2 and TMPRSS2. The culture medium was 10% FBS DMEM.

SARS-CoV-2 infection paradigm

When Sertoli cells reach a high confluency (>90%) they are trypsinized and plated onto transwells at 10^6 cells/cm^2. Upon reaching an acceptable TEER (described below) the infection can begin. Virus stock is serially diluted to an MOI of 0.01 in the culture medium. The Sertoli cell medium is removed and the Sertoli cells are rinsed with 1x PBS twice. The viral dilution is then added so that 100 µL are added to the apical side of each transwell. The basal side does not receive virus. Swirl to disperse the virus then incubate at 35 °C for 15 minutes. After incubation add the overlay and incubate for 6 hours. After 6 hours remove the medium and rinse both the apical and basal layers. Fresh 10% FBS DMEM supplemented with 1:1000 testosterone is added. Continue incubation for 48 hours.

Overlay Medium

Prepare overlay medium by mixing 2.4% Avicel RC-581 with 2x Overlay Medium (1:1) to make a 1.2% Avicel overlay. Size of plaques can be influenced by the Avicel concentration: lower (0.8%) to make plaques larger or higher (1.5%) to make plaques smaller. 1.2% was used. Calculate the amount needed by multiplying the total number of plates by 25mL.

Plaque Assays

50 µL of stock virus and serially diluted virus were used to infect Vero E6 cells transfected with TMPRSS2 and ACE2 on a six well plate seeded with ~ 10^6 cells/well 24 hours before infection. After a 15-minute incubation the overlay is added and left to incubate for 6 hours. Then incubate for 48 hours. Following incubation rinse the plates twice with 1x PBS ensuring Avicel is removed. Immediately fix cells with Methanol:Acetone (80:20) for 10 minutes at room temperature. Plates can be immersed in a bin of Methanol:Acetone (80:20) and carried out of containment for staining in BSL2 labs. Following fixation, remove Methanol:Acetone from wells by dumping on absorbent pads. Allow plates to completely air-dry. Plates are now ready to either be fixed with Crystal Violet Plates can be stored for staining at ambient temperature if needed. Add 1-2 mL Crystal Violet Working Solution to each well and incubate at room temperature for about 10 minutes. Remove crystal violet from each well back and wash residual crystal violet left on each well with DI water. Count clear spots (plaques) on purple background. This allows confirmation of viral presence at appropriate concentrations. Following the 48-hour infection of the Sertoli cells 50 µL of apical

side medium is added to a VERO E6 plate as previously described. This ensures viral infection and viral shedding.

Transepithelial Electrical Resistance (TEER) measurement

The functionality of the blood-testis barrier was assessed by performing transepithelial electrical resistance as previously described.[378] Confluent cultures were trypsinized and seeded at 1 $x10^6$ cells/ cm^2 in the apical (upper) chamber of the 12mm diameter Transwell (Costar, 0.4 µm pore size) coated with Matrigel (Corning). The TEER of the cells was measured daily using an Epithelial Ohmmeter (EVOM, World Precision Instruments, Inc.) in ohms (Ω) x cm^2, with chopstick electrode probes as previously described [366,379]. The plates would be left at room temperature alongside the TEER probe submerged in media for 20 minutes to acclimate. Each well was measured three times in three locations and averaged to provide TEER per well. Following TEER measurement, cells were refed and supplemented with testosterone (Sigma) until the end of the experiment. Upon reaching a daily average TEER of 200Ω (2-3 days), the cells were infected with SARS-CoV-2 variants at an MOI of 0.01 for 6 hours. Following the infection paradigm, the medium was removed, and the cells were rinsed and refed. Then TEER was recorded, and the infection continued for 48 hours. Following the 48 hours TEER measurements were recorded a second time. Student's t-test was performed on JMP between each variant and the control so that p=0.05. To test for outliers the quantiles range and Huber's outlier test were performed in JMP.

Paracellular Flux (Permeability) Assay

After the TEER measurements following infection the NHP and human Sertoli cells were equilibrated with Ringer's solution for 15 minutes at 35°C, then the apical chamber was replaced with Ringers and 50mg/mL Texas Red-labeled dextran (10 kDa; Thermo Fisher) and 2mg/mL Calcein (0.63 kDa; Thermo Fisher) as described.[380] Over two hours, the transwells were moved to new basal chambers every 30 minutes, and 100mL of media was collected from the basal side of the chamber and used for measuring fluorescent intensity. This was incubated at 35°C during the 30 minutes. Fluorescence was measured at wavelengths Ex485/Em525 nanometers for Calcein and Ex585/Em625 nanometers for dextran using a SpectraMax iD5 microplate reader (Molecular Devices). The amount of flux was determined by a standard curve and was graphed as the additive amount of calcein or dextran appearing in the lower chamber of the Transwell plotted versus time. Student's t-test was performed on JMP between each group and the control so that p=0.05. To test for outliers the quantiles range and Huber's outlier test were performed in JMP.

3.9 AUTHOR AFILIATIONS AND CONTRIBUTIONS

We are grateful to Dr. Anthony Chan and his provision of NHP testicular tissue through Emory National Primate Research Center, Dr. Kyle Orwig for his provision of human testis cells through the University of Pittsburgh, and Dr. Stephen Tompkins for his provision of SARS-CoV-2 samples.

1. **Department of Environmental Health Science, College of Public Health, University of Georgia, Athens, GA, USA** R. Clayton Edenfield, Krista M. Symosko, In Ki Cho & Charles A. Easley IV
2. **Regenerative Bioscience Center, University of Georgia, Athens, GA, USA** R. Clayton Edenfield, Krista M. Symosko, In Ki Cho & Charles A. Easley IV

3. **Center for Vaccines and Immunology, Department of Infectious Diseases, College of Veterinary Medicine, University of Georgia, Athens, GA, USA** Cheryl A. Jones, Scott K Johnson, and Stephen M. Tampkins
4. **Division of Pulmonary, Allergy, Critical Care and Sleep Medicine, Department of Medicine and Department of Cell Biology, Emory University School of Medicine, Atlanta, Georgia, USA** Kristen F. Easley & Michael Koval

R.C.E. performed the core experiments and designed the project; K.S.C. and S.B.P. aided in Sertoli cell culture, TEER, Dye Flux, and qRT-PCR; C.A.J. and S.K.J. cultured and quantified SARS-CoV-2 variants and aided in experiments; SMT provided invaluable oversight into virus pathology and experimental design; K.F.E. and M.K. provided invaluable training and oversight for TEER and Dye Flux; I.K.C. aided in Sertoli cell isolation; C.A.E. provided oversight and final approval for the manuscript.

CHAPTER 4

IMPACT OF ALCOHOL USE DISORDER ON THE BLOOD-TESTIS BARRIER[3]

[3] To be submitted to *Scientific Reports*

4.1 ABSTRACT

Alcohol is one of the most used recreational substances, with increasing use since the COVID-19 pandemic. Notably, there are several clinical cases of alcohologenic reversible azoospermia. However, how alcohol affects the blood-testis barrier has yet to be elucidated. Here we provide a novel *in vitro* blood-testis barrier model to investigate the impacts of alcohol on the blood-testis barrier. We show that clinically relevant ethanol concentrations can reversibly alter *in vitro* barrier function, suggesting a non-hormonal mechanism for alcohologenic reversible azoospermia. Employing transepithelial electrical resistance and Dye Flux assays, we show that barrier integrity deteriorates following chronic exposure to 10, 60, and 100mM of ethanol. Furthermore, 48 hours of withdrawal was sufficient to partially restore the formed barrier at 10 and 60mM. We also observed differential gene expression in key Sertoli cell and tight junction genes: *SOX9*, *AR*, *GATA4*, *CLDN3*, *CLDN4*, and *CLDN11*. At 100mM, we observed an increase in cytokines associated with barrier degradation: IL-8, IL-22, and MCP1. Finally, we show that this barrier degradation is likely not caused by cell death. Altogether we provide a model that mimics the blood-testis barrier and its clinical manifestations following chronic alcohol consumption, suggesting a non-hormonal mechanism for alcohologenic reversible azoospermia.

4.2 ALCOHOL USE AND CONSUMPTION

Human consumption of alcohol predates history.[381] Alcohol is a toxic, psychoactive, and addictive drug that is widely accepted and commonly used in

society. Over 2.3 billion adults (≥15) having consumed it in the past year and more than 80% having used it in in their lifetime in high-income countries.[382] The total alcohol consumption in 2016 was 6.4L per person on average. 18.2% of the world population and 26.9% of the United States population participate in heavy episodic drinking (HED), consuming the equivalent of 60g or more of pure alcohol on at least one monthly occasion.[382,383] Furthermore, alcohol abuse is linked to premature death and disability across the globe, with males at a higher risk of 7.1% compared to females at 2.2%. It is also responsible for 10% of all deaths among those aged from 15 to 49.[384] In the United States in 2015, 86.4% of adults reported alcohol consumption, with 56% reporting consumption in the last month.[383] During the COVID-19 pandemic, alcohol consumption increased globally. Stress related to the COVID-19 pandemic was associated with drinking more and more often.[385] Western countries, particularly the US, saw the largest increase in alcohol consumption, with Europe, the US, and Canada reporting a 20% increase in alcohol consumption.[386] In the US, alcohol sales increased by 55% during the opening weeks of pandemic lockdowns. Additionally, there was a 300% increase in alcohol sales by e-commerce. Persistent and excessive alcohol consumption leads to alcohol use disorders (AUDs) and various psychiatric issues, heightens susceptibility to other health ailments such as cancers, and is a teratogen during pregnancy. These consequences pose significant public health challenges, result in substantial economic costs, and exact a considerable human toll.[387]

Alcohol is linked to a diverse range of negative health consequences. In 2016, alcohol use was associated with eight significant disease categories, including both immediate and long-term effects, leading to an annual loss of 133 million disability-adjusted life years.[387] After unintentional injuries alcohol-attributable burden of disease causes gastrointestinal disease, infectious diseases, intentional injuries, cardiovascular diseases and diabetes mellitus, malignant neoplasms, and epilepsy. Alcohol consumption is connected to the occurrence and progression of several infectious diseases, such as lower respiratory infections, HIV/AIDS, other sexually transmitted diseases, and tuberculosis. The primary mechanisms behind these connections involve the impairment of both innate and acquired immune systems, as well as impaired decision-making during intoxication.[388]

4.3 ALCOHOL CONSUMPTION AND MALE FERTILITY

Alcohol consumption is associated with liver, kidney, cardiovascular, and respiratory disease. HED is associated with alcohol poisoning and increased respiratory rate, heart rate, and body temperature, making it a serious health hazard.[382] Alcoholism is associated with liver disease, resulting in hormonal imbalances.[383] Further, 34% of men with alcohol induced advanced liver cirrhosis also displayed testicular atrophy.[389] Chronic alcohol abuse is also associated with altering male fertility. Hormones, seminal output and quality, and testicular structure are all altered by excess alcohol consumption. Testosterone decreases with chronic consumption of alcohol. However, there is contradictory evidence regarding the levels of gonadotropin, follicle-stimulating hormone (FSH),

luteinizing hormone (LH), and estradiol. [383,390] Leydig cell count and morphology are altered,[390] sperm concentration and motility decrease, and there is an increase in abnormal sperm morphology, chromatin condensation defects, and sperm DNA fragmentation.[390,391] Furthermore, in the sperm of chronic alcohol abuse patients, there are changes in RNA, aberrant gene methylation, and alterations in apoptotic proteins.[390] There are also reported health impacts of offspring from paternal alcoholics, including low fetal/birth rate, limited offspring growth, nervous system anomalies, altered reproductive development, increased psychopathologies, heart defects, and incidence of cancer.[390] Autopsy reports have confirmed that in moderate to high alcohol consumption, there are slight alterations in sperm morphology, arrested sperm development, and Sertoli cell-only syndrome.[392]

There have also been several cases of reversible azoospermia in alcohol use disorder (AUD) patients. Brzek, 1987, is the first to observe alcohologenic reversible azoospermia.[393] Sermondade et al. report a patient with azoospermia and a negative testicular biopsy. This was reversible following three months of alcohol withdrawal.[394] Guthauser et al. report a 27-year-old patient with AUD displaying HED and infertility for five years and no history of cryptorchidism, orchitis, testicular torsion, chemotherapy, or radiation therapy. Five sperm analyses were completed from alcohol withdrawal to 20 months later. Six months after withdrawal, normal semen counts, motility, and oligo/asthenozoospermia were observed. Importantly, intracytoplasmic sperm injection was successfully carried out and pregnancy was achieved following alcohol cessation.[395] Vicari et

al. also show reversible azoospermia, and 3 months following alcohol withdrawal, pregnancy was achieved.[396] While HED patients are observed to have low fertility[397], low to moderate amounts of alcohol do not appear to affect male fecundity.[397-401]

While there is evidence that alcohol consumption can impact the testis and male fertility, little has been done to address its impact on the blood-testis barrier or provide a possible mechanism for alcoholgenic reversible azoospermia. Sertoli cells are critical for male fertility.[402] They provide nutrients and support to differentiating germ cells and comprise the blood-testis barrier (BTB). BTB integrity is necessary to protect sperm. Additionally, Sertoli cells create an immunoprivileged environment in the testes protecting immunogenic germ cells from immune system intrusion.[403] Furthermore, the immunoprivileged environment allows for a local innate immunity protecting from microbial infections. Testicular cytokines are instrumental in inter-compartmental intercellular communication, regulation of steroidogenesis, and immunoregulation.[404] Alterations in levels of cytokines, such as MCP-1 and IL-8, can modify male fertility.[404-406] Destruction or dysfunction of the BTB leads to various negative outcomes in male fertility.[41]

Sertoli cells are shown to be negatively impacted by alcohol. Zhu et al. show that in vivo and in vitro rat Sertoli cells are biochemically affected by alcohol. They exposed the cells to up to 200mM of ethanol for 48 hours, observing changes in constituent and secreted proteins.[407] Studies have also shown that ethanol is toxic to Sertoli cells at 500mM and that in mice,

consumption of alcoholic beverages can reduce Sertoli cell count.[408,409] One unpublished study has shown alcohol may impact the rat blood-testis barrier by showing an increase in the influx of Gd-PTDM MRI contrast agent across the BTB in response to alcohol consumption.[410] Alongside evidence that alcohol impacts Sertoli cells and the BTB, there is also evidence that alcohol impacts other blood barriers in the body. Wood et al. show that long-term alcohol exposure weakens tight junctions while not affecting adherens junctions in epithelial cells in a way reversible after cessation.[411] Schlingman et al. also show tight junction changes in response to chronic alcohol use.[412] Additionally, Wei et al. show that long-term alcohol consumption can damage the blood-brain barrier altering barrier-forming proteins, increasing inflammatory factors, and causing cognitive dysfunction.[413] Therefore, here we hypothesized that clinically relevant levels of alcohol are sufficient to cause blood-testis barrier degradation.

To assess the impacts of alcohol on the blood-testis barrier, we created the first *in vitro* nonhuman primate BTB model using *Rhesus macaque* Sertoli cells, which were then exposed to clinically relevant levels of alcohol. Concentrations of 10, 60, and 100 mM of ethanol were used, equivalent to a range of mild inebriation to requiring hospitalization.[414-416] We used transepithelial electrical resistance (TEER) and Dye Flux assays to evaluate the integrity of the in *vitro* formed barrier. To assess if alterations in tight junction proteins caused any changes, we performed qRT-PCR on claudins 3, 4, and 11 in addition to SOX9, GATA4, and AR. Additionally, we performed an Annexin V assay to indicate Sertoli cell health. Finally, a cytokine panel was performed to determine

any signs of inflammation. This is the first description of nonhormonal alcohol induced blood-testis barrier degradation as well as providing a possible mechanism for alcohologenic reversible azoospermia.

4.4 RESULTS: SERTOLI CELL ISOLATION AND CULTURE

Because other experiments have shown an indirect or hormone-dependent mechanism of the effects of alcohol on the BTB, we aimed to test Sertoli cells and BTB directly. To do this we isolated Sertoli cells from adult *Rhesus macaques* tissue as described. [366] Following tissue mincing the cells were isolated using a Percoll gradient and plated. Purification continued by differential plating and visual analysis (Figure 1 A). Sertoli cell identity was confirmed by immunostaining for GATA4, Sox9, and WT1 on adult nhp testis and isolated cells (Figure 1 B, C). After culturing to a high confluency (over 95%), the cells were plated onto transwells for the experiments. The Sertoli cells were plated at a high density of 10^6 cells/cm^2 to encourage barrier formation. Testosterone was added to aid in barrier formation and help the barrier last for at least 10 days [367]. Once the barrier reached a TEER of 200 Ohm x cm^2 we began performing experiments.

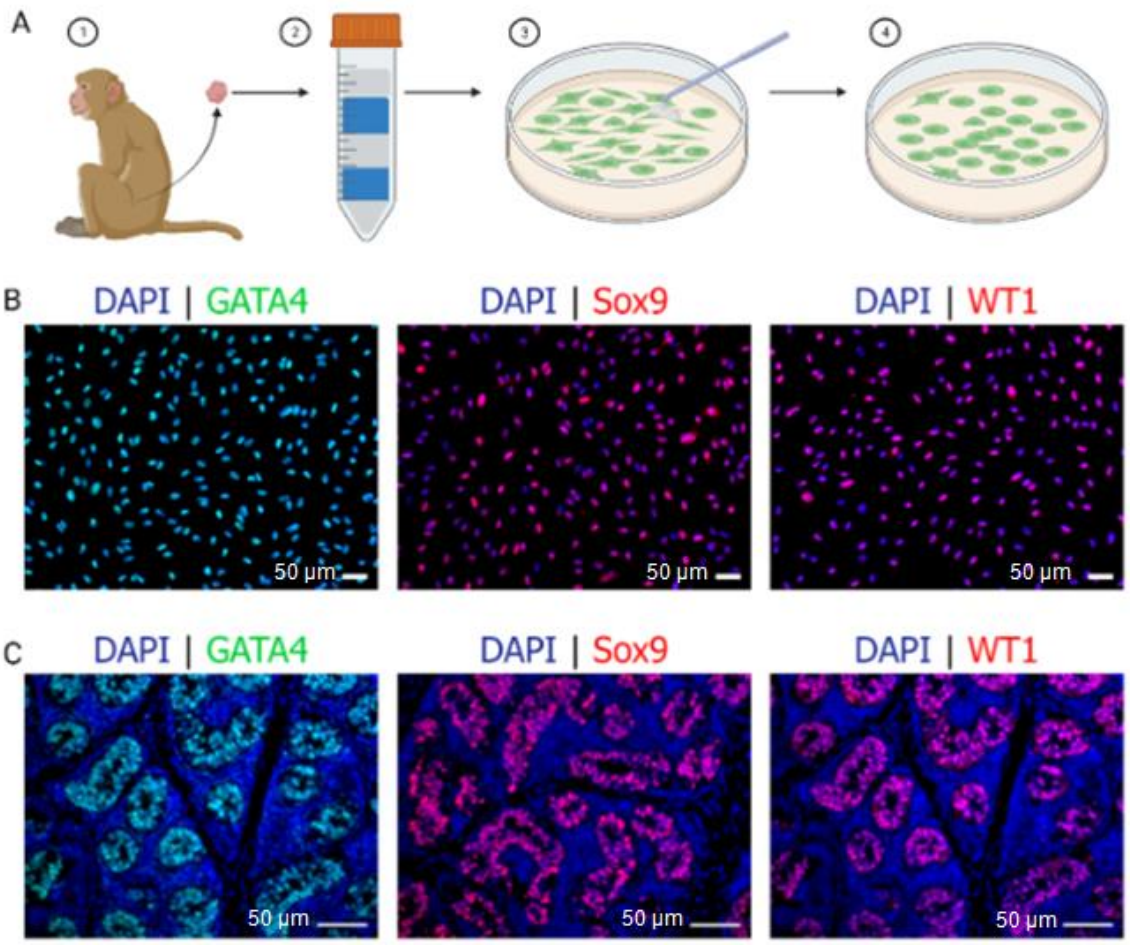
A
1
2
3
4
B
DAPI | GATA4
DAPI | Sox9
DAPI | WT1
50 µm
50 µm
50 µm
C
DAPI | GATA4
DAPI | Sox9
DAPI | WT1
50 µm
50 µm
50 µm

Figure 4.1: Sertoli cell isolation confirmation by imaging

Image A describes how we isolated and purified Sertoli cells. We choose to isolate Sertoli cells from *Rhesus macaque* because human cells can be hard to obtain, and immortalized cells are not always reliable as a model. Following tissue digestion, gravity sedimentation, and Percoll separation cells were differentially plated and cells that did not have Sertoli-like morphology were scraped from the plate. This was done until the cell population appeared 95% pure. We immunostained the remaining cell population with Sertoli cell markers, GATA4, WT1, and Sox9 to ensure successful Sertoli cell isolation. Image B shows these cells. Image C shows these markers on immunostained monkey testis tissue. We show similar expression of GATA4, Sox9, and WT1 between the isolated Sertoli cells and those still in tissue.

4.5 RESULTS: ALCOHOL CAUSES BLOOD-TESTIS BARRIER BREAKDOWN

Because of the known degradative effect that alcohol has on other barriers, like those in the lungs [417], intestines [418], and brain [413] alongside what is known about its impact on the testis, we hypothesized that alcohol will have similar degradative effects on the BTB. To test this, we created an *in vitro* BTB from primary nhp Sertoli cells. We then exposed the barrier to clinically relevant levels of alcohol to assess what direct effects it may have on BTB integrity. Finally, to recreate the observed clinical manifestations of alcohologenic reversible azoospermia we exposed the cells to alcohol chronically for 3 or 8 days and then allowed them 48 hours to recover. To measure barrier integrity, we performed TEER and Dye Flux, two assays that are regularly used [379,380].

TER measures electrical resistance of a barrier between two nodes of a voltmeter probe. We describe a dose-dependent reduction in TEER in response to 10, 60, and 100mM of ethanol over 10 days (Figure 2 A). Additionally, we allowed some formed barriers to recover for 48 hours without any treatment. We observed an increase in TEER in these recovery samples at the 48-hour mark. Importantly, this recovery was only observed to a significant extent in the 10 and 60mM treated groups (Figure 2 B). In the 100mM group, a significant increase in TEER was not observed; however, there was an upward trend after 48 hours. These data indicate that ethanol can reversibly harm the formed blood-testis barrier.

Dye Flux measures how much dye can pass through the formed barrier over a 2-hour time course. Here we show that both calcein and dextran pass through the barrier at a higher concentration in our treated cells when compared to the control. On day 5, dextran is significant at 10, 60, and 100mM, (Figure 3 C) and Calcein is significant at 60 and 100mM (Figure 3 A). Interestingly, by day 10, this effect plateaus, with only 100mM being significantly different in dextran and Calcein (Figure 3 B & D). This mimics clinical observations of lower alcohol consumption exhibiting fewer testicular manifestations. The recovery groups showed no significant differences (Figure 3 E-H) except for dextran at 100mM on day 5 (Figure 3 G). Notably, there was also a decrease in Calcein on day 5 at 60mM in the recovery group (Figure 3 E). These data support the TEER data showing that ethanol at high concentrations can negatively impact the formed barrier and that 48 hours of ethanol withdrawal will allow the barrier to recover.

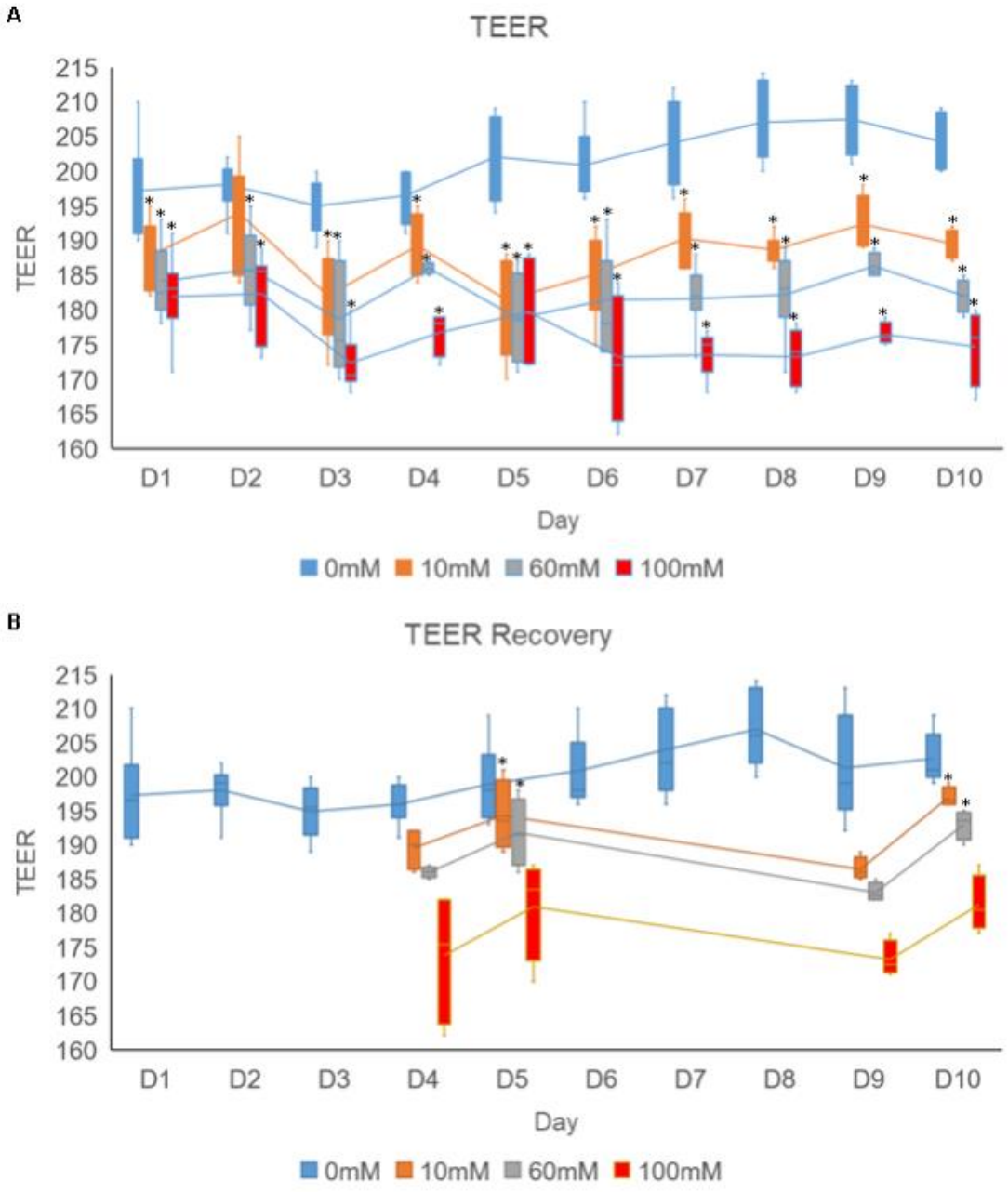
A
TEER
TEER
215
210
205
200
195
190
185
180
175
170
165
160
D1
D2
D3
D4
D5
D6
D7
D8
D9
D10
Day
0mM
10mM
60mM
100mM
B
TEER Recovery
TEER
215
210
205
200
195
190
185
180
175
170
165
160
D1
D2
D3
D4
D5
D6
D7
D8
D9
D10
Day
0mM
10mM
60mM
100mM

Figure 4.2: Barrier integrity and recovery assessed by Transepithelial Electrical Resistance

Image A (top) shows TEER decrease in response to EtOH. Significance was determined by a student's t-test so that $P<0.05$ and is shown as *. The control for each day was used to determine differences between the dosed populations for their respective day. Importantly, almost all doses are significantly lower than the control for their respective day. Image B shows each 24 hours of recovery. TEER was measured on days 4, 5, 9, and 10 to determine how effective recovery was. Significance was determined by a student's t-test so that $P<0.05$ and is shown as *. However, in this case, the control is the continuously dosed population within its respective day and dose. We observe that the 10mM and 60mM groups have a significantly higher TEER than the continuously dosed groups on days 5 and 10. To confirm this we also determined that there was no significant difference in these groups and the true control pictured above in blue. Only day 2 at the lowest dose was not significant. However, higher doses and durations appear to require longer recovery times. Overall, we show that alcohol has a profound effect on the blood-testis barrier that increases with concentration and time. Furthermore, these effects can be ameliorated by allowing alcohol withdrawal.

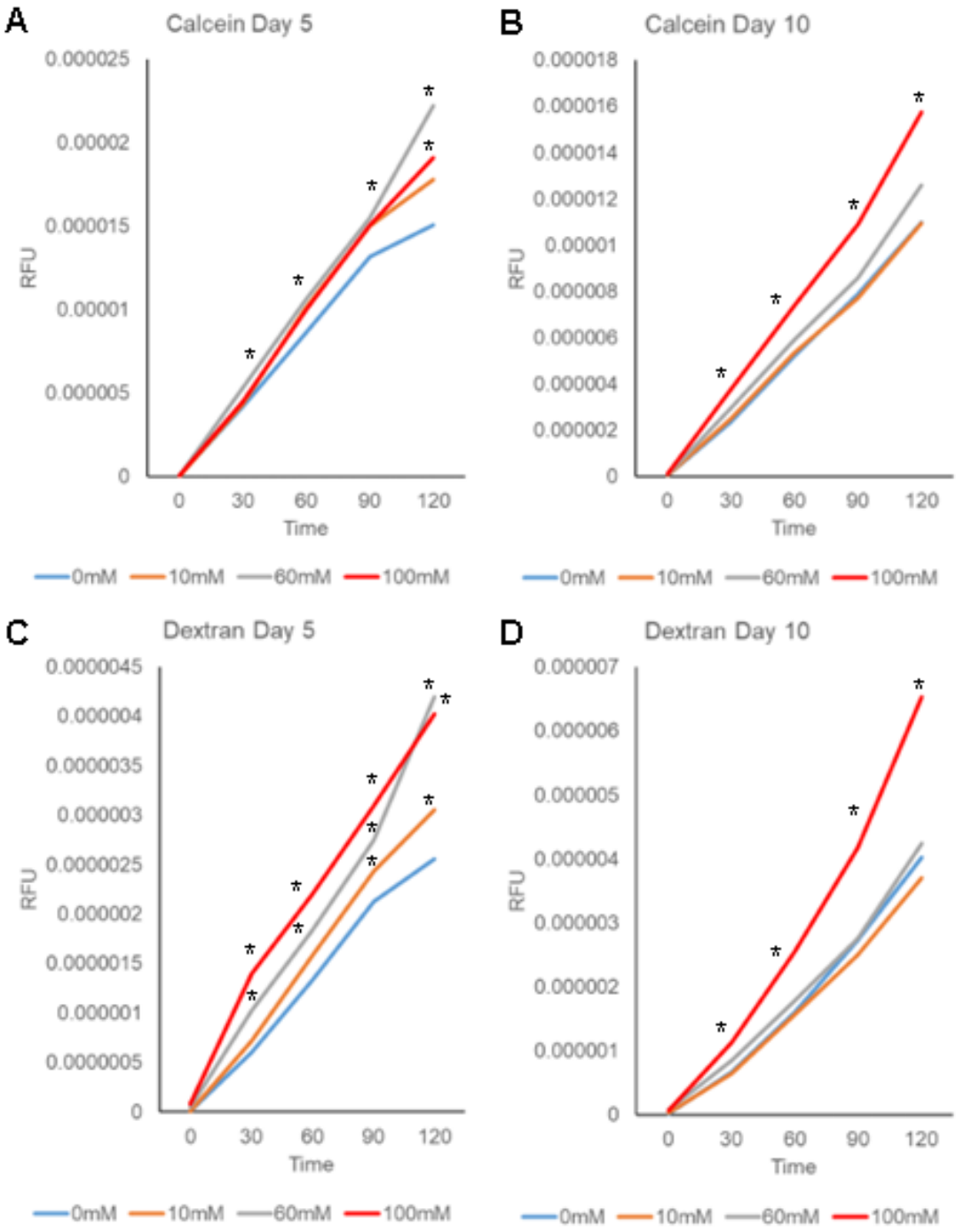
A
Calcein Day 5
RFU
0.000025
0.00002
0.000015
0.00001
0.000005
0
0 30 60 90 120
Time
0mM 10mM 60mM 100mM
B
Calcein Day 10
RFU
0.000018
0.000016
0.000014
0.000012
0.00001
0.000008
0.000006
0.000004
0.000002
0
0 30 60 90 120
Time
0mM 10mM 60mM 100mM
C
Dextran Day 5
RFU
0.0000045
0.000004
0.0000035
0.000003
0.0000025
0.000002
0.0000015
0.000001
0.0000005
0
0 30 60 90 120
Time
0mM 10mM 60mM 100mM
D
Dextran Day 10
RFU
0.000007
0.000006
0.000005
0.000004
0.000003
0.000002
0.000001
0
0 30 60 90 120
Time
0mM 10mM 60mM 100mM

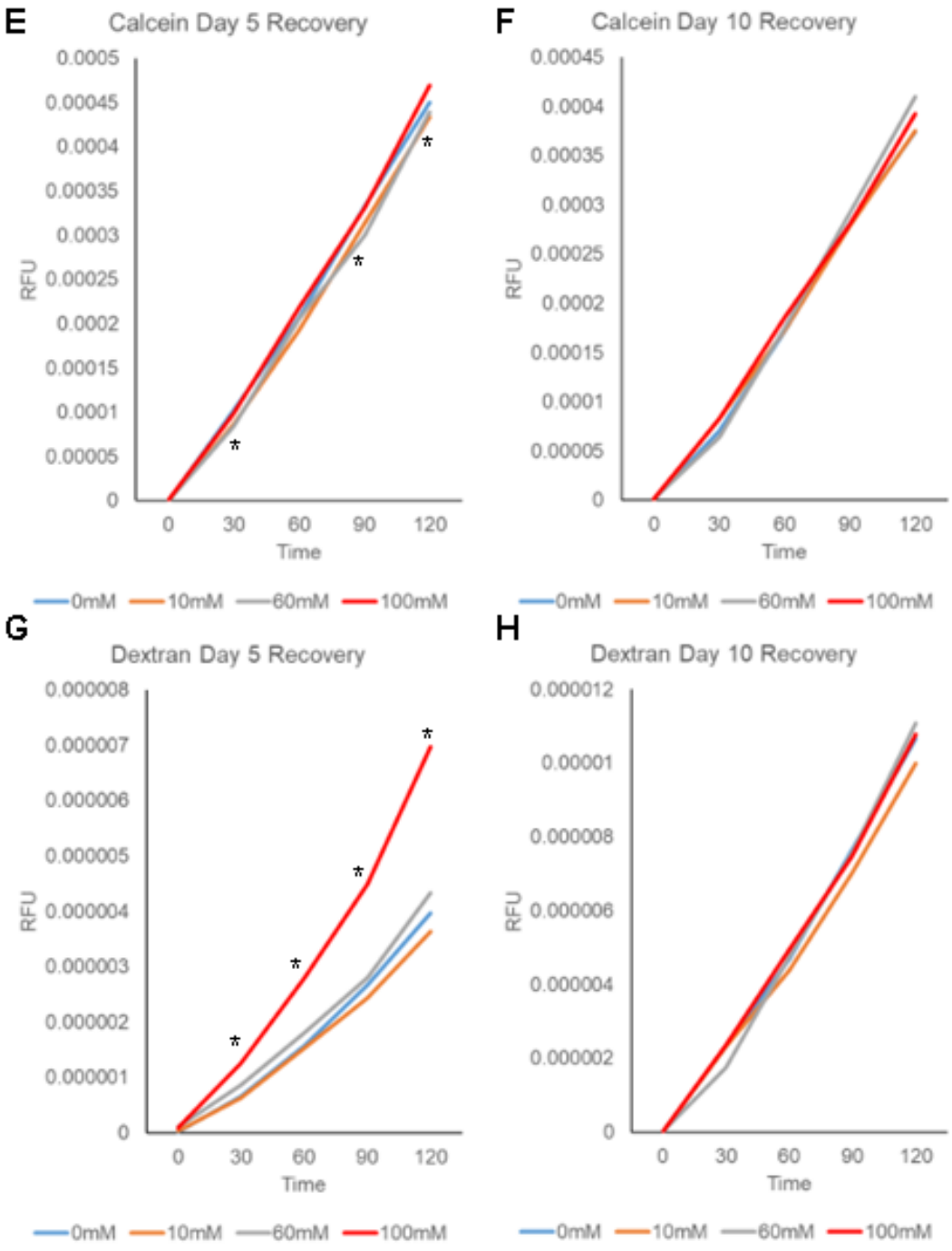
E
Calcein Day 5 Recovery
RFU
Time
0mM
10mM
60mM
100mM
F
Calcein Day 10 Recovery
RFU
Time
0mM
10mM
60mM
100mM
G
Dextran Day 5 Recovery
RFU
Time
0mM
10mM
60mM
100mM
H
Dextran Day 10 Recovery
RFU
Time
0mM
10mM
60mM
100mM

Figure 4.3: Barrier integrity assessed by Dye Flux

Images A and B show the flow of Calcein through the barrier increase over the course of ten days in response to alcohol dosing. 100mM EtOH is significantly higher than the control on both days 5 and 10 and 60mM is higher than the control on day 5. Images C and D show the flow of Dextran through the barrier on days 5 and 10. Again the highest dose is significantly higher than the control on both days. Additionally, on day 5 60mM and 10mM also show a significantly higher flow through of Dextran than the control. In short, high levels of alcohol can impact the formed barrier allowing small molecules to pass through. Intriguingly, the acute dose appears to have a larger impact than the chronic one; however, the chronic 100mM dose will allow close to twice as much dye through. Images E-H show dye pass-through following 48 hours of recovery. Image G shows the only case where Dextran or Calcein flow through the barrier was significantly higher than the control; this is where Dextran is significantly higher at all time points. Interestingly, at day 5 Calcein flows through the barrier the least in the group treated with 60mM EtOH. Overall, these data show that a recovery time of 48 hours is sufficient to restore barrier integrity regarding small molecules passing through at 10 and 60mM. Significance was determined by a student's t-test so that $P<0.05$ and is shown as *.

4.6 ALCOHOL INDUCES GENE EXPRESSION CHANGES IN SERTOLI CELLS

The BTB is made up of multiple different junctional proteins that work together to build a unique barrier. This barrier is very tight yet dynamic in nature to allow the migration of spermatogonia into the lumen. Several sources led us to suspect that alcohol could be altering tight junctions [411-413]. To observe changes in the expression of genes related to tight junction formation, we performed qRT-PCR and measured genes important for BTB (CLDN3, CLDN4, and (CLDN11) and Sertoli cell function [419,420] (*Sox9*, *AR*, and *GATA4*). Because Sertoli cells are critical for nursing developing spermatogonia as well as maintaining the BTB we wanted to assess common Sertoli cell markers to assess their health. *Sox9* is vital during Sertoli cell differentiation, however its role in the adult testis is not understood. Strikingly, *Sox9* is upregulated in patients with impaired spermatogenesis [421].

At day 5, *CLDN3* and *CLDN4* were upregulated in treated cells compared to controls (Figure 4 A), and the recovery samples were significantly lower at 10 and 60mM (Figure 4 B) however, they are lower than the control. On day 10 there is a similar trend in *CLDN3* and *CLDN4* in both the treated and recovery groups (Figure 4 C and D); however, there is a difference at 60mM. *CLDN11* is expressed much more similarly to the control, even at 100mM. Interestingly, the recovery samples express lower *CLDN11* at 10 and 60mM on days 5 and 10 (Figure 4 B and D), and there is no difference in *CLDN11* between treated and recovered samples at 100mM on days 5 or 10.

At day 5, *AR* is only different between the treated and recovered samples at 10mM (Figure 4 A and B), in which the treated is upregulated compared to the control. At 60 and 100mM on day 5, the treated and recovered samples are similar to the control. However, by day 10, the recovered samples were all significantly lower than the treated cells and were more similar to the control (Figure 4 C and D).

At day 5, *GATA4* was upregulated in the treated groups at 10, 60, and 100mM and in the recovered groups at 60 and 100mM (Figure 4 A and C). Significantly, the recovered samples at the lowest dose are the closest to the control on day 5. This trend continues for *Sox9*.

At day 5, *Sox9* is also upregulated in the treated groups at all doses and in the recovered groups at 60 and 100mM (Figure 4 A B). By day 10, *GATA4* expression is like the control in both groups except for the 10 and 60mM recovery (Figure 4 C and D). Notably, GATA4 expression is significantly lower in the recovery group at 60mM. *Sox9* at day 10 has all groups upregulated except for 60mM recovery (Figure 4 C and D), which is much lower and most like the control.

Because of the unique nature of the BTB being characterized as a tight but dynamic barrier any changes to the integrity of the barrier could have significant impacts on male fertility. If the barrier becomes too strong then cell migration of spermatogonia may not be possible alternatively if the barrier cannot be maintained, then immune and xenobiotic/toxicant intrusion may occur both of which would be detrimental[422,423]. Broadly, alcohol appears to cause CLDN3, 4,

and 11 gene expression to increase. Importantly, an increase in CLDN11 expression has been associated with decreased spermatogenesis, including in hypospermatogenesis, spermatocytic and maturation arrest, and Sertoli cell only (SCO) testes [424] all common symptoms in AUD patients.

We show that chronic EtOH treatment increases expression of *Sox9* and that after 8 days, 48 hours of recovery is insufficient to return *Sox9* levels to normal. However, recovery is possible following 3 days of treatment. Androgen receptor (AR) is vital for Sertoli cell maturation and function[425,426]. Generally, *AR* will increase in Sertoli cells in a testosterone free environment before puberty. Additionally, *AR* inhibition is linked to an increase in BTB permeability. Following 10 days of chronic EtOH exposure we observe an increase in AR. However, 48 hours is enough to bring the expression levels close to control. *GATA4* is also important for Sertoli cell and testicular development and function and without it Sertoli cell dysfunction and metabolic defects, impaired fertility, and BTB breakdown will occur [427,428].However, *GATA4* appears to be largely unchanged by ethanol.

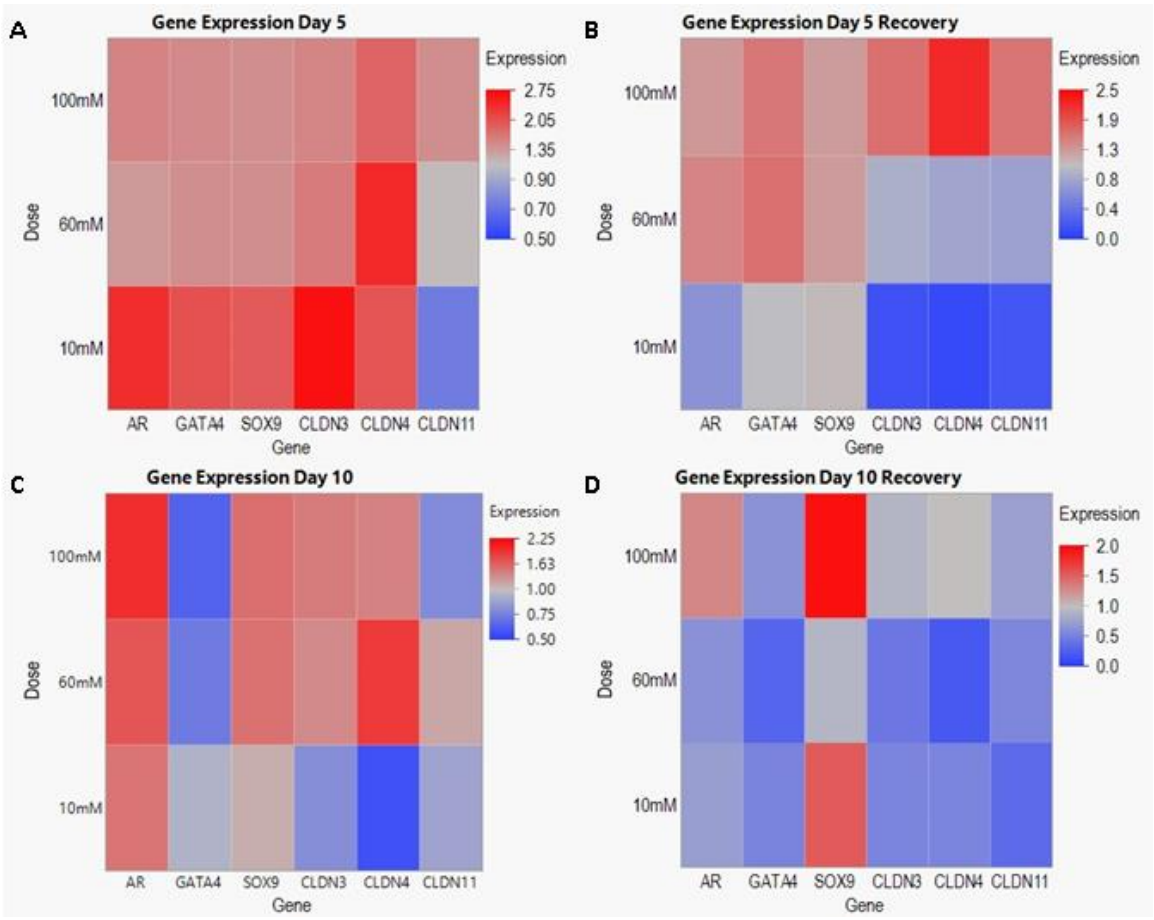
A
Gene Expression Day 5
Expression
2.75
2.05
1.35
0.90
0.70
0.50
Dose
100mM
60mM
10mM
AR
GATA4
SOX9
CLDN3
CLDN4
CLDN11
Gene
B
Gene Expression Day 5 Recovery
Expression
2.5
1.9
1.3
0.8
0.4
0.0
Dose
100mM
60mM
10mM
AR
GATA4
SOX9
CLDN3
CLDN4
CLDN11
Gene
C
Gene Expression Day 10
Expression
2.25
1.63
1.00
0.75
0.50
Dose
100mM
60mM
10mM
AR
GATA4
SOX9
CLDN3
CLDN4
CLDN11
Gene
D
Gene Expression Day 10 Recovery
Expression
2.0
1.5
1.0
0.5
0.0
Dose
100mM
60mM
10mM
AR
GATA4
SOX9
CLDN3
CLDN4
CLDN11
Gene

Figure 4.4: Using quantitative real-time Polymerase Chain Reaction to assess gene expression associated with blood-testis barrier function

qRT-PCR is used to show gene expression of Sertoli cell markers AR, GATA4, and SOX9 and claudins 3, 4, and 11. 3 and 11 are notably important for the formation of the BTB as they guide differentiating gametes into the lumen. All gene expressions are normalized to GAPDH, and the results are normalized to the control. Most genes are upregulated in response to dosing. His upregulation may be in response to barrier degradation. Images A and B show day five and C and D show day 10. Images B and D show the recovery samples. The recovery is noticeably lower, and we show several differences between the recovered and non-recovered cells. Particularly on day 5 at 10mM and day 10 at 60mM. Following recovery, gene expression of claudins in the groups exposed to 60 and 100mM EtOH remain high while the 10mM group is low on both days 5 and 10.

4.7 CLINICALLY RELEVANT DOSES OF ALCOHOL DISRUPT THE BTB WITHOUT CAUSING CELL DEATH

High concentrations of alcohol are shown to be toxic to Sertoli cells and reduce their count [408,409]. We wanted to ensure that the concentrations chosen would not cause Sertoli cell death.

We performed the Annexin V assay to determine if the observed negative impact on the formed BTB was from Sertoli cell death and degradation. Annexin V showed no changes in dead cells after 10 days of treatment (Figure 7). However, there are some changes in apoptotic stages. While there is no increase in dead cells there is a decrease in the number of live cells. This appears to be because of an increase in early-stage apoptotic cells. Early stage apoptotic cells are characterized in this protocol by being Annexin V positive and 7-ADD negative. Annexin V binds to phosphatidylserine (PS) and 7-AAD binds to the DNA. Alcohol induced stress may lead to the exposure of PS on the outer surface of the cell membrane allowing Annexin V binding. However, the barrier is not disrupted to the point of allowing 7-AAD to bind to the DNA.

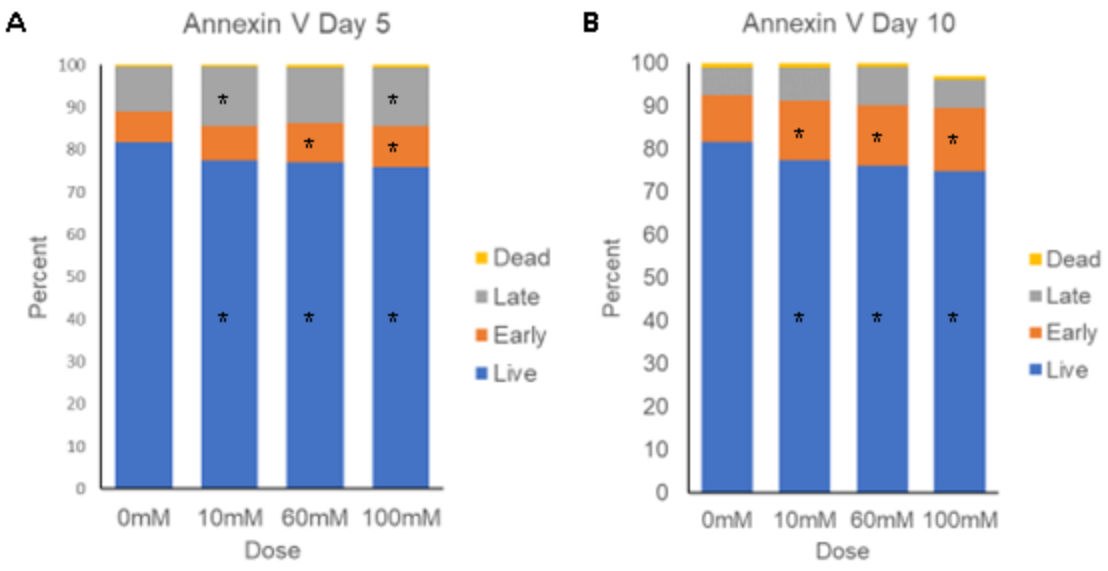
A
Annexin V Day 5
Percent
Dose
0mM
10mM
60mM
100mM
Dead
Late
Early
Live
B
Annexin V Day 10
Percent
Dose
0mM
10mM
60mM
100mM
Dead
Late
Early
Live

Figure 4.5: Using Annexin V to determine cell health

The Annexin V assay is used to determine if alcohol's impact on barrier integrity is caused by the death of cells. There is no significant difference in dead cells; however, there are differences in the early and late apoptotic and live cells. Significance is determined by the student's t-test so that $p<0.05$ and is shown as *. 10mM appears to have the least effect and 100mM the most, as expected. Interestingly, by day 10 there is no significant difference between late apoptotic cells, only early. While each dose has a significantly lower live population for both days this is best explained by some cells moving towards apoptosis. However, as there is no significant difference in dead cells this may just be evidence that the cells are somewhat unhealthy but not dying. Overall, the cells appear healthy enough to assess barrier integrity.

4.8 CYTOKINES ARE ALTERED IN RESPONSE TO ALCOHOL

Sertoli cells provide the testis with an immune privileged microenvironment by building and maintaining the blood-testis barrier and modulating the innate and adaptive immune processes through the production of immunoregulatory compounds [429]. While we have shown that alcohol is directly causing BTB breakdown, thereby altering the immunological microenvironment, we wanted to observe if there were any alterations to the immunoregulatory secretions of Sertoli cells.

We performed a cytokine panel to detect if any cytokines that may impact barrier integrity or cause immune dysregulation were released during treatment. We observed a significant increase ($p<0.05$) in IL-8 and MCP-1 at day 5 between 100mM and the control (Figure 8). While not significant ($p=0.051$), IL-22 trended higher in the 100mM group. Eotaxin, GM-CSF, IP-10, M-CSF, and MIP-1a are largely unaffected by EtOH treatment in our model. After 10 days of treatment, no significant changes existed in any of the observed cytokines.

Under normal conditions IL-8 is not highly expressed by Sertoli cells. However, it is observed during chronic inflammatory conditions caused by Zika infection in a similar model [430]. IL-8 is an inflammatory cytokine that is upregulated by complement systems [431]. Furthermore, it has been shown that alcohol consumption can activate these complement systems [432]. MCP-1 is an inflammatory chemokine [433] that has been shown to increase in response to the Sertoli cell toxicant mono-(2-ethylhexyl) phthalate, altering the immune microenvironment [434]. It is also observed during chronic inflammatory conditions

caused by Zika infection [430]. Alcohol consumption also causes an increase in MCP-1 in the brain playing a role in the neurotoxic effects of alcohol [435]. Furthermore, MCP-1 and IL-8 have both been associated with a decrease in overall health in AUD patients [436]. We showed that in addition to the destruction of the physical immunological microenvironment alcohol also alters the immunoregulatory secretions of Sertoli cells.

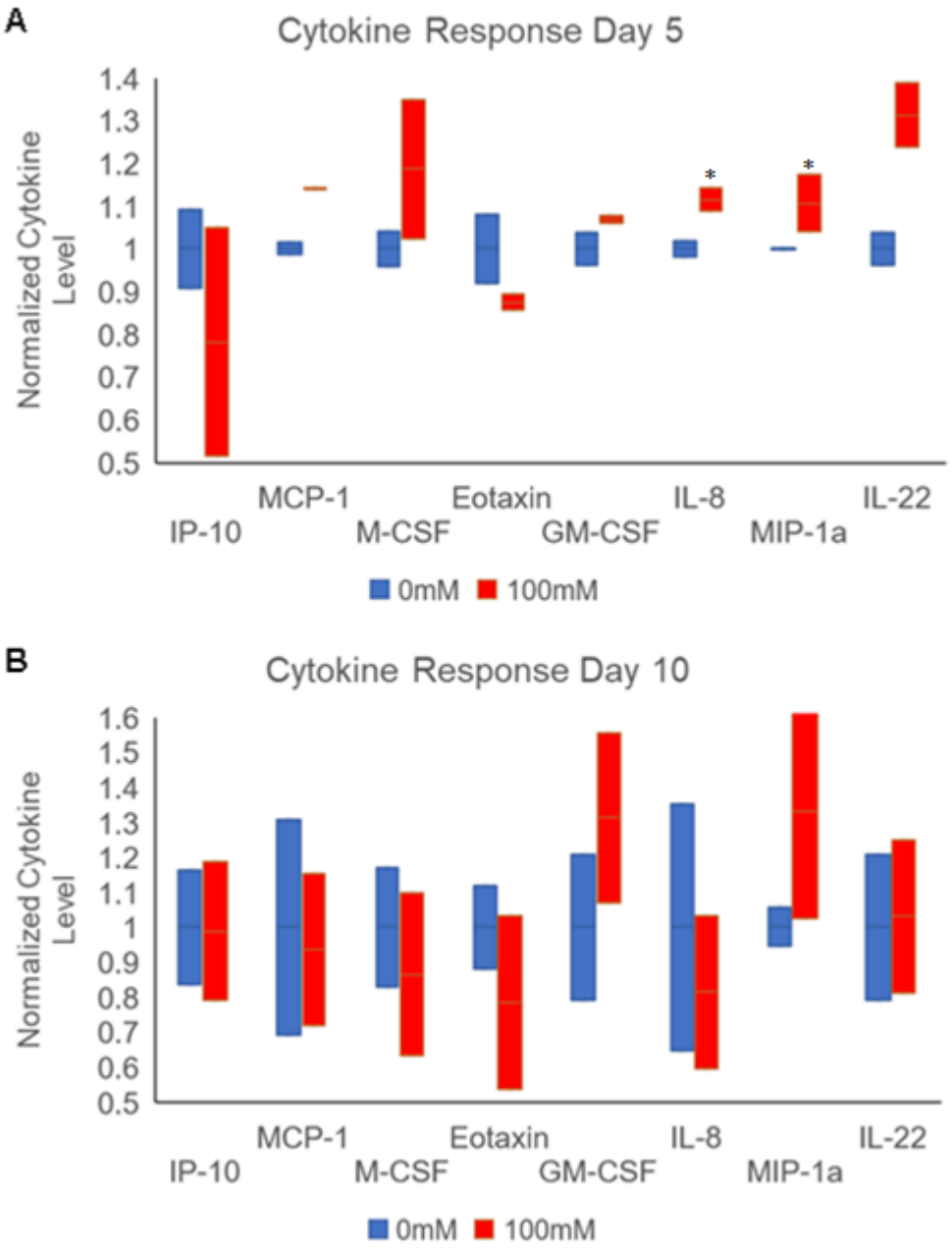
A
Cytokine Response Day 5
Normalized Cytokine Level
1.4
1.3
1.2
1.1
1
0.9
0.8
0.7
0.6
0.5
*
*
IP-10
MCP-1
M-CSF
Eotaxin
GM-CSF
IL-8
MIP-1a
IL-22
0mM
100mM
B
Cytokine Response Day 10
Normalized Cytokine Level
1.6
1.5
1.4
1.3
1.2
1.1
1
0.9
0.8
0.7
0.6
0.5
IP-10
MCP-1
M-CSF
Eotaxin
GM-CSF
IL-8
MIP-1a
IL-22
0mM
100mM

Figure 4.6: Using a cytokine panel to determine any possible changes in immune function

A cytokine panel showed that IL-8 (P=0.0435) and MCP-1a (P=0.0283) were significantly altered in response to 100µM EtOH. IL-22 (P=.051) also showed some change. Significance was determined by a two-sample t-test and is shown as *. Results were normalized to the control mean for graphing. On day 5 all cytokines except IP-10 and Eotaxin appear to increase. However, by day 10 they are much closer to control but GM-CSF and MIP-1a remain elevated. This immunomodulation may be partially responsible for immune intrusion and reported reversible azoospermia and Sertoli cell-only syndrome in heavy drinkers.

4.9 DISCUSSION

This study shows that clinically relevant ethanol doses can negatively and reversibly impact the blood-testis barrier *in vitro*. These findings are compatible with clinical reports of alcoholgenic reversible azoospermia. Because of the increase in drinking and binge drinking in Western countries, especially the US, it is essential to elucidate what effects excessive drinking may have on male fertility, particularly as this may contribute to the worldwide decline in sperm count. To test this, we formed an *in vitro* blood-testis barrier from nhp Sertoli cells. *Rhesus macaque* is a well-established animal model most like humans. However, as toxicology assays move away from animal models, it will be essential to establish translational *in vitro* models to aid in determining when it may be necessary to use a whole organism. Additionally, human primary Sertoli cells are much more challenging to obtain and maintain. This unique model system allows us to bridge these gaps.

Upon formation, these *in vitro* barriers were exposed to clinically relevant levels of EtOH for extended periods. Half of them were allowed to recover for 48 hours to model alcohol withdrawal in humans. These barriers significantly recovered compared to those that received a continuous dose. This mimics the clinical manifestation of alcohologenic reversible azoospermia. While this has been documented for decades, its mechanism is not well elucidated. Here we show for the first time that alcohol can non-hormonally damage the BTB. This is confirmed by TEER and Dye Flux assays. Furthermore, this damage occurs

without killing large populations of Sertoli cells as confirmed by the Annexin V assay.

Additionally, we point to mechanisms that this damage may occur through alterations in junctional barriers. We used qRT-PCR to show changes in gene expression in our formed barriers in response to alcohol and withdrawal from it. We observed an increase in CLDN3, 4, and 11 expression in response to alcohol exposure. Notably, an increase in CLDN11 has been associated with symptoms similar to alcohologenic azoospermia. Unfortunately, claudin localization could not be determined due to a lack of immunocytochemistry primary antibodies that specifically react with *Rhesus macaque* claudins. However, other relevant *Rhesus macaque* proteins can be immunolocalized such as *Sox9*.

In addition to changes in gene expression, we observed changes in cytokine levels. We saw significant changes in cytokines associated with barrier breakdown and tight junction alterations particularly IL-8 and MCP-1. These cytokines work in tandem with the physical BTB to form the immune privilege of the testes. If either are harmed, then male fertility may be at risk. Together these data support our hypothesis that blood-testis barrier breakdown and recovery may be a critical etiology in alcohologenic reversible azoospermia.

Alcohol is widely used. It has several impacts throughout the body and causes alcohologenic reversible azoospermia; however, the etiology of this syndrome still needs to be fully elucidated. Using a novel *in vitro* BTB model, we showed that ethanol can nonhormonally and reversibly damage the BTB. TEER and Dye Flux assays show barrier integrity deterioration following exposure to

10, 60, and 100mM of ethanol. Allowing 48 hours of withdrawal caused partial restoration of the formed barrier at 10 and 60mM. Key Sertoli cell genes *SOX9*, *AR*, and *GATA4* and tight junction genes *CLDN3*, *CLDN4*, and *CLDN11* expression changed in response to alcohol and withdrawal. At 100mM, cytokines associated with barrier degradation increased: IL-8. IL-22, and MCP1. Finally, Annexin V show that barrier degradation is not caused by cell death but by changes in the formed barrier. This data also indicates immunological changes that put male fertility at risk. Altogether we present a model that mimics the blood-testis barrier and its clinical manifestations and suggest a possible etiology for alcohologenic reversible azoospermia.

4.10 METHODS

Sertoli Cell Isolation and Culture

All procedures were approved by the Emory University Institutional Animal Care and Use Committee and were performed in accordance with the Animal Welfare Act and the US Department of Health and Human Services "Guide for the Care and Use of Laboratory Animals" (National Research Council, 2011). The Emory National Primate Research Center is fully accredited by the Association for Assessment and Accreditation of Laboratory Animal Care (AAALAC) International. Testicular biopsies were obtained from Rhesus macaques from Dr. Chan, previously at the Emory National Primate Research Center were sectioned as previously described.[366] The biopsies were stored in liquid nitrogen until needed. Following thaw, the tissue was briefly minced further, and the germ cells were separated out by gravity sedimentation while in 80mL of HBSS and P/S.

Then the remaining pellet undergoes an enzyme digestion while being shaken at 300 rpm at 37C for 15 minutes. Digestion media contains 80mL HBSS with P/S, 10 mL trypsin (2.5%), 10 mL collagenase type IV (1%), and 2 mL DNase (1 mg/mL). The digested solution was then passed through a metal sieve to remove any undigested or connective tissue. 0.1% soybean trypsin inhibitor was then added to halt digestion. The solution was then centrifuged at 200g for 5 min, the supernatant was discarded, and DMEM F12 with P/S was added in a 10:1 volume ratio. The solution then rests at room temp for 30 minutes. The pellet is enriched for tubular fragments cells and the supernatant for interstitial cells. The interstitial cells are removed and stored in liquid nitrogen. The pellet can now be resuspended in PBS with 1M glycine and 2mM EDTA and pipetted for 10 min to remove peritubular cells. Gravity sedimentation was then used to isolate out Sertoli cells and tubular fragments. Both were plated and cultured in DMEM F12 15% FBS with P/S. Culture media is refreshed every other day. The Sertoli cells are then purified by visual analysis and differential plating. At passage 3 the Sertoli cells were cultured at 35℃ with 10% FBS DMEM with P/S.

Immunostaining

Sertoli cells were cultured on coverslips in 6-well plates, with DMEM + 10% FBS medium changed every other day. Once they reached a good confluency (over 90%), cells were fixed with 2% PFA for 20 minutes, washed with PBS and stored at 4°C until staining was performed. Permeabilization was carried out using 0.2% Triton X (Millipore, # 9410-OP) in PBS for 10 minutes at room temperature. After two washes with PBS for 5 minutes each, non-specific binding of antibodies was

blocked using CAS-block (Thermo Fisher Scientific, # 008120) for 15 minutes at room temperature. Cells were then incubated overnight with the following primary antibodies diluted in PBS with 10% CAS Block: mouse anti-human GATA4 at 1:200 (Santa Cruz Biotechnology, # sc-25310), rabbit anti-human WT1 at 1:100 (Santa Cruz Biotechnology, # sc-192), rabbit anti-human Sox9 at 1:250 (Millipore Sigma, # AB5535). On the next day, the coverslips were washed three times with PBS containing 0.05% Tween 20 (Bio-Rad, # 170-6531) and incubated with appropriate secondary antibodies donkey-anti-mouse IgG Alexa Fluor 488 or donkey- anti-rabbit IgG Alexa Fluor 594, both at 1:100 for 1 hour at room temperature. After two PBS washes, coverslips were mounted on slides using Vectashield with DAPI (Vector, #H-1200-10) and analyzed using fluorescence microscopy.

For tissue staining, 6 weeks-old testes were fixed overnight in 4% PFA at 4°C, dehydrated and subsequently embedded in paraffin. Slides with 5 µm thick sections were prepared, deparaffinized with xylene and rehydrated in ethanol, then antigen retrieval was performed by boiling them for 10 min in citrate buffer (Vector, # H-3300-250). After cooling for approximately 30 min, slides were washed twice in PBS and permeabilized in cold 100% methanol for 10 min, followed by 10 min in 0.2% Triton-X in PBS. Slides were washed in PBS twice and blocking was performed with CAS-block (Thermo Fisher Scientific, # 008120) for 30 minutes at room temperature. After blocking, sections were incubated with the primary antibodies at the dilutions described above, in a humid chamber overnight at 4°C. On the next day, slides were washed three

times with PBS containing 0.05% Tween 20, incubated with the appropriate secondary antibodies at 1:500 dilution in PBS with 10% CAS Block, for 1 hour at room temperature, washed with PBS and mounted with Vectashield with DAPI for imaging.

Transepithelial Electrical Resistance (TEER) measurement

The functionality of the blood-testis barrier was assessed by performing transepithelial electrical resistance as previously described.[378] Confluent cultures were trypsinized and seeded at 1 $x10^6$ cells/ cm^2 in the apical (upper) chamber of the 12mm diameter Transwell (Costar, 0.4 µm pore size) coated with Matrigel (Corning). The TEER of the cells was measured daily using an Epithelial Ohmmeter (EVOM, World Precision Instruments, Inc.) in ohms (Ω) x cm^2, with chopstick electrode probes as previously described [366,379]. The plates would be left at room temperature alongside the TEER probe submerged in media for 20 minutes to acclimate. Each well was measured three times in three locations and averaged to provide TEER per well. Following TEER measurement, cells were refed and supplemented with testosterone (Sigma) until the end of the experiment. Upon reaching a daily average TEER of 200Ω (2-3 days), the cells were dosed with 0, 10, 60, or 100 mM EtOH. The TEER measurements were recorded, and media changes and measurements occurred for 5 to 10 consecutive days. Recovery experiments were allowed 48 hours of withdrawal following 3 or 8 days of alcohol treatment and were measured following the above protocol also measured daily. Student's t-test was performed on JMP between each group and the control so that p=0.05.

Paracellular Flux (Permeability) Assay

After the TEER measurements on the fifth and tenth days for both the nonrecovery and recovery groups, the NHP Sertoli cells were equilibrated with Ringer's solution for 15 minutes at 35°C, and then the medium in the apical chamber was replaced with Ringers and 50mg/mL Texas Red-labeled dextran (10 kDa; Thermo Fisher) and 2mg/mL Calcein (0.63 kDa; Thermo Fisher) as described.[380] Over two hours, the transwells were moved to new basal chambers every 30 minutes, and 100mL of media was collected from the basal side of the chamber and used for measuring fluorescence intensity. The plates were incubated at 35°C during the 30 minutes. Fluorescence was measured at wavelengths Ex485/Em525 nanometers for Calcein and Ex585/Em625 nanometers for dextran using a SpectraMax iD5 microplate reader (Molecular Devices). The amount of flux was compared to a standard curve and was graphed as the additive amount of calcein or dextran appearing in the lower chamber of the Transwell plotted versus time. Student's t-test was performed on JMP between each group and the control so that p=0.05.

RNA Extraction and quantification

Cells were lifted from the transwells by removing the media and adding 200uL of Tryp LE. The cells were then allowed to incubate for 5 minutes at 35°C. After 5 minutes 200uL of 10% FBS DMEM. The cells were then scraped and vigorously pipetted, then rinsed with an extra 200uL, then counted, and pelleted by centrifugation. RNA was extracted following the RNeasy Plus Mini Kit (Qiagen) instructions from the control and ethanol treated NHP Sertoli cells. After the

TEER was measured on the fifth or tenth day, to yield four biological replicates (*n* = 4). RNA integrity was measured using the NanoDrop 2000c spectrophotometer (Thermo Scientific), and only samples with 260/280 ratios >2.0 were accepted for further processing. The samples were stored at -80°C until qRT-qPCR analysis (<1 month).

RT-qPCR analysis

Each RNA sample (500ng) was reversed transcribed to cDNA for RT-qPCR using the iScript cDNA Synthesis Kit (Bio-Rad) per manufacturer's instructions. Quantitative PCR was performed with 500 µg cDNA and the iQ SYBR Green Supermix (Bio-Rad) per the manufacturer's instructions using the CFX Connect Real-Time PCR Detection System (Bio-Rad). The amplification parameters were the initial denaturation of 3 min at 95 °C, 40 cycles of 15-second denaturation at 95 °C, and 1 minute at 57 °C for annealing and extension. After the final PCR cycle, a melt curve analysis was performed at the following parameters: 5 seconds per step, 65 °C to 95 °C at 0.5 °C increments.

All PCR primers (Integrated DNA Technologies, **Table 4.1**) were designed and validated for specificity and amplification efficiency to NHP genes *AR*, *SOX9*, *GATA4, CLDN3, CLDN4,* and *CLDN11*. *CLDN5* was designed but was not able to amplify. This is most likely because of how short the gene is. *GAPDH* was used as an internal control for normalization. All genes were normalized to *GAPDH* and then to the control so that the control is equal to one. For each experiment (day, dose, and recovery status), there were 6 replicates for each gene. (**Table 4.1**)

Gene	Forward Primer Sequence (5’ – 3’)	Reverse Primer Sequence (5’-3’)
AR	GGATGGGGCTCATGGTGTTT	GCCCATCCACTGGAATAATGC
SOX9	GGGCAAGCTCTGGAGACTTCTG	GGGAGATGTGCGTCTGCTC
GATA4	CGGCACCCCAATCTCGTAG	GCGGGAGGCAGACAGC
CLDN3	CGAGTCGTACACCTTGCACT	GGCAGCAACATCATCACGTC
CLDN4	AAAGTGCCTTTGTTGGCCTG	CGAGTGTGAGCAGACCAGTT
CLDN11	CACCAATGACTGGGTGGTGA	CAGGACTGAGGCAGCAATCA

Table 4.1: **Oligonucleotide primers**

Oligonucleotide primers were used for PCR amplification of cDNAs isolated from control and treated NHP Sertoli cells.

Annexin V Assay

Cell apoptosis was determined by the Muse™ Annexin V assay kit (Thermo Fischer). An n of 3 was used for each control and dose. Upon finishing the dosing paradigm, the media was aspirated and TrypLE was added. The cells were incubated for 5 minutes and then an equal amount of 10% FBS DMEM was added. 100µL of cell suspension at a concentration of 10^5 to 10^7 was added to 100µL of Muse Annexin V and Dead Cell Reagent. The mixture was incubated for 20 minutes in the dark at room temperature and then run on the Guava Muse Cell Analyzer. Gating was done to include all cell populations. Student's t-test was performed on JMP between each group and the control so that p=0.05.

Human Cytokine Panel

The panel follows the Human Cytokine/Chemokine/Growth Factor Panel A kit (Millipore). 250uL of media were taken from 8 transwells for the control and 100mM EtOH groups and pooled into 2 samples for each group to have 4 biological replicates averaged and represented. The plate was first washed and decanted. The control was media only and the Assay Buffer was used as the background. Next 25µL of sample were added to each well and then 25µL of well mixed beads. We then incubated the mixture for two hours at room temperature. Following incubation, the wells were washed 3 times with 200µL wash buffer. Then 25µL of detection antibodies were added and left to incubate at room temperature for 1 hour. Next, 25µL of Streptavidin-Phycoerythrin was added per well and left to incubate at room temperature for 30 minutes. Then 3 washes were performed with 200µL of wash buffer and 150µL of Sheath Fluid was added

per well. Finally, the 96 well plate was run on a Luminex plate reader. Statistics were run on JMP utilizing the student's t test so that p=0.05.

4.11 AUTHOR AFILIATIONS AND CONTRIBUTIONS

We are grateful to Dr. Anthony Chan and his provision of NHP testicular tissue through Emory National Primate Research Center.

NIH R01-HL137112, R01-AA025854 (MK), F31-AA029000 (KFE)

5. **Department of Environmental Health Science, College of Public Health, University of Georgia, Athens, GA, USA** R. Clayton Edenfield, Krista M. Symosko & Charles A. Easley IV
6. **Regenerative Bioscience Center, University of Georgia, Athens, GA, USA** R. Clayton Edenfield, Krista M. Symosko & Charles A. Easley IV
7. **Division of Pulmonary, Allergy, Critical Care and Sleep Medicine, Department of Medicine and Department of Cell Biology, Emory University School of Medicine, Atlanta, Georgia, USA** Kristen F. Easley & Michael Koval
8. **Department of Biochemistry and Molecular Biology, University of Calgary, Calgary, AB, Canada** Nathalia de Lima e Martins Lara, Ina Dobrinski

R.C.E. performed the core experiments and designed the project; K.S.C. and S.B.P. aided in Sertoli cell culture, TEER, Dye Flux, and qRT-PCR; K.F.E. and M.K. provided invaluable training and oversight for TEER and Dye Flux; N.L.M.L. and I.D. helped with immunostaining and Sertoli cell confirmation; I.K.C. aided in Sertoli cell isolation; C.A.E. provided oversight and final approval for the manuscript.

CHAPTER 5

IMPROVING *IN VITRO* SPERMATOGENESIS[4]

[4] To be submitted to *Nature*

5.1 ABSTRACT

There is a growing need for stem cell-based therapies and toxicological model regarding male reproductive health. However, many of the current models ignore key spatiotemporal aspects of the testicular microenvironment. Here we propose several modifications to a preexisting *in vitro* spermatogenesis model. These modifications better mimic the testicular microenvironment resulting in a more efficient and effective model.

5.2 IN VITRO SPERMATOGENESIS AS A REGENERATIVE THERAPY AND TOXICOLOGICAL TOOL

Spermatogenesis is the basis for male reproduction and after puberty, males typically produce tens to hundreds of millions of motile sperm.[437] However, approximately 15% of couples worldwide face difficulties with natural conception, and about half of these cases can be attributed to male factors.[10] To combat this, advances in assisted reproductive technologies have allowed the reproductive community to overcome most types of male infertility. Techniques like in vitro fertilization-intracytoplasmic sperm injection (IVF-ICSI) have made pregnancies and live births possible using even a single viable and functional sperm.[438] Nevertheless, IVF-ICSI is not a viable option for patients with no detectable sperm, a condition known as azoospermia.

A diagnosis of azoospermia is made when there is a complete absence of sperm observed in at least two semen samples, even after a microscopic evaluation of a centrifuged sample is conducted. Men with non-obstructive azoospermia (NOA) caused by inherent factors are limited to treatment by

microdissection testicular sperm extraction which is only 50% successful. This method might result in a live birth for 10-25% of couples.[439,440] The remaining patients have no other viable options. Furthermore, NOA can be caused by gonadotoxic extrinsic factors like chemotherapy and radiotherapy.[441,442] For patients where sperm banking is not possible, like prepubertal patients, there is currently no alternative treatment. Therefore, there is a pressing need for regenerative treatment approaches, especially for individuals with NOA who do not have retrievable sperm or for survivors of prepubertal cancer.

As male factor infertility is on the rise it is vital to know what role environmental toxicants play in this. Traditionally, these studies have relied on animals to investigate chemical toxicity. However, animals have extreme differences in physiology, absorption, distribution, metabolism, excretion, and reproduction. Animals have been very useful thus far, but more human-like models are required. The Environmental Protection Agency plans to cut funding for vertebrate research by 30% by 2025 and eliminate it by 2035.[443] Additionally, the Food and Drug Administration no longer requires new medicines to be tested in animal to receive FDA approval.[444] As these traditional models are phased out there is a need for a human-like model to investigate environmental impacts on male fertility that does not rely on human tissue.

A potential approach for both is in stem cell derived *in vitro* spermatogenesis. While there has been plenty of success using other *in vivo*, *ex vivo*, and non-stem cell *in vitro* systems, stem cell systems offer unique advantages. Stem cells provide a mechanism to study human reproduction using

genetically distinct backgrounds including that of the patient. This manuscript will focus on two types of stem cells that are extremely valuable for research: embryonic stem cells (ESCs) and induced pluripotent stem cells (iPSCs). Human ESCs (hESCs) are pluripotent cells that give rise to all somatic cells in the embryo. They have been a staple for research since their derivation in 1998.[445] These cell lines are created using immunosurgical methods to isolate and culture of the inner cell mass. Generation of these cell lines currently requires the destruction of the embryo raising ethical concerns.[446] Human iPSCs (hiPSCs) are able to bypass these concerns as they are derived from somatic cells via Oct3/4, Sox2, Klf4, and c-Myc (Yamanaka factors).[447] hiPSCs offer several benefits to hESCs in the regenerative realm as they are a renewable source and can be patient derived. However, hESCs may be more applicable to the toxicology field as these cell lines are better standardized for use in multiple labs.

Easley et al. produced the first stem cell-based model for human *in vitro* spermatogenesis, producing haploid spermatid-like cells from ESCs and iPSCs.[448] This model has had great success in testing male reproductive toxicants like 2-bromopropane, 1,2,dibromo-3-chloropropne, hexabromocyclododecane, tetrabromobisphenol A, polybrominated biphenyl-153, and perfluorinated alkyl substances.[347-349,449] Furthermore, this model is shown to work with NHP ESCs able to generate haploid spermatid-like cells able to fertilize NHP oocytes and produce blastocysts.[450]

5.3 THE NEED FOR IMPROVEMENT

Spermatogenesis is a complex biological process orchestrated spatiotemporally by a network of cells with distinctive functions with distinctive functions within a highly organized tubular structure. While the model provided by Easley et al. is a powerful tool for studying toxicological effect on spermatogenesis and has great potential as a regenerative therapy it neglects several spatiotemporal aspects of spermatogenesis.[450] Additionally, this model is relatively inefficient and cannot produce large amounts of round spermatids. While there are several models that recapitulate spatial or temporal aspects of spermatogenesis none of these models provide both or the same benefits to regenerative therapy or the toxicological sciences.[451] Furthermore, complete *in vitro* spermatogenesis has yet to be accomplished. This manuscript will discuss multiple improvements to the model described by Easley et al. by better mimicking the spatiotemporal microenvironment of the testis.

In Easley et al. 2021, NHP pluripotent stem cells were differentiated into spermatid like cells. Briefly, these lines were cultured at 37° C for 10 days on STO-feeder cells in mouse spermatogonial stem cell (SSC) medium containing: MEM α (Thermo Fisher), 0.2% bovine serum albumin (Sigma), 5 µg/mL of insulin (Sigma), 10 µg/mL of transferrin (Sigma), 60 µM of putrescine (Sigma), 2 mM of L-glutamine (Invitrogen), 50 µM of β-mercaptoethanol (Sigma), 1 ng/mL of human basic fibroblast growth factor (R&D Systems), 20 ng/mL of glial cell line-derived neurotrophic factor (R&D Systems), 30 nM of sodium selenite (Sigma), 2.36 µM of stearic acid (Sigma), 1.02 µM of oleic acid (Sigma), 2.71 µM of linoleic acid (Sigma), 0.43 µM of linolenic acid (Sigma), 10 mM of 4-(2-

hydroxyethyl)-1-piperazineethane-sulfonic acid (Sigma), and 0.5x penicillin/streptomycin (Thermo Fisher). Cells were replenished with fresh medium every other day, and SSC medium was gassed with a blood gas mixture (5% CO_2, 5% O_2, 90% N_2 gas) before use.[450]

Due to the complex nature of spermatogenesis SSCs are exposed to multiple factors at various time points. Particularly post and pre-meiosis as they sit in two different regions of the BTB. This model fails to recapitulate these timing effects and neglects multiple spermatogenic factors.[452] To improve on this model system, a stepwise co-culture method that better incorporates factors involved with spermatogenesis, provides a better microenvironment, and is temperature adjusted to promote spermatogenesis was designed. Several protocols including Easley et al. were modified by Dr. Anthony Chan, Dr. In Ki Cho, and Clayton Edenfield.[453-459]

5.4 BUILDING A STEPWISE CO-CULTURE MODEL

The foremost problem was the use of non-testicular mouse cells. STO feeder cells are often used for establishing embryonic stem cells and maintaining them in an undifferentiated state.[460] Sertoli cells were used in their place. Sertoli cells have already been extensively covered in this manuscript but briefly, these cells maintain spermatogenesis through their secretions and cellular contacts. To preserve that role Sertoli cells were added as the feeder layer. These Sertoli cells were isolated from human and NHP primary testis tissue. They were isolated as previously described (Chapter 3 and 4). The Sertoli cells are refed every other day as described in Chapter 4 cultured to a high confluency (>90%) and then

mitomycin C treated. Mitomycin C (MMC) is an antitumoral antibiotic that is commonly used to inhibit the growth of feeder cells.[461] It does so by selectively inhibiting the synthesis of DNA. The MMC inactivated Sertoli cells are then plated onto Matrigel coated plates at a density of ~1x10^6 cells/60 cm^2. Sertoli feeder systems have successfully been used several times in the clinic.[462-464]

A notable feature of the testis is its location outside of the abdominal cavity. Generally, testicular temperature is lower than body temperature and while this temperature varies between species in primates it is approximately 2° C. Increasing testicular temperature to core body temperature will lead to morphological abnormalities in spermatozoa through impairments to spermiogenesis and meiosis.[465] Stem cells however, are cultured at 37° C. To account for this difference in required temperatures for optimum growth based on cell type the differentiation starts in the 37° C incubator and is then moved to the 35° C incubator on day 3. By day 3 most of the stem cells have begun to differentiate into spermatogonial stem cells and will therefore be better suited for the 35° C incubator.[466]

Finally, several changes were made to the factors supplemented to the media. 1% FBS is added to ensure the feeder layer can survive during the 15-day differentiation. To support differentiation leukemia inhibitory factor (LIF), epidermal growth factor (EGF), follicle stimulating hormone (FSH), human chorionic gonadotropin (HCG), estradiol, testosterone, and retinoic acid (RA) are added. Testosterone is produced by Leydig cells and primarily acts upon Sertoli cells.[239] In the absence of testosterone or functional androgen receptors

spermatogenesis will not progress beyond meiosis indicating it play an indirect role in meiosis.[367] LIF is a pleiotropic cytokine that controls the proliferation and survival of stem cells like primordial germ cell and gonocytes.[467] Peritubular myoid cells are thought to produce LIF.[468] EGF is a cytokine that promotes cell proliferation. In the testis Leydig cells primarily produce EGF but so can germ cells.[469] It is thought that EGF can modulate spermatogenesis especially spermatogonial proliferation.[470] HCG is commonly used to treat male infertility associated with decreased luteinizing hormone levels.[471] Estradiol is converted from testosterone and is produced in immature germ cells, spermatozoa, Leydig cells, and Sertoli cells. Estradiol is known to regulate spermatogenic proliferation, differentiation, survival, and apoptosis. It is involved in Sertoli tight junction modulation and Leydig cell function. Estradiol can enhance fertilizing capacity and induce sperm acrosome reaction and capacitation.[472] FSH is a pituitary gonadotropin and targets the Sertoli cells to produce regulatory molecules and nutrients needed for spermatogenesis.[473] RA plays a key role in spermatogonia differentiation preceding meiosis and is critical for entering meiosis.[474,475] RA inhibits genes involved in spermatogonia proliferation and activates genes involved in spermatogonia differentiation, meiosis, and progression.[476] CYP26 inhibitor is also added to prevent RA degradation by CYP26.

In addition to RA, nutrient signaling ALSO plays a role in meiosis.[453] While Sertoli cells are present in our culture they do not appear to form a true BTB nor the niches that are present *in vivo*. It is believed that during the intermediate phase of the BTB the Sertoli cells will restrict the flow of nutrients to signal

meiosis. To mimic that in vitro a nutrient restriction medium is used on days 10 and 11. The nutrient restriction medium is 90% EBSS and 10% 1% FBS SSC.[453] RA is also added during this time to push any non-haploid cells into meiosis.

GDNF and BFGF are still added in this protocol however, when they are added in the differentiation has been altered. bFGF is produced by many cells including Sertoli, Leydig, and many stages of germ cells. bFGF plays an important regulator of germ cell differentiation. However, plays an important role in maintaining the pluripotency of stem cells and has been shown to have a negative impact on differentiation. It is thought that bFGF primarily acts upon SSCs to maintain proliferation and plasticity.[452] GDNF is secreted by Sertoli cells and peritubular myoid cells. It is very important for SSC proliferation and differentiation. However, it may cause a bottleneck before meiosis.[452] Therefore, GDNF is added from day 5 to day 10 and is dropped during the last five days.

Briefly, the Stepwise Co-culture Protocol (SWCC) will be presented here. On Day -2, Matrigel coat the plates and store in 37 °C incubator. On Day -1 Mitomycin C treated cells are plated onto Matrigel coated plates at a density of $1x10^6$ cells/60 cm^2 with 10% FBS DMEM medium. They are placed into the 35 °C incubator overnight. Day 0, stem cells are plated onto the MMC Sertoli cell plates at a ratio of 2:5 mL stem cell suspension to medium on plate with mTESR medium. They are placed in the 37 °C incubator overnight. On Day 1 the medium is changed to 1% SSC supplemented with LIF and bFGF and placed in the 37 °C. Day 3, the medium is changed and replaced with 1% FBS SSC supplemented with LIF, bFGF, testosterone, RA, and CYP inhibitor and is placed

in the 35 °C incubator for the remainder of the differentiation. On Day 5, the medium is replaced with 1% FBS SSC and supplemented with LIF, GDNF, testosterone, and the cocktail consisting of EGF, rFSH, estradiol, and hCG. Day 7 and 9 are the same as Day 5. On Day 10 the medium is replaced with nutrient restriction medium consisting of a 1:9 ratio of 1% FBS SSC to EBSS and supplemented with RA and CYP inhibitor. On Day 12 the medium is changed to 1% FBS SSC supplemented with testosterone, the cocktail, and half as much RA and CYP inhibitor. Day 14, medium is changed to 1% FBS SSC supplemented with testosterone, the cocktail, and ¼ as much RA and CYP inhibitor. On Day 15, the protocol has reached its terminus and analysis can begin. Importantly, the quality and density of the stem cells after seeding on the Sertoli cells greatly affects differentiation. Additionally, a high purity (above 90%) is required for this protocol. The difference between the SWCC and previous protocol (SCC) is further described in **Figure 5.1** and the methods section.

To evaluate the effectiveness of the new protocol, several assays were conducted, including cell cycle analysis, qRT-PCR, and immunocytochemistry. Multiple markers were used to assess different stages of spermatogenesis.

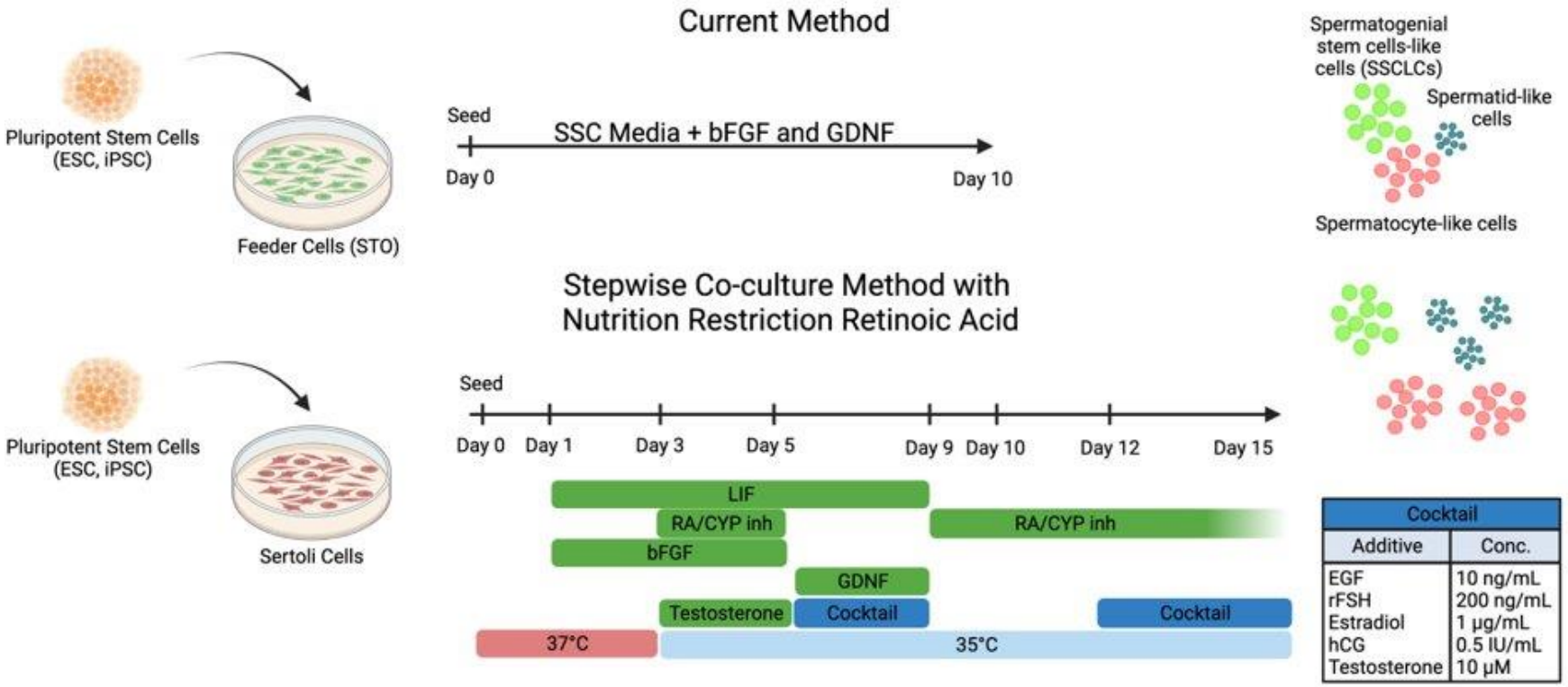

Cocktail	
Additive	Conc.
EGF	10 ng/mL
rFSH	200 ng/mL
Estradiol	1 µg/mL
hCG	0.5 IU/mL
Testosterone	10 µM

Figure 5.1 Stepwise co-culture with nutrient restriction and retinoic acid stimulation method

Here we describe the stepwise co-culture model with nutrient restriction and retinoic acid and how it compares to the previous method.

5.5 RESULTS: USING DNA CONTENT TO ASSESS TOTAL HAPLOIDY

Cell cycle assays are commonly used as a toxicological assay to determine environmental exposures that disrupt the cell cycle. It has even been used to assess how environmental toxicants effect cell cycle in the model provided by Easley et al.[448,449] This works by assessing DNA content using propidium iodide to detect DNA content supplied by the Muse® Cell Cycle Kit (Luminex). Using this kit haploid percentage was generated from flow cytometry analyses. Because haploid cells have half the DNA content of their diploid counterparts it is easy to count the percentage of haploid cells using this method.

Overall, the data show an increase in the effectiveness of the SWCC method from the previous method as measured by the Cell Cycle Kit. Haploid percentage increases from ~5% on average with the previous method to over 20% on average with the SWCC method (**Figure 5.2**).

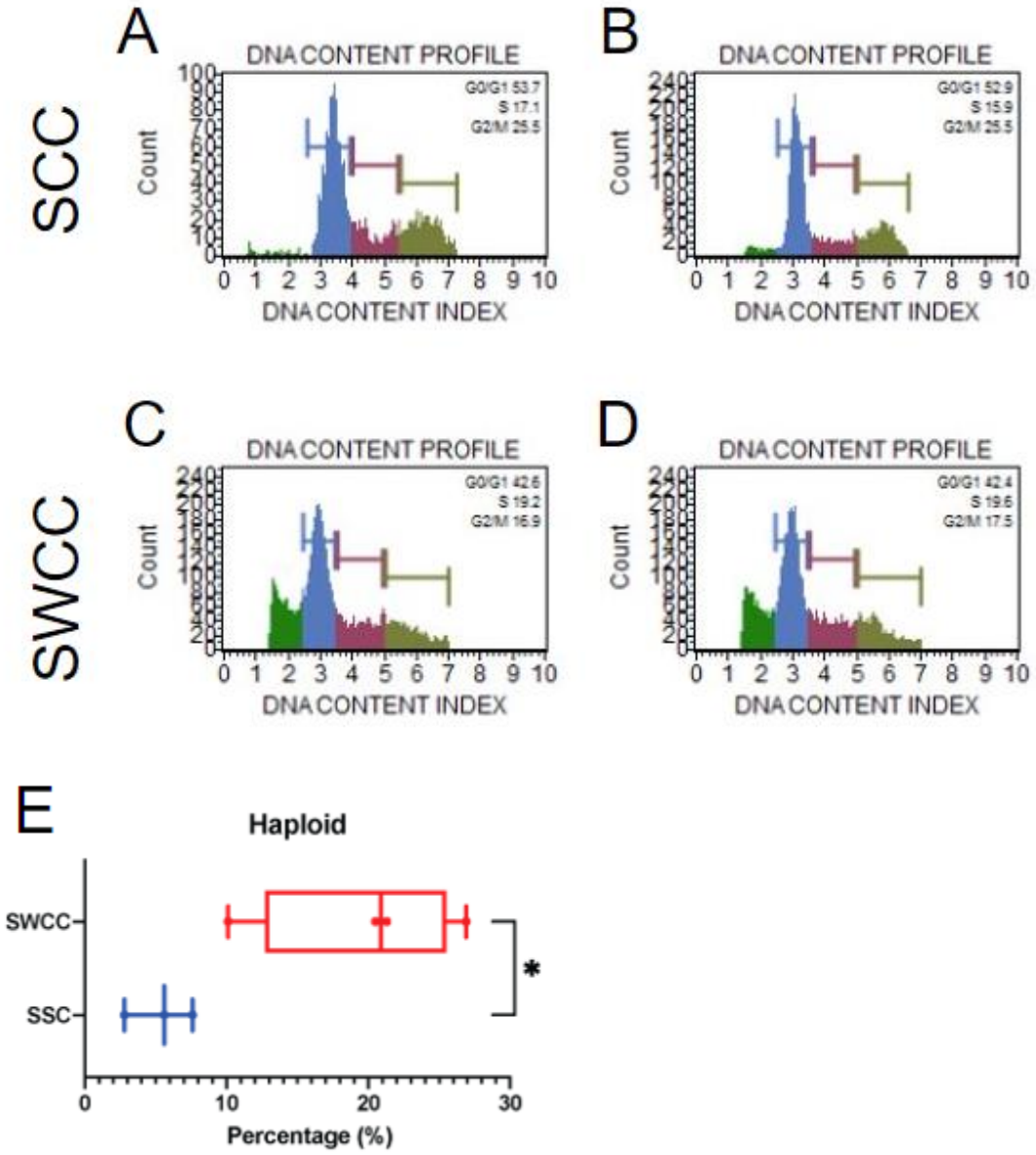
A
B
C
D
E
SCC
SWCC
DNA CONTENT PROFILE
Count
DNA CONTENT INDEX
G0/G1 53.7
S 17.1
G2/M 25.5
G0/G1 52.9
S 15.9
G2/M 25.5
G0/G1 42.6
S 19.2
G2/M 16.9
G0/G1 42.4
S 19.6
G2/M 17.5
Haploid
SWCC
SSC
*
Percentage (%)

Figure 5.2: Cell cycle analysis shows greater production of haploid cells under SWCC protocol

In images A-D haploidy is shown by the leftmost green peak. Image A and B show differentiations under the previous differentiation protocol (SCC). They average ~5% haploid cells. Image C and D show differentiations using the SWCC protocol. They average ~20% haploid cells. Image E shows the average haploid count of both A and B and C and D and that C and D have significantly more haploid cells than A and B.

5.6 RESULTS: USING REAL-TIME QRT-PCR TO ASSESS SPERMATOGENIC MARKERS *IN VITRO*

Real-Time Quantitative Reverse Transcriptase PCR allows reliable detection and measurement of PCR products. It can be used to determine the relative and absolute quantification of gene expression. Here it is used to measure the expression of spermatogenic genes in the primordial germ cell (PGC), spermatogonial stem cell (SSC), spermatogonia (SPG), spermatocyte and spermatid stages (**Figure 5.3**). The list of genes was selected based on comparative systematic review and meta-analysis of primary research articles. Stage specific genes are used to determine differentiation success.

For the PGC/SSC stage there is no specific SSC marker and so a panel must be used for best results *DPPA3, DAZL, ZBTB16, UCHL1, DDX4, TESMIN,* and *DHRS13* were used*. DPPA3* (also known as *Pgc7* or *Stella*) is expressed in a small number of cells of the proximal posterior epiblast that form the PGC and have high alkaline phosphatase activity.[477] *DAZL* is a germ cell-specific RNA binding protein that is essential for developing PGC upon their arrival in the gonad. In its absence germ cells do not develop beyond the PGC stage.[477] *ZBTB16* is important for SSC development, promotes SSC maintenance, and lowers during the first wave of spermatogenesis.[478] *UCHL1* is known to be expressed in the SSC stage.[479,480] *DDX4* is a germ cell marker and its expression pattern is localized to SSCs, spermatocytes, and spermatids.[481] *TESMIN* and *DHRS13* are associated with meiosis and spermatogenesis.[482,483]

Spermatogonia genes that were tested include *ID4*, *NANOS2*, *TCN2*, *MAGEA4*, *GFRA1*, *RAD51*, *CT55*, *PIWIL2*, *EGR4*, *STRA8*, *PLPPR5*, *GDNF*, *ASB9*, *NANOS3*, *TMEM55A*, *CDT1*, *ISOC1*, *NMT2*, *SYCP3*, *MEIOB*, *MLH1*, *DMC1*, *LIF*, *HSD17B14*, *FGF2*, and *ARMC1*. *ID4* levels dictate the transition between the stem cell and progenitor capacity in spermatogonia.[484] *NANOS2* is a known marker of SSC and undifferentiated spermatogonia in multiple species.[485] *GFRA1* (GDNF family receptor alpha-1) is localized in the SSC pool and SPG region.[485] *TCN2* and *NANOS3* are found in SSC/SPG population.[486] Common SPG markers used in single cell RNA-Seq include *MAGEA4*, *STRA8*, *SYCP3*, *NANOS3*, *EGR4*, *PIWIL2*, *FGF2*, and *ASB9* and *PLPPR5* is an SPG/SSC marker.[487] SYCP3 is also expressed in spermatocytes. [488]*RAD51* is essential for the maintenance of spermatogonia and meiotic progression.[489] *CT55* is primarily observed in the cytoplasm of spermatocytes and spermatogonia but also the acrosome and flagellum of early and late spermatids.[490] *TMEM55A* is upregulated in SPG populations.[491] *CDT1* controls mitotic progression in SPG cells.[492] Spermatogonia and spermatocytes express *MLH1*, *RAD51*, *DMC1*, *ISOC1*, and *MEIOB*.[493] Because of the transient state of spermatogonia they often express genes also found in SSCs and spermatocytes.

Spermatocyte genes that were tested include *HSD17B3*, *C9ORF57*, *CETN3, MGAT4D*, *PHOSPHO2,* and *TPPP3. HSD17B3* is most often expressed in Leydig cells but can also be in spermatids.[466] C9ORF57, CETN3, MGAT4D, PHOSPHO2, and TPPP3 are all found in spermatocytes using single cell RNA-Seq.[493,494]

Spermatid stage gene expression was also observed. *C17ORF98*, *ENPP2*, *LRRC3B*, *PRSS37*, *PRSS58*, *TP53TG5*, *PRM1*, *PRM2*, *TET1*, *TET2*, *TET3*, *TNP1*, *TNP2*, *ACRBP*, *FSCN3*, and *PHOSPHO1* were all tested. *C17ORF98* is expressed in early spermatids, PRSS58 is expressed in mid stage spermatids, and *FSCN3* is expressed in late stage spermatids.[488] *PRM1* and *TNP1* are also expressed in spermatids.[488,493] ENPP2 is involved in the production of lysophosphatidic acid production, a molecular component influencing male fertility.[495] LRRC3B is shown to be expressed in spermatids.[493] *PRSS37* is found in late stage spermatid and sperm and is a marker of its functionality as low expression levels of *PRSS37* is associated with unexplained male fertility.[496] *TP53TG5* is observed in late stage spermatids in single cell RNA-Seq of *Cynomolgus macaque*.[497] *PRM2* and *TNP2* are both expressed postmeiotically in round and elongating spermatids.[498] *TET 1-3* are expressed successively throughout different stages of spermatogenesis with their levels associated with male fertility. *TET2* is expressed in late stage spermatocytes, while *TET1* is expressed in the nuclei of early stage round spermatids, and *TET3* is expressed in late stage spermatids.[499] *ACRBP* is expressed in both spermatids and spermatozoa and catalyzes the conversion of proacrosin to acrosin.[500] *PHOSPHO1* has a sperm-specific isoform and is essential for the completion of spermatogenesis.[501]

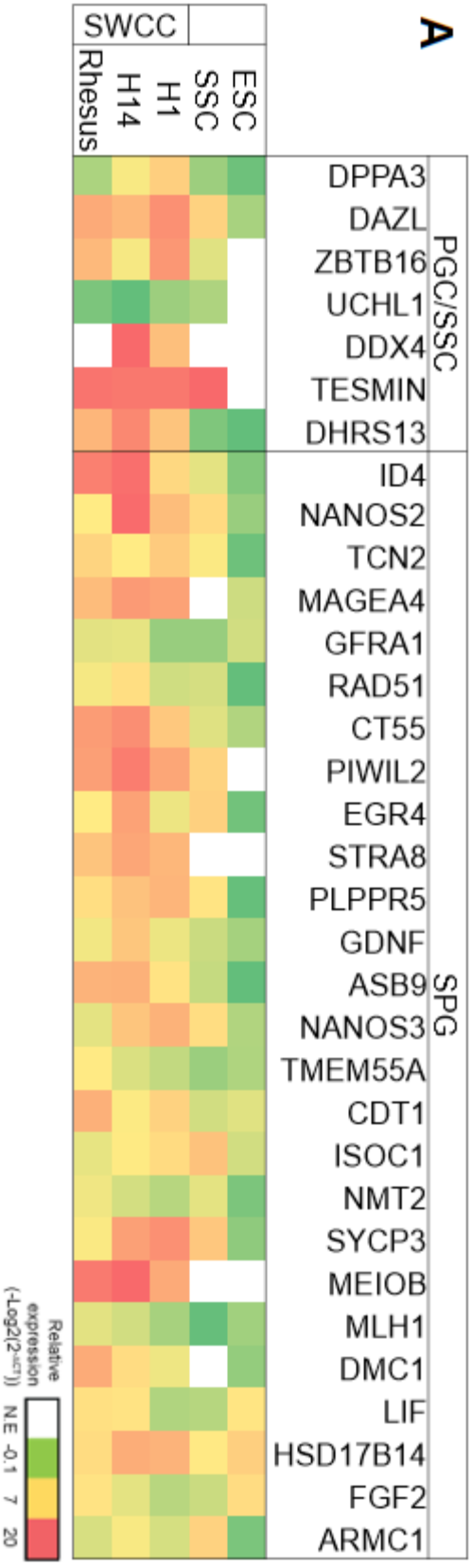
A
SWCC
ESC
SSC
H1
H14
Rhesus
PGC/SSC
SPG
DPPA3
DAZL
ZBTB16
UCHL1
DDX4
TESMIN
DHRS13
ID4
NANOS2
TCN2
MAGEA4
GFRA1
RAD51
CT55
PIWIL2
EGR4
STRA8
PLPPR5
GDNF
ASB9
NANOS3
TMEM55A
CDT1
ISOC1
NMT2
SYCP3
MEIOB
MLH1
DMC1
LIF
HSD17B14
FGF2
ARMC1
Relative expression (-Log2(2^-dCT))
NE
-0.1
7
20

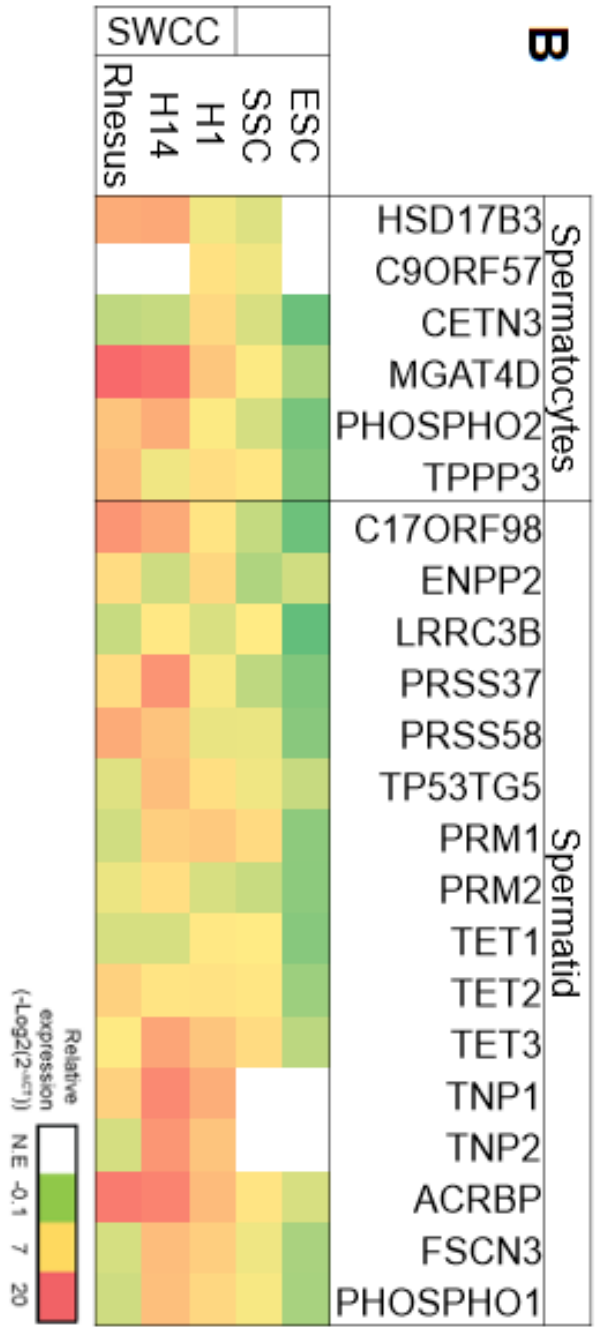
B
SWCC
ESC
SSC
H1
H14
Rhesus
Spermatocytes
HSD17B3
C9ORF57
CETN3
MGAT4D
PHOSPHO2
TPPP3
Spermatid
C17ORF98
ENPP2
LRRC3B
PRSS37
PRSS58
TP53TG5
PRM1
PRM2
TET1
TET2
TET3
TNP1
TNP2
ACRBP
FSCN3
PHOSPHO1
Relative expression (-Log2(2^-ΔCT))
N.E
-0.1
7
20

Figure 5.3: Using real time qRT-PCR to assess spermatogenic markers *in vitro*

The ESCs show little to no expression of spermatogenic genes. The SSC has higher expression of almost all spermatogenic genes when compared to the ESCs and the SWCC protocol has higher expression than the SSC. Image A shows the expression levels of PGC, SSC, and SPG associated gene. Broadly, the SWCC protocol has higher expression In genes associated with all stages but notably higher expression meiosis associated genes in the SPG stage. Interestingly, there is a higher expression of PGC and SSC associated genes. This could be because less cells are entering the SPG stage in the SWCC compared to the SSC stage or just that there are more cells produced. Given that there are higher amounts of spermatocyte and spermatid associated genes it is most likely the latter (Image B). Many late-stage spermatid and spermatozoa are observed at a higher level using the SWCC protocol like PRSS37, TET3, and ACRBP. Interestingly, H14 appears to have higher expression of spermatogenic genes perhaps pointing to a genetic cause. The *Rhesus macaque* differentiation also has a similar but differential gene expression indicative of a closely related species.

5.7 RESULTS: USING IMMUNOCYTOCHEMISTRY TO DETERMINE SUCCESS OF THE STEPWISE CO-CULTURE PROTOCOL

Immunocytochemistry (ICC) is a technique used to visualize proteins in cells of interest; here it is used to assess the success of the SWCC protocol (**Figure 5.4**). γH2A.X is a prominent event that occurs at double strand breaks that are associated with chromatin remodeling in round spermatids.[502] SYCP3 is involved with meiotic chromosome segregation and spermatogenesis and are present within the nucleus as a worm-like structure.[503] Acrosin (ACR) is a digestive enzyme that aids in the penetration of the zona pellucida and is located within the inner acrosome membrane. It is used to mark spermatids and spermatozoa via ICC.[504] DMC1 is found in late stage spermatocytes and is required for the homologous synapsis of chromosomes in meiosis; it is punctate within the nucleus.[505] MLH1 is in both pre- and meiotic cells. In meiotic cells it is necessary for meiotic crossing over. It is small and punctate.[506] Protamine 1 (PRM1) is sperm specific and binds to DNA causing spermatid chromatin condensation post meiosis.[507]

The ICC that was performed shows multiple confirmations of spermatogenesis and notably meiosis as well. γH2A.X and SYCP3 are shown together and appear as they would be expected to within the nucleus. MLH1 and DMC1 also appear as they should, punctate within the nucleus. PRM1 being bound to DNA appears the same as the Hoechst staining used for DNA as expected. SYCP3, however, does not appear as expected, although it is in the

correct place. Because of its location within the nucleus, it is hard to visualize without proper preparation.

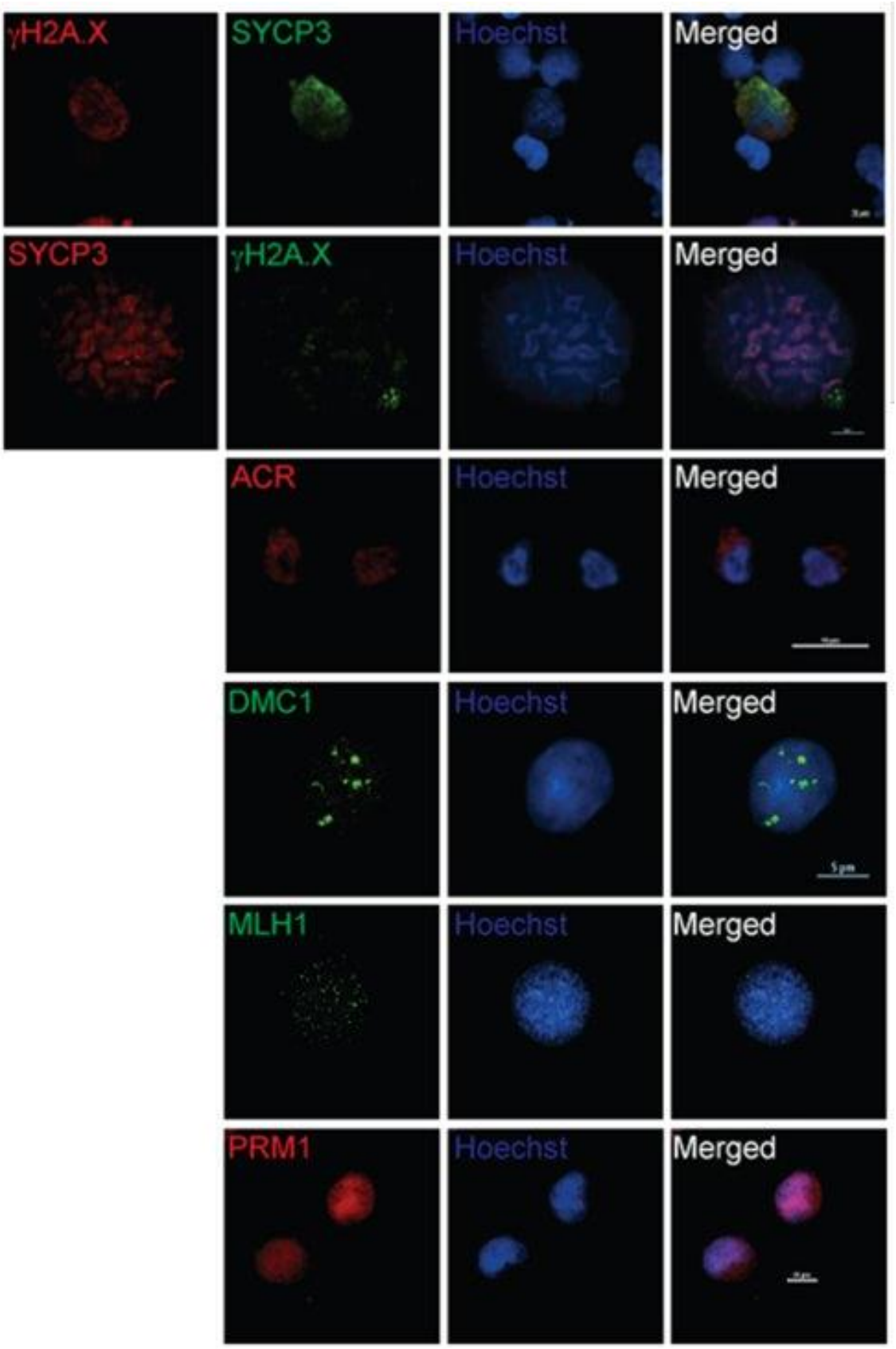
γH2A.X
SYCP3
Hoechst
Merged
SYCP3
γH2A.X
Hoechst
Merged
ACR
Hoechst
Merged
DMC1
Hoechst
Merged
MLH1
Hoechst
Merged
PRM1
Hoechst
Merged

Figure 5.4: Immunocytochemistry to visualize key meiotic markers in *in vitro* differentiated spermatids

Here, ICC provides confirmation of spermatogenesis, emphasizing meiosis. γH2A.X and SYCP3 display the anticipated nuclear localization. MLH1 and DMC1 exhibit the expected punctate pattern within the nucleus. PRM1 binding to DNA corresponds to Hoechst staining. Notably, SYCP3, although correctly located, appears differently from the anticipated pattern.

5.8 MATERIALS AND METHODS

Human stem cell Culture

The stem cells are cultured on Matrigel plates, and the medium is changed every other day with MTESR + P/S. They are incubated at 37 °C at 5% CO2. They are passaged about every five days with dispase.

Stem cell Passaging

Stem cell plates are observed for shape, size, debris, differentiation, and confluency. Aspirate media and rinse with DMEM F12. Add 5 mL of dispase and incubate for ~7 minutes or until a bright halo appears around the stem cell colonies. Aspirate dispase and add fresh media. Scrape the cells and collect them in a conical tube. Distribute the cells on the new plates. For maintenance add about 1 mL onto a 10 cm plate. For starting an experiment add about 4 mL onto a 10 cm plate.

Human Sertoli cell culture

Sertoli cells were isolated from de-identified human testis cell suspensions kindly provided by Dr. Kyle Orwig at the University of Pittsburgh. The sample number of the provided cells are Human Core – 18092304 – testis cells. The suspensions were stored in liquid nitrogen until needed at a concentration of ~20 x 10^6 cells/mL. Following thaw, the germ cells were separated out by gravity sedimentation while in 10mL of HBSS and P/S. The remaining pellet undergoes a brief enzyme digestion while being shaken at 300 rpm at 37C for 5 minutes. Digestion media contains 80mL HBSS with P/S, 10 mL trypsin (2.5%), 10 mL

collagenase type IV (1%), and 2 mL DNase (1 mg/mL). 0.1% soybean trypsin inhibitor was then added to halt digestion. The solution was then centrifuged at 200g for 5 min, the supernatant was discarded, and DMEM F12 with P/S was added in a 10:1 volume ratio. The solution then rests at room temp for 30 minutes. The pellet is enriched for tubular fragments cells and the supernatant for interstitial cells. The interstitial cells can be further isolated on a discontinuous Percoll gradient. The pellet can now be resuspended in PBS with 1M glycine and 2mM EDTA and pipetted for 10 min to remove peritubular cells. Gravity sedimentation was then used to isolate out Sertoli cells and tubular fragments. Both were plated and cultured in DMEM F12 15% FBS with P/S. Culture media is refreshed every other day. The Sertoli cells are then purified by visual analysis and differential plating. At passage 3 the Sertoli cells were cultured at 35℃ with 10% FBS DMEM12 with 5mL P/S and 5 mL Glutamax supplemented with 1:1000 FSH and 1:2000 EGF.[377] The cells medium is changed every other day.

Sertoli cell mitomycin C treatment

Mitomycin C media is prepared by adding 10 µL Mito C for every 1 mL of 10% FBS DMEM. 5 mL of this media is added to each >95% confluency 10 cm plate. The plates are incubated at 35 °C for 4.5 hours. Properly dispose of the mitomycin C medium. The cells can now be collected for liquid nitrogen storage or used for an experiment.

SSC medium

2g of BSA is dissolved in 1000 mL of MEM Alpha. Then two bottles af ascorbic acid are prepared and added along with penstrp, Hepes, BME, lipid mixture,

insulin, transferrin, and sodium selenite. For 1% FBS just add 10 mL of FBS. The mixture is then filter sterilized.

Name	Stock	Final Concentration	Volume (500mL)	Company	Catalog
MEM Alpha			500mL	Invitrogen	12561-072
BSA Fraction V		0.20%	50 mg	MP Biomedicals	08810661
Insulin (ug/mL)	10 mg/mL	5 ug/mL	10 uL	Sigma	15500
Transferrin (ug/mL)	100mg/mL		100 uL	Sigma	T1283
BME (M)	1000x stock	50 uM	100 uL		
Human recombinant bFGF (ng/mL)	1 ug/mL	1 ng/mL	10 uL ***	PeproTech	100-18B
Human recombinant GDNF (ng/mL)	20 ug/mL	20 ng/mL	200 uL ***	PeproTech	450-10
Sodium Selenite Na_2SeO_3(nM)	$3x10^{-4}$ M	30 nM	10 uL	Sigma	S5261
HEPES (mM)	1 M	10 mM	5 mL		
Pen/Strep		0.5 x	2.5 mL		

Stepwise Co-culture Differentiation

Mitomycin C-treated cells are seeded onto Matrigel-coated plates and incubated overnight. The hESCs are passaged onto these as previously described. The differentiation starts the following day. 1% FBS is added to the SSC medium and then this is further supplemented with specific combinations of growth factors and hormones at different stages: retinoic acid (1 µM) is introduced on days 3, 10, and 13 (at 0.5 µM), while bFGF (1ng/mL) is administered on days 1-4, and GDNF (20 ng/mL) was given on days 5-10. Testosterone (10 µM) is included from day 3 to 10. Additionally, a cocktail containing EGF (10ng/mL), FSH (200 ng/mL)

estradiol (1 µg/mL), and hCG (0.5 IU/mL) was added from day 5 until the completion. On days 10 and 11 10% SSC medium with 90% EBSS is added.

Immunocytochemistry

Aspirate the medium from the cells and add 4% paraformaldehyde and incubate at room temperature for 15 minutes. Next wash the cells with PBS. Then add 5% BSA Blocking Buffer (5% BSA, 5% goat serum, 0.1% triton-x in PBS) and incubate at room temperature for one hour. Aspirate and add 5% Blocking Buffer with primary antibodies. Block overnight at 4 °C. The next day, aspirate the blocking buffer with the primary antibodies and wash with 0.1% triton-x PBS for 10 minutes on a cell shaker. Repeat twice. Then add 0.1% triton-x PBS with appropriate secondary antibody at 1:1000. Stain for one hour at room temperature shielded from light. Then wash as previously described. Following wash add PBS with Hoeschst 33342 at 1:1000 and stain for 15 minutes at room temperature shielded from the light.

RT-qPCR analysis

Each RNA sample (500ng) was reversed transcribed to cDNA for RT-qPCR using the iScript cDNA Synthesis Kit (Bio-Rad) per manufacturer's instructions. Quantitative PCR was performed with 500 µg cDNA and the iQ SYBR Green Supermix (Bio-Rad) per the manufacturer's instructions using the CFX Connect Real-Time PCR Detection System (Bio-Rad). The amplification parameters were the initial denaturation of 3 min at 95 °C, 40 cycles of 15-second denaturation at 95 °C, and 1 minute at 57 °C for annealing and extension. After the final PCR

cycle, a melt curve analysis was performed at the following parameters: 5 seconds per step, 65 °C to 95 °C at 0.5 °C increments.

CHAPTER 6

CONCLUSION: PREDICTING HOW MULTIPLE INSULTS COULD IMPACT THE BLOOD-TESTIS BARRIER AND SPERMATOGENESIS[5]

[5] To be submitted to *Scientific Reports*

6.1 ABSTRACT

Male fertility has been declining the past century. This chapter focuses on how alcohol abuse and SARS-CoV-2 infection jointly contribute to harming male reproductive health. It summarizes and contextualizes the previous studies and provides an experimental framework to study the impact of these two exposures on spermatogenesis and the blood-testis barrier. Additionally, it outlines therapeutic implications and preventative strategies to combat alcohol abuse and SARS-CoV-2 infection and their damages to male reproductive health.

6.2 INTRODUCTION

As previously discussed, there has been a decline in human fertility over the past several decades. Approximately 10% of males experience fertility problems, and this number is expected to increase. Generally, this influx in male infertility is associated with a corresponding reduction in sperm concentration and testosterone levels. This decline in male reproductive health has been observed worldwide.

Multiple explanations have been given to explain this decline in male reproductive health including environmental toxicants, endocrine disrupting chemicals, lifestyle, and genetic conditions. However, there is likely not one specific culprit. Because of the complexity of interactions between one's environment and their reproductive health, it can be hard to identify a single cause that disrupts their reproductive health, especially on a worldwide scale. The overall decline in male reproductive health is best explained by a variety of

interacting insults that have the combined effect of reducing one's fertility. The exact combination will widely vary between individuals.

Furthermore, male reproductive health itself is a complex process requiring numerous cells to work together for spermatogenesis and fertility to be possible. The three major cell types involved in spermatogenesis are the germ cells, Sertoli cells, and Leydig cells. Germ cells are the most important, consisting of spermatogonial stem cells up to mature sperm. They are responsible for the packaging and delivering of the paternal genetic and epigenetic information required for reproduction. Sertoli cells are nurse cells. They provide key nutrients and signaling to germ cells allowing for spermatogenesis to occur. Additionally, they make up the blood-testis barrier to keep the germ cells safe from xenotoxicants and immune cells. The Leydig cells provide necessary hormones and cell signaling to both germ cells and Sertoli cells to ensure successful spermatogenesis. There are other important cell types required for spermatogenesis; however, these three are the primary ones. For spermatogenesis to successfully occur, all these cell types must be functioning properly. Any insult that effects one of them may disrupt male reproductive health. The more insults there are to one or more of these cell types, the greater the risk to male reproductive health.

To discuss how multiple insults can impact male reproductive health, this chapter will focus on SARS-CoV-2 and alcohol, their individual effects on the three major cell types, and their possible combined impact on those same cell

types. Furthermore, how to test these insults and their combined impact on the three major cell types will also be discussed.

6.3 SARS-COV-2 INFECTION AND MALE REPRODUCTIVE HEALTH

As this topic has been extensively covered in this manuscript, this section will be brief. SARS-CoV-2 infection is primarily dependent on the presence of viral entry proteins ACE2 and TMPRSS2. Spermatogonial stem cells and spermatogonia express both proteins while spermatocytes and spermatids only express TMPRSS2. Sertoli and Leydig cells, however, only express ACE2, which is the primary target of the SARS-CoV-2 spike protein.[353] Because of the testicular expression of SARS-CoV-2 viral entry proteins, male reproductive health could be at risk from SARS-CoV-2 infection.

A recent study by Li et al. has shown that SARS-CoV-2 can enter Leydig cells and affect testosterone production *in vitro*. They showed Leydig cells of hamsters infected with SARS-CoV-2 had SARS-CoV-2 nucleocapsid present. They also demonstrated that a SARS-CoV-2 spike-pseudotyped viral vector could enter human Leydig-like cells and cause an increase in testosterone production.[508] While interesting, this study did not rely on actual SARS-CoV-2 virus or Leydig cells. Furthermore, the resulting evidence that testosterone production increased is opposite to what is observed clinically.[353] Because SARS-CoV-2 infection is known to alter testosterone production and Leydig cells express the viral entry protein, more research is required to understand the role that SARS-CoV-2 infection may have on testosterone production and the Leydig cells.

Sertoli cells also express the SARS-CoV-2 viral entry protein ACE2, indicating their potential susceptibility to SARS-CoV-2. There is also clinical evidence of SARS-CoV-2 infection disrupting blood-testis barrier function. In addition to the clinical evidence, there is growing evidence that SARS-CoV-2 can negatively impact barrier function and Sertoli cells.[358] Furthermore, we provide evidence that SARS-CoV-2 infection can alter blood-testis barrier integrity. This is indicated by an influx in dye across the barrier and a decrease in the electrical resistance of the barrier.

Because early-stage germ cells sit outside the BTB and express both SARS-CoV-2 viral entry proteins they are at risk for influence from SARS-CoV-2 infection. Yang et al. has demonstrated excessive germ cell dam.[312] Ma et al. also show germ cell damage characterized by apoptosis.[317] A 2023 article from Garrouch et al. provide evidence that patients struggling with infertility had worse sperm parameters following the COVID-19 pandemic.[509] Specifically, they noted a significant decrease in total and progressive sperm motility and a significant increase in the percentage of morphologically abnormal spermatozoa during the pandemic. This study provides some evidence that SARS-CoV-2 infection may worsen male reproductive health by the impact it has on the germ cells. However, there are some confounding factors. The patients already had infertility issues and they were not confirmed to have had COVID-19. Unfortunately, there have not been many studies assessing how SARS-CoV-2 infection can impact the male germ cells. There have been post-mortem studies; however, these cases represent the worst pathologies of SARS-CoV-2 infection and do not

represent the majority of COVID-19 cases. Furthermore, there have been no *in vitro* studies able to assess the direct impact of SARS-CoV-2 infection on the germ cells.

The epigenetic impact of SARS-CoV-2 infection on male germ cells has also not been studied. Viruses are known to epigenetically impact the host in many ways: directly, through viral proteins interacting with host epigenetic proteins, indirectly, through viral triggering of host epigenetic pathways, locally, by altering the epigenetic status of the infected cell or organ, and systemically, by altering the epigenetic status of uninfected cells or organs. Virtually all pathogens influence the host epigenome in some way. [510,511] SARS-CoV-2 related viruses like SARS-CoV-1 and MERS-CoV are associated with causing differentially methylated CpG sites and exploit DNA methylators and histone modifiers. It is suggested that COVID-19 utilizes similar mechanisms.[512] In COVID-19 patients, differentially methylated CpG sites have been observed in multiple organs outside the testis. Considering the testicular and epigenetic effects of SARS-CoV-2 infection, it is vital to learn what impacts the infection may have on the sperm epigenome. SARS-CoV-2 infection may cause epigenetic alterations to the male germline. Fever, an observed symptom of COVID-19, is known to cause sperm DNA damage and epigenetic alterations.[513,514] Additionally, increased testicular cytokines, like those associated with COVID-19, may impair male fertility and cause epigenetic changes in sperm. [515,516,517] However, only two studies have attempted to observe virus induced sperm epigenetic changes. The studies show this is possible in both *Toxoplasma gondii* infection and sepsis in

rodents. [518,519] While there is no direct evidence of viral-induced epigenetic alterations in human sperm, considering the number of COVID-19 cases in reproductive aged males, the testicular damage associated with SARS-CoV-2 infection, and the known affect SARS-CoV-2 infection can have on the epigenome, there is no better time to interrogate whether COVID-19 can alter the paternal epigenome.[520]

To better understand the impacts of SARS-CoV-2 infection on male fertility, more research will need to be done. Several studies have addressed the impact of COVID-19 on male fertility. However, these studies tend to focus on the most severe cases or the indirect effects of SARS-CoV-2 infection.[353] Not many studies have assessed the direct impact of SARS-CoV-2 infection on Sertoli, Leydig, and germ cells. Specifically, infection will need to be replicated in the three major cell types using human primary cells. We expect that SARS-CoV-2 infection of the Sertoli cells will cause blood-testis barrier disruption. We have already shown this via TEER and Dye Flux. However, we hypothesize that cytokine analysis will reveal altered production of cytokines important for spermatogenesis and immune function and that RNAseq will show alterations in gene expression of genes important for BTB regulation and Sertoli cell health. A coculture model of Sertoli cells and germ cells would be beneficial to observe any changes in the Sertoli-germ cell interactions caused by SARS-CoV-2 infection. It is likely that SARS-CoV-2 infection will disrupt the junctions between these cells. SARS-CoV-2 infection of the Leydig cells will likely alter hormone production. This has been observed clinically and in vitro but with conflicting results. More

research is required to elucidate the cause behind these conflicting results. A coculture system that combines the Leydig cells alongside Sertoli and germ cells would be beneficial. This type of system would allow for the study of multiple testicular interactions and how damage to one cell type could further damage another following SARS-CoV-2 infection.

6.4 ALCOHOL USE AND MALE REPRODUCTIVE HEALTH

Alcohol has been used throughout human history and its impact on human health is overwhelmingly negative. As heavy drinking has increased following the COVID-19 pandemic, hopefully this research question receives more attention in the future, especially since a majority of male alcoholics are in reproductive age and may be interested in becoming fathers.[390] This section will focus on the overall effect of alcohol on the three major testicular cell types.

Leydig cells are the primary source of testosterone production in males. Therefore, altered testosterone levels often indicate Leyd cell dysfunction. However, this is not always the case as any damage to the HPG axis could disrupt testosterone production. Animal studies indicate that alcohol consumption will reduce testosterone levels.[390] However, animal studies also note reduced levels of LH and FSH following alcohol abuse. This indicates that alcohol could be causing damage to the hypothalamus or pituitary resulting in a reduction in testosterone production.[390] Importantly, one animal study has noted alcohol induced alterations to Leydig cell number and morphology.[521] In humans, there is contradicting evidence on the levels of FSH, LH, and testosterone. However, it appears that alcohol abuse alters these levels.[390]

As previously discussed, alcohol has been demonstrated to have detrimental effects on Sertoli cells.[407] Furthermore, some evidence shows that alcohol may disrupt the BTB as it is able to do in other barriers throughout the body. Previously, we showed that alcohol use can disrupt the barrier formed by primary NHP Sertoli cells. Specifically, we show that TEER significantly decreases while Dye Flux significantly increases in response to alcohol. Furthermore, we show that the barrier is able to recover to some extent following 48 hrs of withdrawal which matches the clinical data.[393] In addition to effects on the barrier, we show that Sertoli cell gene expression is altered in response to alcohol. Specifically, we show that tight junction and Sertoli cell function gene expression is altered in response to alcohol. Additionally, we show cytokines involved with BTB regulation and the local testicular immune system are altered in response to alcohol. Furthermore, these changes do not appear to be the cause of Sertoli cell death.

Male germ cells have also been shown to be impacted by alcohol abuse. In animals, semen quality is altered, characterized by reduced sperm concentration and motility, increased abnormal sperm morphology, and defects in chromatin condensation.[390] Similar results are observed in humans. Alcohol abuse is associated with reduced sperm concentration, altered semen volume and increased abnormal morphology, increased sperm DNA fragmentation, and defects in chromatin condensation.[390] There have also been observed effects on gene transcription and genetic and epigenetic regulation. In animals, there is reported altered expression of RNA involved in sperm function and proteins

involved in apoptosis, and aberrant gene acetylation of sperm DNA from alcohol abuse.[390] In humans, there is an observed altered expression of RNA involved in sperm function and aberrant gene methylation in sperm DNA.[390]

Alcohol's impact on the sperm epigenome has been described by Chastain et al.[522] Briefly, alcohol consumption has been shown to decrease methylation in imprinted genes H19 and IG-DMR in human sperm. In rodents, there is decreased methylation in the imprinted genes H19 and Peg3, decreased methylation of the BDNF promoter, increased methylation of DAT, and decreased cytosine methyltransferase in sperm.[522]

6.5 STEM CELL RESEARCH AND MALE REPRODUCTIVE HEALTH

As Chapter 5 extensively covered the need for an improved spermatogenesis model, this section will provide a brief overview of stem cell research in the context of male reproduction and an overview of the methodologies and findings from Chapter 5. With the increasing prevalence of male factor infertility, understanding the role of environmental exposures is crucial. Traditionally, research on toxicity has leaned heavily on animal studies. However, due to significant disparities between humans and animals, these models, while valuable, have limitations. Recognizing this, there is a growing demand for models that closely resemble human biology. Regulations from the FDA and EPA are exacerbating this shift away from traditional models, highlighting the necessity for human-like alternatives to study environmental impacts on male fertility; especially, ones that do not rely exclusively on human tissue. Additionally, the rise of male factor infertility necessitates a model that has

high potential for transfer into clinical settings. Human embryonic and induced pluripotent stem cells offer a great model system for both needs.

Previously, we described that human stem cells can be differentiated into spermatid-like cells. We produced an advanced model system that allows for increased production of spermatid-like cells and better mimics the spatiotemporal testicular microenvironment. This is demonstrated by immunocytochemistry and qRT-PCR data showing late-stage spermatogenic and meiotic markers and cell sorting data showing an increased number of haploid cells.

6.6 IMPLICATIONS OF INSULT INTERPLAY

The complexity of environmental exposures necessitates the use of mixtures and multiple exposures because most people are not exposed to just one toxicant but rather multiple and often simultaneously. Chapter 7 discusses how chronic alcohol use can prime bronchial cells for barrier dysfunction and altered inflammatory response. Here, we use that same framework to discuss how multiple insults could interact to impact male fertility. Specifically, we discuss how chronic alcohol use and SARS-CoV-2 infection could alter the blood-testis barrier and spermatogenesis. Additionally, we discuss how to test this and expected results. Importantly, conducting experiments with live SARS-CoV-2 necessitates the use of a biosafety level 3 (BSL3) facility, which consequently limits the scope of experiments that can be performed. Therefore, this discussion will not extensively cover experiments that are unlikely to be performed.

Chapter 4 provided an insight into what chronic alcohol abuse can do to the BTB. Broadly we observed reductions in barrier integrity, alterations in gene

expression associated with barrier junctions and Sertoli cell function, and an increase in proinflammatory secretions. Additionally, we have insight into how SARS-CoV-2 infection can impact BTB integrity from Chapter 3. We observed a decrease in barrier integrity from SARS-CoV-2 infection. Variants better adapted for immune invasion had less of an impact on barrier integrity. We hypothesize that chronic alcohol abuse will alter the barrier to be more susceptible to SARS-CoV-2 disruption.

Interestingly, one study by Balasubramanian et al. shows that ethanol exposure can increase the amount of viral entry proteins, like ACE2 and TMPRSS2 in the brains of mice.[523] If ethanol exposure also causes an increase in viral entry proteins in Sertoli cells, then it is likely that chronic alcohol abuse could worsen the impacts of SARS-CoV-2 infection for male reproductive health. This would likely be from an increase in infectivity of Sertoli cells. Additionally, ethanol exposure and SARS-CoV-2 infection already disrupts the barrier. Therefore, it is likely that together further barrier disruption will occur. Additionally, the proinflammatory effect of ethanol exposure on the barriers may prime the barriers for further insult by SARS-CoV-2 infection.

To test this, we would expose the in vitro formed barrier to ethanol for 5 days. qRT-PCR and ICC can be used to assess the presence and possible increase in viral entry proteins or upregulation of their gene expression. Following ethanol exposure, the barriers would then be exposed to SARS-CoV-2 variants of concern at an MOI of 0.01 for 6 hours as previously described. To observe if cytokines influence SARS-CoV-2 infection and barrier disruption,

proinflammatory cytokines can be supplemented prior to infection. Because some of these cytokines, like IL-8 and MCP-1, can increase barrier permeability it is likely that SARS-CoV-2 infection could further disrupt the barrier. In the testis, barrier disruption coupled with a proinflammatory state could have severe consequences to male reproductive health by allowing immune intrusion into the seminiferous tubule.

Several studies have shown that SARS-CoV-2 infection and alcohol abuse can alter semen concentration, sperm morphology, DNA aberration, cause defects in chromatin condensation, and alter sperm epigenetics.[353,390,522] However, most of this data comes from clinical reports and *in vivo* experiments. While valuable, this data does little to interrogate the mechanisms. We propose that both exposures be tested in the in vitro spermatogenesis model presented in Chapter 5. The previous iteration of this model has already been used to test multiple environmental exposures.[347,348,449] Greeson et al. have shown that the model can be used to replicate the impact of environmental exposures on the male gamete epigenome in a way that is consistent with human epidemiological studies.[348] With the improvements made to that model it now better mimics the testicular microenvironment, and should better mimic environmental exposures.

Exposing this new model to ethanol should result in altered spermatogenesis. This can be characterized by defects in chromatin, DNA aberration, and a decrease in DNA methylation at imprinted genes like H19 as previously observed.[522] Because it takes time to differentiate the stem cells into germ cells it is recommended to not begin exposures until day three, when most

of the cells have begun to differentiate. A downside to this model is that maturation is not completed. This means that things like sperm morphology and motility cannot be assessed. Additionally, as there are no seminal vesicle or prostate gland structures in this model, there are no ways to measure semen concentration. However, a solution to this is to measure haploid count as a proxy for semen concentration and sperm count. It is likely that haploid count would decrease in response to ethanol exposure. One downside to having Sertoli cells present in the culture is that it may be more difficult to measure direct effects of ethanol on the germ cells. Because we have previously shown that ethanol can negatively affect Sertoli cells, any observed damage to the germ cells could be caused, at least in part, by disrupting the interaction between Sertoli and germ cells. To account for this, it may be beneficial to forgo using Sertoli cells during experiments in which the Sertoli-germ cell interactions may interfere with the experimental outcome.

SARS-CoV-2 infection is also likely to alter spermatogenesis in this model. Specifically, we may see changes in haploid count and epigenetic alterations. Because it takes time to differentiate the stem cells into germ cells, it is recommended to not begin exposures until day three, when most of the cells have begun to differentiate. SARS-CoV-2 is likely to interact with early-stage germ cells because of the viral entry proteins that are present on them.[353] This direct interaction with the germ cells may lead to epigenetic alterations and poor spermatogenic outcomes like a decrease in cell count, a reduction in late stage spermatogenic markers, and changes to the chromatin. To test for infection, viral

RNA presence can be determined via qRT-PCR and a LAMP assay. Additionally, viral presence can be shown via ICC. Haploid cell count will have to be tested using a cell sorter within the BSL3 facility, as this requires live cells. Alterations to the germ cells may also occur from changes to the Sertoli cell signaling rather than direct germ cell interactions. Again, the Sertoli cells may be removed if they interfere with the experimental outcome. Being able to remove and integrate the Sertoli cells allows for a better understanding of the interactions that Sertoli cells have with germ cells and how environmental exposures may alter that interaction. Because of the indirect and systemic impact that SARS-CoV-2 infection can have on cells regardless of their infection status, the ability to remove the Sertoli cells may be helpful. In addition, to removing the Sertoli cells, it may be beneficial to replace the live virus with just the spike protein. This way, it can be observed if these alterations to the germ cells are from infection or just interactions between the spike protein and ACE2. Viruses tend to epigenetically target the immune system, by methylating genes related to immune function and interfering with RNAs associated with immune response.[512] Because of the preexisting immunosuppressive state of the testis, it is difficult to tell what impact SARS-CoV-2 infection will have. To test for methylation changes, the DNA will have to be isolated within the BSL3 facility before it is removed. Following DNA isolation, DNA methylation changes can be observed as described in Greeson et al.[348] It will be important to observe changes in methylation in imprinted regions as this can have a profound effect on the offspring.

COVID-19 is known to have multiple comorbidities and risk factors.[353] We explore how alcohol can lead to a worsening in barrier function during SARS-CoV-2 infection in bronchial cells in Chapter 7. Alcohol consumption and SARS-CoV-2 infection can individually affect reproductive health, including spermatogenesis, through various mechanisms. Alcohol abuse disrupts hormone regulation, impair testicular function, and affect sperm quality and production.[390] SARS-CoV-2 infection can cause inflammation and oxidative stress, disrupts hormone regulation, impair testicular function, and affects sperm quality and production.[353] Furthermore, chronic alcohol abuse can weaken the immune system, making individuals more susceptible to infection.

When these factors are combined, the potential for adverse effects on spermatogenesis could be higher.

To test how ethanol exposure and SARS-CoV-2 infection could impact spermatogenesis, we recommend using the model presented in Chapter 5. Because it takes time to differentiate the stem cells into germ cells it is recommended to not begin exposures until day three, when most of the cells have begun to differentiate. Infection will need to be confirmed via RNA presence and ICC. To test ethanol as a risk factor it would be best to begin with ethanol exposure and then later continue with SARS-CoV-2 infection. Starting ethanol on day 3 and SARS-CoV-2 infection on day 5 may be a good way mimic this type of exposure *in vitro*. As previously discussed, ethanol exposure to the Sertoli cells may impair their supportive function, potentially disrupting the nurturing environment necessary for spermatid development. Additionally, the Sertoli cells

may produce inflammatory cytokines in response to ethanol exposure. These inflammatory cytokines, like IL-6, may put the germ cells at further risk than if they were just exposed to ethanol. To test this, an ELIZA based cytokine panel should be performed. Furthermore, adding cytokines instead of ethanol will help to elucidate what role inflammation plays in germ cell damage and SARS-CoV-2 infection. Again, removing the Sertoli cells could be beneficial to better observe the direct impact of these two exposures on the germ cells. It is likely that these two exposures will cause oxidative stress and apoptosis. However, there is no good way to measure this in the BSL3 facility. Because both ethanol exposure and SARS-CoV-2 infection can induce epigenetic changes, it is likely that together they could alter epigenetic regulation and might affect gene expression patterns critical for spermatogenesis. To examine DNA methylation changes, DNA isolation must take place within the BSL3 facility before removal. After DNA isolation, DNA methylation changes can be analyzed as described in Greeson et al.[348] Monitoring DNA methylation alterations in imprinted regions is crucial, as these changes can significantly impact the offspring. The combined exposure is likely to cause a decrease in DNA methylation at imprinted genes like H19 as previously observed.[522] Overall, we expect ethanol exposure and SARS-CoV-2 infection to have a worse impact on spermatogenesis than just one of the exposures alone.

6.7 THERAPEUTIC IMPLICATIONS AND PREVENTATIVE STRATEGIES

Ethanol exposure and SARS-CoV-2 infection can indeed have implications for male reproductive health, particularly concerning the blood-testis

barrier and spermatogenesis. To combat these effects, therapeutic intervention may be necessary. Oxidative stress is likely to be a concern; however, it may be difficult to test for this given the restrictions of the facility. Regardless, antioxidant supplements could help mitigate the oxidative stress induced by both ethanol and viral infections, potentially protecting sperm and testicular cells. Given the role of inflammation in both conditions, anti-inflammatory medications might be considered to manage immune responses and reduce inflammation in the reproductive system. While not readily studied in our system because of the lack of Leydig cells, hormonal alterations are also of concern. If hormonal imbalances occur due to testicular damage, hormone replacement therapies might be considered to restore normal hormonal levels. These therapeutic interventions should take place if patients are unable to conceive after one year, have low sperm count, and have had a history of chronic alcohol abuse or recent SARS-CoV-2 infection.

While therapeutic interventions may restore the individual's fertility, it is best if the individual did not have these insults to begin with, as these damages may be irreversible or cause damage to the next generation if left untreated. Education and awareness are often the best ways to prevent harm. Public awareness campaigns can be used to educate the public about potential risks of excessive alcohol consumption and the importance of taking protective measures against SARS-CoV-2 infection. Making lifestyle modifications can have a profound impact on protecting male reproductive health. Encouraging moderate alcohol consumption or abstinence can significantly reduce the risk of alcohol-

induced reproductive damage. Maintaining a healthy lifestyle by exercising regularly, keeping a balanced diet, and managing stress can boost overall immunity and reproductive health. Using personal protective equipment in high-risk environments can reduce the risk of SARS-CoV-2 infection. Early detection and treatment is also vital. Regular health check-ups can help in the early detection of any reproductive health issues, allowing for timely intervention and management. As variants of concern continue to emerge, vaccine development will play a pivotal role in protecting people and male reproductive health. Research into effective vaccines against SARS-CoV-2 can significantly reduce the risk of infection. Vaccination not only protects against the virus but can also prevent potential reproductive complications associated with the infection. It is important to note that these strategies are general and may evolve with ongoing research.

CHAPTER 7

EPILOGUE: CHRONIC ALCOHOL USE PRIMES BRONCHIAL CELLS FOR BARRIER DYSFUNCTION AND ALTERED INFLAMMATORY RESPONSE DURING SARS-COV-2 INFECTION[6]

[6]524 Easley, K. F. *et al.* Chronic alcohol use primes bronchial cells for altered inflammatory response and barrier dysfunction during SARS-CoV-2 infection. *American Journal of Physiology-Lung Cellular and Molecular Physiology* **0**, null, doi:10.1152/ajplung.00381.2022. Reprinted here with permission of the publisher under Creative Commons license CC BY 4.0 http://creativecommons.org/licenses/by/4.0/.

Chronic alcohol use primes bronchial cells for barrier dysfunction and altered inflammatory response during SARS-CoV-2 infection

Kristen F. Easley[1], R. Clayton Edenfield[2,3], Megan Jane Lott[2], Ryan C. Reed[1], Jayasri Das Sarma[4,5], Ashish J. Mehta[1,6], Bashar S. Staitieh[1], Erin K. Lipp[2], In Ki Cho[2,3], Scott K. Johnson[7], Cheryl A. Jones[7], Anne-Gaelle Bebin-Blackwell[7], Joshua M. Levy[8], S. Mark Tompkins[7], Charles A. Easley 4th[2,3], Michael Koval[1,9]

[1]Division of Pulmonary, Allergy, Critical Care and Sleep Medicine, Emory University School of Medicine, Atlanta, GA, US

[2]Department of Environmental Health Science, College of Public Health, University of Georgia, Athens, GA, US

[3]Regenerative Bioscience Center, University of Georgia, Athens, GA, US

[4]Department of Biological Sciences, Indian Institute of Science Education and Research Kolkata, Mohanpur, Nadia, India

[5]Department of Ophthalmology, University of Pennsylvania, Philadelphia, PA, US.

[6]Atlanta Veterans Affairs Health Care System, Decatur, GA, US

[7]Center for Vaccines and Immunology, University of Georgia, Athens, GA, US

[8]Department of Otolaryngology, Emory University School of Medicine, Atlanta, GA, US

[9]Department of Cell Biology, Emory University School of Medicine, Atlanta, GA, US

Address correspondence to:
Michael Koval, PhD
Emory University School of Medicine
Division of Pulmonary, Allergy, Critical Care and Sleep Medicine
205 Whitehead Building
615 Michael Street
Atlanta, Georgia 30322
United States

Phone: 404-712-2976
Fax: 404-712-2974

Email: mhkoval@emory.edu

Running title: Impact of alcohol on SARS-CoV-2 infection

Keywords: COVID-19, Alcohol Use Disorder, Airway Epithelia, inflammation, tight junction

7.1 ABSTRACT

Alcohol Use Disorder (AUD) is a significant public health concern and people with AUD are more likely to develop severe acute respiratory distress syndrome (ARDS) in response to respiratory infections. To examine whether AUD was a risk factor for more severe outcome in response to SARS-CoV-2 infection, we examined early responses to infection using cultured differentiated bronchial epithelial cells derived from brushings obtained from people with AUD or without AUD. RNAseq analysis determined that cells from people with AUD had a distinct gene expression profile from people without AUD. Bronchial epithelial cells from AUD patients showed a significant decrease in barrier function 72 h post infection, as determined by transepithelial electrical resistance. In contrast, barrier function of non-AUD cells was enhanced 72 h after SARS-CoV-2 infection. AUD cells showed less claudin-7 colocalizing with zonula occludens-1 than non-AUD cells, indicative of disorganized tight junctions. However, both AUD and non-AUD cells showed decreased β-catenin expression following SARS-CoV-2 infection. To determine the impact of AUD on the inflammatory response to SARS-CoV-2 infection, cytokine secretion was measured by multiplex analysis. SARS-CoV-2-infected AUD bronchial cells had enhanced secretion of multiple pro-inflammatory cytokines including TNFα, IL-1β and IFNγ as opposed to non-AUD cells. By contrast, secretion of EGF and GM-CSF, cytokines that can be barrier protective, was enhanced for non-AUD bronchial cells. Taken together, these data support the hypothesis that AUD is a risk factor for COVID-19, where alcohol primes airway epithelial cells for

increased barrier dysfunction and increased inflammation in response to infection by SARS-CoV-2.

7.2 INTRODUCTION

COVID-19 is caused by severe acute respiratory syndrome coronavirus 2 (SARS-CoV-2) and is associated with respiratory failure in the most severe cases [525,526]. It is estimated that a third of COVID-19 patients requiring mechanical ventilation do not survive [527]. Several comorbidities are associated with increased COVID-19 severity, including obesity, diabetes and other chronic diseases [528]. It has long been appreciated that alcohol use disorder (AUD) is a risk factor for increased severity of lung disease [529-531]. This includes increased susceptibility to infectious pneumonia [532-535] and poor outcomes in acute respiratory distress syndrome (ARDS) [536]. As ARDS is a significant pathological consequence of SARS-CoV-2 infection [537], it is noteworthy that people with AUD and COVID-19 have been shown to have a higher rate of hospitalization and mortality [538], suggesting that AUD is a risk factor for increased severity of COVID-19 related illness [539]. Compounding the potential impact of AUD on patient outcomes is the added stress of experiencing the COVID-19 pandemic, which has been associated with substance abuse, including increased alcohol consumption [540,541]. However, the mechanisms by which AUD influences lung epithelial responses to SARS-CoV-2 are not known at present.

Numerous factors associated with AUD contribute to increased inflammation and overall poor lung health. Patients with AUD and animal models of AUD show higher levels of inflammatory cytokines and chemokines in the

airway [542-545], alveolar macrophage dysfunction [546,547] and disruption of the lung microbiome [548]. Additionally, chronic alcohol exposure results in lung epithelial barrier dysfunction, which predisposes ARDS patients to more severe pulmonary edema [549,550]. For instance, lung epithelial barrier permeability is regulated by the apical junctional complex, composed of tight junctions and adherens junctions [551-553]. The impact of alcohol exposure on the expression, organization, and function of lung epithelial tight junction proteins can be demonstrated using in vitro models [545,554-556]. Of note, alveolar epithelial cells isolated from alcohol-fed animals have barrier dysfunction that persists in tissue culture, even in the absence of added ethanol [557].

It is clear that SARS-CoV-2 has the capacity to infect multiple epithelia throughout the respiratory tree [558]. However, whether the impact of AUD on SARS-CoV-2 infection is due to the effects of alcohol on lung epithelia has not been determined. Since AUD is a significant risk factor for ARDS in general [559] and had higher rates of hospitalization following infection with SARS-CoV-2 [538], we hypothesize that AUD would sensitize lung epithelial cells to the effects of SARS-CoV-2 infection.

It is well established that cultured human lung epithelial cells have significant utility for the study of the effects of SARS-CoV-2 infection [560-567], suggesting that an in vitro model would shed light on the impact of AUD on the effects of SARS-CoV-2 infection on lung epithelial cells. To do this, we isolated bronchial brushings from patients with and without AUD, expanded them in a basal cell state and then differentiated them using an air liquid interface (ALI)

culture system using methods previously established by our laboratory [568]. The cells were infected with SARS-CoV-2 and the effect on barrier function, junction protein expression and inflammatory cytokine production were measured. We found that after infection, cells from patients with AUD had a significant decrease in TER and showed enhanced secretion of several pro-inflammatory cytokines including TNFα, IL-1β and IFNγ as compared with non-AUD cells. By contrast, infected non-AUD cells produced significantly higher levels of GM-CSF and EGF than AUD cells, which can have an anti-inflammatory, barrier protective effect on epithelial cells. Taken together, these data support the hypothesis that AUD is a risk factor for COVID-19 and that this is, in part, due to an effect of chronic alcohol exposure on airway epithelial cells.

7.3 MATERIALS AND METHODS

Donor consent. Research involving human research participants was performed in accordance with the Declaration of Helsinki guidelines. All human subject protocols were reviewed and approved by the Emory University Institutional Review Board and the Atlanta Veterans Affairs Health Care System Research and Development Committee. Potential subjects for study enrollment were screened using the Short Michigan Alcohol Screening Test and AUD Identification Test [569,570]. Individuals with a history of AUD were recruited from the Substance Abuse Treatment Program at the Atlanta Veterans Affairs Health Care System, and otherwise healthy control subjects were recruited from general Veterans Affairs medical clinics [571]. Additional subject inclusion criteria included active alcohol abuse, in which the last alcoholic drink was <8d prior to

bronchoscopy. Subjects were excluded if they primarily abused substances other than alcohol, were HIV positive, were >55 y old, or had abnormal chest radiographs.

Airway epithelial cell culture and infection. Cells from bronchial brushings were expanded in co-culture with irradiated 3T3 fibroblast feeder cells in F+Y reprogramming media (FYRM) as previously described [568]. FYRM was changed every other day until the cells were ~70-90% confluent and then the cells were isolated by first removing the 3T3 feeder layer using calcium/magnesium-free phosphate buffered saline supplemented with 1 mM EDTA (PBS/EDTA), followed by detaching epithelial cells by incubating with Accutase (Sigma-Aldrich #A6964) at RT for 10 minutes. Cells were then centrifuged and frozen as P1 stocks. For experiments, cells were thawed, expanded using FYRM and then seeded on Transwell permeable supports pre-coated with type IV collagen (Sigma-Aldrich #C7521) at a density of 150,000 cells per 6.5 mm Transwell (Costar #3450, 24 well) or 350,000 cells per 12 mm Transwell (Costar # 3460, 12 well) in E-ALI medium [568]. E-ALI medium was based on previous formulations with modifications to glucose (150 mg/dl; 8.3 mM), $CaCl_2$ (1 mM), heparin (2 µg/ml), L-glutamine (2.5 mM), hydrocortisone (960 mg/ml), bovine pituitary extract (20 µg/ml), and Mg^{2+} (0.5 µM). E-ALI medium is changed every other day with washing of the apical surface. Using this protocol, monolayers were fully differentiated 14 days after transitioning to ALI.

Differentiated cells were infected at MOI 0.1 for 6h with SARS-CoV-2 USA-WA1/2020 (BEI Resources, # NR-52281), consistent with previously used conditions that minimize overt cell death within a three day window [563]. The cells were then washed with ALI medium and further incubated for 72h. At 6, 24, 48 and 72h post infection, apical surfaces were washed with 0.2 ml E-ALI and 0.5 ml basal medium was collected, banked at -20^{o}C for further analysis and the cells were re-fed. Virus production by infected cells was determined by analysis of plaque forming units (PFU) present in cell culture medium. In brief, at 24, 48 and 72 h post infection, the apical surface was washed with 150 µl medium/well, and basolateral medium was also collected. To measure PFUs, a dilution series of the media was produced and plated onto confluent Vero E6 cells (100 µl/well) that were incubated for 72 h and then stained with crystal violet. Data are presented as total PFUs secreted over the entire 72 h period. In all cases, virus shedding was only detected in apical washes, there was no virus present in basolateral media. In some experiments, virus infection was confirmed using a LAMP assay kit (New England BioLabs, # E2019S) according to the manufacturer's instructions.

RNA-seq Analysis. Differentiated non-infected AUD and non-AUD cells harvested from Transwells were flash frozen and submitted to Azenta Life Sciences for RNA extraction and bulk RNA-Seq. Sequencing Configuration: library preparation, Illumina, 2x150bp, ~350M raw paired-end reads (~105GB), single index, per lane. RNA-seq reads were analyzed for differential gene expression, alternative splicing and gene ontology (GO) enrichment analysis.

The heat map of differentially expressed genes (p-adj. value < 0.05) was generated using Galaxy Project. All samples had a similar distribution of normalized read counts (**Supplemental Figure 7.1**).

Transepithelial Resistance (TER) and Dye Flux. TER was measured using an EVOM Voltohmmeter (World Precision Instruments, #EVOM2). Before measuring, cells were washed with Dulbecco's Phosphate Buffered Saline containing Ca^{+2} and Mg^{+2} (DPBS, Corning # 21-030-CV) followed by a 15-minute incubation at 37^{o}C in Ringer's solution (140 mM NaCl, 5 mM KCl, 0.36 mM K_2HPO_4, 0.44mM KH_2PO_4, 1.3 mM $CaCl_2 \bullet 2\ H_2O$, 0.5 mM $MgCl_2 \bullet 6\ H_2O$, 4.2 mM $NaHCO_3$, 10 mM Na HEPES, 10 mM glucose). Cells that had a pre-infection TER at least 750 Ohm x cm^2 or higher were used for further analysis. To facilitate comparison between different cells, TER values were normalized to pre-infection values obtained at t = 0 h for each condition examined. Dye Flux measurements were performed using calcein and 10 kDa Texas Red dextran and quantified as previously described [380].

Immunofluorescence Microscopy. Cells on Transwell permeable supports were rinsed with DPBS then fixed with 4% paraformaldehyde (PFA) for 10 minutes at RT in the dark. This was followed by a DPBS rinse and 2 minutes of fixation in 1:1 methanol/acetone at RT. Cells were then washed 3x with DPBS. Cells were permeabilized in 0.5% Triton X-100/DPBS++ for 5 minutes, followed by two 5-minute incubations in blocking solution (0.5% Triton X-100 and 5% Goat

serum in DPBS). Primary antibodies were added (diluted in 3% BSA in DPBS) and incubated overnight at 4ºC. The cells were washed 3x with DPBS and then incubated for 1h at RT with fluorescent secondary antibodies diluted in 3% BSA. The secondary antibodies were removed and the cells were further incubated for 10 minutes in Hoechst 33342 (ThermoFIsher # 62249) diluted 1:1000 in DPBS to stain nuclei. Cells were washed 3x with DPBS, and Transwells were mounted on slides using Vectashield mounting solution (Vector Labs #H-1000-10).

Primary antibodies used for immunofluorescence were: mouse anti-ZO-1 (Invitrogen #339100, 1:500 dilution), rabbit anti-β-catenin (Abcam ab32572, 1:400 dilution), Rabbit anti-claudin 7 (Abcam #ab27487, 1:200 dilution). Secondary antibodies used for immunofluorescence were: Alexa fluor 568 goat anti-mouse (Invitrogen A11031, 1:1500 dilution), Alexa fluor 488 goat anti-rabbit (Invitrogen #A11034, 1:1500 dilution), Alexa fluor 488 anti-mouse (Invitrogen #A11029, 1:1500 dilution), Alexa fluor 568 anti-rabbit (Invitrogen #A11036, 1:1500 dilution). Images were taken using either a Nikon Ti Eclipse with epifluorescence and processed using 3D deconvolution or a Nikon A1R confocal and processed using Nikon Elements and Image J.

Cytokine Analysis. Apical washes and basolateral medium that were collected at 6, 24, 48 and 72h after SARS-CoV-2 infection were analyzed and the total amount of cytokine secreted was determined by measuring cytokine concentration multiplied by total volume. E-ALI medium collected at each time-

point following SARS-CoV-2 infection was analyzed using the MILLIPLEX Human Cytokine / Chemokine / Growth Factor Panel A kit (Cat # HCYTA-60K-PX38) according to the manufacturer's instructions, modified to accommodate the BSL-3 facility. After Streptavidin-Phycoerythrin incubation, all wells on the assay plate were washed twice with assay buffer followed by the addition of 200 µl 4% PFA and the samples were further incubated for 17 h 4^{o}C to denature any virus that was present prior to analysis. Data represent the total pg secreted at different timepoints and are also presented as the total pg secreted apically or basolaterally over a 72h period.

Statistics. Statistics were calculated using Graphpad Prism 8.0 and significance was determined using ordinary one-way ANOVA with Sidak's multiple comparison test (aggregate TER) the Kruskal Wallis one-way ANOVA test (cytokine analysis) or the one-way ANOVA test with Fisher's LSD Test (barrier function analysis).

7.4 RESULTS: RNA-SEQ REVEALS THAT AUD AND NON-AUD AIRWAY CELLS HAVE DIFFERENTIAL GENE EXPRESSION PROFILES

In this study, we used cells derived from airway brushings obtained from three individuals with AUD and three non-AUD individuals. The best matched samples available consisted of lung brushings from Black or African American males (**Table 7.1**). Smoking status varied for each subject but in aggregate, these samples had comparable representative non-smokers and smokers. These airway epithelial cells were proliferated as basal cells and then differentiated using ALI cultures as described in Methods.

Sample ID	Age	Sex	Height, in.	Weight, lbs	BMI	Race	Ethnicity	Current Smoker?	Pack Year History
AUD 1	50	Male	65	145	24.1	Black or African American	Not Hispanic or Latino	Yes	3
AUD 2	53	Male	71	201	28.0	Black or African American	Not Hispanic or Latino	Yes	26
AUD 3	51	Male	71	173	24.1	Black or African American	Not Hispanic or Latino	No	0
AUD 4	43	Female	69	263	38.8	Black or African American	Not Hispanic or Latino	No	0
Non-AUD 1	20	Male	77	195	23.1	Black or African American	n/a	No	0
Non-AUD 2	29	Male	66	172	27.8	Black or African American	Not Hispanic or Latino	Yes	4
Non-AUD 3	58	Male	66	135	21.8	Black or African American	Not Hispanic or Latino	Yes	45

Table 7.1: Sample donor characteristics

RNAseq, barrier function and cytokine analysis were done using cells from donors AUD 1, AUD 2, AUD 3, non-AUD 1, non-AUD 2, and non-AUD 3. Immunofluorescence analysis was done using cells from donors AUD 1, AUD 2, AUD 4, non-AUD 1, non-AUD 2, and non-AUD 3. AUD, alcohol use disorder; BMI, body mass index.

To determine whether there were AUD dependent differences in gene expression, we analyzed the cultures by RNA-seq. Normalized read counts were comparable for all six samples (**Supplemental Figure 7.1**). As shown by hierarchical clustering (**Figure 7.1A**), the samples stratified by AUD status showed distinct patterns of upregulated and downregulated genes. Further analysis by volcano plot showed that there were 117 up-regulated genes and 47 down-regulated genes in AUD cells compared to non-AUD cells (**Figure 7.1B**). A full list of differentially expressed (DE) genes can be found in Supplemental Table 1. Note that both AUD and non-AUD cells were cultured in the absence of added ethanol in the medium, indicating that any changes in gene expression were persistent during the cell culture and differentiation process, likely due to epigenetic reprogramming as a result of AUD.

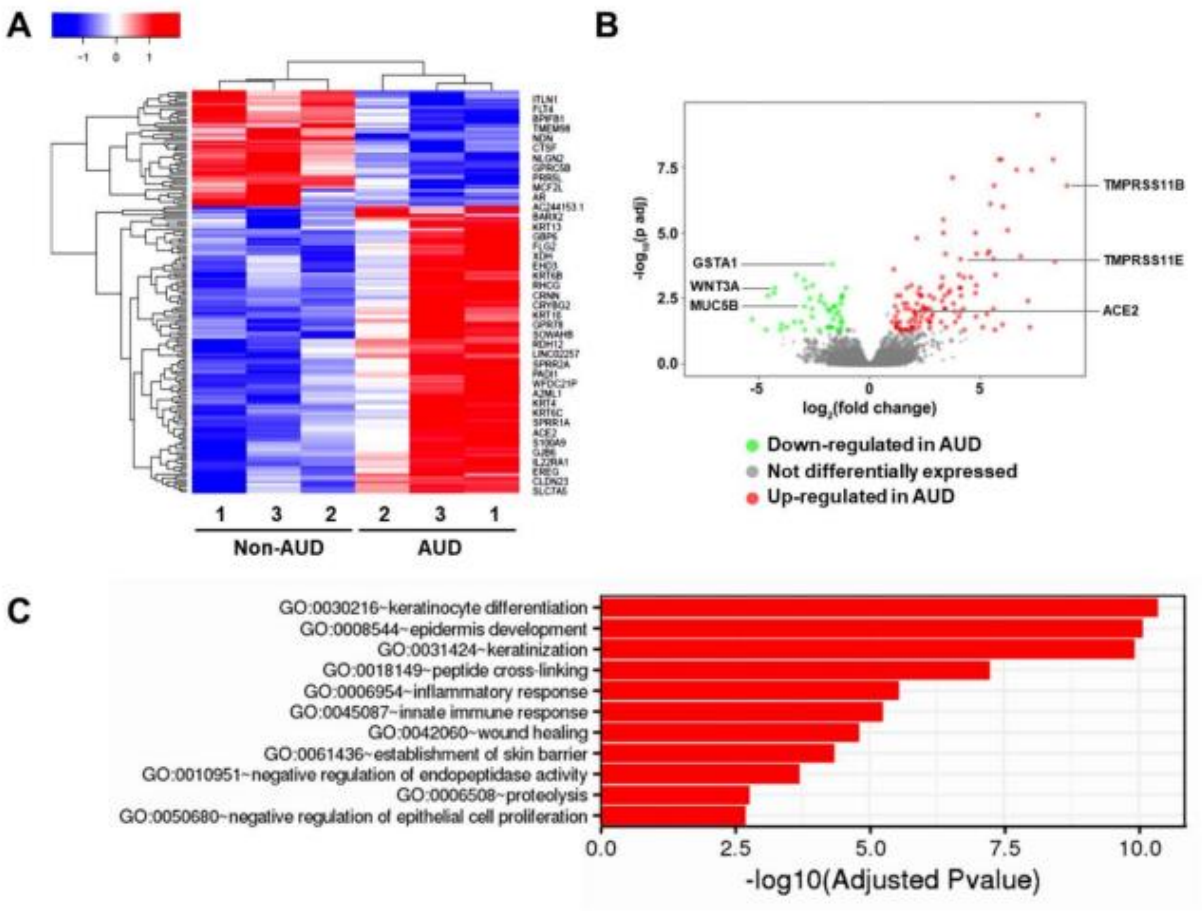
A
-1
0
1
1
3
2
2
3
1
Non-AUD
AUD
B
-log10(p adj)
7.5
5.0
2.5
0.0
-5
0
5
log2(fold change)
TMPRSS11B
TMPRSS11E
ACE2
GSTA1
WNT3A
MUC5B
Down-regulated in AUD
Not differentially expressed
Up-regulated in AUD
C
GO:0030216~keratinocyte differentiation
GO:0008544~epidermis development
GO:0031424~keratinization
GO:0018149~peptide cross-linking
GO:0006954~inflammatory response
GO:0045087~innate immune response
GO:0042060~wound healing
GO:0061436~establishment of skin barrier
GO:0010951~negative regulation of endopeptidase activity
GO:0006508~proteolysis
GO:0050680~negative regulation of epithelial cell proliferation
0.0
2.5
5.0
7.5
10.0
-log10(Adjusted Pvalue)

Figure 7.1: Differentiated bronchial cells from non-AUD and AUD patients were subject to RNA sequencing.

(A) Heat map representation of all 164 differentially expressed genes. Down-regulated genes are in blue and up-regulated genes are in red, in respect to AUD cells. Select DE genes are located on right. (B) Volcano plot representation of all genes. Green dots represent down-regulated genes in AUD cells, red dots represent up-regulated genes in AUD cells and grey dots represent genes that were not differentially expressed. SARS-CoV-2 receptor genes were upregulated in AUD cells. Genes required for proper function and maintenance of bronchial cells were down-regulated in AUD cells. (C) Differentially expressed genes were clustered by their gene ontology. Enrichment of gene ontology terms was tested using Fisher exact test (GeneSCF v1.1-p2). Shown are the top 11 significantly enriched gene ontology terms with an adjusted P-value less than 0.05 in the differentially expressed gene set.

Shown in **Figure 7.1C** is Gene Ontology (GO) enrichment analysis reflecting the top 11 GO terms, of which 5 relate to epidermal differentiation and barrier function and 2 relate to inflammation. The DE genes categorized into these GO categories can be found in **Tables 7.2 and 7.3**. Among the epidermally related upregulated genes are small proline rich proteins (SPRRs) that are largely expressed in the epidermis and have bactericidal properties [572]. Moreover, SPRR3 has been found to play a role in allergic airway inflammation, where knockdown of SPRR3 reduced the number of inflammatory cells in the BAL fluid [572].

Gene Name	Log 2 Fold Change	Adj. *P* Value
ABCA12	2.09	0.02
CALML5	4.57	0
CRNN	7.32	0
EMP1	2.29	0.03
EREG	2.2	0
FLG2	5.11	0.04
GRHL3	2.27	0
KLK6	3.85	0.01
KLK7	3.75	0
KRT10	1.66	0.05
KRT13	3.87	0.03
KRT16	3.23	0.02
KRT24	8.36	0
KRT4	3.63	0
KRT6B	3.79	0
KRT6C	3.27	0
KRT78	6.64	0
SCEL	2.42	0.01
SPINK5	4.83	0
SPINK7	5.66	0.05
SPRR1A	6.23	0
SPRR1B	4.06	0
SPRR2A	5.96	0
SPRR2D	5.62	0
SPRR2E	5.68	0
SPRR3	7.59	0
TGM1	2.73	0.02

Table 7.2: Genes upregulated by AUD related to epidermal differentiation.

Alphabetically sorted list of genes enriched in AUD cells, as determined by Gene Ontogeny (GO) analysis for GO:0030216: keratinocyte differentiation, GO:0008544: epidermis development, GO:0031424: keratinization, GO:0018149: peptide cross-linking, GO:0061436: establishment of skin barrier.

Gene Name	Log 2 Fold Change	Adj. *P* Value
BDKRB2	1.24	0
C6	2.75	0.01
CLEC7A	1.28	0.01
ECM1	3.57	0
IL1RN	2.07	0.01
IL22RA1	2.72	0
IL36A	6.82	0
IL36RN	4.04	0.01
KRT16	3.23	0.02
MGLL	2.29	0
PGLYRP4	1.22	0.04
S100A12	4.13	0
S100A8	4.78	0
S100A9	2.28	0.01

Table 7.3: Genes upregulated by AUD related to inflammation.

Alphabetically sorted list of genes enriched in AUD cells, as determined by Gene Ontogeny (GO) analysis for GO:0030216: keratinocyte differentiation, GO:0008544: epidermis development, GO:0031424: keratinization, GO:0018149: peptide cross-linking, GO:0061436: establishment of skin barrier.

The genes upregulated by AUD related to inflammation (**Table 7.3**) reflect a relatively mild phenotype and include receptor antagonist genes such as IL1RN and IL36RN. Genes classically associated with inflammation, such as TNFα, IL-1β, IFNγ and IL-6, were comparably expressed by AUD and non-AUD cells at baseline. However, there were some proinflammatory genes that were upregulated, most notably S100A8, S100A9 and S100A12. These genes are damage-associated molecular pattern (DAMP) molecules [573], that have been linked to several pathological states, including severe asthma [574,575].

In addition, AUD cells had decreased expression of glutathione S-transferase alpha 1 (GSTA1), WNT3A and MUC5B, which are enhanced in non-AUD cells. Since these genes play roles in protection from oxidative stress, airway repair and clearance of respiratory particulates and pathogens, respectively [576,577], the decreased levels of expression of these genes is consistent with AUD airway epithelial cells being sensitized to injury and/or infection.

Among the genes up-regulated in AUD are several that have been implicated in SARS-CoV-2 infection, including ACE2, which encodes the receptor that binds the virus spike protein, and two TMPRSS isoforms: TMPRSS11B and TMPRSS11E. While the TMPRSS2 isoform is best known for activating the SARS-CoV-2 spike protein, one study found enhanced fusion between 293 cells expressing SARS-CoV-2 S and 293 cells expressing hACE2 and TMPRSS11E [578]. Taken together, these data suggested that AUD status of donor cells is an

independent determinant of gene expression of bronchial epithelial cells that may impact their response to SARS-CoV-2 infection.

7.5 RESULTS: SARS-COV-2 INFECTION IMPAIRS BARRIER FUNCTION OF AUD CELLS

Prior to infection, we measured transepithelial resistance (TER) and paracellular flux of calcein and 10 kDa Texas Red dextran as indices of barrier integrity. By and large, barrier function was comparable when comparing bronchial epithelial cells derived from AUD and non-AUD brushings, with some individual variability (**Figure 7.2**). This is in contrast to alveolar epithelial cells, which consistently have impaired barrier function when chronically exposed to alcohol in vivo [554].

The cells with TER values shown in **Figure 7.2A** were infected with the Washington strain of SARS-CoV-2 at 0.1 MOI. TER values were measured at intervals over the course of a 72h time course and normalized to baseline values to facilitate comparisons for each condition examined (**Figure 7.3**). In each of the three different AUD isolates, SARS-CoV-2 infection caused a significant decrease in TER (**Figure 7.3A-C**). On the other hand, the three different non-AUD cell isolates showed an increase in TER 72 h following infection (**Figure 7.3D-F**).

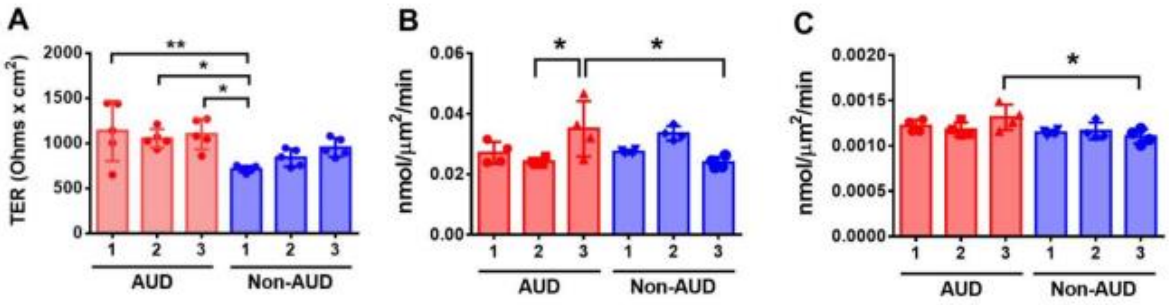
A
TER (Ohms x cm^2)
2000
1500
1000
500
0
**
*
*
1 2 3 1 2 3
AUD
Non-AUD
B
nmol/µm^2/min
0.06
0.04
0.02
0.00
*
*
1 2 3 1 2 3
AUD
Non-AUD
C
nmol/µm^2/min
0.0020
0.0015
0.0010
0.0005
0.0000
*
1 2 3 1 2 3
AUD
Non-AUD

Figure 7.2: Baseline barrier function of AUD and non-AUD airway cells.

A. TER values of all samples immediately prior to infection. Non-AUD 1 had a lower TER compared to AUD 1 (**p=0.007) and AUD 2 (*p=0.04) and AUD 3 (*p=0.01). n=3 biological replicates per condition consisting of 5 Transwells per group. Values represent mean + SD in each case. B,C. Cells were incubated with a mixture of calcein (B) and 10 kDa Texas Red Dextran (C) over a 2 h period and the rate of flux from the apical to basolateral surface was determined. B. the amount of calcein flux was higher for AUD 3 vs AUD2 (*p=0.029) and vs non-AUD 3 (* p=0.024). C the amount of 10kDa Texas Red Dextran flux was higher for AUD 3 than non-AUD 3 (* p=0.032). n=3 biological replicates per condition consisting of 4 Transwells per group.

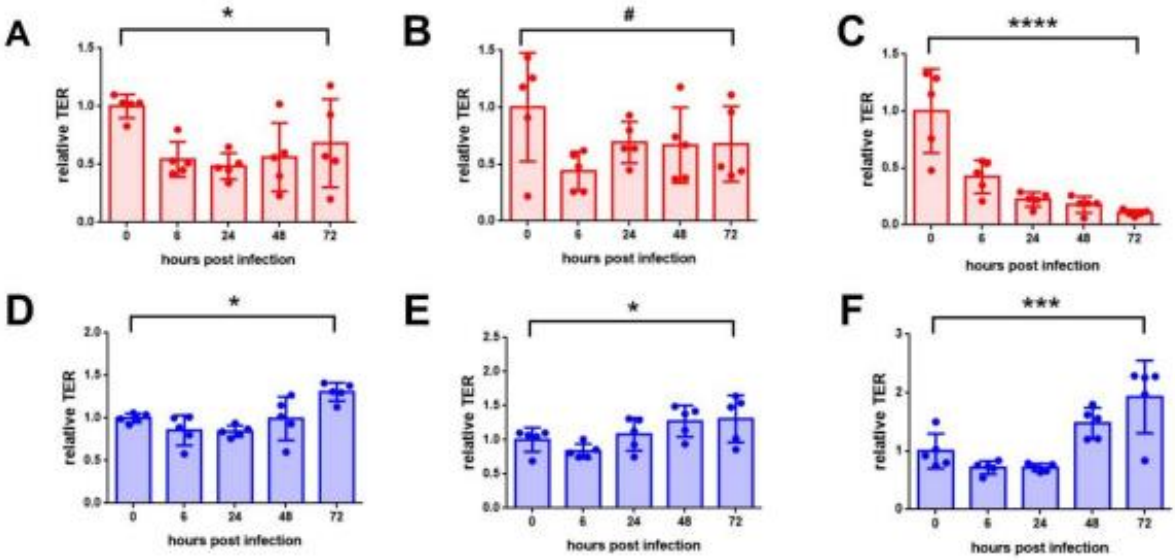
A
B
C
D
E
F
relative TER
hours post infection
0
6
24
48
72
*
#
****
***

Figure 7.3: AUD cells have impaired barrier function following SARS-CoV-2 infection.

Differentiated bronchial cells from AUD (A-C, red) and non-AUD (D-F, blue) subjects were infected with SARS-CoV-2. TER was measured immediately prior to infection (t=0) and at 6, 24, 48 and 72 h post infection, normalized to values at t=0. AUD cells showed decreased barrier function 72h after infection (A, * p=0.04; B, # p=0.12; C, **** p< 0.0001). By contrast, non-AUD cells showed increased barrier function 72 h after infection (D, ** p=0.0047; E, # p=0.051; F, *** p=0.0003). n=3 biological replicates consisting of 5 Transwells per group. Values represent mean $\pm$ SD in each case.

Differences in TER post infection did not correlate with the level of virus production, since infected AUD cells produced comparable or lower levels of SARS-CoV-2 as compared with infected non-AUD cells (**Figure 7.4**). Note that virus secretion was only detected from the apical surface; there was not any virus detectable in the basolateral medium. The lack of detectable basolateral virus was consistent with Dye Flux measurements from infected cells, which did not show enhanced paracellular substrate diffusion in response to infection (**Supplemental Figure 7.2**), in contrast to TER measurements (**Figure 7.3**).

Taken together, these data support a model where the AUD bronchial epithelial cell junctions are more sensitive to SARS-CoV-2 infection than non-AUD cell junctions. To determine whether the differential effects of SARS-CoV-2 infection on TER were due to differences between AUD and non-AUD cells in epithelial junction organization, we used confocal and deconvolution immunofluorescence microscopy (**Figure 7.5**). Over the course of our experiments, the tight junction scaffold protein zonula occludens-1 (ZO-1) remained predominantly tight junction-associated. Also, total levels of ZO-1 were unchanged by SARS-CoV-2 infection (**Figure 7.5E**).

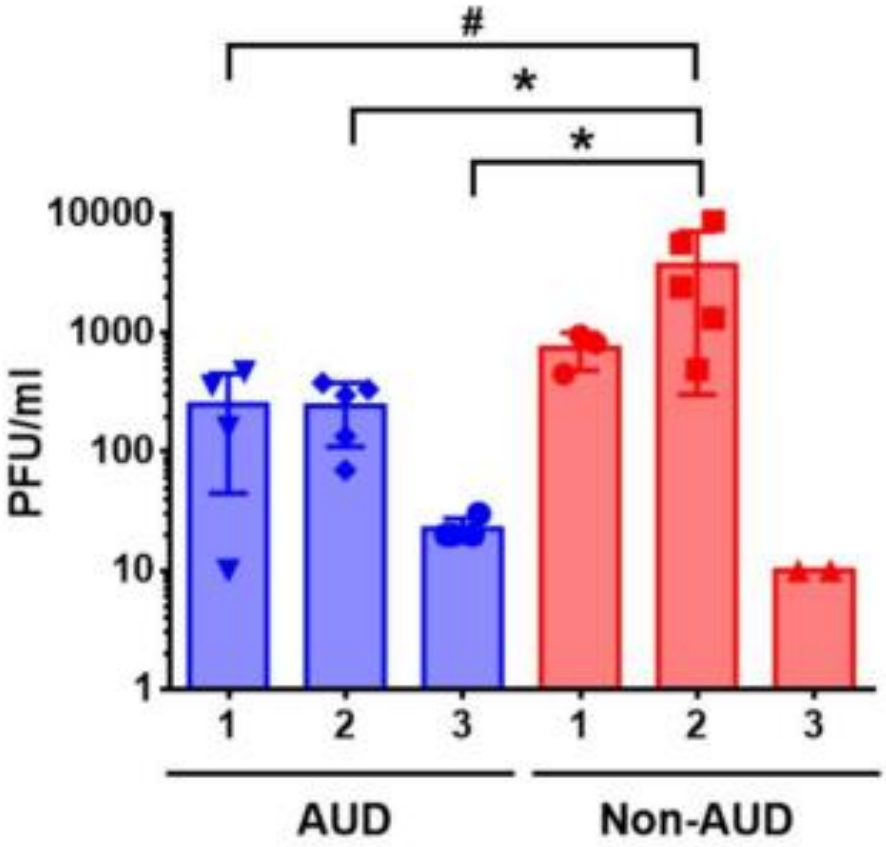
#
*
*
10000
1000
100
10
1
PFU/ml
1
2
3
1
2
3
AUD
Non-AUD

Figure 7.4: Virus shedding from infected cells.

AUD and non-AUD Cells were infected with SARS-CoV-2 at MOI 0.1 for 6 h. Medium was collected from apical surface washes over a 72h period and total plaque forming units (PFU) were determined using Vero E6 cells as described in Methods. Non-AUD 2 cells showed the highest levels of virus shedding, which was higher than the amount of virus shed from AUD cells (*p=0.04; # p=0.06) n=3 biological replicates consisting of 2-5 Transwells per group. Samples of basolateral medium did not contain detectable levels of SARS-CoV-2.

We also examined one of the major transmembrane tight junction proteins responsible for bronchial epithelial barrier function, claudin-7 [579]. At baseline, there was significantly more claudin-7 present in non-AUD than in AUD bronchial epithelial cells (**Figure 7.5F**), potentially rendering the AUD cells more sensitive to barrier dysfunction. Note that most of the claudin-7 expressed by bronchial cells is present on the lateral plasma membrane (**Figure 7.5A**, xz), that is not colocalized with ZO-1 and does not contribute to barrier function [580]. Infection eliminated the significance of the difference in total claudin-7, however, having less ZO-1 associated with tight junctions in infected AUD cells (**Figure 7.5C**) is anticipated to result in decreased barrier function.

In contrast to ZO-1 and claudin-7, levels of β-catenin, an adherens junction scaffold protein, were significantly diminished in response to SARS-CoV-2 infection (**Figure 7.5B, D, G**). A similar effect of SARS-CoV-2 on β-catenin expression has been reported for infected endothelial cells [581,582] and has been implicated in the disruption of vascular barrier function due to COVID-19. However, infection had a similar effect on total β-catenin in AUD and non-AUD cells, suggesting that this does not account for the differential effect of infection on barrier function of bronchial epithelial cells. Instead, the decrease in airway epithelial β-catenin following SARS-CoV-2 infection more likely reflects another cell response that is unaffected by AUD, such as translocation of junction localized β-catenin to mediate wnt signaling [583].

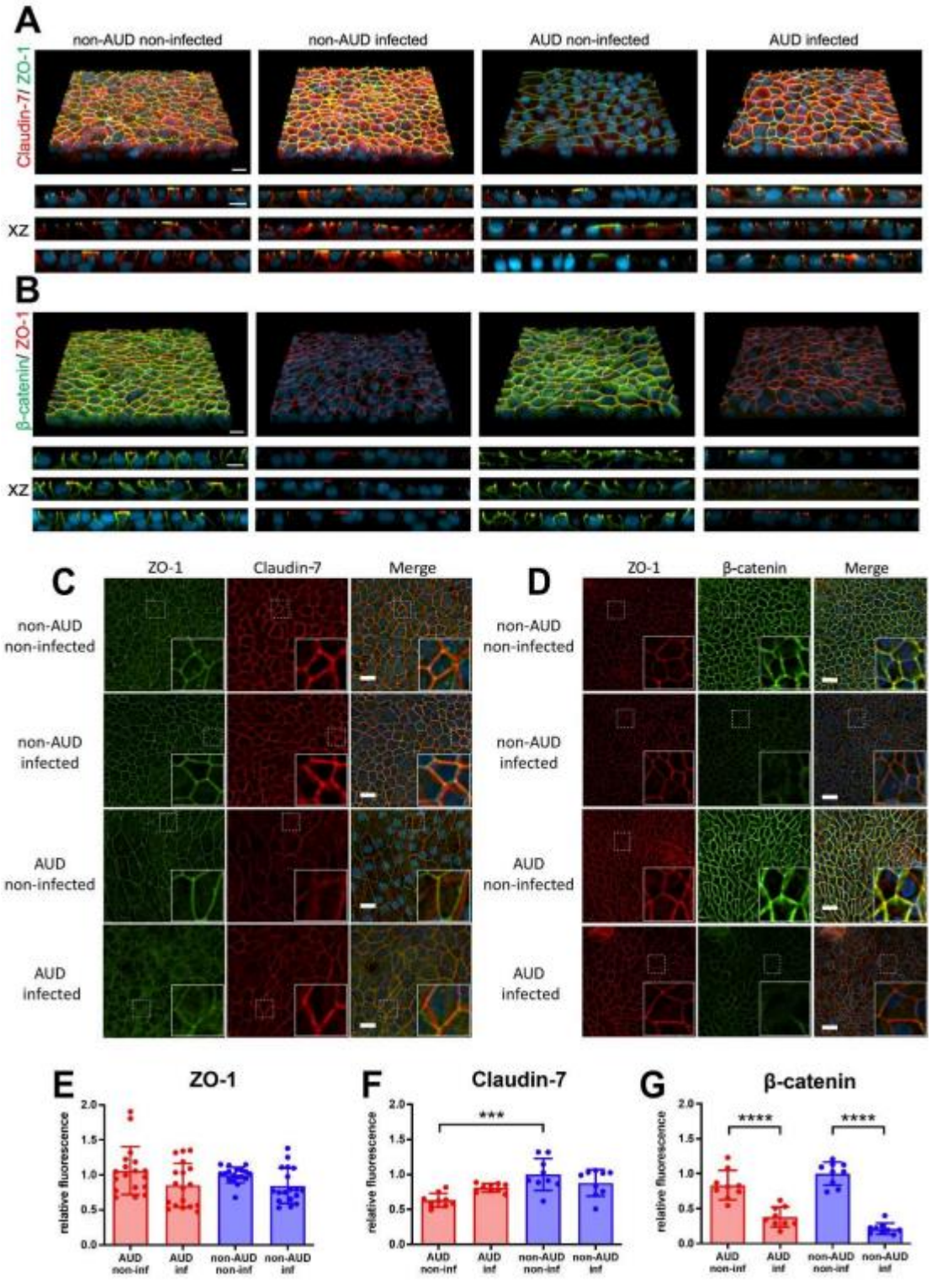
A
non-AUD non-infected
non-AUD infected
AUD non-infected
AUD infected
Claudin-7/ ZO-1
XZ
B
β-catenin/ ZO-1
XZ
C
ZO-1
Claudin-7
Merge
non-AUD non-infected
non-AUD infected
AUD non-infected
AUD infected
D
ZO-1
β-catenin
Merge
non-AUD non-infected
non-AUD infected
AUD non-infected
AUD infected
E
ZO-1
relative fluorescence
AUD non-inf
AUD inf
non-AUD non-inf
non-AUD inf
F
Claudin-7
***
relative fluorescence
AUD non-inf
AUD inf
non-AUD non-inf
non-AUD inf
G
β-catenin
****
****
relative fluorescence
AUD non-inf
AUD inf
non-AUD non-inf
non-AUD inf

Figure 7.5: Changes to non-AUD and AUD bronchial cell junctions in response to SARS-CoV-2 infection.

A-D. Cells 72h post infection or mock infection were fixed and immunostained for ZO-1 (green) and claudin-7 (red) and DAPI (blue) (A,C) or ZO-1 (red), β-catenin (green) and DAPI (blue) (B,D) and imaged by confocal (A,B) and deconvolution (C,D) fluorescence microscopy. A,B. Top panels show a 3D projection, the bottom panels represent xz projections from three biological replicates for each condition. Bar, 10 micron. C,D. xy projections of representative images. White dotted squares represent the location of insets in the bottom right corner of each image. Bar, 20 micron. E-G. Relative fluorescence measurements for showed little effect SARS-CoV-2 infection on total intensity of ZO-1 (C) and claudin-7 (D), however there was a significant decrease in total β-catenin 72 h post-infection (****, $p<0.0001$, n= 3 fields each from 3 biological replicates). Also, there was significantly less claudin-7 in non-infected AUD cells compared to non-infected non-AUD cells (***, $p=0.001$, n= 3 fields each from 3 biological replicates), although this difference diminished 72h post-infection. Values represent mean $\pm$ SD in each case.

7.6 DIFFERENTIAL SECRETION OF CYTOKINES BY INFECTED AUD AND NON-AUD CELLS

We then performed multiplex analysis of cytokine secretion by SARS-CoV-2 infected cells. In general, most of the pro-inflammatory cytokines we measured showed higher levels of secretion by AUD cells during the initial 72h period post-infection as compared to non-AUD cells (**Figure 7.6**, **Supplemental Figure 7.3**). Notable among these cytokines are TNFα, IL-1β and IFNγ (Figure 6A-C), where differences in IL-1β and IFNγ secretion between AUD and non-AUD cells were significant and there was a trending higher level of TNFα secretion by AUD cells at 6 and 24 h after infection. These cytokines have been found to be up-regulated in COVID-19 patients [584] and have the capacity to cause barrier dysfunction [585,586]. This is consistent with the effect we observed on barrier function in **Figure 7.3**. On the other hand, non-AUD cells secreted more Epidermal Growth Factor (EGF) over the 72h time course compared to AUD cells (Figure 6D). In addition, there was a trend towards increased Granulocyte Macrophage Colony Stimulating Factor (GM-CSF) secretion by infected non-AUD cells compared to AUD cells (Figure 6E). Both EGF [587,588] and GM-CSF [545]) have been associated with improved lung epithelial barrier function, which is consistent with the effect of SARS-CoV-2 infection on non-AUD cells observed in **Figure 7.4**.

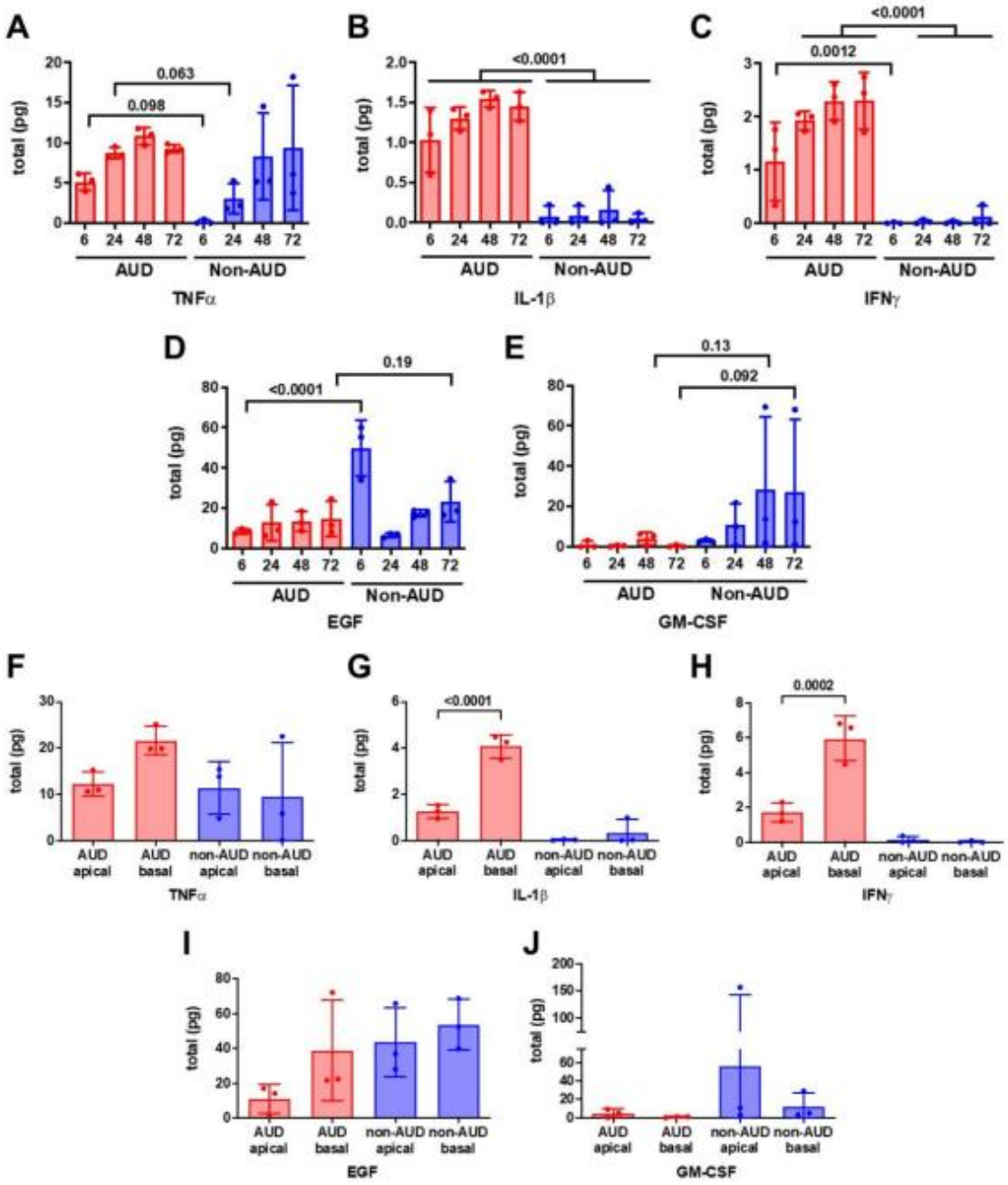
A
B
C
D
E
F
G
H
I
J
total (pg)
0.063
0.098
<0.0001
0.0012
0.19
0.13
0.092
0.0002
6 24 48 72 6 24 48 72
AUD
Non-AUD
TNFα
IL-1β
IFNγ
EGF
GM-CSF
AUD apical
AUD basal
non-AUD apical
non-AUD basal

Figure 7.6: Pro-inflammatory cytokines were preferentially secreted by AUD cells in a polarized manner in response to infection.

Differentiated bronchial cells from non-AUD and AUD patients were infected with SARS-CoV-2 and analyzed for cytokine secretion at 6, 24, 48 and 72 h post infection (A-E) or analyzed for apical and basolateral secretion over the entire time course (F-J). There was a trending or significant increase in pro-inflammatory cytokine secretion (TNFα, IL-1β, and IFNγ) by AUD cells at some or all timepoints. There was a trending or significant increase in anti-inflammatory cytokines by non-AUD cells at some timepoints. AUD cells secreted significantly more basolateral IL-1β, and IFNγ. There was equivalent apical and basolateral secretion of TNFα, EGF and GM-CSF by AUD cells. For all 5 cytokines, non-AUD cells secreted equal amounts apically and basolaterally. n=3 biological replicates consisting of samples from 3 Transwells per group. Values represent mean + SD in each case.

An additional sixteen cytokines were preferentially secreted by AUD cells at least at one timepoint (Supplemental Figure 3). It is noteworthy that AUD cells secreted more IL-17A, IL-17F and IL-25/IL-17E (**Supplemental Figure 7.3L, M, P**), as IL-17 strongly correlates with severe COVID-19 (94). Nine additional cytokines were found to be equivalently secreted from AUD and non-AUD cells during the 72 h time course, including IL-1α and IL-13 (**Supplemental Figure 7.4**). Total IL-6 secretion was also comparable for AUD and non-AUD cells over the 72h period, however, there appeared to be a lag in IL-6 secretion by non-AUD cells (**Supplemental Figure 7.4F**). Other cytokines equivalently secreted by AUD and non-AUD cells included IL-4 and TNFβ (**Supplemental Figure 7.4**). AUD cells also secreted three anti-inflammatory cytokines in response to infection: IL-1RA, IL-10 and IL-22 (**Supplemental Figure 7.4**). Of these, it is noteworthy that elevated IL-1RA and IL-10 have been associated with severe COVID-19, likely reflecting an attempt by the host to mount a protective response [589-591].

We also assessed apical and basolateral secretion of cytokines and found that AUD cells had significantly greater basolateral secretion of IFNγ and IL-1β, while secretion of TNFα, EGF, GM-CSF was not significantly polarized (**Figure 7.6F-J**). Seventeen additional cytokines from our multiplex analysis were found to be secreted in a polarized manner (**Supplemental Figure 7.5**). We observed a variety of polarity profiles, including eight cytokines that were significantly secreted basolaterally from AUD cells while five cytokines were significantly

secreted basolaterally from non-AUD cells. CCL5/RANTES and M-CSF were significantly secreted apically from AUD cells while IL-7 and IL-22 were significantly secreted basolaterally in both AUD and non-AUD cells (**Supplemental Figure 7.5 B,F,M,O**). On the other hand, eight cytokines secreted by infected cells did not show significant polarity in secretion (**Supplemental Figure 7.6**).

Taken together, these results support a model in which AUD cells were primed for an early, enhanced innate immune response to SARS-CoV-2 infection when compared with non-AUD cells, which can have a deleterious effect on cell function.

7.7 DISCUSSION

The effect of SARS-COV-2 infection on human primary bronchial cells in culture has been examined by others [561-565,567], however, this study is the first analysis of the effects of AUD on cell responses to SARS-CoV-2 infection. Our data support a model where AUD and non-AUD differ in their inflammatory response to SARS-CoV-2 infection. This was not due to AUD cells having a strong pro-inflammatory phenotype at baseline, but instead reflected a phenotypic shift that sensitized them to mount an earlier innate inflammatory response to SARS-CoV-2 infection than non-AUD cells.

Our study is the first to focus on samples obtained from Black or African American subjects concerning the effects of AUD on SARS-CoV-2 infection

(**Table 7.1**). In the United States, African American populations have disproportionally higher rates of SARS-CoV-2 infection, hospitalization, and COVID-19-related mortality, according to a systematic review of numerous studies [592]. This is a multifactorial issue due in part to adverse social determinants of health and increased prevalence of comorbidities [593]. While we were unable to adjust for smoking in our study, we did have 2 smokers represented in each of the AUD and non-AUD samples, making the percentage of smokers 66%. This percentage of smokers in the AUD patient samples is equivalent to the percentage of chronic alcohol users who smoke at least one pack of cigarettes a day, which is 70% [594].

RNA-seq analysis of our samples revealed 164 DE genes with the majority up-regulated in AUD cells. Gene Ontology (GO) enrichment analysis showed that the most significant GO terms enriched for AUD samples related to epidermal/keratinocyte differentiation and barrier function. In particular there was enhanced expression of genes related to a cornified barrier, including CRNN, several SPRR genes and FLG2. This, in combination with decreased MUC5B expressed by AUD cells, suggests that the molecular nature of AUD and non-AUD cells is likely to be different, even though their barrier function was numerically equivalent. As one example of how this could have functional ramifications related to the impact of AUD on lung function, increased SPRR3 expression has previously been associated with lung inflammation [572]. We also found that CEACAM5, a gene encoding a cell adhesion protein, was upregulated

in AUD cells. CEACAM5 is also upregulated in bronchial cells from patients with severe type-2 asthma [595], further suggesting a pro-inflammatory phenotype.

Bailey et al. [596] performed RNA-seq analysis of unexpanded bronchial brushings from 19 non-AUD people and 18 people with AUD. We found that there were some DE genes found in our RNAseq analysis that were represented in the Bailey et al. dataset (**Table 7.4**, uncorrected for smoking status), however this required using a less stringent measure of significance for the Bailey dataset, namely DEs with a significant raw p value, even though the adj p value was not significant. One explanation for an overall difference in the DE datasets could be demographic differences between sample donors in the two different studies. Another difference is that we analyzed cells that were propagated and differentiated as opposed to brushings that were directly analyzed, so they could represent different classes of cell phenotypes.

Gene Name	Current Study			Bailey et al. (75)		
	Log 2 Fold Change	*P* Value	Adj. *P* Value	Log 2 Fold Change	*P* Value	Adj. *P* Value
CEACAM7	4.82	0	0	2.58	0.014	0.180
S100A8	4.78	0	0	2.10	0.021	0.210
CYSRT1	3.43	0	0	1.06	0.018	0.195
CEACAM5	3.39	0	0.01	4.18	0.001	0.055
PADI1	3.33	0	0	1.55	0.015	0.186
ABCA12	2.09	0	0.02	2.34	0.010	0.160
CRYBG2	1.62	0	0.01	1.32	0.017	0.192
PLBD1	1.41	0	0.05	0.77	0.008	0.142
BDKRB2	1.24	0	0	0.42	0.052	0.309
GPRC5B	−1.63	0	0.02	−0.84	0.023	0.223
MUC5B	−2.93	0	0.01	−2.05	0.004	0.102
CYP2A13	−3.99	0	0.05	−2.09	0.002	0.085
ITLN1	−4.57	0	0	−3.18	0.011	0.161

Table 7.4: Genes altered by AUD status.

Examples of genes comparably differentially regulated in our comparison of cultured AUD and non-AUD cells and data from Bailey et al. (2020), which were processed for AUD status, but not for smoking status. Although both sets of data had significant p values, the adjusted p value for these genes was not significant for the Bailey, et al. data, which is a limitation of this analysis.[596]

After infection with SARS-CoV-2, cells from patients with AUD had a robust inflammatory response, including higher levels of TNFα, IL-1β and IFNγ secreted than infected non-AUD cells. Several other proinflammatory cytokines were also preferentially secreted by infected AUD cells as compared with non-AUD cells (**Supplemental Figure 7.3**). However, there were also several cytokines that were comparably secreted by infected AUD and non-AUD cells. For instance, over the 72h period following infection, IL-6 secretion was comparable for AUD and non-AUD cells (**Supplemental Figure 7.4F**), although AUD cells had an earlier IL-6 response than non-AUD cells. Other studies examining SARS-CoV-2-exposed bronchial cells have also showed that IL-6 was produced at 72 h after infection [561,564,567], consistent with the response we observed in non-AUD cells. Although there is a correlation of systemic IL-6 levels with disease severity [589,597], it is not the sole determinant and an overall inflammatory profile should be considered. Surprisingly, we found that SARS-CoV-2 infected, non-AUD cells secreted two protective cytokines, EGF and GM-CSF, that were less prominent in infected AUD cells. EGF in particular has been shown to promote lung epithelial cell barrier function [587,588]. Moreover, administration of EGF to septic mice has been shown to lessen the severity of sepsis, even in alcohol fed mice, in part by protecting gut barrier function [598].

Interpreting roles for GM-CSF in bronchial epithelial cell behavior is complex, since it has both pro- and anti- inflammatory effects, depending on the amount, context and presence of other inflammatory mediators [599]. Consistent with the

protective effect of GM-CSF, GM-CSF deficient mice exhibit pulmonary alveolar proteinosis (PAP) [600], which ultimately led to therapies including inhaled GM-CSF to treat this disease [601]. There is also evidence that ARDS survival correlates with the amount of GM-CSF present in lung lavage fluid [545,602]. This is due to stimulation of the PU.1 transcription factor by autocrine stimulation of lung epithelial cells by GM-CSF and this pathway was found to be impaired as a result of chronic alcohol ingestion in a rodent model [603]. This would be consistent with impairment of GM-CSF signaling by AUD cells as a contributor to barrier dysfunction due to SARS-CoV-2 (**Figure 7.1**) and supports the potential for GM-CSF administration as a therapeutic approach in severe COVID-19 [604,605]. However, the use of administered GM-CSF to treat non-COVID ARDS has had mixed success, where it was shown to improve the ratio of arterial oxygen partial pressure to fractional inspired oxygen (PaO2/FIO2) [606], but it did not increase the number of ventilator-free days in ARDS patients [607].

We found that AUD cells showed a significant decrease in TER in response to SARS-CoV-2 infection, however non-AUD cells showed an increase in TER. Previous analysis of infected airway cells has shown a minimal effect of SARS-CoV-2 infection on TER over a 6 day period [563] or over a 30 day period following an initial drop, with some fluctuations [562]. Although the enhancement of TER by non-AUD cells was unexpected, it was consistent with another study demonstrating that SARS-CoV-2 infection of bronchial epithelial cells showed a

transient decrease in TER followed by a rebound to higher TER when measured over a 7-day time course post infection [608].

Another likely mechanism of diminished barrier function is the influence of viral proteins on assembly of the tight junction complex, even in the absence of viral shedding. In particular, interference of the SARS-CoV envelope protein (E protein) with ZO-1 association with tight junctions was originally demonstrated for SARS-CoV-1 [609]. Subsequently SARS-CoV-2 E protein has been found to bind to ZO-1 as well [610-613]. Whether this is occurring in SARS-CoV-2 infected airway cells to interfere with tight junctions remains to be determined. Disruption of ZO-1 can also influence the distribution of claudin-7 between the tight junction (barrier forming) and lateral (non-barrier forming) pools. Regardless of the mechanism, cell polarity is largely retained, since infected airway cells *in vitro* show low levels of basolateral virus shedding relative to apical shedding [562,608] and cytokine secretion is also polarized, as seen here and in other reports [561,564].

In contrast to ZO-1 and claudin-7, levels of β-catenin, an adherens junction scaffold protein, were significantly diminished in response to SARS-CoV-2 infection irrespective of whether the cells were from people with or without AUD (Figure 5B, D, G). A similar effect of SARS-CoV-2 on β-catenin expression has been reported for infected endothelial cells [581,582] and has been implicated in the disruption of vascular barrier function due to COVID-19. However, since SARS-CoV-2 infection had a similar effect on total β-catenin in AUD and non-AUD cells,

this does not account for the differential effect of infection on barrier function of bronchial epithelial cells. Instead, the decrease in airway epithelial β-catenin following SARS-CoV-2 infection more likely reflects another cell response. For instance, decreased expression and junction localization of β-catenin could alter airway cell responses to infection by having an impact on wnt signaling [583].

We found that the effects of AUD on human airway epithelial cell responses to SARS-CoV-2 infection were maintained by cultured cells and did not require the presence of alcohol in the culture medium. This finding is consistent with our data using lung epithelial cells isolated from alcohol fed rodents [554,555,557] and suggests that the cells may by epigenetically reprogrammed in response to chronic alcohol exposure. In fact, alcohol consumption has been linked to epigenetic modification of the central nervous system as a mechanism underlying addiction [614], which further suggests that epigenetic reprogramming also can occur in the lung in response to AUD. Consistent with this possibility, it has previously been shown that alcohol inhibits Thy-1 expression by lung fibroblasts by DNA methylation induced by TGF-β1 [615,616]. The effects of epigenetic reprogramming of lung epithelia by alcohol remain to be determined.

Our findings that non-AUD cells had a relatively mild response to SARS-CoV-2 infection is likely to reflect the cell culture conditions we used. Here we used medium that supports bronchial cell differentiation and also contains normal resting glucose levels [568]. However, several media commonly used to support

airway epithelial cell differentiation have high glucose concentrations, including media based on LHC Basal:DMEM-H and Pneumocult-ALI both of which contain ~ 300 mg/dL glucose [568]. Thus, one consideration in interpreting results obtained with cultured airway epithelial cells is that their response to SARS-CoV-2 infection may be sensitive to medium glucose content, which would be consistent with diabetes as a risk factor for increased severity of COVID-19 [617].

Here we compared primary bronchial epithelial cells derived from AUD and non-AUD patients that were grown, differentiated, and treated under the same conditions to demonstrate that AUD cells showed early sensitivity to SARS-CoV-2 infection. As early onset of severe disease is a likely determinant of further disease progression, our data add AUD as a risk factor for increased severity of COVID-19 related illness [539] due to the combined impact of alcohol and SARS-CoV-2 infection on airway epithelial barrier function and inflammation. This underscores the importance of considering AUD status when treating COVID-19 patients and the likely utility of targeting the lung epithelium when considering treatment options.

7.8 FUNDING, ACKNOWLEDGEMENTS, AND AUTHOR CONTRIBUTIONS

Funding

This project was supported by R01-AA025854 (MK, CAE), F31-AA029000 (KFE) and the Indo-U.S. Science & Technology Forum (IUSSTF) Virtual Networks for COVID-19 (Ref: IUSSTF/VN-COVID/107/2020), India (MK, JDS).

Acknowledgements

We thank Michael Kulik and Ted Ross from the University of Georgia for assistance in the BSL-3 facility.

Author contributions

CAE, MK, KFE, RCE, EKL, MJL and AGBB designed and executed experiments. BSS and AJM provided airway cell brushings. KFE, RCR and RCE cultured cells, performed imaging and cytokine analysis. CAE, RCE, AGBB, CAJ, SKJ and SMT performed all BSL-3 experiments. RCE, MK, CAE, and KFE analyzed the data, compiled the figures, and wrote the first draft of manuscript. MK, JDS, IKC, JML and CAE provided feedback and interpreted results. All of the co-authors edited and approved the manuscript

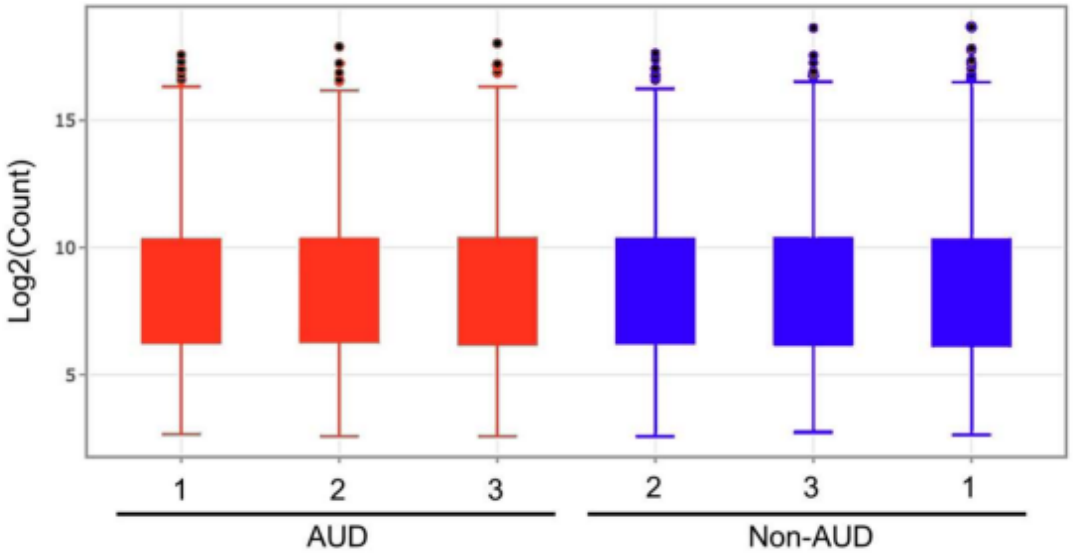
Log2(Count)
15
10
5
1
2
3
2
3
1
AUD
Non-AUD

Supplemental Figure 7.1: Distribution of normalized read accounts

Shown in the normalization of original read counts used to determine differentially expressed genes. These values show that the samples analyzed had comparable read sequencing depth.

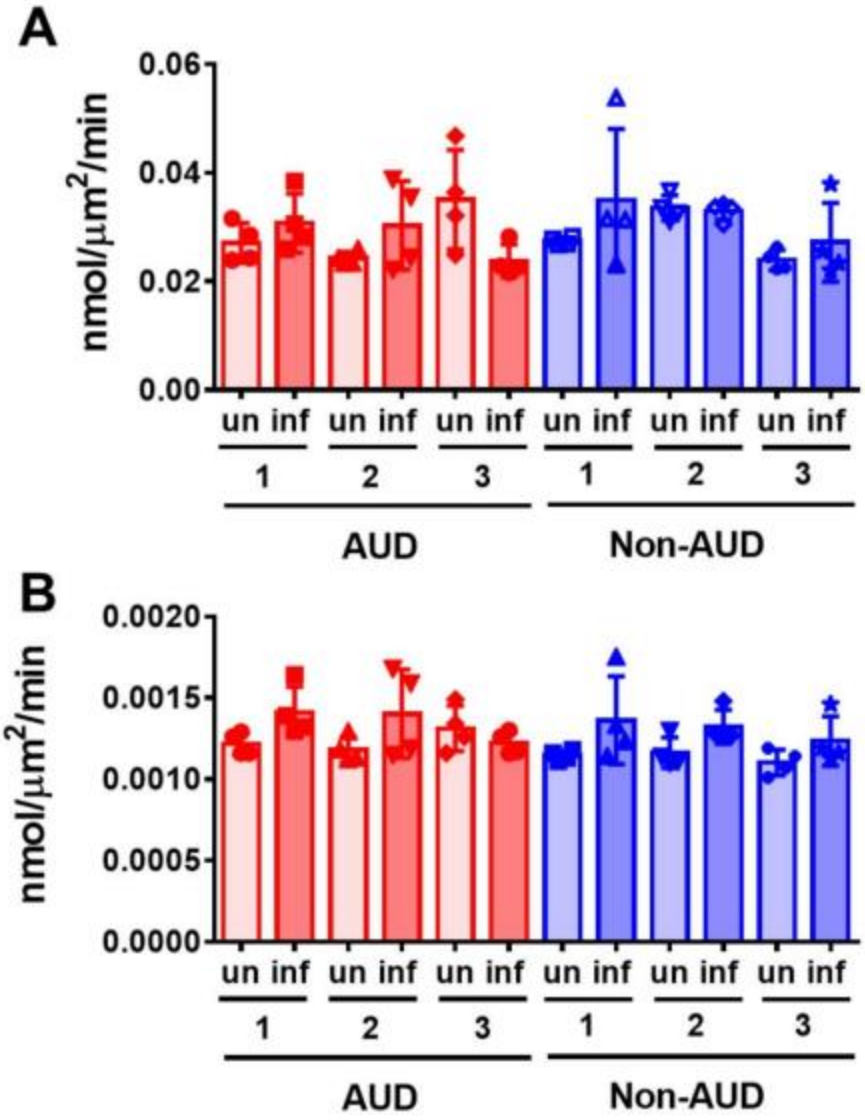
A
nmol/μm²/min
0.06
0.04
0.02
0.00
un inf un inf un inf un inf un inf un inf
1 2 3 1 2 3
AUD
Non-AUD
B
nmol/μm²/min
0.0020
0.0015
0.0010
0.0005
0.0000
un inf un inf un inf un inf un inf un inf
1 2 3 1 2 3
AUD
Non-AUD

Supplemental Figure 7.2: Dye Flux measurements of paracellular permeability

Paracellular permeability of AUD and non-AUD cells to calcein (A) and 10kDa Texas Red dextran (B) are shown for uninfected (un) and infected (inf) monolayers. N=3 biological replicates, 4 transwells each, representing mean ± SD. Paracellular flux was comparable for uninfected and infected cells. There were not any significant differences in flux due to AUD infection status. Uninfected cell data is also represented in Figure 2B,C in the main body of the text.

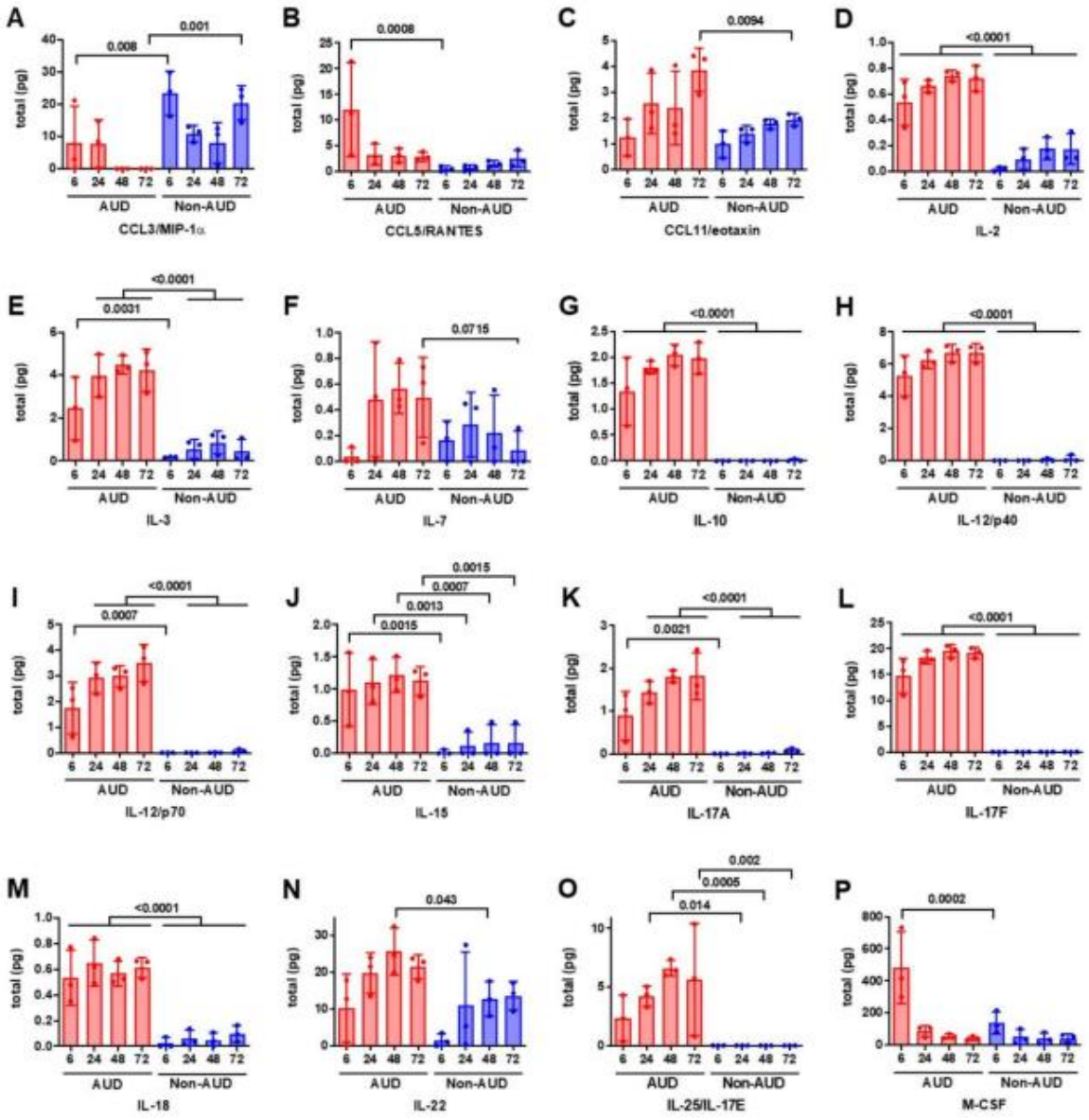
A
0.008
0.001
total (pg)
6 24 48 72 6 24 48 72
AUD Non-AUD
CCL3/MIP-1α
B
0.0008
CCL5/RANTES
C
0.0094
CCL11/eotaxin
D
<0.0001
IL-2
E
<0.0001
0.0031
IL-3
F
0.0715
IL-7
G
<0.0001
IL-10
H
<0.0001
IL-12/p40
I
<0.0001
0.0007
IL-12/p70
J
0.0015
0.0007
0.0013
0.0015
IL-15
K
<0.0001
0.0021
IL-17A
L
<0.0001
IL-17F
M
<0.0001
IL-18
N
0.043
IL-22
O
0.002
0.0005
0.014
IL-25/IL-17E
P
0.0002
M-CSF

Supplemental Figure 7.3: Secreted cytokines showing significant differences between AUD and non-AUD cells in response to infection

Differentiated bronchial cells from non-AUD and AUD patients were infected with SARS-CoV-2 and analyzed for cytokine secretion using a multiplex assay. Shown is cytokine secretion at 6, 24, 48 and 72 h post infection. n=3 biological replicates consisting of samples from 3 Transwells per group. Values represent mean + SD in each case, p values are shown above each graph.

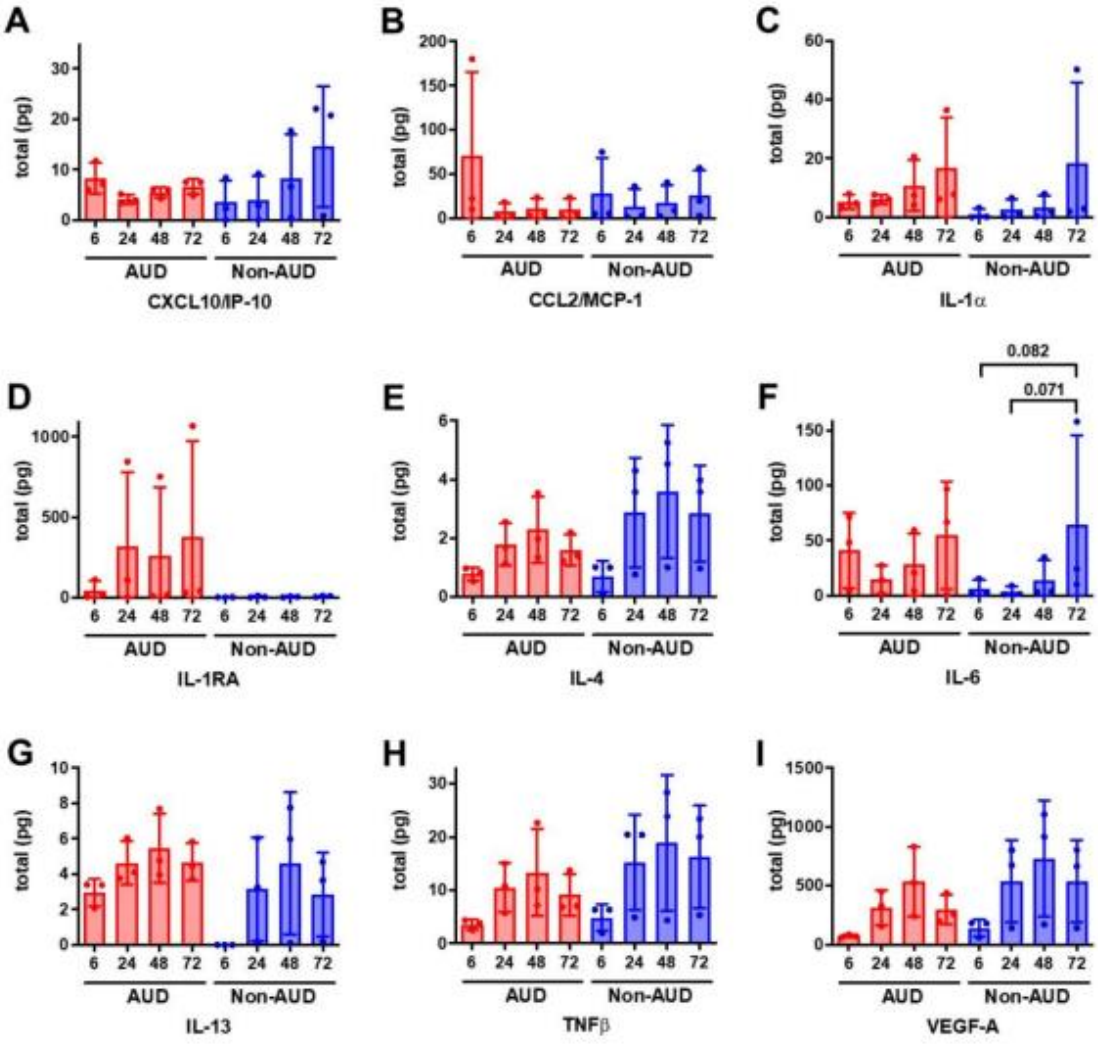
A
total (pg)
30
20
10
0
6 24 48 72 6 24 48 72
AUD
Non-AUD
CXCL10/IP-10
B
total (pg)
200
150
100
50
0
6 24 48 72 6 24 48 72
AUD
Non-AUD
CCL2/MCP-1
C
total (pg)
60
40
20
0
6 24 48 72 6 24 48 72
AUD
Non-AUD
IL-1α
D
total (pg)
1000
500
0
6 24 48 72 6 24 48 72
AUD
Non-AUD
IL-1RA
E
total (pg)
6
4
2
0
6 24 48 72 6 24 48 72
AUD
Non-AUD
IL-4
F
0.082
0.071
total (pg)
150
100
50
0
6 24 48 72 6 24 48 72
AUD
Non-AUD
IL-6
G
total (pg)
10
8
6
4
2
0
6 24 48 72 6 24 48 72
AUD
Non-AUD
IL-13
H
total (pg)
30
20
10
0
6 24 48 72 6 24 48 72
AUD
Non-AUD
TNFβ
I
total (pg)
1500
1000
500
0
6 24 48 72 6 24 48 72
AUD
Non-AUD
VEGF-A

Supplemental Figure 7.4: Secreted cytokines that did not show significant differences between AUD and non-AUD cells in response to infection

Differentiated bronchial cells from non-AUD and AUD patients were infected with SARS-CoV-2 and analyzed for cytokine secretion using a multiplex assay. Shown is cytokine secretion at 6, 24, 48 and 72 h post infection. Shown are cytokines that were equivalently secreted by AUD cells and non-AUD cells at each timepoint. n=3 biological replicates consisting of samples from 3 Transwells per group. Values represent mean + SD in each case, p values are shown above the graph in F.

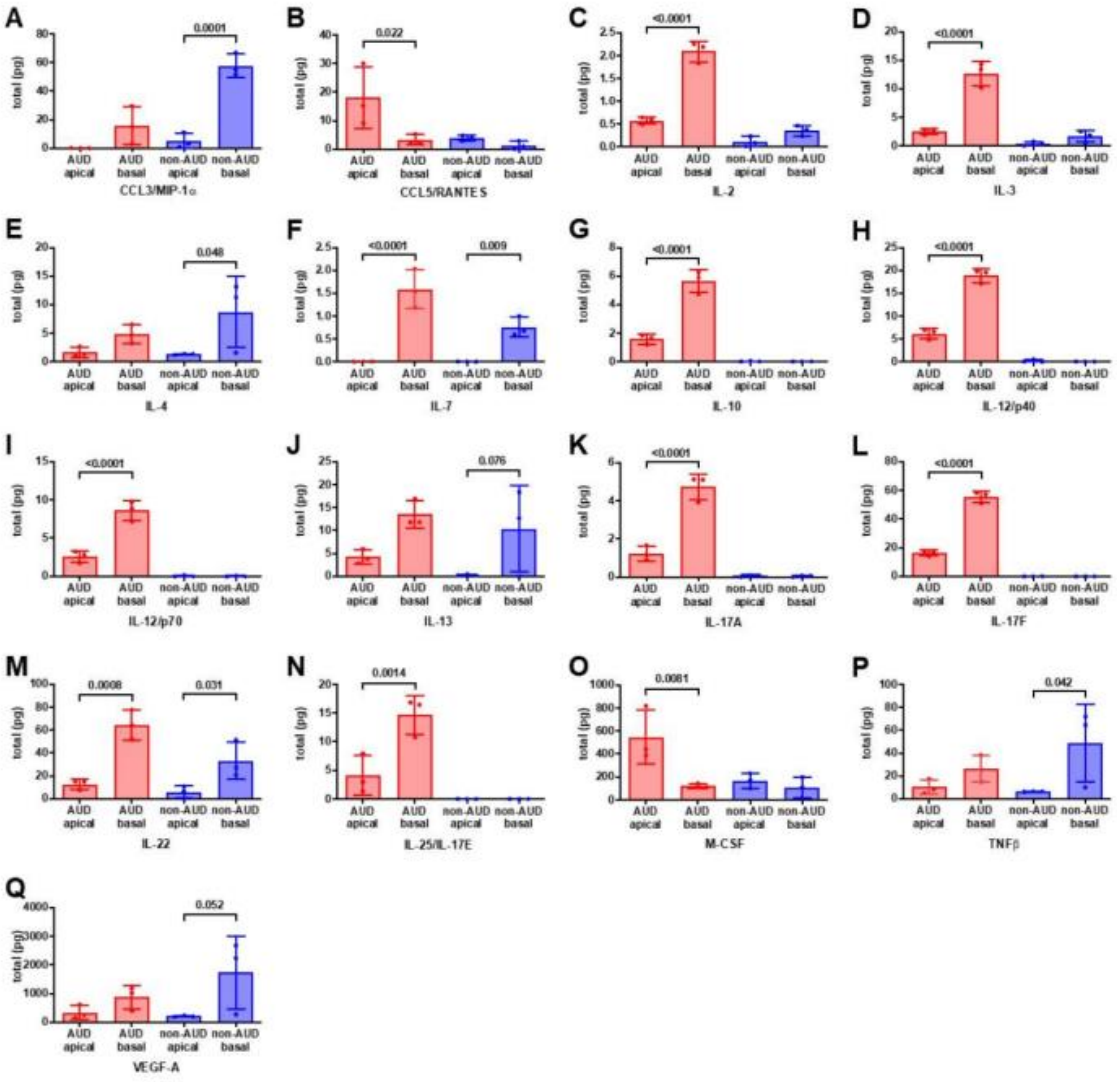
A
0.0001
total (pg)
AUD apical
AUD basal
non-AUD apical
non-AUD basal
CCL3/MIP-1α
B
0.022
CCL5/RANTES
C
<0.0001
IL-2
D
<0.0001
IL-3
E
0.048
IL-4
F
<0.0001
0.009
IL-7
G
<0.0001
IL-10
H
<0.0001
IL-12/p40
I
<0.0001
IL-12/p70
J
0.076
IL-13
K
<0.0001
IL-17A
L
<0.0001
IL-17F
M
0.0008
0.031
IL-22
N
0.0014
IL-25/IL-17E
O
0.0081
M-CSF
P
0.042
TNFβ
Q
0.052
VEGF-A

Supplemental Figure 7.5: Secreted cytokines showing significant differences in polarized secretion in response to infection

Differentiated bronchial cells from non-AUD and AUD patients were infected with SARS-CoV-2 and analyzed for cytokine secretion using a multiplex assay. Shown is apical and basolateral cytokine secretion over the entire time course. n=3 biological replicates consisting of samples from 3 Transwells per group. Values represent mean + SD in each case, p values are shown above each graph.

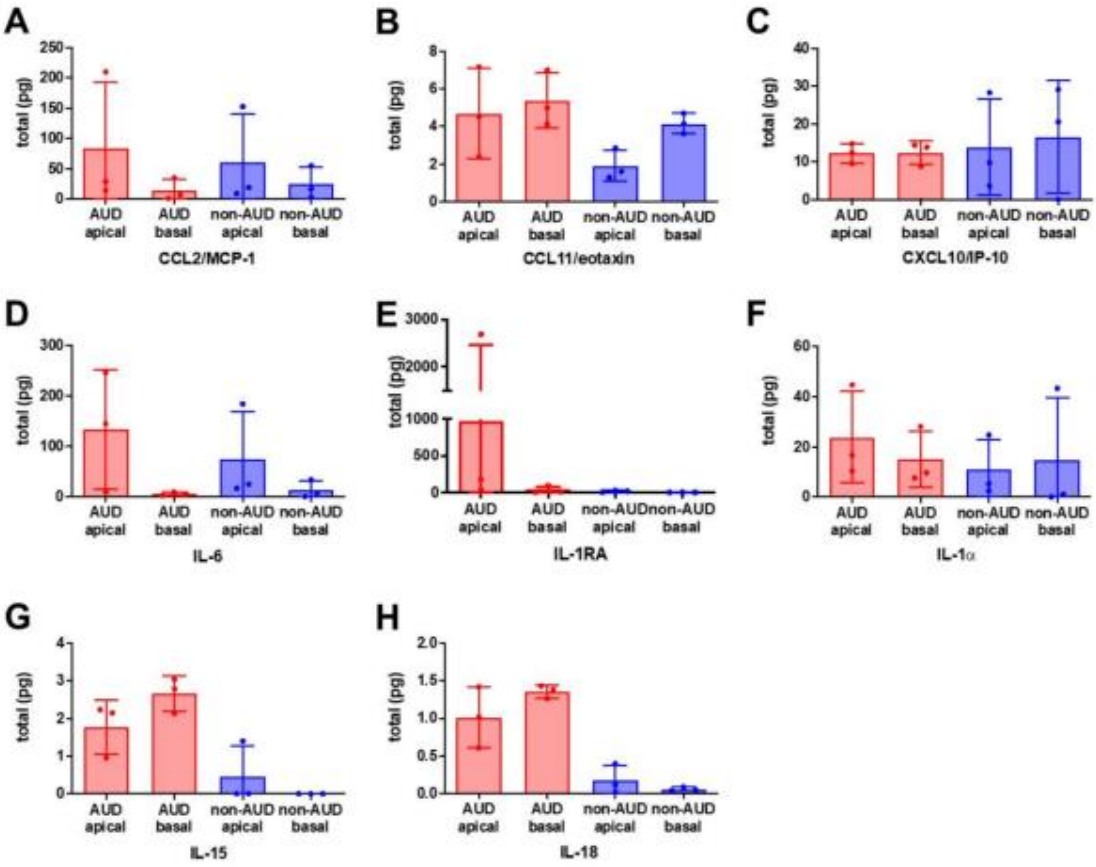
A
total (pg)
250
200
150
100
50
0
AUD apical
AUD basal
non-AUD apical
non-AUD basal
CCL2/MCP-1
B
total (pg)
8
6
4
2
0
AUD apical
AUD basal
non-AUD apical
non-AUD basal
CCL11/eotaxin
C
total (pg)
40
30
20
10
0
AUD apical
AUD basal
non-AUD apical
non-AUD basal
CXCL10/IP-10
D
total (pg)
300
200
100
0
AUD apical
AUD basal
non-AUD apical
non-AUD basal
IL-6
E
total (pg)
3000
2000
1000
500
0
AUD apical
AUD basal
non-AUD apical
non-AUD basal
IL-1RA
F
total (pg)
60
40
20
0
AUD apical
AUD basal
non-AUD apical
non-AUD basal
IL-1α
G
total (pg)
4
3
2
1
0
AUD apical
AUD basal
non-AUD apical
non-AUD basal
IL-15
H
total (pg)
2.0
1.5
1.0
0.5
0.0
AUD apical
AUD basal
non-AUD apical
non-AUD basal
IL-18

Supplemental Figure 7.6: Secreted cytokines that did not show significant differences in polarized secretion in response to infection

Differentiated bronchial cells from non-AUD and AUD patients were infected with SARS-CoV-2 and analyzed for cytokine secretion using a multiplex assay. Shown is apical and basolateral cytokine secretion over the entire time course. n=3 biological replicates consisting of samples from 3 Transwells per group. Values represent mean + SD in each case.

REFERENCES

1 Fund, U. N. P. 8 Billion Lives, Infinite Possibilities the case for rights and choices. (United Nations Population Fund, UNFPA Division fo Communications and Strategic Partnerships, 2023).

2 Davis, K. Low fertility in evolutionary perspective. *Population and Development Review* **12**, 48-65 (1986).

3 Aitken, R. J. The changing tide of human fertility. *Hum Reprod* **37**, 629-638, doi:10.1093/humrep/deac011 (2022).

4 Lerch, M. Regional variations in the rural-urban fertility gradient in the global South. *PLoS One* **14**, e0219624 (2019).

5 White, M. J. *et al.* Urbanization and fertility: An event-history analysis of coastal Ghana. *Demography* **45**, 803-816 (2008).

6 Liu, D. H. & Raftery, A. E. How do education and family planning accelerate fertility decline? *Population and development review* **46**, 409-441 (2020).

7 Jones, G. W. Delayed marriage and very low fertility in Pacific Asia. *Population and development review* **33**, 453-478 (2007).

8 Louis, J. F. *et al.* The prevalence of couple infertility in the United States from a male perspective: evidence from a nationally representative sample. *Andrology* **1**, 741-748 (2013).

9 Chandra, A., Copen, C.E., & Stephen, E.H. Infertility and Impaired Fecundity in the United States, 1982-2010: Data From the National Survey of Family Growth. 1-19 (2013).

10 Agarwal, A., Mulgund, A., Hamada, A. & Chyatte, M. R. A unique view on male infertility around the globe. *Reprod Biol Endocrinol* **13**, 37, doi:10.1186/s12958-015-0032-1 (2015).

11 Pizzorno, J. Environmental Toxins and Infertility. *Integr Med (Encinitas)* **17**, 8-11 (2018).

12 Sharma, R., Biedenharn, K. R., Fedor, J. M. & Agarwal, A. Lifestyle factors and reproductive health: taking control of your fertility. *Reprod Biol Endocrinol* **11**, 66, doi:10.1186/1477-7827-11-66 (2013).

13 Carlsen, E., Giwercman, A., Keiding, N. & Skakkebæk, N. E. Evidence for decreasing quality of semen during past 50 years. *British medical journal* **305**, 609-613 (1992).

14 Swan, S. H., Elkin, E. P. & Fenster, L. The question of declining sperm density revisited: an analysis of 101 studies published 1934-1996. *Environmental health perspectives* **108**, 961-966 (2000).

15 Swan, S. H., Elkin, E. P. & Fenster, L. Have sperm densities declined? A reanalysis of global trend data. *Environmental health perspectives* **105**, 1228-1232 (1997).

16 Levine, H. *et al.* Temporal trends in sperm count: a systematic review and meta-regression analysis. *Human reproduction update* **23**, 646-659 (2017).

17 Aitken, R. J. in *Seminars in reproductive medicine.* 003-020 (Thieme Medical Publishers, Inc. 333 Seventh Avenue, 18th Floor, New York, NY …).

18 Lv, M.-Q. *et al.* Temporal trends in semen concentration and count among 327 373 Chinese healthy men from 1981 to 2019: a systematic review. *Human Reproduction* **36**, 1751-1775 (2021).

19 Swan, S. H. & Colino, S. *Count down: how our modern world is threatening sperm counts, altering male and female reproductive development, and imperiling the future of the human race*. (Simon and Schuster, 2022).

20 Perheentupa, A. *et al.* A cohort effect on serum testosterone levels in Finnish men. *European journal of endocrinology* **168**, 227-233 (2013).

21 Travison, T. G., Araujo, A. B., O'Donnell, A. B., Kupelian, V. & McKinlay, J. B. A population-level decline in serum testosterone levels in American men. *The Journal of Clinical Endocrinology & Metabolism* **92**, 196-202 (2007).

22 Chodick, G., Epstein, S. & Shalev, V. Secular trends in testosterone-findings from a large state-mandate care provider. *Reproductive biology and endocrinology* **18**, 1-5 (2020).

23 La Merrill, M. A. *et al.* Consensus on the key characteristics of endocrine-disrupting chemicals as a basis for hazard identification. *Nature Reviews Endocrinology* **16**, 45-57, doi:10.1038/s41574-019-0273-8 (2020).

24 Duh-Leong, C., Maffini, M. V., Kassotis, C. D., Vandenberg, L. N. & Trasande, L. The regulation of endocrine-disrupting chemicals to minimize

their impact on health. *Nature Reviews Endocrinology* **19**, 600-614, doi:10.1038/s41574-023-00872-x (2023).

25 Rodprasert, W., Toppari, J. & Virtanen, H. E. Environmental toxicants and male fertility. *Best Practice & Research Clinical Obstetrics & Gynaecology* **86**, 102298, doi:https://doi.org/10.1016/j.bpobgyn.2022.102298 (2023).

26 Kumar, M. *et al.* Environmental Endocrine-Disrupting Chemical Exposure: Role in Non-Communicable Diseases. *Frontiers in Public Health* **8**, doi:10.3389/fpubh.2020.553850 (2020).

27 Skakkebæk, N. E. *et al.* Environmental factors in declining human fertility. *Nature Reviews Endocrinology* **18**, 139-157, doi:10.1038/s41574-021-00598-8 (2022).

28 Sharma, R., Harlev, A., Agarwal, A. & Esteves, S. C. Cigarette smoking and semen quality: a new meta-analysis examining the effect of the 2010 World Health Organization laboratory methods for the examination of human semen. *European urology* **70**, 635-645 (2016).

29 Ricci, E. *et al.* Semen quality and alcohol intake: a systematic review and meta-analysis. *Reproductive biomedicine online* **34**, 38-47 (2017).

30 Hatch, E. E. *et al.* Intake of sugar-sweetened beverages and fecundability in a North American preconception cohort. *Epidemiology (Cambridge, Mass.)* **29**, 369 (2018).

31 Ma, J. *et al.* Association between BMI and semen quality: an observational study of 3966 sperm donors. *Human Reproduction* **34**, 155-162 (2019).

32 Sermondade, N. *et al.* BMI in relation to sperm count: an updated systematic review and collaborative meta-analysis. *Human reproduction update* **19**, 221-231 (2013).

33 Vaamonde, D., Da Silva-Grigoletto, M. E., García-Manso, J. M., Barrera, N. & Vaamonde-Lemos, R. Physically active men show better semen parameters and hormone values than sedentary men. *European journal of applied physiology* **112**, 3267-3273 (2012).

34 Gaskins, A. J. *et al.* Physical activity and television watching in relation to semen quality in young men. *British journal of sports medicine* **49**, 265-270 (2015).

35 Lalinde-Acevedo, P. C. *et al.* Physically active men show better semen parameters than their sedentary counterparts. *International journal of fertility & sterility* **11**, 156 (2017).

36 França, L. R., Hess, R. A., Dufour, J. M., Hofmann, M. & Griswold, M. The Sertoli cell: one hundred fifty years of beauty and plasticity. *Andrology* **4**, 189-212 (2016).

37 Petersen, C. & Söder, O. The Sertoli Cell – A Hormonal Target and 'Super' Nurse for Germ Cells That Determines Testicular Size. *Hormone Research* **66**, 153-161, doi:10.1159/000094142 (2006).

38 Oatley, J. M. & Brinster, R. L. The germline stem cell niche unit in mammalian testes. *Physiol Rev* **92**, 577-595, doi:10.1152/physrev.00025.2011 (2012).

39 Li, N., Wang, T. & Han, D. Structural, cellular and molecular aspects of immune privilege in the testis. *Frontiers in immunology* **3**, 152 (2012).

40 Fijak, M. & Meinhardt, A. The testis in immune privilege. *Immunological reviews* **213**, 66-81 (2006).

41 Mruk, D. D. & Cheng, C. Y. The Mammalian Blood-Testis Barrier: Its Biology and Regulation. *Endocr Rev* **36**, 564-591, doi:10.1210/er.2014-1101 (2015).

42 Gilula, N. B., Fawcett, D. W. & Aoki, A. The Sertoli cell occluding junctions and gap junctions in mature and developing mammalian testis. *Developmental biology* **50**, 142-168 (1976).

43 Yan Cheng, C. & Mruk, D. D. in *Sertoli Cell Biology (Second Edition)* (ed Michael D. Griswold) 333-383 (Academic Press, 2015).

44 Russell, L. Movement of spermatocytes from the basal to the adluminal compartment of the rat testis. *American Journal of Anatomy* **148**, 313-328 (1977).

45 Setchell, B., Voglmayr, J. & Waites, G. A blood-testis barrier restricting passage from blood into rete testis fluid but not into lymph. *The Journal of physiology* **200**, 73-85 (1969).

46 Moroi, S. *et al.* Occludin is concentrated at tight junctions of mouse/rat but not human/guinea pig Sertoli cells in testes. *American Journal of Physiology-Cell Physiology* **274**, C1708-C1717 (1998).

47 Ikenouchi, J. *et al.* Tricellulin constitutes a novel barrier at tricellular contacts of epithelial cells. *The Journal of cell biology* **171**, 939-945 (2005).

48 Krug, S. M. *et al.* Tricellulin forms a barrier to macromolecules in tricellular tight junctions without affecting ion permeability. *Molecular biology of the cell* **20**, 3713-3724 (2009).

49 Tsukita, S., Tanaka, H. & Tamura, A. The Claudins: From Tight Junctions to Biological Systems. *Trends in Biochemical Sciences* **44**, 141-152, doi:https://doi.org/10.1016/j.tibs.2018.09.008 (2019).

50 Lapointe, T. K. & Buret, A. G. Interleukin-18 facilitates neutrophil transmigration via myosin light chain kinase-dependent disruption of occludin, without altering epithelial permeability. *American Journal of Physiology-Gastrointestinal and Liver Physiology* **302**, G343-G351 (2012).

51 Zhou, B. *et al.* Claudin-18–mediated YAP activity regulates lung stem and progenitor cell homeostasis and tumorigenesis. *The Journal of clinical investigation* **128**, 970-984 (2018).

52 Ding, L. *et al.* Inflammation and disruption of the mucosal architecture in claudin-7–deficient mice. *Gastroenterology* **142**, 305-315 (2012).

53 Walsh, S. V., Hopkins, A. M. & Nusrat, A. Modulation of tight junction structure and function by cytokines. *Advanced drug delivery reviews* **41**, 303-313 (2000).

54 Escudero-Esparza, A., Jiang, W. G. & Martin, T. A. Claudin-5 participates in the regulation of endothelial cell motility. *Molecular and cellular biochemistry* **362**, 71-85 (2012).

55 Ikari, A. *et al.* Phosphorylation of paracellin-1 at Ser217 by protein kinase A is essential for localization in tight junctions. *Journal of cell science* **119**, 1781-1789 (2006).

56 Van Itallie, C. M. *et al.* Phosphorylation of claudin-2 on serine 208 promotes membrane retention and reduces trafficking to lysosomes. *Journal of cell science* **125**, 4902-4912 (2012).

57 Stamatovic, S. M., Dimitrijevic, O. B., Keep, R. F. & Andjelkovic, A. V. Protein kinase Cα-RhoA cross-talk in CCL2-induced alterations in brain endothelial permeability. *Journal of Biological Chemistry* **281**, 8379-8388 (2006).

58 Chihara, M., Otsuka, S., Ichii, O., Hashimoto, Y. & Kon, Y. Molecular dynamics of the blood–testis barrier components during murine spermatogenesis. *Molecular reproduction and development* **77**, 630-639 (2010).

59 Meng, J., Holdcraft, R. W., Shima, J. E., Griswold, M. D. & Braun, R. E. Androgens regulate the permeability of the blood–testis barrier. *Proceedings of the National Academy of Sciences* **102**, 16696-16700 (2005).

60 De Gendt, K. *et al.* A Sertoli cell-selective knockout of the androgen receptor causes spermatogenic arrest in meiosis. *Proceedings of the National Academy of Sciences* **101**, 1327-1332 (2004).

61 Meng, J., Greenlee, A. R., Taub, C. J. & Braun, R. E. Sertoli cell-specific deletion of the androgen receptor compromises testicular immune privilege in mice. *Biology of reproduction* **85**, 254-260 (2011).

62 Wang, R.-S. *et al.* Androgen receptor in sertoli cell is essential for germ cell nursery and junctional complex formation in mouse testes. *Endocrinology* **147**, 5624-5633 (2006).

63 Hellani, A. *et al.* Developmental and hormonal regulation of the expression of oligodendrocyte-specific protein/claudin 11 in mouse testis. *Endocrinology* **141**, 3012-3019 (2000).

64 Lui, W.-Y., Lee, W. M. & Cheng, C. Y. Transforming growth factor-β3 perturbs the inter-Sertoli tight junction permeability barrier in vitro possibly mediated via its effects on occludin, zonula occludens-1, and claudin-11. *Endocrinology* **142**, 1865-1877 (2001).

65 Tu'uhevaha, J., Sluka, P., Foo, C. F. & Stanton, P. G. Claudin-11 expression and localisation is regulated by androgens in rat Sertoli cells in vitro. *Reproduction* **133**, 1169-1179 (2007).

66 Florin, A. *et al.* Androgens and postmeiotic germ cells regulate claudin-11 expression in rat Sertoli cells. *Endocrinology* **146**, 1532-1540 (2005).

67 Gye, M. Changes in the expression of claudins and transepithelial electrical resistance of mouse Sertoli cells by Leydig cell coculture. *International journal of andrology* **26**, 271-278 (2003).

68 Mruk, D. D. & Cheng, C. Y. Sertoli-Sertoli and Sertoli-germ cell interactions and their significance in germ cell movement in the seminiferous epithelium during spermatogenesis. *Endocr Rev* **25**, 747-806, doi:10.1210/er.2003-0022 (2004).

69 Crisóstomo, L. *et al.* Molecular mechanisms and signaling pathways involved in the nutritional support of spermatogenesis by Sertoli cells. *Sertoli Cells: Methods and Protocols*, 129-155 (2018).

70 Yin, J. *et al.* Regulatory effects of autophagy on spermatogenesis. *Biology of reproduction* **96**, 525-530 (2017).

71 Ni, F.-D., Hao, S.-L. & Yang, W.-X. Multiple signaling pathways in Sertoli cells: recent findings in spermatogenesis. *Cell Death & Disease* **10**, 541, doi:10.1038/s41419-019-1782-z (2019).

72 Yefimova, M. G. *et al.* Phagocytosis by Sertoli cells: analysis of main phagocytosis steps by confocal and electron microscopy. *Sertoli cells: methods and protocols*, 85-101 (2018).

73 Boj, M., Chauvigné, F., Zapater, C. & Cerdà, J. Gonadotropin-activated androgen-dependent and independent pathways regulate aquaporin expression during teleost (Sparus aurata) spermatogenesis. *PLoS One* **10**, e0142512 (2015).

74 Deng, Q. *et al.* Vesicle-associated membrane protein-associated protein a is involved in androgen receptor trafficking in mouse Sertoli cells. *International Journal of Endocrinology* **2018** (2018).

75 Zhang, J. J. *et al.* Identification of microRNAs for regulating adenosine monophosphate-activated protein kinase expression in immature boar Sertoli cells in vitro. *Molecular Reproduction and Development* **86**, 450-464 (2019).

76 Santos, N. C. & Kim, K. H. Activity of retinoic acid receptor-alpha is directly regulated at its protein kinase A sites in response to follicle-stimulating hormone signaling. *Endocrinology* **151**, 2361-2372 (2010).

77 Ye, L. *et al.* Toxic effects of T i O 2 nanoparticles in primary cultured rat sertoli cells are mediated via a dysregulated C a2+/PKC/p38 MAPK/NF-κ B cascade. *Journal of Biomedical Materials Research Part A* **105**, 1374-1382 (2017).

78 Lei, T. *et al.* Galectin-1 enhances TNFα-induced inflammatory responses in Sertoli cells through activation of MAPK signalling. *Scientific Reports* **8**, 3741 (2018).

79 Itman, C. *et al.* Developmentally regulated SMAD2 and SMAD3 utilization directs activin signaling outcomes. *Developmental dynamics: an official publication of the American Association of Anatomists* **238**, 1688-1700 (2009).

80 Wang, X. N. *et al.* The Wilms tumor gene, Wt1, is critical for mouse spermatogenesis via regulation of sertoli cell polarity and is associated with non-obstructive azoospermia in humans. *PLoS genetics* **9**, e1003645 (2013).

81 Young, J. C., Wakitani, S. & Loveland, K. L. in *Seminars in cell & developmental biology.* 94-103 (Elsevier).

82 Itman, C. & Loveland, K. L. SMAD expression in the testis: An insight into BMP regulation of spermatogenesis. *Developmental Dynamics* **237**, 97-111, doi:https://doi.org/10.1002/dvdy.21401 (2008).

83 Mendis, S. H. S., Meachem, S. J., Sarraj, M. A. & Loveland, K. L. Activin A Balances Sertoli and Germ Cell Proliferation in the Fetal Mouse Testis1. *Biology of Reproduction* **84**, 379-391, doi:10.1095/biolreprod.110.086231 (2010).

84 Zhang, X.-J., Wen, X.-X., Zhao, L. & He, J.-P. Immunolocalization of Smad4 protein in the testis of domestic fowl (Gallus domesticus) during postnatal development. *Acta Histochemica* **114**, 429-433, doi:https://doi.org/10.1016/j.acthis.2011.08.003 (2012).

85 Archambeault, D. R. & Yao, H. H.-C. Loss of smad4 in Sertoli and Leydig cells leads to testicular dysgenesis and hemorrhagic tumor formation in mice. *Biology of Reproduction* **90**, 62, 61-10 (2014).

86 Petricca, S. *et al.* Tebuconazole and Econazole Act Synergistically in Mediating Mitochondrial Stress, Energy Imbalance, and Sequential Activation of Autophagy and Apoptosis in Mouse Sertoli TM4 Cells: Possible Role of AMPK/ULK1 Axis. *Toxicol Sci* **169**, 209-223, doi:10.1093/toxsci/kfz031 (2019).

87 Bertoldo, M. J. *et al.* Specific deletion of AMP-activated protein kinase (α1AMPK) in mouse Sertoli cells modifies germ cell quality. *Mol Cell Endocrinol* **423**, 96-112, doi:10.1016/j.mce.2016.01.001 (2016).

88 Tartarin, P. *et al.* Inactivation of AMPKα1 induces asthenozoospermia and alters spermatozoa morphology. *Endocrinology* **153**, 3468-3481, doi:10.1210/en.2011-1911 (2012).

89 Gautam, M., Bhattacharya, I., Rai, U. & Majumdar, S. S. Hormone induced differential transcriptome analysis of Sertoli cells during postnatal maturation of rat testes. *PLoS One* **13**, e0191201, doi:10.1371/journal.pone.0191201 (2018).

90 De Cesaris, P. *et al.* Tumor necrosis factor-alpha induces interleukin-6 production and integrin ligand expression by distinct transduction pathways. *J Biol Chem* **273**, 7566-7571, doi:10.1074/jbc.273.13.7566 (1998).

91 De Cesaris, P. *et al.* Activation of Jun N-terminal kinase/stress-activated protein kinase pathway by tumor necrosis factor alpha leads to intercellular adhesion molecule-1 expression. *J Biol Chem* **274**, 28978-28982, doi:10.1074/jbc.274.41.28978 (1999).

92 Hirai, K. *et al.* HST-1/FGF-4 protects male germ cells from apoptosis under heat-stress condition. *Exp Cell Res* **294**, 77-85, doi:10.1016/j.yexcr.2003.11.012 (2004).

93 Jiang, X. *et al.* The roles of fibroblast growth factors in the testicular development and tumor. *J Diabetes Res* **2013**, 489095, doi:10.1155/2013/489095 (2013).

94 Godet, M., Sabido, O., Gilleron, J. & Durand, P. Meiotic progression of rat spermatocytes requires mitogen-activated protein kinases of Sertoli cells and close contacts between the germ cells and the Sertoli cells. *Dev Biol* **315**, 173-188, doi:10.1016/j.ydbio.2007.12.019 (2008).

95 Hasegawa, K., Namekawa, S. H. & Saga, Y. MEK/ERK signaling directly and indirectly contributes to the cyclical self-renewal of spermatogonial stem cells. *Stem Cells* **31**, 2517-2527, doi:10.1002/stem.1486 (2013).

96 Galardo, M. N. *et al.* Different signal transduction pathways elicited by basic fibroblast growth factor and interleukin 1β regulate CREB phosphorylation in Sertoli cells. *J Endocrinol Invest* **36**, 331-338, doi:10.3275/8582 (2013).

97 Crépieux, P. *et al.* The ERK-dependent signalling is stage-specifically modulated by FSH, during primary Sertoli cell maturation. *Oncogene* **20**, 4696-4709, doi:10.1038/sj.onc.1204632 (2001).

98 Li, M. W. *et al.* Tumor necrosis factor {alpha} reversibly disrupts the blood-testis barrier and impairs Sertoli-germ cell adhesion in the seminiferous epithelium of adult rat testes. *J Endocrinol* **190**, 313-329, doi:10.1677/joe.1.06781 (2006).

99 Hedger, M. P. in *Knobil and Neill's Physiology of Reproduction (Fourth Edition)* (eds Tony M. Plant & Anthony J. Zeleznik) 805-892 (Academic Press, 2015).

100 Kaur, G., Thompson, L. A. & Dufour, J. M. Sertoli cells – Immunological sentinels of spermatogenesis. *Seminars in Cell & Developmental Biology* **30**, 36-44, doi:https://doi.org/10.1016/j.semcdb.2014.02.011 (2014).

101 Luca, G. *et al.* Sertoli cells for cell transplantation: pre-clinical studies and future perspectives. *Andrology* **6**, 385-395, doi:https://doi.org/10.1111/andr.12484 (2018).

102 Tung, K. S. K. *et al.* Egress of sperm autoantigen from seminiferous tubules maintains systemic tolerance. *The Journal of Clinical Investigation* **127**, 1046-1060, doi:10.1172/JCI89927 (2017).

103 O'Donnell, L. *et al.* Sperm proteins and cancer-testis antigens are released by the seminiferous tubules in mice and men. *Faseb j* **35**, e21397, doi:10.1096/fj.202002484R (2021).

104 Bloom, D. E. & Cadarette, D. Infectious Disease Threats in the Twenty-First Century: Strengthening the Global Response. *Front Immunol* **10**, 549, doi:10.3389/fimmu.2019.00549 (2019).

105 Grubaugh, N. D. *et al.* Tracking virus outbreaks in the twenty-first century. *Nat Microbiol* **4**, 10-19, doi:10.1038/s41564-018-0296-2 (2019).

106 Roychoudhury, S. *et al.* Viral Pandemics of the Last Four Decades: Pathophysiology, Health Impacts and Perspectives. *Int J Environ Res Public Health* **17**, doi:10.3390/ijerph17249411 (2020).

107 Evenson, D. P., Jost, L. K., Corzett, M. & Balhorn, R. Characteristics of human sperm chromatin structure following an episode of influenza and high fever: a case study. *J Androl* **21**, 739-746 (2000).

108 Lugar, D. W., Ragland, D. & Stewart, K. R. Influenza outbreak causes reduction in semen quality of boars. *JSHAP* **25**, 303-307 (2017).

109 Sergerie, M., Mieusset, R., Croute, F., Daudin, M. & Bujan, L. High risk of temporary alteration of semen parameters after recent acute febrile illness. *Fertil Steril* **88**, 970.e971-977, doi:10.1016/j.fertnstert.2006.12.045 (2007).

110 Devi, B. Y., Sharma, G. & Polasa, H. Induction of chromosomal aberrations in mice spermatocytes by unpurified & purified human influenza viruses. *Indian J Med Res* **86**, 506-510 (1987).

111 Mead, P. S. *et al.* Zika Virus Shedding in Semen of Symptomatic Infected Men. *N Engl J Med* **378**, 1377-1385, doi:10.1056/NEJMoa1711038 (2018).

112 Mansuy, J. M. *et al.* Zika virus: high infectious viral load in semen, a new sexually transmitted pathogen? *Lancet Infect Dis* **16**, 405, doi:10.1016/s1473-3099(16)00138-9 (2016).

113 Chan, J. F. *et al.* Zika Virus Infection in Dexamethasone-immunosuppressed Mice Demonstrating Disseminated Infection with Multi-organ Involvement Including Orchitis Effectively Treated by Recombinant Type I Interferons. *EBioMedicine* **14**, 112-122, doi:10.1016/j.ebiom.2016.11.017 (2016).

114 Matusali, G. *et al.* Zika virus infects human testicular tissue and germ cells. *J Clin Invest* **128**, 4697-4710, doi:10.1172/jci121735 (2018).

115 Clancy, C. S., Van Wettere, A. J., Siddharthan, V., Morrey, J. D. & Julander, J. G. Comparative Histopathologic Lesions of the Male Reproductive Tract during Acute Infection of Zika Virus in AG129 and

Ifnar(-/-) Mice. *Am J Pathol* **188**, 904-915, doi:10.1016/j.ajpath.2017.12.019 (2018).

116 Govero, J. *et al.* Zika virus infection damages the testes in mice. *Nature* **540**, 438-442, doi:10.1038/nature20556 (2016).

117 Joguet, G. *et al.* Effect of acute Zika virus infection on sperm and virus clearance in body fluids: a prospective observational study. *Lancet Infect Dis* **17**, 1200-1208, doi:10.1016/s1473-3099(17)30444-9 (2017).

118 Avelino-Silva, V. I. *et al.* Potential effect of Zika virus infection on human male fertility? *Rev Inst Med Trop Sao Paulo* **60**, e64, doi:10.1590/s1678-9946201860064 (2018).

119 Akhigbe, R. E. *et al.* Viral Infections and Male Infertility: A Comprehensive Review of the Role of Oxidative Stress. *Front Reprod Health* **4**, 782915, doi:10.3389/frph.2022.782915 (2022).

120 Shereen, M. A., Khan, S., Kazmi, A., Bashir, N. & Siddique, R. COVID-19 infection: Origin, transmission, and characteristics of human coronaviruses. *J Adv Res* **24**, 91-98, doi:10.1016/j.jare.2020.03.005 (2020).

121 World Health Organization. WHO Coronavirus (COVID-19) Dashboard. World Health Organizationhttps://covid19.who.int/ (2021).

122 Lithander, F. E. *et al.* COVID-19 in older people: a rapid clinical review. *Age Ageing* **49**, 501-515, doi:10.1093/ageing/afaa093 (2020).

123 Fakhry AbdelMassih, A. *et al.* Obese communities among the best predictors of COVID-19-related deaths. *Cardiovasc Endocrinol Metab* **9**, 102-107, doi:10.1097/xce.0000000000000218 (2020).

124 Fang, L., Karakiulakis, G. & Roth, M. Are patients with hypertension and diabetes mellitus at increased risk for COVID-19 infection? *Lancet Respir Med* **8**, e21, doi:10.1016/s2213-2600(20)30116-8 (2020).

125 AbdelMassih, A. F. *et al.* A multicenter consensus: A role of furin in the endothelial tropism in obese patients with COVID-19 infection. *Obes Med* **19**, 100281, doi:10.1016/j.obmed.2020.100281 (2020).

126 Zheng, Z. *et al.* Risk factors of critical & mortal COVID-19 cases: A systematic literature review and meta-analysis. *J Infect* **81**, e16-e25, doi:10.1016/j.jinf.2020.04.021 (2020).

127 Cevik, M., Bamford, C. G. G. & Ho, A. COVID-19 pandemic-a focused review for clinicians. *Clin Microbiol Infect* **26**, 842-847, doi:10.1016/j.cmi.2020.04.023 (2020).

128 Stasi, C., Fallani, S., Voller, F. & Silvestri, C. Treatment for COVID-19: An overview. *Eur J Pharmacol* **889**, 173644, doi:10.1016/j.ejphar.2020.173644 (2020).

129 Zhang, J. J. *et al.* Clinical characteristics of 140 patients infected with SARS-CoV-2 in Wuhan, China. *Allergy* **75**, 1730-1741, doi:10.1111/all.14238 (2020).

130 Mao, L. *et al.* Neurologic Manifestations of Hospitalized Patients With Coronavirus Disease 2019 in Wuhan, China. *JAMA Neurol* **77**, 683-690, doi:10.1001/jamaneurol.2020.1127 (2020).

131 Wu, P. *et al.* Characteristics of Ocular Findings of Patients With Coronavirus Disease 2019 (COVID-19) in Hubei Province, China. *JAMA Ophthalmol* **138**, 575-578, doi:10.1001/jamaophthalmol.2020.1291 (2020).

132 Nishiga, M., Wang, D. W., Han, Y., Lewis, D. B. & Wu, J. C. COVID-19 and cardiovascular disease: from basic mechanisms to clinical perspectives. *Nat Rev Cardiol* **17**, 543-558, doi:10.1038/s41569-020-0413-9 (2020).

133 Zheng, Y. Y., Ma, Y. T., Zhang, J. Y. & Xie, X. COVID-19 and the cardiovascular system. *Nat Rev Cardiol* **17**, 259-260, doi:10.1038/s41569-020-0360-5 (2020).

134 Puelles, V. G. *et al.* Multiorgan and Renal Tropism of SARS-CoV-2. *N Engl J Med* **383**, 590-592, doi:10.1056/NEJMc2011400 (2020).

135 Trypsteen, W., Van Cleemput, J., Snippenberg, W. V., Gerlo, S. & Vandekerckhove, L. On the whereabouts of SARS-CoV-2 in the human body: A systematic review. *PLoS Pathog* **16**, e1009037, doi:10.1371/journal.ppat.1009037 (2020).

136 Carfì, A., Bernabei, R. & Landi, F. Persistent Symptoms in Patients After Acute COVID-19. *Jama* **324**, 603-605, doi:10.1001/jama.2020.12603 (2020).

137 Lopez-Leon, S. *et al.* More than 50 long-term effects of COVID-19: a systematic review and meta-analysis. *Sci Rep* **11**, 16144, doi:10.1038/s41598-021-95565-8 (2021).

138 Groff, D. *et al.* Short-term and Long-term Rates of Postacute Sequelae of SARS-CoV-2 Infection: A Systematic Review. *JAMA Netw Open* **4**, e2128568, doi:10.1001/jamanetworkopen.2021.28568 (2021).

139 Weiss, S. R. & Leibowitz, J. L. Coronavirus pathogenesis. *Adv. Virus Res.* **81** (2011).

140 Mesel-Lemoine, M. A human coronavirus responsible for the common cold massively kills dendritic cells but not monocytes. *J. Virol.* **86** (2012).

141 Zhou, P. A pneumonia outbreak associated with a new coronavirus of probable bat origin. *Nature* **579** (2020).

142 Chen, N. Epidemiological and clinical characteristics of 99 cases of 2019 novel coronavirus pneumonia in Wuhan, China: a descriptive study. *Lancet* **395** (2020).

143 Zhu, Z. From SARS and MERS to COVID-19: a brief summary and comparison of severe acute respiratory infections caused by three highly pathogenic human coronaviruses. *Respir. Res.* **21** (2020).

144 Liu, Y. Viral dynamics in mild and severe cases of COVID-19. *Lancet Infect. Dis.* **20** (2020).

145 Zhao, S. Preliminary estimation of the basic reproduction number of novel coronavirus (2019-nCoV) in China, from 2019 to 2020: a data-driven analysis in the early phase of the outbreak. *Int. J. Infect. Dis.* **92** (2020).

146 Liu, Y., Gayle, A. A., Wilder-Smith, A. & Rocklöv, J. The reproductive number of COVID-19 is higher compared to SARS coronavirus. *J. Travel. Med.* **27** (2020).

147 Lipsitch, M. Transmission dynamics and control of severe acute respiratory syndrome. *Science* **300** (2003).

148 Majumder, M. S., Rivers, C., Lofgren, E. & Fisman, D. Estimation of MERS-coronavirus reproductive number and case fatality rate for the spring 2014 Saudi Arabia outbreak: insights from publicly available data. *PLoS Curr.*, doi:10.1371/currents.outbreaks.98d2f8f3382d84f390736cd5f5fe133c (2014).

149 V'kovski, P., Kratzel, A., Steiner, S., Stalder, H. & Thiel, V. Coronavirus biology and replication: implications for SARS-CoV-2. *Nat. Rev. Microbiol.* **19** (2021).

150 Astuti, I. & Ysrafil. Severe acute respiratory syndrome coronavirus 2 (SARS-CoV-2): an overview of viral structure and host response. *Diabetes Metab. Syndr.* **14** (2020).

151 Li, F. Structure, function, and evolution of coronavirus spike proteins. *Annu. Rev. Virol.* **3** (2016).

152 Xu, X. Evolution of the novel coronavirus from the ongoing Wuhan outbreak and modeling of its spike protein for risk of human transmission. *Sci. China Life Sci.* **63** (2020).

153 Li, F., Li, W., Farzan, M. & Harrison, S. C. Structure of SARS coronavirus spike receptor-binding domain complexed with receptor. *Science* **309** (2005).

154 Li, F. Conformational states of the severe acute respiratory syndrome coronavirus spike protein ectodomain. *J. Virol.* **80** (2006).

155 Yuan, Y. Cryo-EM structures of MERS-CoV and SARS-CoV spike glycoproteins reveal the dynamic receptor binding domains. *Nat. Commun.* **8** (2017).

156 Perlman, S. & Netland, J. Coronaviruses post-SARS: update on replication and pathogenesis. *Nat. Rev. Microbiol.* **7** (2009).

157 Wang, N. Structure of MERS-CoV spike receptor-binding domain complexed with human receptor DPP4. *Cell Res.* **23** (2013).

158 Walls, A. C. Structure, function, and antigenicity of the SARS-CoV-2 spike glycoprotein. *Cell* **181** (2020).

159 Li, W. Angiotensin-converting enzyme 2 is a functional receptor for the SARS coronavirus. *Nature* **426** (2003).

160 Raj, V. S. Dipeptidyl peptidase 4 is a functional receptor for the emerging human coronavirus-EMC. *Nature* **495** (2013).

161 Towler, P. ACE2 X-ray structures reveal a large hinge-bending motion important for inhibitor binding and catalysis. *J. Biol. Chem.* **279** (2004).

162 Wong, S. K., Li, W., Moore, M. J., Choe, H. & Farzan, M. A 193-amino acid fragment of the SARS coronavirus S protein efficiently binds angiotensin-converting enzyme 2. *J. Biol. Chem.* **279** (2004).

163 Chen, Y., Guo, Y., Pan, Y. & Zhao, Z. J. Structure analysis of the receptor binding of 2019-nCoV. *Biochem. Biophys. Res. Commun.* **525** (2020).

164 Glowacka, I. Evidence that TMPRSS2 activates the severe acute respiratory syndrome coronavirus spike protein for membrane fusion and reduces viral control by the humoral immune response. *J. Virol.* **85** (2011).

165 Heurich, A. TMPRSS2 and ADAM17 Cleave ACE2 differentially and only proteolysis by TMPRSS2 augments entry driven by the severe acute respiratory syndrome coronavirus spike protein. *J. Virol.* **88** (2014).

166 Henrich, S. The crystal structure of the proprotein processing proteinase furin explains its stringent specificity. *Nat. Struct. Mol. Biol.* **10** (2003).

167 Shang, J. Structural basis of receptor recognition by SARS-CoV-2. *Nature* **581** (2020).

168 Wrapp, D. Cryo-EM structure of the 2019-nCoV spike in the prefusion conformation. *Science* **367** (2020).

169 Kim, Y. Crystal structure of Nsp15 endoribonuclease NendoU from SARS-CoV-2. *Protein Sci.* **29** (2020).

170 Meng, T. The insert sequence in SARS-CoV-2 enhances spike protein cleavage by TMPRSS. Preprint at. *bioRxiv*, doi:10.1101/2020.02.08.926006 (2020).

171 Hasan, A. A review on the cleavage priming of the spike protein on coronavirus by angiotensin-converting enzyme-2 and furin. *J. Biomol. Struct. Dyn.* **39** (2020).

172 Millet, J. K., Jaimes, J. A. & Whittaker, G. R. Molecular diversity of coronavirus host cell entry receptors. *FEMS Microbiol. Rev.* **45** (2020).

173 Hoffmann, M., Kleine-Weber, H. & Pöhlmann, S. A multibasic cleavage site in the spike protein of SARS-CoV-2 is essential for infection of human lung cells. *Mol. Cell* **78** (2020).

174 Ranta, N. The plasma level of proprotein convertase FURIN in patients with suspected infection in the emergency room: a prospective cohort study. *Scand. J. Immunol.* **82** (2015).

175 Xia, S. The role of furin cleavage site in SARS-CoV-2 spike protein-mediated membrane fusion in the presence or absence of trypsin. *Signal. Transduct. Target. Ther.* **5** (2020).

176 Duffy, S. Why are RNA virus mutation rates so damn high? *PLoS Biol.* **16** (2018).

177 Li, Q. The impact of mutations in SARS-CoV-2 spike on viral infectivity and antigenicity. *Cell* **182** (2020).

178 Ozono, S. SARS-CoV-2 D614G spike mutation increases entry efficiency with enhanced ACE2-binding affinity. *Nat. Commun.* **12** (2021).

179 Vöhringer, H. S. Genomic reconstruction of the SARS-CoV-2 epidemic in England. *Nature*, doi:10.1038/s41586-021-04069-y (2021).

180 Guruprasad, L. Human SARS CoV-2 spike protein mutations. *Proteins* **89** (2021).

181 Qiao, Y. Targeting transcriptional regulation of SARS-CoV-2 entry factors ACE2and TMPRSS2. *Proc. Natl Acad. Sci. USA* **118** (2021).

182 Lucas, J. M. The androgen-regulated protease TMPRSS2 activates a proteolytic cascade involving components of the tumor microenvironment and promotes prostate cancer metastasis. *Cancer Discov.* **4** (2014).

183 Younis, J. S., Skorecki, K. & Abassi, Z. The double edge sword of testosterone's role in the COVID-19 pandemic. *Front. Endocrinol.*, doi:10.3389/fendo.2021.607179 (2021).

184 Bilinska, K., Jakubowska, P., Bartheld, C. S. & Butowt, R. Expression of the SARS-CoV-2 entry proteins, ACE2 and TMPRSS2, in cells of the olfactory epithelium: identification of cell types and trends with age. *ACS Chem. Neurosci.* **11** (2020).

185 Dugail, I., Amri, E. Z. & Vitale, N. High prevalence for obesity in severe COVID-19: possible links and perspectives towards patient stratification. *Biochimie* **179** (2020).

186 Holly, J. M. P., Biernacka, K., Maskell, N. & Perks, C. M. Obesity, diabetes and COVID-19: an infectious disease spreading from the east collides with the consequences of an unhealthy western lifestyle. *Front. Endocrinol.* **11** (2020).

187 Shibata, S. Hypertension and related diseases in the era of COVID-19: a report from the Japanese Society of Hypertension Task Force on COVID-19. *Hypertens. Res.* **43** (2020).

188 Bui, L. T. Chronic lung diseases are associated with gene expression programs favoring SARS-CoV-2 entry and severity. *Nat. Commun.* **12** (2021).

189 Zipeto, D., Palmeira, J. d. F., Argañaraz, G. A. & Argañaraz, E. R. ACE2/ADAM17/TMPRSS2 interplay may be the main risk factor for COVID-19. *Front. Immunol.*, doi:10.3389/fimmu.2020.576745 (2020).

190 Kočar, E., Režen, T. & Rozman, D. Cholesterol, lipoproteins, and COVID-19: Basic concepts and clinical applications. *Biochim. Biophys. Acta Mol. Cell Biol. Lipids* **1866** (2021).

191 Brake, S. J. Smoking Upregulates angiotensin-converting enzyme-2 receptor: a potential adhesion site for novel coronavirus SARS-CoV-2 (Covid-19). *J. Clin. Med.* **9** (2020).

192 Wu, Q., Coumoul, X., Grandjean, P., Barouki, R. & Audouze, K. Endocrine disrupting chemicals and COVID-19 relationships: a computational systems biology approach. Preprint at. *medRxiv*, doi:10.1101/2020.07.10.20150714 (2020).

193 Braun, E. & Sauter, D. Furin-mediated protein processing in infectious diseases and cancer. *Clin. Transl. Immunol.* **8** (2019).

194 Hoffmann, M. SARS-CoV-2 cell entry depends on ACE2 and TMPRSS2 and is blocked by a clinically proven protease inhibitor. *Cell* **181** (2020).

195 Sungnak, W. SARS-CoV-2 entry factors are highly expressed in nasal epithelial cells together with innate immune genes. *Nat. Med.* **26** (2020).

196 Zhao, M. M. Cathepsin L plays a key role in SARS-CoV-2 infection in humans and humanized mice and is a promising target for new drug development. *Signal. Transduct. Target. Ther.* **6** (2021).

197 Samavati, L. & Uhal, B. D. ACE2, Much more than just a receptor for SARS-COV-2. *Front. Cell. Infect. Microbiol.* **10** (2020).

198 Chi, M. Dexmedetomidine promotes breast cancer cell migration through Rab11-mediated secretion of exosomal TMPRSS2. *Ann. Transl. Med.* **8** (2020).

199 Kuba, K., Imai, Y. & Penninger, J. M. Angiotensin-converting enzyme 2 in lung diseases. *Curr. Opin. Pharmacol.* **6** (2006).

200 Takahashi, H. Upregulation of the renin-angiotensin-aldosterone-ouabain system in the brain Is the core mechanism in the genesis of all types of hypertension. *Int. J. Hypertens.* **2012** (2012).

201 Okamura, A. Upregulation of renin-angiotensin system during differentiation of monocytes to macrophages. *J. Hypertens.* **17** (1999).

202 Paz Ocaranza, M. Counter-regulatory renin–angiotensin system in cardiovascular disease. *Nat. Rev. Cardiol.* **17** (2020).

203 Iwai, M. & Horiuchi, M. Devil and angel in the renin–angiotensin system: ACE–angiotensin II–AT1 receptor axis vs. ACE2–angiotensin-(1–7)–Mas receptor axis. *Hypertens. Res.* **32** (2009).

204 Kuriakose, J., Montezano, A. C. & Touyz, R. M. ACE2/Ang-(1-7)/Mas1 axis and the vascular system: vasoprotection to COVID-19-associated vascular disease. *Clin. Sci.* **135** (2021).

205 Karnik, S. S., Singh, K. D., Tirupula, K. & Unal, H. Significance of angiotensin 1–7 coupling with MAS1 receptor and other GPCRs to the

renin-angiotensin system: IUPHAR Review 22. *Br. J. Pharmacol.* **174** (2017).

206 Ingraham, N. E. Understanding the renin-angiotensin-aldosterone-SARS-CoV-axis: a comprehensive review. *Eur. Respir. J.* **56** (2020).

207 Xiao, L., Sakagami, H. & Miwa, N. ACE2: the key molecule for understanding the pathophysiology of severe and critical conditions of COVID-19: demon or angel? *Viruses* **12** (2020).

208 Verdecchia, P., Cavallini, C., Spanevello, A. & Angeli, F. The pivotal link between ACE2 deficiency and SARS-CoV-2 infection. *Eur. J. Intern. Med.* **76** (2020).

209 Imai, Y., Kuba, K. & Penninger, J. M. The discovery of angiotensin-converting enzyme 2 and its role in acute lung injury in mice. *Exp. Physiol.* **93** (2008).

210 Zhang, H., Penninger, J. M., Li, Y., Zhong, N. & Slutsky, A. S. Angiotensin-converting enzyme 2 (ACE2) as a SARS-CoV-2 receptor: molecular mechanisms and potential therapeutic target. *Intensive Care Med.* **46** (2020).

211 Ekholm, M., Kahan, T., Jörneskog, G., Brinck, J. & Wallén, N. H. Haemostatic and inflammatory alterations in familial hypercholesterolaemia, and the impact of angiotensin II infusion. *J. Renin Angiotensin Aldosterone Syst.* **16** (2015).

212 Beyerstedt, S., Casaro, E. B. & Rangel, É. B. COVID-19: angiotensin-converting enzyme 2 (ACE2) expression and tissue susceptibility to SARS-CoV-2 infection. *Eur. J. Clin. Microbiol. Infect. Dis.* **40** (2021).

213 Zapater, P., Novalbos, J., Gallego-Sandín, S., Hernández, F. T. & Abad-Santos, F. Gender differences in angiotensin-converting enzyme (ACE) activity and inhibition by enalaprilat in healthy volunteers. *J. Cardiovasc. Pharmacol.* **43** (2004).

214 Komukai, K., Mochizuki, S. & Yoshimura, M. Gender and the renin–angiotensin–aldosterone system. *Fundam. Clin. Pharmacol.* **24** (2010).

215 Reyes, J. G. The hypoxic testicle: physiology and pathophysiology. *Oxid. Med. Cell Longev.* **2012** (2012).

216 Colli, L. G. Systemic arterial hypertension leads to decreased semen quality and alterations in the testicular microcirculation in rats. *Sci. Rep.* **9** (2019).

217 Pacurari, M., Kafoury, R., Tchounwou, P. B. & Ndebele, K. The renin-angiotensin-aldosterone system in vascular inflammation and remodeling. *Int. J. Inflamm.* **2014** (2014).

218 Guo, J. H., Huang, Q., Studholme, D. J., Wu, C. Q. & Zhao, Z. Transcriptomic analyses support the similarity of gene expression between brain and testis in human as well as mouse. *Cytogenet. Genome Res.* **111** (2005).

219 McGavern, D. B. & Kang, S. S. Illuminating viral infections in the nervous system. *Nat. Rev. Immunol.* **11** (2011).

220 Jackson, L., Eldahshan, W., Fagan, S. C. & Ergul, A. Within the brain: the renin angiotensin system. *Int. J. Mol. Sci.* **19** (2018).

221 Xia, H. & Lazartigues, E. Angiotensin-converting enzyme 2 in the brain: properties and future directions. *J. Neurochem.* **107** (2008).

222 Song, E. Neuroinvasion of SARS-CoV-2 in human and mouse brain. *J. Exp. Med.* **218** (2021).

223 Paterson, R. W. The emerging spectrum of COVID-19 neurology: clinical, radiological and laboratory findings. *Brain* **143** (2020).

224 Castilho, A. C. S., Fontes, P. K., Franchi, F. F., Santos, P. H. & Razza, E. M. Renin-angiotensin system on reproductive biology, renin-angiotensin system - past, present and future. *IntechOpen*, doi:10.5772/66997 (2017).

225 Gianzo, M. Angiotensin II type 2 receptor is expressed in human sperm cells and is involved in sperm motility. *Fertil. Steril.* **105** (2016).

226 Leal, M. C. The role of angiotensin-(1-7) receptor Mas in spermatogenesis in mice and rats. *J. Anat.* **214** (2009).

227 Leung, P. S. & Sernia, C. The renin-angiotensin system and male reproduction: new functions for old hormones. *J. Mol. Endocrinol.* **30** (2003).

228 Paul, M., Mehr, A. P. & Kreutz, R. Physiology of local renin-angiotensin systems. *Physiol. Rev.* **86** (2006).

229 Reis, A. B. Angiotensin (1-7) and its receptor Mas are expressed in the human testis: implications for male infertility. *J. Mol. Histol.* **41** (2010).

230 Valdivia, A. Role of angiotensin-(1-7) via MAS receptor in human sperm motility and acrosome reaction. *Reproduction* **159** (2020).

231 Campbell, D. J. Clinical relevance of local renin angiotensin systems. *Front. Endocrinol.* **5** (2014).

232 Shibahara, H. Activity of testis angiotensin converting enzyme (ACE) in ejaculated human spermatozoa. *Int. J. Androl.* **24** (2001).

233 Illiano, E., Trama, F. & Costantini, E. Could COVID-19 have an impact on male fertility? *Andrologia* **52** (2020).

234 Younis, J. S., Abassi, Z. & Skorecki, K. Is there an impact of the COVID-19 pandemic on male fertility? The ACE2 connection. *Am. J. Physiol. Endocrinol. Metab.* **318** (2020).

235 Sèdes, L. Cholesterol: a gatekeeper of male fertility? *Front. Endocrinol.* **9** (2018).

236 Kerr, J. B. Ultrastructure of the seminiferous epithelium and intertubular tissue of the human testis. *J. Electron. Microsc. Tech.* **19** (1991).

237 Garcia, T. X. & Hofmann, M. C. Regulation of germ line stem cell homeostasis. *Anim. Reprod.* **12** (2015).

238 Rato, L. Metabolic regulation is important for spermatogenesis. *Nat. Rev. Urol.* **9** (2012).

239 Smith, L. B. & Walker, W. H. The regulation of spermatogenesis by androgens. *Semin. Cell Dev. Biol.* **30** (2014).

240 Guo, J. The adult human testis transcriptional cell atlas. *Cell Res.* **28** (2018).

241 Bhang, D. H. Testicular endothelial cells are a critical population in the germline stem cell niche. *Nat. Commun.* **9** (2018).

242 Mayerhofer, A. Human testicular peritubular cells: more than meets the eye. *Reproduction* **145** (2013).

243 Schuppe, H. C. Chronic orchitis: a neglected cause of male infertility? *Andrologia* **40** (2008).

244 Tortorec, A. L. From ancient to emerging infections: the odyssey of viruses in the male genital tract. *Physiol. Rev.* **100** (2020).

245 Liu, W., Han, R., Wu, H. & Han, D. Viral threat to male fertility. *Andrologia* **50** (2018).

246 Dejucq, N. & Jégou, B. Viruses in the mammalian male genital tract and their effects on the reproductive system. *Microbiol. Mol. Biol. Rev.* **65** (2001).

247 Cheng, C. Y. & Mruk, D. D. The blood-testis barrier and its implications for male contraception. *Pharmacol. Rev.* **64** (2012).

248 Almeida, R. d. N. The cellular impact of the ZIKA virus on male reproductive tract immunology and physiology. *Cells* **9** (2020).

249 Patel, D. P. The impact of SARS-CoV-2 and COVID-19 on male reproduction and men's health. *Fertil. Steril.* **115** (2021).

250 Siemann, D. N., Strange, D. P., Maharaj, P. N., Shi, P. Y. & Verma, S. Zika virus infects human Sertoli cells and modulates the integrity of the in vitro blood-testis barrier model. *J. Virol.* **91** (2017).

251 Leda, A. R. Selective disruption of the blood–brain barrier by Zika virus. *Front. Microbiol.* **10** (2019).

252 Hanchard, J., Capó-Vélez, C. M., Deusch, K., Lidington, D. & Bolz, S. S. Stabilizing cellular barriers: raising the shields against COVID-19. *Front. Endocrinol.* **11** (2020).

253 Buzhdygan, T. P. The SARS-CoV-2 spike protein alters barrier function in 2D static and 3D microfluidic in-vitro models of the human blood–brain barrier. *Neurobiol. Dis.* **146** (2020).

254 Sivabakya, T. K. & Srinivas, G. Lung barrier function in COVID-19? *SN Compr. Clin. Med.* **2** (2020).

255 Zhang, L. SARS-CoV-2 crosses the blood–brain barrier accompanied with basement membrane disruption without tight junctions alteration. *Signal. Transduct. Target. Ther.* **6** (2021).

256 Lukassen, S. SARS-CoV-2 receptor ACE2 and TMPRSS2 are primarily expressed in bronchial transient secretory cells. *EMBO J.* **39** (2020).

257 Hamming, I. Tissue distribution of ACE2 protein, the functional receptor for SARS coronavirus. A first step in understanding SARS pathogenesis. *J. Pathol.* **203** (2004).

258 Xu, H. High expression of ACE2 receptor of 2019-nCoV on the epithelial cells of oral mucosa. *Int. J. Oral. Sci.* **12** (2020).

259 Bourgonje, A. R. Angiotensin-converting enzyme 2 (ACE2), SARS-CoV-2 and the pathophysiology of coronavirus disease 2019 (COVID-19). *J. Pathol.* **251** (2020).

260 Salamanna, F., Maglio, M., Landini, M. P. & Fini, M. Body localization of ACE-2: on the trail of the keyhole of SARS-CoV-2. *Front. Med.* **7** (2020).

261 Li, S. SARS-CoV-2 triggers inflammatory responses and cell death through caspase-8 activation. *Signal. Transduct. Target. Ther.* **5** (2020).

262 Deinhardt-Emmer, S. SARS-CoV-2 causes severe epithelial inflammation and barrier dysfunction. *J. Virol.* **95** (2021).

263 Gkogkou, E., Barnasas, G., Vougas, K. & Trougakos, I. P. Expression profiling meta-analysis of ACE2 and TMPRSS2, the putative anti-inflammatory receptor and priming protease of SARS-CoV-2 in human cells, and identification of putative modulators. *Redox Biol.* **36** (2020).

264 Pan, F. No evidence of severe acute respiratory syndrome–coronavirus 2 in semen of males recovering from coronavirus disease 2019. *Fertil. Steril.* **113** (2020).

265 Stanley, K. E., Thomas, E., Leaver, M. & Wells, D. Coronavirus disease-19 and fertility: viral host entry protein expression in male and female reproductive tissues. *Fertil. Steril.* **114** (2020).

266 Pan, P. P., Zhan, Q. T., Le, F., Zheng, Y. M. & Jin, F. Angiotensin-converting enzymes play a dominant role in fertility. *Int. J. Mol. Sci.* **14** (2013).

267 Verma, S., Saksena, S. & Sadri-Ardekani, H. ACE2 receptor expression in testes: implications in coronavirus disease 2019 pathogenesis†. *Biol. Reprod.* **103** (2020).

268 Wang, Z. & Xu, X. scRNA-seq profiling of human testes reveals the presence of the ACE2 receptor, a target for SARS-CoV-2 infection in spermatogonia, Leydig and Sertoli cells. *Cells* **9** (2020).

269 Douglas, G. C. The novel angiotensin-converting enzyme (ACE) homolog, ACE2, is selectively expressed by adult Leydig cells of the testis. *Endocrinology* **145** (2004).

270 Navarra, A., Albani, E., Castellano, S., Arruzzolo, L. & Levi-Setti, P. E. Coronavirus disease-19 infection: implications on male fertility and reproduction. *Front. Physiol.* **11** (2020).

271 Fan, C., Lu, W., Li, K., Ding, Y. & Wang, J. ACE2 expression in kidney and testis may cause kidney and testis infection in COVID-19 patients. *Front. Med.* **7** (2021).

272 Song, H., Seddighzadeh, B., Cooperberg, M. R. & Huang, F. W. Expression of ACE2, the SARS-CoV-2 receptor, and TMPRSS2 in prostate epithelial cells. *Eur. Urol.* **78** (2020).

273 Zhou, L. SARS-CoV-2 targets by the pscRNA profiling of ACE2, TMPRSS2 and furin proteases. *iScience* **23** (2020).

274 Lazartigues, E., Qadir, M. M. & Mauvais-Jarvis, F. Endocrine significance of SARS-CoV-2's reliance on ACE2. *Endocrinology* **161** (2020).

275 Pal, R. & Banerjee, M. COVID-19 and the endocrine system: exploring the unexplored. *J. Endocrinol. Invest.* **43** (2020).

276 Piticchio, T., Moli, R., Tumino, D. & Frasca, F. Relationship between betacoronaviruses and the endocrine system: a new key to understand the COVID-19 pandemic — a comprehensive review. *J. Endocrinol. Invest.* **44** (2021).

277 Çayan, S., Uğuz, M., Saylam, B. & Akbay, E. Effect of serum total testosterone and its relationship with other laboratory parameters on the prognosis of coronavirus disease 2019 (COVID-19) in SARS-CoV-2 infected male patients: a cohort study. *Aging Male* **23** (2020).

278 Ma, L. Evaluation of sex-related hormones and semen characteristics in reproductive-aged male COVID-19 patients. *J. Med. Virol.* **93** (2021).

279 Toufexis, D., Rivarola, M. A., Lara, H. & Viau, V. Stress and the reproductive axis. *J. Neuroendocrinol.* **26** (2014).

280 Pal, R. COVID-19, hypothalamo-pituitary-adrenal axis and clinical implications. *Endocrine* **68** (2020).

281 Leow, M. K. S. Hypocortisolism in survivors of severe acute respiratory syndrome (SARS). *Clin. Endocrinol.* **63** (2005).

282 Zhao, J. M. Clinical pathology and pathogenesis of severe acute respiratory syndrome. *Zhonghua Shi Yan He Lin. Chuang Bing. Du. Xue Za Zhi* **17** (2003).

283 Xu, J. Orchitis: a complication of severe acute respiratory syndrome (SARS)1. *Biol. Reprod.* **74** (2006).

284 Wang, S., Zhou, X., Zhang, T. & Wang, Z. The need for urogenital tract monitoring in COVID-19. *Nat. Rev. Urol.* **17** (2020).

285 Cardona Maya, W. D., Plessis, S. S. & Velilla, P. A. SARS-CoV-2 and the testis: similarity with other viruses and routes of infection. *Reprod. Biomed. Online* **40** (2020).

286 Marca, A. Testicular pain as an unusual presentation of COVID-19: a brief review of SARS-CoV-2 and the testis. *Reprod. Biomed. Online* **41** (2020).

287 Ediz, C. Is there any association of COVID-19 with testicular pain and epididymo-orchitis? *Int. J. Clin. Pract.* **75** (2021).

288 Kim, J., Thomsen, T., Sell, N. & Goldsmith, A. J. Abdominal and testicular pain: an atypical presentation of COVID-19. *Am. J. Emerg. Med.* **38** (2020).

289 Bridwell, R. E., Merrill, D. R., Griffith, S. A., Wray, J. & Oliver, J. J. A coronavirus disease 2019 (COVID-19) patient with bilateral orchitis. *Am. J. Emerg. Med.* **42** (2021).

290 Gagliardi, L. Orchiepididymitis in a boy with COVID-19. *Pediatr. Infect. Dis. J.* **39** (2020).

291 Chen, L. Ultrasound imaging findings of acute testicular infection in patients with coronavirus disease 2019: a single-center-based study in Wuhan, China. *J. Ultrasound Med.* **40** (2020).

292 Falahieh, F. M. Effects of moderate COVID-19 infection on semen oxidative status and parameters 14 and 120 days after diagnosis. *Reprod. Fertil. Dev.* **33** (2021).

293 Li, H. Impaired spermatogenesis in COVID-19 patients. *EClinicalMedicine* **28** (2020).

294 Salciccia, S. Interplay between male testosterone levels and the risk for subsequent invasive respiratory assistance among COVID-19 patients at hospital admission. *Endocrine* **70** (2020).

295 Rastrelli, G. Low testosterone levels predict clinical adverse outcomes in SARS-CoV-2 pneumonia patients. *Andrology* **9** (2021).

296 Wei, L. Endocrine cells of the adenohypophysis in severe acute respiratory syndrome (SARS). *Biochem. Cell Biol.* **88** (2010).

297 Sharun, K., Tiwari, R. & Dhama, K. SARS-CoV-2 in semen: potential for sexual transmission in COVID-19. *Int. J. Surg.* **84** (2020).

298 Li, D., Jin, M., Bao, P., Zhao, W. & Zhang, S. Clinical characteristics and results of semen tests among men with coronavirus disease 2019. *JAMA Netw. Open* **3** (2020).

299 Mohseni, A. H., Taghinezhad-S, S., Xu, Z. & Fu, X. Body fluids may contribute to human-to-human transmission of severe acute respiratory

syndrome coronavirus 2: evidence and practical experience. *Chin. Med.* **15** (2020).

300 He, W. Impact of SARS-CoV-2 on male reproductive health: a review of the literature on male reproductive involvement in COVID-19. *Front. Med.* **7** (2020).

301 Atkinson, B. Presence and persistence of zika virus RNA in semen, United Kingdom, 2016. *Emerg. Infect. Dis.* **23** (2017).

302 Li, F. Distinct mechanisms for TMPRSS2 expression explain organ-specific inhibition of SARS-CoV-2 infection by enzalutamide. *Nat. Commun.* **12** (2021).

303 Zupin, L., Pascolo, L., Zito, G., Ricci, G. & Crovella, S. SARS-CoV-2 and the next generations: which impact on reproductive tissues? *J. Assist. Reprod. Genet.* **37** (2020).

304 Marca, A., Niederberger, C., Pellicer, A. & Nelson, S. M. COVID-19: lessons from the Italian reproductive medical experience. *Fertil. Steril.* **113** (2020).

305 Donoghue, M. A novel angiotensin-converting enzyme–related carboxypeptidase (ACE2) converts angiotensin I to angiotensin 1-9. *Circ. Res.* **87** (2000).

306 Vaarala, M. H., Porvari, K. S., Kellokumpu, S., Kyllönen, A. P. & Vihko, P. T. Expression of transmembrane serine protease TMPRSS2 in mouse and human tissues. *J. Pathol.* **193** (2001).

307 Pinto, B. G. G. ACE2 expression is increased in the lungs of patients with comorbidities associated with severe COVID-19. *J. Infect. Dis.* **222** (2020).

308 Erbay, G. Short-term effects of COVID-19 on semen parameters: a multicenter study of 69 cases. *Andrology* **9** (2021).

309 Aquila, I. SARS-CoV-2 pandemic: review of the literature and proposal for safe autopsy practice. *Arch. Pathol. Lab. Med.* **73** (2020).

310 Bian, X. W. & Team, T. C. P. Autopsy of COVID-19 patients in China. *Natl Sci. Rev.* **7** (2020).

311 Massarotti, C. SARS-CoV-2 in the semen: where does it come from? *Andrology* **9** (2021).

312 Yang, M. Pathological findings in the testes of COVID-19 patients: clinical implications. *Eur. Urol. Focus.* **6** (2020).

313 Duarte-Neto, A. N. Testicular pathology in fatal COVID-19: a descriptive autopsy study. *Andrology*, doi:10.1111/andr.13073 (2021).

314 Nie, X. Multi-organ proteomic landscape of COVID-19 autopsies. *Cell* **184** (2021).

315 Moghimi, N. COVID-19 disrupts spermatogenesis through the oxidative stress pathway following induction of apoptosis. *Apoptosis* **26** (2021).

316 Peirouvi, T. COVID-19 disrupts the blood-testis barrier through the induction of inflammatory cytokines and disruption of junctional proteins. *Inflamm. Res.* **26** (2021).

317 Ma, X. Pathological and molecular examinations of postmortem testis biopsies reveal SARS-CoV-2 infection in the testis and spermatogenesis damage in COVID-19 patients. *Cell Mol. Immunol.* **18** (2021).

318 Achua, J. K. Histopathology and ultrastructural findings of fatal COVID-19 infections on testis. *World J. Mens Health* **39** (2021).

319 Maiese, A. Autopsy findings in COVID-19-related deaths: a literature review. *Forensic Sci. Med. Pathol.* **17** (2020).

320 Ruiz, S. I., Zumbrun, E. E. & Nalca, A. in Animal Models for the Study of Human Disease 2nd edn (ed. Conn, P. M.) 853901 (Academic Press, 2017).

321 González, R. & Dobrinski, I. Beyond the mouse monopoly: studying the male germ line in domestic animal models. *ILAR J.* **56** (2015).

322 Roberts, A. Animal models and vaccines for SARS-CoV infection. *Virus Res.* **133** (2008).

323 Agrawal, A. S. Generation of a transgenic mouse model of middle east respiratory syndrome coronavirus infection and disease. *J. Virol.* **89** (2015).

324 Tao, X. Characterization and demonstration of the value of a lethal mouse model of middle east respiratory syndrome coronavirus infection and disease. *J. Virol.* **90** (2016).

325 Bao, L. The pathogenicity of SARS-CoV-2 in hACE2 transgenic mice. *Nature* **583** (2020).

326 Martina, B. E. E. Virology: SARS virus infection of cats and ferrets. *Nature* **425** (2003).

327 Sia, S. F. Pathogenesis and transmission of SARS-CoV-2 in golden hamsters. *Nature* **583** (2020).

328 Campos, R. K. SARS-CoV-2 infects hamster testes. *Microorganisms* **9** (2021).

329 Estes, J. D., Wong, S. W. & Brenchley, J. M. Nonhuman primate models of human viral infections. *Nat. Rev. Immunol.* **18** (2018).

330 Osuna, C. E. & Whitney, J. B. Nonhuman primate models of Zika virus infection, immunity, and therapeutic development. *J. Infect. Dis.* **216** (2017).

331 Haagmans, B. L. & Osterhaus, A. D. M. E. Nonhuman primate models for SARS. *PLoS Med.* **3** (2006).

332 Wit, E. Middle East respiratory syndrome coronavirus (MERS-CoV) causes transient lower respiratory tract infection in rhesus macaques. *Proc. Natl Acad. Sci. USA* **110** (2013).

333 Chao Shan, Y. F. Y. & Yang, X. L. Infection with novel coronavirus (SARS-CoV-2) causes pneumonia in the rhesus macaques. *Cell Res.* **30** (2020).

334 Totura, A. Small particle aerosol exposure of African Green monkeys to MERS-CoV as a model for highly pathogenic coronavirus infection. *Emerg. Infect. Dis. J.* **26** (2020).

335 Neff, E. African green monkey Zika models. *Lab. Anim.* **49** (2020).

336 Laksono, B. M. Studies into the mechanism of measles-associated immune suppression during a measles outbreak in the Netherlands. *Nat. Commun.* **9** (2018).

337 Alves-Lopes, J. P., Söder, O. & Stukenborg, J. B. Testicular organoid generation by a novel in vitro three-layer gradient system. *Biomaterials* **130** (2017).

338 Yin, L. High-content image-based single-cell phenotypic analysis for the testicular toxicity prediction induced by bisphenol A and its analogs bisphenol S, bisphenol AF, and tetrabromobisphenol A in a three-dimensional testicular cell co-culture model. *Toxicol. Sci.* **173** (2020).

339 Sakib, S., Voigt, A., Goldsmith, T. & Dobrinski, I. hree-dimensional testicular organoids as novel in vitro models of testicular biology and toxicology. *Environ. Epigenet* **5** (2019).

340 Fatehullah, A., Tan, S. H. & Barker, N. Organoids as an in vitro model of human development and disease. *Nat. Cell Biol.* **18** (2016).

341 Chen, K. G., Park, K. & Spence, J. R. Studying SARS-CoV-2 infectivity and therapeutic responses with complex organoids. *Nat. Cell Biol.* **23** (2021).

342 Baert, Y. Primary human testicular cells self-organize into organoids with testicular properties. *Stem Cell Rep.* **8** (2017).

343 Strange, D. P. Human testicular organoid system as a novel tool to study Zika virus pathogenesis. *Emerg. Microbes Infect.* **7** (2018).

344 Zhang, B. Z. SARS-CoV-2 infects human neural progenitor cells and brain organoids. *Cell Res.* **30** (2020).

345 Chu, H. Comparative replication and immune activation profiles of SARS-CoV-2 and SARS-CoV in human lungs: an ex vivo study with implications for the pathogenesis of COVID-19. *Clin. Infect. Dis.* **71** (2020).

346 Yuen, C. K. Suppression of SARS-CoV-2 infection in ex-vivo human lung tissues by targeting class III phosphoinositide 3-kinase. *J. Med. Virol.* **93** (2021).

347 Easley, C. A. T. Assessing reproductive toxicity of two environmental toxicants with a novel in vitro human spermatogenic model. *Stem Cell Res.* **14** (2015).

348 Greeson, K. W. Detrimental effects of flame retardant, PBB153, exposure on sperm and future generations. *Sci. Rep.* **10** (2020).

349 Steves, A. N. Per- and polyfluoroalkyl substances impact human spermatogenesis in a stem-cell-derived model. *Syst. Biol. Reprod. Med.* **64** (2018).

350 Ballering, A. V., Oertelt-Prigione, S., Olde Hartman, T. C. & Rosmalen, J. G. M. Sex and Gender-Related Differences in COVID-19 Diagnoses and SARS-CoV-2 Testing Practices During the First Wave of the Pandemic: The Dutch Lifelines COVID-19 Cohort Study. *J Womens Health (Larchmt)* **30**, 1686-1692, doi:10.1089/jwh.2021.0226 (2021).

351 Park, S. *et al.* Unreported SARS-CoV-2 Home Testing and Test Positivity. *JAMA Network Open* **6**, e2252684-e2252684, doi:10.1001/jamanetworkopen.2022.52684 (2023).

352 HHS. (2023).

353 Edenfield, R. C. & Easley, C. A. Implications of testicular ACE2 and the renin–angiotensin system for SARS-CoV-2 on testis function. *Nature Reviews Urology* **19**, 116-127, doi:10.1038/s41585-021-00542-5 (2022).

354 Wang, P. *et al.* Blood–brain barrier injury and neuroinflammation induced by SARS-CoV-2 in a lung–brain microphysiological system. *Nature Biomedical Engineering*, doi:10.1038/s41551-023-01054-w (2023).

355 Song, H. *et al.* Detection of blood–brain barrier disruption in brains of patients with COVID-19, but no evidence of brain penetration by SARS-CoV-2. *Acta Neuropathologica* **146**, 771-775, doi:10.1007/s00401-023-02624-7 (2023).

356 Proust, A. *et al.* Differential effects of SARS-CoV-2 variants on central nervous system cells and blood–brain barrier functions. *Journal of Neuroinflammation* **20**, 184, doi:10.1186/s12974-023-02861-3 (2023).

357 Fiorito, S. *et al.* Is the epithelial barrier hypothesis the key to understanding the higher incidence and excess mortality during COVID-19 pandemic? The case of Northern Italy. *Allergy* **77**, 1408-1417, doi:https://doi.org/10.1111/all.15239 (2022).

358 Kang, K. *et al.* SARS-CoV-2 Structural Proteins Modulated Blood-Testis Barrier-Related Proteins through Autophagy in the Primary Sertoli Cells. *Viruses* **15**, doi:10.3390/v15061272 (2023).

359 Ly, J., Campos, R. K., Hager-Soto, E. E., Camargos, V. N. & Rossi, S. L. Testicular pathological alterations associated with SARS-CoV-2 infection. *Frontiers in Reproductive Health* **5**, doi:10.3389/frph.2023.1229622 (2023).

360 Fan, Y. *et al.* SARS-CoV-2 Omicron variant: recent progress and future perspectives. *Signal Transduction and Targeted Therapy* **7**, 141, doi:10.1038/s41392-022-00997-x (2022).

361 Gili, R. & Burioni, R. SARS-CoV-2 before and after Omicron: two different viruses and two different diseases? *Journal of Translational Medicine* **21**, 251, doi:10.1186/s12967-023-04095-6 (2023).

362 Dai, P. *et al.* SARS-CoV-2 and male infertility: from short- to long-term impacts. *J Endocrinol Invest* **46**, 1491-1507, doi:10.1007/s40618-023-02055-x (2023).

363 Che, B. W. *et al.* Effects of mild/asymptomatic COVID-19 on semen parameters and sex-related hormone levels in men: a systematic review and meta-analysis. *Asian J Androl* **25**, 382-388, doi:10.4103/aja202250 (2023).

364 Dijokaite-Guraliuc, A. *et al.* Antigenic characterization of SARS-CoV-2 Omicron subvariant BA.4.6. *Cell Discovery* **8**, 127, doi:10.1038/s41421-022-00493-0 (2022).

365 Channabasappa, N. K., Niranjan, A. K. & Emran, T. B. SARS-CoV-2 variant omicron XBB.1.5: challenges and prospects - correspondence. *Int J Surg* **109**, 1054-1055, doi:10.1097/js9.0000000000000276 (2023).

366 Gaur, M., Ramathal, C., Reijo Pera, R. A., Turek, P. J. & John, C. M. Isolation of human testicular cells and co-culture with embryonic stem cells. *Reproduction* **155**, 153-166, doi:10.1530/rep-17-0346 (2018).

367 Walker, W. H. Testosterone signaling and the regulation of spermatogenesis. *Spermatogenesis* **1**, 116-120, doi:10.4161/spmg.1.2.16956 (2011).

368 Santos, W. J., Guiraldi, L. M. & Lucheis, S. B. Should we be concerned about COVID-19 with nonhuman primates? *Am J Primatol* **82**, e23158, doi:10.1002/ajp.23158 (2020).

369 Nova, N. Cross-Species Transmission of Coronaviruses in Humans and Domestic Mammals, What Are the Ecological Mechanisms Driving Transmission, Spillover, and Disease Emergence? *Frontiers in Public Health* **9**, doi:10.3389/fpubh.2021.717941 (2021).

370 Munster, V. J. *et al.* Respiratory disease in rhesus macaques inoculated with SARS-CoV-2. *Nature* **585**, 268-272, doi:10.1038/s41586-020-2324-7 (2020).

371 Gibbons, A. Captive gorillas test positive for coronavirus. *Science* (2021).

372 Melin, A. D., Janiak, M. C., Marrone, F., Arora, P. S. & Higham, J. P. Comparative ACE2 variation and primate COVID-19 risk. *Communications Biology* **3**, 641, doi:10.1038/s42003-020-01370-w (2020).

373 Cao, Y. *et al.* BA.2.12.1, BA.4 and BA.5 escape antibodies elicited by Omicron infection. *Nature* **608**, 593-602, doi:10.1038/s41586-022-04980-y (2022).

374 Ao, D., He, X., Hong, W. & Wei, X. The rapid rise of SARS-CoV-2 Omicron subvariants with immune evasion properties: XBB.1.5 and BQ.1.1 subvariants. *MedComm (2020)* **4**, e239, doi:10.1002/mco2.239 (2023).

375 Groenheit, R. *et al.* Rapid emergence of omicron sublineages expressing spike protein R346T. *The Lancet Regional Health – Europe* **24**, doi:10.1016/j.lanepe.2022.100564 (2023).

376 Qu, P. *et al.* Distinct Neutralizing Antibody Escape of SARS-CoV-2 Omicron Subvariants BQ.1, BQ.1.1, BA.4.6, BF.7 and BA.2.75.2. *bioRxiv*, doi:10.1101/2022.10.19.512891 (2022).

377 Guo, Y. *et al.* Long-term culture and significant expansion of human Sertoli cells whilst maintaining stable global phenotype and AKT and SMAD1/5 activation. *Cell Communication and Signaling* **13**, 20, doi:10.1186/s12964-015-0101-2 (2015).

378 Mruk, D. D. & Cheng, C. Y. An in vitro system to study Sertoli cell blood-testis barrier dynamics. *Methods Mol Biol* **763**, 237-252, doi:10.1007/978-1-61779-191-8_16 (2011).

379 Srinivasan, B. *et al.* TEER measurement techniques for in vitro barrier model systems. *J Lab Autom* **20**, 107-126, doi:10.1177/2211068214561025 (2015).

380 Stewart, T. *et al.* Calibrated flux measurements reveal a nanostructure-stimulated transcytotic pathway. *Exp Cell Res* **355**, 153-161, doi:10.1016/j.yexcr.2017.03.065 (2017).

381 Dudley, R. & Maro, A. Human Evolution and Dietary Ethanol. *Nutrients* **13**, 2419 (2021).

382 Iranpour, A. & Nakhaee, N. A Review of Alcohol-Related Harms: A Recent Update. *Addict Health* **11**, 129-137, doi:10.22122/ahj.v11i2.225 (2019).

383 Van Heertum, K. & Rossi, B. Alcohol and fertility: how much is too much? *Fertil Res Pract* **3**, 10, doi:10.1186/s40738-017-0037-x (2017).

384 Organization, W. H. *Health Topics: Alcohol*, <https://www.who.int/health-topics/alcohol#tab=tab_1> (2023).

385 Schecke, H., Bohn, A., Scherbaum, N. & Mette, C. Alcohol use during COVID-19 pandemic on the long run: findings from a longitudinal study in Germany. *BMC Psychology* **10**, 266, doi:10.1186/s40359-022-00965-8 (2022).

386 Bantounou, M. A. A narrative review of the use of alcohol during the Covid-19 pandemic; effects and implications. *Journal of Addictive Diseases* **41**, 30-40, doi:10.1080/10550887.2022.2058852 (2023).

387 MacKillop, J. *et al.* Hazardous drinking and alcohol use disorders. *Nature Reviews Disease Primers* **8**, 80, doi:10.1038/s41572-022-00406-1 (2022).

388 Morojele, N. K., Shenoi, S. V., Shuper, P. A., Braithwaite, R. S. & Rehm, J. Alcohol Use and the Risk of Communicable Diseases. *Nutrients* **13**, 3317 (2021).

389 Lloyd, C. W. & Williams, R. H. Endocrine changes associated with Laennec's cirrhosis of the liver. *Am J Med* **4**, 315-330, doi:10.1016/0002-9343(48)90248-4 (1948).

390 Finelli, R., Mottola, F. & Agarwal, A. Impact of Alcohol Consumption on Male Fertility Potential: A Narrative Review. *Int J Environ Res Public Health* **19**, doi:10.3390/ijerph19010328 (2021).

391 Villalta, J. *et al.* Testicular function in asymptomatic chronic alcoholics: relation to ethanol intake. *Alcohol Clin Exp Res* **21**, 128-133 (1997).

392 Pajarinen, J. *et al.* Moderate alcohol consumption and disorders of human spermatogenesis. *Alcohol Clin Exp Res* **20**, 332-337, doi:10.1111/j.1530-0277.1996.tb01648.x (1996).

393 BRZEK, A. Alcohol and Male Fertility (Preliminary Report). *Andrologia* **19**, 32-36, doi:https://doi.org/10.1111/j.1439-0272.1987.tb01853.x (1987).

394 Sermondade, N. *et al.* Progressive alcohol-induced sperm alterations leading to spermatogenic arrest, which was reversed after alcohol withdrawal. *Reproductive BioMedicine Online* **20**, 324-327, doi:https://doi.org/10.1016/j.rbmo.2009.12.003 (2010).

395 Guthauser, B., Boitrelle, F., Plat, A., Thiercelin, N. & Vialard, F. Chronic Excessive Alcohol Consumption and Male Fertility: A Case Report on Reversible Azoospermia and a Literature Review. *Alcohol and Alcoholism* **49**, 42-44, doi:10.1093/alcalc/agt133 (2013).

396 Vicari, E., Arancio, A., Giuffrida, V., D'Agata, R. & Calogero, A. E. A case of reversible azoospermia following withdrawal from alcohol consumption. *Journal of Endocrinological Investigation* **25**, 473-476, doi:10.1007/BF03344041 (2002).

397 Curtis, K. M., Savitz, D. A. & Arbuckle, T. E. Effects of Cigarette Smoking, Caffeine Consumption, and Alcohol Intake on Fecundability. *American Journal of Epidemiology* **146**, 32-41, doi:10.1093/oxfordjournals.aje.a009189 (1997).

398 Olsen, J., Bolumar, F., Boldsen, J. & Bisanti, L. Does moderate alcohol intake reduce fecundability? A European multicenter study on infertility and subfecundity. European Study Group on Infertility and Subfecundity. *Alcohol Clin Exp Res* **21**, 206-212 (1997).

399 Jensen, T. K. *et al.* Alcohol and male reproductive health: a cross-sectional study of 8344 healthy men from Europe and the USA. *Hum Reprod* **29**, 1801-1809, doi:10.1093/humrep/deu118 (2014).

400 Povey, A. C. *et al.* Modifiable and non-modifiable risk factors for poor semen quality: a case-referent study. *Hum Reprod* **27**, 2799-2806, doi:10.1093/humrep/des183 (2012).

401 de Jong, A. M., Menkveld, R., Lens, J. W., Nienhuis, S. E. & Rhemrev, J. P. Effect of alcohol intake and cigarette smoking on sperm parameters and pregnancy. *Andrologia* **46**, 112-117, doi:10.1111/and.12054 (2014).

402 O'Donnell, L., Smith, L. B. & Rebourcet, D. Sertoli cells as key drivers of testis function. *Seminars in Cell & Developmental Biology* **121**, 2-9, doi:https://doi.org/10.1016/j.semcdb.2021.06.016 (2022).

403 Zhao, S., Zhu, W., Xue, S. & Han, D. Testicular defense systems: immune privilege and innate immunity. *Cell Mol Immunol* **11**, 428-437, doi:10.1038/cmi.2014.38 (2014).

404 Loveland, K. L. *et al.* Cytokines in Male Fertility and Reproductive Pathologies: Immunoregulation and Beyond. *Frontiers in Endocrinology* **8**, doi:10.3389/fendo.2017.00307 (2017).

405 Meineke, V., Frungieri, M. B., Jessberger, B., Vogt, H. & Mayerhofer, A. Human testicular mast cells contain tryptase: increased mast cell number and altered distribution in the testes of infertile men. *Fertil Steril* **74**, 239-244, doi:10.1016/s0015-0282(00)00626-9 (2000).

406 Frungieri, M. B. *et al.* Number, distribution pattern, and identification of macrophages in the testes of infertile men. *Fertil Steril* **78**, 298-306, doi:10.1016/s0015-0282(02)03206-5 (2002).

407 Zhu, Q., Van Thiel, D. H. & Gavaler, J. S. Effects of ethanol on rat Sertoli cell function: studies in vitro and in vivo. *Alcohol Clin Exp Res* **21**, 1409-1417 (1997).

408 Farghali, H. *et al.* Effect of ethanol on energy status and intracellular calcium of Sertoli cells: a study using immobilized perfused cells. *Endocrinology* **133**, 2749-2755, doi:10.1210/endo.133.6.8243299 (1993).

409 Figueiro, F. D. *et al.* Effect of alcoholic beverages on progeny and reproduction of mice. *Brazilian Journal of Pharmaceutical Sciences* **53** (2017).

410 Van Thiel DH, F. H., Gavaler JS, Ho C *P-NMR as a tool to investigate the testicular toxicity of ethanol in vivo* (NIAAA Research Monograph 21, 1991).

411 Wood, S. *et al.* Chronic alcohol exposure renders epithelial cells vulnerable to bacterial infection. *PLoS One* **8**, e54646, doi:10.1371/journal.pone.0054646 (2013).

412 Schlingmann, B. L. *et al.* Alveolar Barrier Function in Alcoholic Lung Syndrome Is Impaired by Tight Junction Destabilization. *Ann Am Thorac Soc* **12**, S75-76 (2015).

413 Wei, J. *et al.* Blood-brain barrier integrity is the primary target of alcohol abuse. *Chem Biol Interact* **337**, 109400, doi:10.1016/j.cbi.2021.109400 (2021).

414 Szabo, G., Mandrekar, P., Dolganiuc, A., Catalano, D. & Kodys, K. Reduced alloreactive T-cell activation after alcohol intake is due to impaired monocyte accessory cell function and correlates with elevated IL-10, IL-13, and decreased IFNgamma levels. *Alcohol Clin Exp Res* **25**, 1766-1772 (2001).

415 Overgaard, C. E. *et al.* The relative balance of GM-CSF and TGF-β1 regulates lung epithelial barrier function. *Am J Physiol Lung Cell Mol Physiol* **308**, L1212-1223, doi:10.1152/ajplung.00042.2014 (2015).

416 Clinic, C. *Blood Alcohol Content (BAC)*, <https://my.clevelandclinic.org/health/diagnostics/22689-blood-alcohol-content-bac#:~:text=BAC%200.30%25%20to%200.40%25%3A,potentially%20fatal%20blood%20alcohol%20level.> (2022).

417 Smith, P., Jeffers, L. A. & Koval, M. Effects of different routes of endotoxin injury on barrier function in alcoholic lung syndrome. *Alcohol* **80**, 81-89, doi:https://doi.org/10.1016/j.alcohol.2018.08.007 (2019).

418 Wang, Y. *et al.* Effects of alcohol on intestinal epithelial barrier permeability and expression of tight junction-associated proteins. *Mol Med Rep* **9**, 2352-2356, doi:10.3892/mmr.2014.2126 (2014).

419 Morrow, C. M., Mruk, D., Cheng, C. Y. & Hess, R. A. Claudin and occludin expression and function in the seminiferous epithelium. *Philos Trans R Soc Lond B Biol Sci* **365**, 1679-1696, doi:10.1098/rstb.2010.0025 (2010).

420 You, X., Chen, Q., Yuan, D., Zhang, C. & Zhao, H. Common markers of testicular Sertoli cells. *Expert Rev Mol Diagn* **21**, 613-626, doi:10.1080/14737159.2021.1924060 (2021).

421 Lan, K. C. *et al.* Up-regulation of SOX9 in sertoli cells from testiculopathic patients accounts for increasing anti-mullerian hormone expression via impaired androgen receptor signaling. *PLoS One* **8**, e76303, doi:10.1371/journal.pone.0076303 (2013).

422 Cheng, C. Y. & Mruk, D. D. The blood-testis barrier and its implications for male contraception. *Pharmacol Rev* **64**, 16-64, doi:10.1124/pr.110.002790 (2012).

423 Mruk, D. D. & Cheng, C. Y. Sertoli-Sertoli and Sertoli-Germ Cell Interactions and Their Significance in Germ Cell Movement in the

Seminiferous Epithelium during Spermatogenesis. *Endocrine Reviews* **25**, 747-806, doi:10.1210/er.2003-0022 (2004).

424 Nah, W. H., Lee, J. E., Park, H. J., Park, N. C. & Gye, M. C. Claudin-11 expression increased in spermatogenic defect in human testes. *Fertility and Sterility* **95**, 385-388, doi:https://doi.org/10.1016/j.fertnstert.2010.08.023 (2011).

425 Edelsztein, N. Y. & Rey, R. A. Importance of the Androgen Receptor Signaling in Gene Transactivation and Transrepression for Pubertal Maturation of the Testis. *Cells* **8**, doi:10.3390/cells8080861 (2019).

426 Wang, J. M., Li, Z. F. & Yang, W. X. What Does Androgen Receptor Signaling Pathway in Sertoli Cells During Normal Spermatogenesis Tell Us? *Front Endocrinol (Lausanne)* **13**, 838858, doi:10.3389/fendo.2022.838858 (2022).

427 Schrade, A. *et al.* GATA4 Regulates Blood-Testis Barrier Function and Lactate Metabolism in Mouse Sertoli Cells. *Endocrinology* **157**, 2416-2431, doi:10.1210/en.2015-1927 (2016).

428 Kyrönlahti, A. *et al.* GATA4 regulates Sertoli cell function and fertility in adult male mice. *Mol Cell Endocrinol* **333**, 85-95, doi:10.1016/j.mce.2010.12.019 (2011).

429 Washburn, R. L., Hibler, T., Kaur, G. & Dufour, J. M. Sertoli Cell Immune Regulation: A Double-Edged Sword. *Front Immunol* **13**, 913502, doi:10.3389/fimmu.2022.913502 (2022).

430 Siemann, D. N., Strange, D. P., Maharaj, P. N., Shi, P.-Y. & Verma, S. Zika Virus Infects Human Sertoli Cells and Modulates the Integrity of the In Vitro Blood-Testis Barrier Model. *Journal of Virology* **91**, 10.1128/jvi.00623-00617, doi:doi:10.1128/jvi.00623-17 (2017).

431 Washburn, R. L. *et al.* Sertoli Cells Express Accommodation, Survival, and Immunoregulatory Factors When Exposed to Normal Human Serum. *Biomedicines* **11**, 1650 (2023).

432 Santiesteban-Lores, L. E., Carneiro, M. C., Isaac, L. & Bavia, L. Complement System in Alcohol-Associated Liver Disease. *Immunol Lett* **236**, 37-50, doi:10.1016/j.imlet.2021.05.007 (2021).

433 Singh, S., Anshita, D. & Ravichandiran, V. MCP-1: Function, regulation, and involvement in disease. *International Immunopharmacology* **101**, 107598, doi:https://doi.org/10.1016/j.intimp.2021.107598 (2021).

434 Stermer, A. R. *et al.* Mono-(2-ethylhexyl) phthalate-induced Sertoli cell injury stimulates the production of pro-inflammatory cytokines in Fischer

344 rats. *Reprod Toxicol* **69**, 150-158, doi:10.1016/j.reprotox.2017.02.013 (2017).

435 Zhang, K. & Luo, J. Role of MCP-1 and CCR2 in alcohol neurotoxicity. *Pharmacol Res* **139**, 360-366, doi:10.1016/j.phrs.2018.11.030 (2019).

436 Kazmi, N. *et al.* An exploratory study of pro-inflammatory cytokines in individuals with alcohol use disorder: MCP-1 and IL-8 associated with alcohol consumption, sleep quality, anxiety, depression, and liver biomarkers. *Frontiers in Psychiatry* **13**, doi:10.3389/fpsyt.2022.931280 (2022).

437 Heller, C. H. & Clermont, Y. KINETICS OF THE GERMINAL EPITHELIUM IN MAN. *Recent Prog Horm Res* **20**, 545-575 (1964).

438 Wang, J. & Sauer, M. V. In vitro fertilization (IVF): a review of 3 decades of clinical innovation and technological advancement. *Ther Clin Risk Manag* **2**, 355-364, doi:10.2147/tcrm.2006.2.4.355 (2006).

439 Flannigan, R. K. & Schlegel, P. N. Microdissection testicular sperm extraction: preoperative patient optimization, surgical technique, and tissue processing. *Fertil Steril* **111**, 420-426, doi:10.1016/j.fertnstert.2019.01.003 (2019).

440 Achermann, A. P. P., Pereira, T. A. & Esteves, S. C. Microdissection testicular sperm extraction (micro-TESE) in men with infertility due to nonobstructive azoospermia: summary of current literature. *Int Urol Nephrol* **53**, 2193-2210, doi:10.1007/s11255-021-02979-4 (2021).

441 Ghieh, F., Mitchell, V., Mandon-Pepin, B. & Vialard, F. Genetic defects in human azoospermia. *Basic Clin Androl* **29**, 4, doi:10.1186/s12610-019-0086-6 (2019).

442 Meistrich, M. L. Male gonadal toxicity. *Pediatr Blood Cancer* **53**, 261-266, doi:10.1002/pbc.22004 (2009).

443 Grimm, D. EPA plan to end animal testing splits scientists. *Science* **365**, 1231, doi:10.1126/science.365.6459.1231 (2019).

444 Wadman, M. FDA no longer has to require animal testing for new drugs. *Science* **379**, 127-128 (2023).

445 Thomson, J. A. *et al.* Embryonic stem cell lines derived from human blastocysts. *Science* **282**, 1145-1147, doi:10.1126/science.282.5391.1145 (1998).

446 Vazin, T. & Freed, W. J. Human embryonic stem cells: derivation, culture, and differentiation: a review. *Restor Neurol Neurosci* **28**, 589-603, doi:10.3233/rnn-2010-0543 (2010).

447 Takahashi, K. *et al.* Induction of Pluripotent Stem Cells from Adult Human Fibroblasts by Defined Factors. *Cell* **131**, 861-872, doi:10.1016/j.cell.2007.11.019 (2007).

448 Easley, C. A. T. Direct differentiation of human pluripotent stem cells into haploid spermatogenic cells. *Cell Rep.* **2** (2012).

449 Steves, A. N. *et al.* Ubiquitous Flame-Retardant Toxicants Impair Spermatogenesis in a Human Stem Cell Model. *iScience* **3**, 161-176, doi:10.1016/j.isci.2018.04.014 (2018).

450 Khampang, S. *et al.* Blastocyst development after fertilization with in vitro spermatids derived from nonhuman primate embryonic stem cells. *F S Sci* **2**, 365-375, doi:10.1016/j.xfss.2021.09.001 (2021).

451 Robinson, M., Sparanese, S., Witherspoon, L. & Flannigan, R. Human in vitro spermatogenesis as a regenerative therapy — where do we stand? *Nature Reviews Urology* **20**, 461-479, doi:10.1038/s41585-023-00723-4 (2023).

452 Rombaut, C., Mertes, H., Heindryckx, B. & Goossens, E. Human in vitro spermatogenesis from pluripotent stem cells: in need of a stepwise differentiation protocol? *Molecular Human Reproduction* **24**, 47-54, doi:10.1093/molehr/gax065 (2017).

453 Zhang, X., Gunewardena, S. & Wang, N. Nutrient restriction synergizes with retinoic acid to induce mammalian meiotic initiation in vitro. *Nature Communications* **12**, 1758, doi:10.1038/s41467-021-22021-6 (2021).

454 Duggal, G. *et al.* Exogenous supplementation of Activin A enhances germ cell differentiation of human embryonic stem cells†. *Molecular Human Reproduction* **21**, 410-423, doi:10.1093/molehr/gav004 (2015).

455 Kanatsu-Shinohara, M. *et al.* Long-term proliferation in culture and germline transmission of mouse male germline stem cells. *Biol Reprod* **69**, 612-616, doi:10.1095/biolreprod.103.017012 (2003).

456 Zhao, Y. *et al.* In Vitro Modeling of Human Germ Cell Development Using Pluripotent Stem Cells. *Stem Cell Reports* **10**, 509-523, doi:10.1016/j.stemcr.2018.01.001 (2018).

457 Zhou, Q. *et al.* Complete Meiosis from Embryonic Stem Cell-Derived Germ Cells In Vitro. *Cell Stem Cell* **18**, 330-340, doi:10.1016/j.stem.2016.01.017 (2016).

458 Valli, H. *et al.* Germline stem cells: toward the regeneration of spermatogenesis. *Fertil Steril* **101**, 3-13, doi:10.1016/j.fertnstert.2013.10.052 (2014).

459 Hermann, B. P. *et al.* Characterization, cryopreservation, and ablation of spermatogonial stem cells in adult rhesus macaques. *Stem Cells* **25**, 2330-2338, doi:10.1634/stemcells.2007-0143 (2007).

460 Murakami, T. *et al.* STO Feeder Cells Are Useful for Propagation of Primarily Cultured Human Deciduous Dental Pulp Cells by Eliminating Contaminating Bacteria and Promoting Cellular Outgrowth. *Cell Med* **6**, 75-81, doi:10.3727/215517913x674234 (2013).

461 Ponchio, L. *et al.* Mitomycin C as an alternative to irradiation to inhibit the feeder layer growth in long-term culture assays. *Cytotherapy* **2**, 281-286, doi:10.1080/146532400539215 (2000).

462 Tesarik, J. *et al.* Differentiation of spermatogenic cells during in-vitro culture of testicular biopsy samples from patients with obstructive azoospermia: effect of recombinant follicle stimulating hormone. *Hum Reprod* **13**, 2772-2781, doi:10.1093/humrep/13.10.2772 (1998).

463 Tesarik, J., Guido, M., Mendoza, C. & Greco, E. Human spermatogenesis in vitro: respective effects of follicle-stimulating hormone and testosterone on meiosis, spermiogenesis, and Sertoli cell apoptosis. *J Clin Endocrinol Metab* **83**, 4467-4473, doi:10.1210/jcem.83.12.5304 (1998).

464 Tesarik, J., Bahceci, M., Ozcan, C., Greco, E. & Mendoza, C. Restoration of fertility by in-vitro spermatogenesis. *Lancet* **353**, 555-556, doi:10.1016/s0140-6736(98)04784-9 (1999).

465 Abdelhamid, M. H. M. *et al.* Mild experimental increase in testis and epididymis temperature in men: effects on sperm morphology according to spermatogenesis stages. *Transl Androl Urol* **8**, 651-665, doi:10.21037/tau.2019.11.18 (2019).

466 Cho, I. K. & Easley, C. A. Recent Developments in In Vitro Spermatogenesis and Future Directions. *Reproductive Medicine* **4**, 215-232 (2023).

467 Piquet-Pellorce, C., Dorval-Coiffec, I., Pham, M. D. & Jégou, B. Leukemia inhibitory factor expression and regulation within the testis. *Endocrinology* **141**, 1136-1141, doi:10.1210/endo.141.3.7399 (2000).

468 Curley, M. *et al.* Leukemia Inhibitory Factor-Receptor is Dispensable for Prenatal Testis Development but is Required in Sertoli cells for Normal Spermatogenesis in Mice. *Scientific Reports* **8**, 11532, doi:10.1038/s41598-018-30011-w (2018).

469 Yan, Y. C., Sun, Y. P. & Zhang, M. L. Testis epidermal growth factor and spermatogenesis. *Arch Androl* **40**, 133-146, doi:10.3109/01485019808987936 (1998).

470 Abé, K., Eto, K. & Abé, S. Epidermal growth factor mediates spermatogonial proliferation in newt testis. *Reprod Biol Endocrinol* **6**, 7, doi:10.1186/1477-7827-6-7 (2008).

471 Lee, J. A. & Ramasamy, R. Indications for the use of human chorionic gonadotropic hormone for the management of infertility in hypogonadal men. *Transl Androl Urol* **7**, S348-s352, doi:10.21037/tau.2018.04.11 (2018).

472 Leavy, M. *et al.* Effects of Elevated β-Estradiol Levels on the Functional Morphology of the Testis - New Insights. *Scientific Reports* **7**, 39931, doi:10.1038/srep39931 (2017).

473 Oduwole, O. O., Peltoketo, H. & Huhtaniemi, I. T. Role of Follicle-Stimulating Hormone in Spermatogenesis. *Front Endocrinol (Lausanne)* **9**, 763, doi:10.3389/fendo.2018.00763 (2018).

474 Busada, J. T. & Geyer, C. B. The Role of Retinoic Acid (RA) in Spermatogonial Differentiation. *Biol Reprod* **94**, 10, doi:10.1095/biolreprod.115.135145 (2016).

475 Gewiss, R. L., Schleif, M. C. & Griswold, M. D. The role of retinoic acid in the commitment to meiosis. *Asian J Androl* **23**, 549-554, doi:10.4103/aja202156 (2021).

476 Li, X. *et al.* The roles of retinoic acid in the differentiation of spermatogonia and spermatogenic disorders. *Clinica Chimica Acta* **497**, 54-60, doi:https://doi.org/10.1016/j.cca.2019.07.013 (2019).

477 Nikolic, A., Volarevic, V., Armstrong, L., Lako, M. & Stojkovic, M. Primordial Germ Cells: Current Knowledge and Perspectives. *Stem Cells Int* **2016**, 1741072, doi:10.1155/2016/1741072 (2016).

478 Hammoud, S. S. *et al.* Transcription and imprinting dynamics in developing postnatal male germline stem cells. *Genes Dev* **29**, 2312-2324, doi:10.1101/gad.261925.115 (2015).

479 Cheng, H., Shang, D. & Zhou, R. Germline stem cells in human. *Signal Transduction and Targeted Therapy* **7**, 345, doi:10.1038/s41392-022-01197-3 (2022).

480 Xu, H. *et al.* Derivation and propagation of spermatogonial stem cells from human pluripotent cells. *Stem Cell Res Ther* **11**, 408, doi:10.1186/s13287-020-01896-0 (2020).

481 Azizi, H., NiaziTabar, A., Mohammadi, A. & Skutella, T. Characterization of DDX4 Gene Expression in Human Cases with Non-Obstructive Azoospermia and in Sterile and Fertile Mice. *J Reprod Infertil* **22**, 85-91, doi:10.18502/jri.v22i2.5793 (2021).

482 Wu, X. *et al.* Transcriptome profiling of laser-captured germ cells and functional characterization of zbtb40 during 17alpha-methyltestosterone-induced spermatogenesis in orange-spotted grouper (Epinephelus coioides). *BMC Genomics* **21**, 73, doi:10.1186/s12864-020-6477-4 (2020).

483 Ma, H. T. *et al.* Stimulated by retinoic acid gene 8 (Stra8) plays important roles in many stages of spermatogenesis. *Asian J Androl* **20**, 479-487, doi:10.4103/aja.aja_26_18 (2018).

484 Helsel, A. R. *et al.* ID4 levels dictate the stem cell state in mouse spermatogonia. *Development* **144**, 624-634, doi:10.1242/dev.146928 (2017).

485 Song, H., Park, H. J., Lee, W. Y. & Lee, K. H. Models and Molecular Markers of Spermatogonial Stem Cells in Vertebrates: To Find Models in Nonmammals. *Stem Cells Int* **2022**, 4755514, doi:10.1155/2022/4755514 (2022).

486 Galdon, G. *et al.* In vitro propagation of XXY human Klinefelter spermatogonial stem cells: A step towards new fertility opportunities. *Frontiers in Endocrinology* **13**, doi:10.3389/fendo.2022.1002279 (2022).

487 Sohni, A. *et al.* The Neonatal and Adult Human Testis Defined at the Single-Cell Level. *Cell Reports* **26**, 1501-1517.e1504, doi:10.1016/j.celrep.2019.01.045 (2019).

488 Ahn, J. *et al.* A novel testis-enriched gene, Samd4a, regulates spermatogenesis as a spermatid-specific factor. *Frontiers in Cell and Developmental Biology* **10**, doi:10.3389/fcell.2022.978343 (2022).

489 Qin, J. *et al.* RAD51 is essential for spermatogenesis and male fertility in mice. *Cell Death Discovery* **8**, 118, doi:10.1038/s41420-022-00921-w (2022).

490 Zhang, G. *et al.* Deficiency of cancer/testis antigen gene CT55 causes male infertility in humans and mice. *Cell Death & Differentiation* **30**, 500-514, doi:10.1038/s41418-022-01098-6 (2023).

491 Prokai, D. *et al.* Spermatogonial Gene Networks Selectively Couple to Glutathione and Pentose Phosphate Metabolism but Not Cysteine Biosynthesis. *iScience* **24**, 101880, doi:10.1016/j.isci.2020.101880 (2021).

492 Yuan, Y. *et al.* Geminin deletion in pre-meiotic DNA replication stage causes spermatogenesis defect and infertility. *J Reprod Dev* **63**, 481-488, doi:10.1262/jrd.2017-036 (2017).

493 Hermann, B. P. *et al.* The Mammalian Spermatogenesis Single-Cell Transcriptome, from Spermatogonial Stem Cells to Spermatids. *Cell Reports* **25**, 1650-1667.e1658, doi:10.1016/j.celrep.2018.10.026 (2018).

494 Di Persio, S. *et al.* Single-cell RNA-seq unravels alterations of the human spermatogonial stem cell compartment in patients with impaired spermatogenesis. *Cell Rep Med* **2**, 100395, doi:10.1016/j.xcrm.2021.100395 (2021).

495 Ye, X., Skinner, M. K., Kennedy, G. & Chun, J. Age-dependent loss of sperm production in mice via impaired lysophosphatidic acid signaling. *Biol Reprod* **79**, 328-336, doi:10.1095/biolreprod.108.068783 (2008).

496 Liu, J. *et al.* Low levels of PRSS37 protein in sperm are associated with many cases of unexplained male infertility. *Acta Biochim Biophys Sin (Shanghai)* **48**, 1058-1065, doi:10.1093/abbs/gmw096 (2016).

497 Lau, X., Munusamy, P., Ng, M. J. & Sangrithi, M. Single-Cell RNA Sequencing of the Cynomolgus Macaque Testis Reveals Conserved Transcriptional Profiles during Mammalian Spermatogenesis. *Developmental Cell* **54**, 548-566.e547, doi:https://doi.org/10.1016/j.devcel.2020.07.018 (2020).

498 Wykes, S. M., Nelson, J. E., Visscher, D. W., Djakiew, D. & Krawetz, S. A. Coordinate expression of the PRM1, PRM2, and TNP2 multigene locus in human testis. *DNA Cell Biol* **14**, 155-161, doi:10.1089/dna.1995.14.155 (1995).

499 Ni, K. *et al.* TET enzymes are successively expressed during human spermatogenesis and their expression level is pivotal for male fertility. *Hum Reprod* **31**, 1411-1424, doi:10.1093/humrep/dew096 (2016).

500 Kato, Y., Kumar, S., Lessard, C. & Bailey, J. L. ACRBP (Sp32) is involved in priming sperm for the acrosome reaction and the binding of sperm to the zona pellucida in a porcine model. *PLoS One* **16**, e0251973, doi:10.1371/journal.pone.0251973 (2021).

501 Silva, J. V., Freitas, M. J. & Fardilha, M. Phosphoprotein phosphatase 1 complexes in spermatogenesis. *Curr Mol Pharmacol* **7**, 136-146, doi:10.2174/1874467208666150126154222 (2014).

502 Blanco-Rodríguez, J. gammaH2AX marks the main events of the spermatogenic process. *Microsc Res Tech* **72**, 823-832, doi:10.1002/jemt.20730 (2009).

503 Rufas, J. S. in *Reference Module in Life Sciences* (Elsevier, 2017).

504 Gholami, K., Pourmand, G., Koruji, M., Ashouri, S. & Abbasi, M. Organ culture of seminiferous tubules using a modified soft agar culture system. *Stem Cell Research & Therapy* **9**, 249, doi:10.1186/s13287-018-0997-8 (2018).

505 Yoshida, K. *et al.* The mouse RecA-like gene Dmc1 is required for homologous chromosome synapsis during meiosis. *Mol Cell* **1**, 707-718, doi:10.1016/s1097-2765(00)80070-2 (1998).

506 Shrestha, K. S., Tuominen, M. M. & Kauppi, L. Mlh1 heterozygosity and promoter methylation associates with microsatellite instability in mouse sperm. *Mutagenesis* **36**, 237-244, doi:10.1093/mutage/geab010 (2021).

507 Ren, S. *et al.* The expression, function, and utilization of Protamine1: a literature review. *Transl Cancer Res* **10**, 4947-4957, doi:10.21037/tcr-21-1582 (2021).

508 Li, L. *et al.* SARS-CoV-2 Enters Human Leydig Cells and Affects Testosterone Production In Vitro. *Cells* **12**, doi:10.3390/cells12081198 (2023).

509 Siwar Garrouch, A. S., Manel Ben Fredj,Rim Kooli,Manel Bousabbeh,Ines Boughzala,Asma Sriha,Awatef Hajjaji,Meriem Mehdi. Deleterious impact of COVID-19 pandemic: Male fertility was not out of the bag. *PLoS One* (2023).

510 Paschos, K. & Allday, M. J. Epigenetic reprogramming of host genes in viral and microbial pathogenesis. *Trends in Microbiology* **18**, 439-447, doi:10.1016/j.tim.2010.07.003 (2010).

511 Saksena, N., Bonam, S. R. & Miranda-Saksena, M. Epigenetic Lens to Visualize the Severe Acute Respiratory Syndrome Coronavirus-2 (SARS-CoV-2) Infection in COVID-19 Pandemic. *Frontiers in Genetics* **12**, doi:10.3389/fgene.2021.581726 (2021).

512 Kgatle, M. M. *et al.* COVID-19 Is a Multi-Organ Aggressor: Epigenetic and Clinical Marks. *Front Immunol* **12**, 752380, doi:10.3389/fimmu.2021.752380 (2021).

513 Zini, A. & Libman, J. Sperm DNA damage: clinical significance in the era of assisted reproduction. *CMAJ* **175**, 495-500, doi:10.1503/cmaj.060218 (2006).

514 Wu, J., Zhang, W. & Li, C. Recent Advances in Genetic and Epigenetic Modulation of Animal Exposure to High Temperature. *Frontiers in Genetics* **11**, doi:10.3389/fgene.2020.00653 (2020).

515 Montazersaheb, S. *et al.* COVID-19 infection: an overview on cytokine storm and related interventions. *Virology Journal* **19**, 92, doi:10.1186/s12985-022-01814-1 (2022).

516 Jiang, L. *et al.* Association of semen cytokines with reactive oxygen species and histone transition abnormalities. *J Assist Reprod Genet* **33**, 1239-1246, doi:10.1007/s10815-016-0756-7 (2016).

517 Loveland, K. L. *et al.* Cytokines in Male Fertility and Reproductive Pathologies: Immunoregulation and Beyond. *Front Endocrinol (Lausanne)* **8**, 307, doi:10.3389/fendo.2017.00307 (2017).

518 Tyebji, S., Hannan, A. J. & Tonkin, C. J. Pathogenic Infection in Male Mice Changes Sperm Small RNA Profiles and Transgenerationally Alters Offspring Behavior. *Cell Reports* **31**, 107573, doi:https://doi.org/10.1016/j.celrep.2020.107573 (2020).

519 Bomans, K. *et al.* Paternal sepsis induces alterations of the sperm methylome and dampens offspring immune responses-an animal study. *Clin Epigenetics* **10**, 89-89, doi:10.1186/s13148-018-0522-z (2018).

520 Kleeman, E. A., Gubert, C. & Hannan, A. J. Transgenerational epigenetic impacts of parental infection on offspring health and disease susceptibility. *Trends Genet* **38**, 662-675, doi:10.1016/j.tig.2022.03.006 (2022).

521 Gavaler, J. S., Perez, H. A., Estes, L. & Van Thiel, D. H. Morphologic alterations of rat Leydig cells induced by ethanol. *Pharmacol Biochem Behav* **18 Suppl 1**, 341-347, doi:10.1016/0091-3057(83)90197-1 (1983).

522 Chastain, L. G. & Sarkar, D. K. Alcohol effects on the epigenome in the germline: Role in the inheritance of alcohol-related pathology. *Alcohol* **60**, 53-66, doi:10.1016/j.alcohol.2016.12.007 (2017).

523 Balasubramanian, N., James, T. D., Selvakumar, G. P., Reinhardt, J. & Marcinkiewcz, C. A. Repeated ethanol exposure and withdrawal alters angiotensin-converting enzyme 2 expression in discrete brain regions: Implications for SARS-CoV-2 neuroinvasion. *Alcoholism: Clinical and Experimental Research* **47**, 219-239, doi:https://doi.org/10.1111/acer.15000 (2023).

524 Easley, K. F. *et al.* Chronic alcohol use primes bronchial cells for altered inflammatory response and barrier dysfunction during SARS-CoV-2 infection. *American Journal of Physiology-Lung Cellular and Molecular Physiology* **0**, null, doi:10.1152/ajplung.00381.2022.

525 Selickman, J., Vrettou, C. S., Mentzelopoulos, S. D. & Marini, J. J. COVID-19-Related ARDS: Key Mechanistic Features and Treatments. *Journal of clinical medicine* **11**, doi:10.3390/jcm11164896 (2022).

526 Lamers, M. M. & Haagmans, B. L. SARS-CoV-2 pathogenesis. *Nature reviews. Microbiology* **20**, 270-284, doi:10.1038/s41579-022-00713-0 (2022).

527 Lim, Z. J. *et al.* Case Fatality Rates for Patients with COVID-19 Requiring Invasive Mechanical Ventilation. A Meta-analysis. *American journal of respiratory and critical care medicine* **203**, 54-66, doi:10.1164/rccm.202006-2405OC (2021).

528 Bigdelou, B. *et al.* COVID-19 and Preexisting Comorbidities: Risks, Synergies, and Clinical Outcomes. *Front Immunol* **13**, 890517, doi:10.3389/fimmu.2022.890517 (2022).

529 Yeligar, S. M. & Wyatt, T. A. Alcohol and lung derangements: An overview. *Alcohol* **80**, 1-3, doi:10.1016/j.alcohol.2019.01.002 (2019).

530 Moss, M., Bucher, B., Moore, F. A., Moore, E. E. & Parsons, P. E. The role of chronic alcohol abuse in the development of acute respiratory distress syndrome in adults. *JAMA* **275**, 50-54 (1996).

531 Mehta, A. J. & Guidot, D. M. Alcohol and the Lung. *Alcohol research : current reviews* **38**, 243-254 (2017).

532 de Roux, A. *et al.* Impact of alcohol abuse in the etiology and severity of community-acquired pneumonia. *Chest* **129**, 1219-1225, doi:10.1378/chest.129.5.1219 (2006).

533 Wyatt, T. A. *et al.* Alcohol potentiates RSV-mediated injury to ciliated airway epithelium. *Alcohol* **80**, 17-24, doi:10.1016/j.alcohol.2018.07.010 (2019).

534 Greenbaum, A. *et al.* Heavy alcohol use as a risk factor for severe outcomes among adults hospitalized with laboratory-confirmed influenza, 2005-2012. *Infection* **42**, 165-170, doi:10.1007/s15010-013-0534-8 (2014).

535 Saitz, R., Ghali, W. A. & Moskowitz, M. A. The impact of alcohol-related diagnoses on pneumonia outcomes. *Arch Intern Med* **157**, 1446-1452 (1997).

536 Berkowitz, D. M., Danai, P. A., Eaton, S., Moss, M. & Martin, G. S. Alcohol abuse enhances pulmonary edema in acute respiratory distress syndrome. *Alcohol Clin Exp Res* **33**, 1690-1696, doi:10.1111/j.1530-0277.2009.01005.x (2009).

537 Voelkel, N. F., Bogaard, H. J. & Kuebler, W. M. ARDS in the time of corona: context and perspective. *Am J Physiol Lung Cell Mol Physiol* **323**, L431-L437, doi:10.1152/ajplung.00432.2021 (2022).

538 Bailey, K. L. *et al.* COVID-19 patients with documented alcohol use disorder or alcohol-related complications are more likely to be hospitalized and have higher all-cause mortality. *Alcohol Clin Exp Res* **46**, 1023-1035, doi:10.1111/acer.14838 (2022).

539 Bailey, K. L., Samuelson, D. R. & Wyatt, T. A. Alcohol use disorder: A pre-existing condition for COVID-19? *Alcohol* **90**, 11-17, doi:10.1016/j.alcohol.2020.10.003 (2021).

540 Sugarman, D. E. & Greenfield, S. F. Alcohol and COVID-19: How Do We Respond to This Growing Public Health Crisis? *J Gen Intern Med* **36**, 214-215, doi:10.1007/s11606-020-06321-z (2021).

541 Calina, D. *et al.* COVID-19 pandemic and alcohol consumption: Impacts and interconnections. *Toxicol Rep* **8**, 529-535, doi:10.1016/j.toxrep.2021.03.005 (2021).

542 Camargo Moreno, M., Lewis, J. B., Kovacs, E. J. & Lowery, E. M. Lung allograft donors with excessive alcohol use have increased levels of human antimicrobial peptide LL-37. *Alcohol* **80**, 109-117, doi:10.1016/j.alcohol.2018.11.003 (2019).

543 Bailey, K. L. *et al.* TLR2 and TLR4 Expression and Inflammatory Cytokines are Altered in the Airway Epithelium of Those with Alcohol Use Disorders. *Alcohol Clin Exp Res* **39**, 1691-1697, doi:10.1111/acer.12803 (2015).

544 Mitchell, P. O. *et al.* Alcohol primes the airway for increased interleukin-13 signaling. *Alcohol Clin Exp Res* **33**, 505-513, doi:10.1111/j.1530-0277.2008.00863.x (2009).

545 Overgaard, C. E. *et al.* The relative balance of GM-CSF and TGF-beta1 regulates lung epithelial barrier function. *Am J Physiol Lung Cell Mol Physiol* **308**, L1212-1223, doi:10.1152/ajplung.00042.2014 (2015).

546 Staitieh, B. S., Egea, E. E., Fan, X., Amah, A. & Guidot, D. M. Chronic Alcohol Ingestion Impairs Rat Alveolar Macrophage Phagocytosis via Disruption of RAGE Signaling. *Am J Med Sci* **355**, 497-505, doi:10.1016/j.amjms.2017.12.013 (2018).

547 Yeligar, S. M., Mehta, A. J., Harris, F. L., Brown, L. A. S. & Hart, C. M. Pioglitazone Reverses Alcohol-Induced Alveolar Macrophage Phagocytic Dysfunction. *J Immunol* **207**, 483-492, doi:10.4049/jimmunol.2000565 (2021).

548 Samuelson, D. R. *et al.* The respiratory tract microbial biogeography in alcohol use disorder. *Am J Physiol Lung Cell Mol Physiol* **314**, L107-L117, doi:10.1152/ajplung.00277.2017 (2018).

549 Burnham, E. L., Halkar, R., Burks, M. & Moss, M. The effects of alcohol abuse on pulmonary alveolar-capillary barrier function in humans. *Alcohol Alcohol* **44**, 8-12, doi:10.1093/alcalc/agn051 (2009).

550 Smith, P., Jeffers, L. A. & Koval, M. Effects of different routes of endotoxin injury on barrier function in alcoholic lung syndrome. *Alcohol* **80**, 81-89, doi:10.1016/j.alcohol.2018.08.007 (2019).

551 Koval, M. in *Lung Epithelial Biology in the Pathogenesis of Pulmonary Disease* (eds V. K. Sidhaye & M. Koval) 1-20 (Academic Press, 2017).

552 Linfield, D. T., Raduka, A., Aghapour, M. & Rezaee, F. Airway tight junctions as targets of viral infections. *Tissue Barriers* **9**, 1883965, doi:10.1080/21688370.2021.1883965 (2021).

553 Wittekindt, O. H. Tight junctions in pulmonary epithelia during lung inflammation. *Pflugers Archiv : European journal of physiology* **469**, 135-147, doi:10.1007/s00424-016-1917-3 (2017).

554 Schlingmann, B. *et al.* Regulation of claudin/zonula occludens-1 complexes by hetero-claudin interactions. *Nat Commun* **7**, 12276, doi:10.1038/ncomms12276 (2016).

555 Lynn, K. S. *et al.* Asymmetric distribution of dynamin-2 and beta-catenin relative to tight junction spikes in alveolar epithelial cells. *Tissue Barriers* **9**, 1929786, doi:10.1080/21688370.2021.1929786 (2021).

556 Simet, S. M. *et al.* Alcohol increases the permeability of airway epithelial tight junctions in Beas-2B and NHBE cells. *Alcohol Clin Exp Res* **36**, 432-442, doi:10.1111/j.1530-0277.2011.01640.x (2012).

557 Fernandez, A. L., Koval, M., Fan, X. & Guidot, D. M. Chronic alcohol ingestion alters claudin expression in the alveolar epithelium of rats. *Alcohol* **41**, 371-379, doi:10.1016/j.alcohol.2007.04.010 (2007).

558 Hou, Y. J. *et al.* SARS-CoV-2 Reverse Genetics Reveals a Variable Infection Gradient in the Respiratory Tract. *Cell* **182**, 429-446 e414, doi:10.1016/j.cell.2020.05.042 (2020).

559 Moss, M. *et al.* Chronic alcohol abuse is associated with an increased incidence of acute respiratory distress syndrome and severity of multiple organ dysfunction in patients with septic shock. *Crit Care Med* **31**, 869-877, doi:10.1097/01.CCM.0000055389.64497.11 (2003).

560 Katsura, H. *et al.* Human Lung Stem Cell-Based Alveolospheres Provide Insights into SARS-CoV-2-Mediated Interferon Responses and Pneumocyte Dysfunction. *Cell stem cell* **27**, 890-904 e898, doi:10.1016/j.stem.2020.10.005 (2020).

561 Vanderheiden, A. *et al.* Type I and Type III Interferons Restrict SARS-CoV-2 Infection of Human Airway Epithelial Cultures. *Journal of virology* **94**, doi:10.1128/JVI.00985-20 (2020).

562 Hao, S. *et al.* Long-Term Modeling of SARS-CoV-2 Infection of In Vitro Cultured Polarized Human Airway Epithelium. *mBio* **11**, doi:10.1128/mBio.02852-20 (2020).

563 Zhu, N. *et al.* Morphogenesis and cytopathic effect of SARS-CoV-2 infection in human airway epithelial cells. *Nat Commun* **11**, 3910, doi:10.1038/s41467-020-17796-z (2020).

564 Wang, R. *et al.* Human airway lineages derived from pluripotent stem cells reveal the epithelial responses to SARS-CoV-2 infection. *Am J Physiol Lung Cell Mol Physiol* **322**, L462-L478, doi:10.1152/ajplung.00397.2021 (2022).

565 Mulay, A. *et al.* SARS-CoV-2 infection of primary human lung epithelium for COVID-19 modeling and drug discovery. *Cell reports* **35**, 109055, doi:10.1016/j.celrep.2021.109055 (2021).

566 Lamers, M. M. *et al.* An organoid-derived bronchioalveolar model for SARS-CoV-2 infection of human alveolar type II-like cells. *The EMBO journal* **40**, e105912, doi:10.15252/embj.2020105912 (2021).

567 Ravindra, N. G. *et al.* Single-cell longitudinal analysis of SARS-CoV-2 infection in human airway epithelium identifies target cells, alterations in gene expression, and cell state changes. *PLoS biology* **19**, e3001143, doi:10.1371/journal.pbio.3001143 (2021).

568 Morgan, R. *et al.* A medium composition containing normal resting glucose that supports differentiation of primary human airway cells. *Sci Rep* **12**, 1540, doi:10.1038/s41598-022-05446-x (2022).

569 Saunders, J. B., Aasland, O. G., Babor, T. F., de la Fuente, J. R. & Grant, M. Development of the Alcohol Use Disorders Identification Test (AUDIT): WHO Collaborative Project on Early Detection of Persons with Harmful Alcohol Consumption--II. *Addiction* **88**, 791-804, doi:10.1111/j.1360-0443.1993.tb02093.x (1993).

570 Selzer, M. L., Vinokur, A. & van Rooijen, L. A self-administered Short Michigan Alcoholism Screening Test (SMAST). *J Stud Alcohol* **36**, 117-126, doi:10.15288/jsa.1975.36.117 (1975).

571 Mehta, A. J., Yeligar, S. M., Elon, L., Brown, L. A. & Guidot, D. M. Alcoholism causes alveolar macrophage zinc deficiency and immune dysfunction. *American journal of respiratory and critical care medicine* **188**, 716-723, doi:10.1164/rccm.201301-0061OC (2013).

572 Zhang, C. *et al.* Small proline-rich proteins (SPRRs) are epidermally produced antimicrobial proteins that defend the cutaneous barrier by direct bacterial membrane disruption. *Elife* **11**, doi:10.7554/eLife.76729 (2022).

573 Foell, D., Wittkowski, H., Vogl, T. & Roth, J. S100 proteins expressed in phagocytes: a novel group of damage-associated molecular pattern molecules. *J Leukoc Biol* **81**, 28-37, doi:10.1189/jlb.0306170 (2007).

574 Aoki, T. *et al.* Expression profiling of genes related to asthma exacerbations. *Clin Exp Allergy* **39**, 213-221, doi:10.1111/j.1365-2222.2008.03186.x (2009).

575 Lee, T. H. *et al.* Elevation of S100 calcium binding protein A9 in sputum of neutrophilic inflammation in severe uncontrolled asthma. *Ann Allergy Asthma Immunol* **111**, 268-275 e261, doi:10.1016/j.anai.2013.06.028 (2013).

576 Roy, M. G. *et al.* Muc5b is required for airway defence. *Nature* **505**, 412-416, doi:10.1038/nature12807 (2014).

577 Mannervik, B. *et al.* Nomenclature for human glutathione transferases. *Biochem J* **282 (Pt 1)**, 305-306, doi:10.1042/bj2820305 (1992).

578 Ou, X. *et al.* Characterization of spike glycoprotein of SARS-CoV-2 on virus entry and its immune cross-reactivity with SARS-CoV. *Nat Commun* **11**, 1620, doi:10.1038/s41467-020-15562-9 (2020).

579 Molina, S. A. *et al.* Junctional abnormalities in human airway epithelial cells expressing F508del CFTR. *Am J Physiol Lung Cell Mol Physiol* **309**, L475-487, doi:10.1152/ajplung.00060.2015 (2015).

580 Lu, Z. *et al.* A non-tight junction function of claudin-7-Interaction with integrin signaling in suppressing lung cancer cell proliferation and detachment. *Mol Cancer* **14**, 120, doi:10.1186/s12943-015-0387-0 (2015).

581 Rauti, R. *et al.* Effect of SARS-CoV-2 proteins on vascular permeability. *Elife* **10**, doi:10.7554/eLife.69314 (2021).

582 Hashimoto, R. *et al.* SARS-CoV-2 disrupts respiratory vascular barriers by suppressing Claudin-5 expression. *Science advances* **8**, eabo6783, doi:10.1126/sciadv.abo6783 (2022).

583 van Zuylen, W. J., Rawlinson, W. D. & Ford, C. E. The Wnt pathway: a key network in cell signalling dysregulated by viruses. *Rev Med Virol* **26**, 340-355, doi:10.1002/rmv.1892 (2016).

584 Montazersaheb, S. *et al.* COVID-19 infection: an overview on cytokine storm and related interventions. *Virol J* **19**, 92, doi:10.1186/s12985-022-01814-1 (2022).

585 Coyne, C. B. *et al.* Regulation of airway tight junctions by proinflammatory cytokines. *Mol Biol Cell* **13**, 3218-3234, doi:10.1091/mbc.e02-03-0134 (2002).

586 Ng, C. T., Fong, L. Y. & Abdullah, M. N. H. Interferon-gamma (IFN-gamma): Reviewing its mechanisms and signaling pathways on the regulation of endothelial barrier function. *Cytokine* **166**, 156208, doi:10.1016/j.cyto.2023.156208 (2023).

587 Chen, S. P. *et al.* Effects of transdifferentiation and EGF on claudin isoform expression in alveolar epithelial cells. *J Appl Physiol (1985)* **98**, 322-328, doi:10.1152/japplphysiol.00681.2004 (2005).

588 Terakado, M. *et al.* The Rac1/JNK pathway is critical for EGFR-dependent barrier formation in human airway epithelial cells. *Am J Physiol Lung Cell Mol Physiol* **300**, L56-63, doi:10.1152/ajplung.00159.2010 (2011).

589 Chen, G. *et al.* Clinical and immunological features of severe and moderate coronavirus disease 2019. *J Clin Invest* **130**, 2620-2629, doi:10.1172/JCI137244 (2020).

590 Huang, C. *et al.* Clinical features of patients infected with 2019 novel coronavirus in Wuhan, China. *Lancet* **395**, 497-506, doi:10.1016/S0140-6736(20)30183-5 (2020).

591 Kalinina, O. *et al.* Cytokine Storm Signature in Patients with Moderate and Severe COVID-19. *Int J Mol Sci* **23**, doi:10.3390/ijms23168879 (2022).

592 Mackey, K. *et al.* Racial and Ethnic Disparities in COVID-19-Related Infections, Hospitalizations, and Deaths : A Systematic Review. *Ann Intern Med* **174**, 362-373, doi:10.7326/M20-6306 (2021).

593 Price-Haywood, E. G., Burton, J., Fort, D. & Seoane, L. Hospitalization and Mortality among Black Patients and White Patients with Covid-19. *N Engl J Med* **382**, 2534-2543, doi:10.1056/NEJMsa2011686 (2020).

594 Patten, C. A., Martin, J. E. & Owen, N. Can psychiatric and chemical dependency treatment units be smoke free? *J Subst Abuse Treat* **13**, 107-118, doi:10.1016/0740-5472(96)00040-2 (1996).

595 Mumby, S. *et al.* CEACAM5 is an IL-13-regulated epithelial gene that mediates transcription in type-2 (T2) high severe asthma. *Allergy* **77**, 3463-3466, doi:10.1111/all.15465 (2022).

596 Bailey, K. L. *et al.* Alcohol Use Disorders Are Associated With a Unique Impact on Airway Epithelial Cell Gene Expression. *Alcohol Clin Exp Res* **44**, 1571-1584, doi:10.1111/acer.14395 (2020).

597 Blanco-Melo, D. *et al.* Imbalanced Host Response to SARS-CoV-2 Drives Development of COVID-19. *Cell* **181**, 1036-1045 e1039, doi:10.1016/j.cell.2020.04.026 (2020).

598 Klingensmith, N. J. *et al.* Epidermal Growth Factor Improves Intestinal Integrity and Survival in Murine Sepsis Following Chronic Alcohol Ingestion. *Shock* **47**, 184-192, doi:10.1097/SHK.0000000000000709 (2017).

599 Bhattacharya, P. *et al.* Dual Role of GM-CSF as a Pro-Inflammatory and a Regulatory Cytokine: Implications for Immune Therapy. *J Interferon Cytokine Res* **35**, 585-599, doi:10.1089/jir.2014.0149 (2015).

600 Dranoff, G. *et al.* Involvement of granulocyte-macrophage colony-stimulating factor in pulmonary homeostasis. *Science* **264**, 713-716, doi:10.1126/science.8171324 (1994).

601 Kelly, A. & McCarthy, C. Pulmonary Alveolar Proteinosis Syndrome. *Semin Respir Crit Care Med* **41**, 288-298, doi:10.1055/s-0039-3402727 (2020).

602 Matute-Bello, G. *et al.* Modulation of neutrophil apoptosis by granulocyte colony-stimulating factor and granulocyte/macrophage colony-stimulating factor during the course of acute respiratory distress syndrome. *Crit Care Med* **28**, 1-7, doi:10.1097/00003246-200001000-00001 (2000).

603 Joshi, P. C. *et al.* GM-CSF receptor expression and signaling is decreased in lungs of ethanol-fed rats. *Am J Physiol Lung Cell Mol Physiol* **291**, L1150-1158, doi:10.1152/ajplung.00150.2006 (2006).

604 Lang, F. M., Lee, K. M., Teijaro, J. R., Becher, B. & Hamilton, J. A. GM-CSF-based treatments in COVID-19: reconciling opposing therapeutic approaches. *Nat Rev Immunol* **20**, 507-514, doi:10.1038/s41577-020-0357-7 (2020).

605 McCormick, T. S., Hejal, R. B., Leal, L. O. & Ghannoum, M. A. GM-CSF: Orchestrating the Pulmonary Response to Infection. *Front Pharmacol* **12**, 735443, doi:10.3389/fphar.2021.735443 (2021).

606 Presneill, J. J., Harris, T., Stewart, A. G., Cade, J. F. & Wilson, J. W. A randomized phase II trial of granulocyte-macrophage colony-stimulating factor therapy in severe sepsis with respiratory dysfunction. *American journal of respiratory and critical care medicine* **166**, 138-143, doi:10.1164/rccm.2009005 (2002).

607 Paine, R., 3rd *et al.* A randomized trial of recombinant human granulocyte-macrophage colony stimulating factor for patients with acute lung injury. *Crit Care Med* **40**, 90-97, doi:10.1097/CCM.0b013e31822d7bf0 (2012).

608 Robinot, R. *et al.* SARS-CoV-2 infection induces the dedifferentiation of multiciliated cells and impairs mucociliary clearance. *Nat Commun* **12**, 4354, doi:10.1038/s41467-021-24521-x (2021).

609 Teoh, K. T. *et al.* The SARS coronavirus E protein interacts with PALS1 and alters tight junction formation and epithelial morphogenesis. *Mol Biol Cell* **21**, 3838-3852, doi:10.1091/mbc.E10-04-0338 (2010).

610 Toto, A. *et al.* Comparing the binding properties of peptides mimicking the Envelope protein of SARS-CoV and SARS-CoV-2 to the PDZ domain of the tight junction-associated PALS1 protein. *Protein science : a publication of the Protein Society* **29**, 2038-2042, doi:10.1002/pro.3936 (2020).

611 De Maio, F. *et al.* Improved binding of SARS-CoV-2 Envelope protein to tight junction-associated PALS1 could play a key role in COVID-19 pathogenesis. *Microbes and infection* **22**, 592-597, doi:10.1016/j.micinf.2020.08.006 (2020).

612 Shepley-McTaggart, A. *et al.* SARS-CoV-2 Envelope (E) protein interacts with PDZ-domain-2 of host tight junction protein ZO1. *PLoS One* **16**, e0251955, doi:10.1371/journal.pone.0251955 (2021).

613 Caillet-Saguy, C. *et al.* Host PDZ-containing proteins targeted by SARS-CoV-2. *FEBS J* **288**, 5148-5162, doi:10.1111/febs.15881 (2021).

614 Berkel, T. D. & Pandey, S. C. Emerging Role of Epigenetic Mechanisms in Alcohol Addiction. *Alcohol Clin Exp Res* **41**, 666-680, doi:10.1111/acer.13338 (2017).

615 Neveu, W. A., Mills, S. T., Staitieh, B. S. & Sueblinvong, V. TGF-beta1 epigenetically modifies Thy-1 expression in primary lung fibroblasts. *American journal of physiology. Cell physiology* **309**, C616-626, doi:10.1152/ajpcell.00086.2015 (2015).

616 Neveu, W. A., Staitieh, B. S., Mills, S. T., Guidot, D. M. & Sueblinvong, V. Alcohol-Induced Interleukin-17 Expression Causes Murine Lung Fibroblast-to-Myofibroblast Transdifferentiation via Thy-1 Down-Regulation. *Alcohol Clin Exp Res* **43**, 1427-1438, doi:10.1111/acer.14110 (2019).

617 Bornstein, S. R. *et al.* Practical recommendations for the management of diabetes in patients with COVID-19. *Lancet Diabetes Endocrinol* **8**, 546-550, doi:10.1016/S2213-8587(20)30152-2 (2020).

APPENDIX

SUPPLEMENTAL TABLES FROM CHAPTER 7

Supplemental Table 1 – Differentially Expressed genes comparing AUD to non-AUD cells

GeneID	GeneName	log2Fold Change	pvalue	padj
ENSG00000185873	TMPRSS11B	8.91	0	0
ENSG00000167916	KRT24	8.36	0	0
ENSG00000172005	MAL	8.28	0	0
ENSG00000163209	SPRR3	7.59	0	0
ENSG00000143536	CRNN	7.32	0	0
ENSG00000170426	SDR9C7	7.24	0	0.04
ENSG00000126233	SLURP1	7.15	0	0
ENSG00000136694	IL36A	6.82	0	0
ENSG00000170423	KRT78	6.64	0	0
ENSG00000169474	SPRR1A	6.23	0	0
ENSG00000189001	SBSN	6.03	0	0
ENSG00000155269	GPR78	6.00	0	0.03
ENSG00000241794	SPRR2A	5.96	0	0
ENSG00000249307	LINC01088	5.84	0	0
ENSG00000203785	SPRR2E	5.68	0	0
ENSG00000145879	SPINK7	5.66	0	0.05
ENSG00000163216	SPRR2D	5.62	0	0
ENSG00000166535	A2ML1	5.60	0	0
ENSG00000280071	FP565260.6	5.59	0	0.01
ENSG00000214711	CAPN14	5.46	0	0
ENSG00000140519	RHCG	5.41	0	0
ENSG00000129455	KLK8	5.33	0	0
ENSG00000166183	ASPG	5.29	0	0.01
ENSG00000143520	FLG2	5.11	0	0.04
ENSG00000133710	SPINK5	4.83	0	0
ENSG00000007306	CEACAM7	4.82	0	0
ENSG00000200033	RNU6-403P	4.80	0	0.01
ENSG00000143546	S100A8	4.78	0	0
ENSG00000174226	SNX31	4.78	0	0
ENSG00000178372	CALML5	4.57	0	0
ENSG00000183671	GPR1	4.28	0	0.05
ENSG00000130600	H19	4.26	0	0
ENSG00000090512	FETUB	4.24	0	0.01
ENSG00000163221	S100A12	4.13	0	0
ENSG00000171476	HOPX	4.12	0	0
ENSG00000087128	TMPRSS11E	4.11	0	0
ENSG00000125998	FAM83C	4.11	0	0.01

Supplemental Table 1, continued

GeneID	GeneName	log2Fold Change	pvalue	padj
ENSG00000169469	SPRR1B	4.06	0	0
ENSG00000238042	LINC02257	4.04	0	0
ENSG00000136695	IL36RN	4.04	0	0.01
ENSG00000171401	KRT13	3.87	0	0.03
ENSG00000167755	KLK6	3.85	0	0.01
ENSG00000185479	KRT6B	3.79	0	0
ENSG00000169035	KLK7	3.75	0	0
ENSG00000170477	KRT4	3.63	0	0
ENSG00000143369	ECM1	3.57	0	0
ENSG00000198488	B3GNT6	3.45	0	0.04
ENSG00000197191	CYSRT1	3.43	0	0
ENSG00000139988	RDH12	3.42	0	0.01
ENSG00000158125	XDH	3.40	0	0.01
ENSG00000071991	CDH19	3.39	0	0
ENSG00000105388	CEACAM5	3.39	0	0.01
ENSG00000142623	PADI1	3.33	0	0
ENSG00000172382	PRSS27	3.33	0	0
ENSG00000214049	UCA1	3.29	0	0
ENSG00000121742	GJB6	3.27	0	0
ENSG00000170465	KRT6C	3.27	0	0
ENSG00000186832	KRT16	3.23	0	0.02
ENSG00000166736	HTR3A	3.19	0	0
ENSG00000161249	DMKN	2.91	0	0
ENSG00000124466	LYPD3	2.85	0	0.01
ENSG00000186806	VSIG10L	2.80	0	0.02
ENSG00000039537	C6	2.75	0	0.01
ENSG00000092295	TGM1	2.73	0	0.02
ENSG00000142677	IL22RA1	2.72	0	0
ENSG00000280693	SH3PXD2A-AS1	2.72	0	0.04
ENSG00000173212	MAB21L3	2.71	0	0.02
ENSG00000197632	SERPINB2	2.61	0	0.02
ENSG00000109321	AREG	2.58	0	0.01
ENSG00000253368	TRNP1	2.55	0	0.01
ENSG00000165794	SLC39A2	2.50	0	0.01
ENSG00000136155	SCEL	2.42	0	0.01
ENSG00000177494	ZBED2	2.40	0	0.01
ENSG00000261040	WFDC21P	2.37	0	0

Supplemental Table 1, continued

GeneID	GeneName	log2Fold Change	pvalue	padj
ENSG00000074211	PPP2R2C	2.35	0	0.02
ENSG00000074416	MGLL	2.29	0	0
ENSG00000134531	EMP1	2.29	0	0.03
ENSG00000163220	S100A9	2.28	0	0.01
ENSG00000158055	GRHL3	2.27	0	0
ENSG00000225833	AC097625.1	2.24	0	0.04
ENSG00000124882	EREG	2.20	0	0
ENSG00000064787	BCAS1	2.14	0	0
ENSG00000144063	MALL	2.14	0	0.01
ENSG00000144452	ABCA12	2.09	0	0.02
ENSG00000197353	LYPD2	2.08	0	0.03
ENSG00000173210	ABLIM3	2.07	0	0.01
ENSG00000136689	IL1RN	2.07	0	0.01
ENSG00000013016	EHD3	2.00	0	0.04
ENSG00000130234	ACE2	1.99	0	0.01
ENSG00000183347	GBP6	1.93	0	0.02
ENSG00000109846	CRYAB	1.92	0	0.04
ENSG00000111344	RASAL1	1.89	0	0
ENSG00000124102	PI3	1.88	0	0.04
ENSG00000089127	OAS1	1.84	0	0.05
ENSG00000166396	SERPINB7	1.80	0	0.01
ENSG00000143382	ADAMTSL4	1.79	0	0.03
ENSG00000134955	SLC37A2	1.69	0	0
ENSG00000183018	SPNS2	1.69	0	0.01
ENSG00000186395	KRT10	1.66	0	0.05
ENSG00000143412	ANXA9	1.63	0	0.05
ENSG00000176092	CRYBG2	1.62	0	0.01
ENSG00000103257	SLC7A5	1.54	0	0
ENSG00000149948	HMGA2	1.43	0	0.05
ENSG00000121316	PLBD1	1.41	0	0.05
ENSG00000261104	AC093904.4	1.40	0	0
ENSG00000276170	AC244153.1	1.38	0	0.02
ENSG00000043039	BARX2	1.32	0	0.04
ENSG00000172243	CLEC7A	1.28	0	0.01
ENSG00000168398	BDKRB2	1.24	0	0
ENSG00000006555	TTC22	1.24	0	0.03
ENSG00000163218	PGLYRP4	1.22	0	0.04

Supplemental Table 1, continued

GeneID	GeneName	log2Fold Change	pvalue	padj
ENSG00000151012	SLC7A11	1.20	0	0.03
ENSG00000140297	GCNT3	1.20	0	0.04
ENSG00000206337	HCP5	1.18	0	0.01
ENSG00000177191	B3GNT8	1.16	0	0.01
ENSG00000253958	CLDN23	1.10	0	0
ENSG00000186212	SOWAHB	1.03	0	0.02
ENSG00000144724	PTPRG	-1.06	0	0
ENSG00000169992	NLGN2	-1.22	0	0
ENSG00000174080	CTSF	-1.22	0	0.03
ENSG00000121064	SCPEP1	-1.23	0	0
ENSG00000135362	PRR5L	-1.27	0	0
ENSG00000138696	BMPR1B	-1.28	0	0
ENSG00000143502	SUSD4	-1.28	0	0.04
ENSG00000145284	SCD5	-1.30	0	0.02
ENSG00000184144	CNTN2	-1.30	0	0.02
ENSG00000006042	TMEM98	-1.31	0	0.05
ENSG00000182636	NDN	-1.40	0	0.01
ENSG00000113594	LIFR	-1.48	0	0.05
ENSG00000065989	PDE4A	-1.53	0	0.01
ENSG00000160180	TFF3	-1.55	0	0.01
ENSG00000115325	DOK1	-1.60	0	0.01
ENSG00000167191	GPRC5B	-1.63	0	0.02
ENSG00000243955	GSTA1	-1.69	0	0
ENSG00000234390	USP27X-AS1	-1.69	0	0.04
ENSG00000198892	SHISA4	-1.74	0	0.01
ENSG00000126217	MCF2L	-1.74	0	0.04
ENSG00000099864	PALM	-1.81	0	0.01
ENSG00000165238	WNK2	-1.83	0	0.04
ENSG00000164199	ADGRV1	-1.90	0	0.04
ENSG00000182853	VMO1	-1.91	0	0.01
ENSG00000116299	KIAA1324	-2.03	0	0
ENSG00000105088	OLFM2	-2.19	0	0
ENSG00000233725	LINC00284	-2.24	0	0
ENSG00000224389	C4B	-2.28	0	0.05
ENSG00000127324	TSPAN8	-2.57	0	0
ENSG00000117507	FMO6P	-2.58	0	0.01
ENSG00000272512	AL645608.8	-2.58	0	0.02

Supplemental Table 1, continued

GeneID	GeneName	log2Fold Change	pvalue	padj
ENSG00000176533	GNG7	-2.69	0	0
ENSG00000162373	BEND5	-2.85	0	0
ENSG00000175344	CHRNA7	-2.91	0	0.05
ENSG00000117983	MUC5B	-2.93	0	0.01
ENSG00000125999	BPIFB1	-2.94	0	0
ENSG00000020633	RUNX3	-3.08	0	0.02
ENSG00000153822	KCNJ16	-3.30	0	0
ENSG00000124191	TOX2	-3.38	0	0.02
ENSG00000169083	AR	-3.72	0	0.04
ENSG00000037280	FLT4	-3.95	0	0.03
ENSG00000197838	CYP2A13	-3.99	0	0.05
ENSG00000154342	WNT3A	-4.27	0	0
ENSG00000215030	RPL13P12	-4.30	0	0
ENSG00000179914	ITLN1	-4.57	0	0
ENSG00000140937	CDH11	-4.65	0	0.05
ENSG00000221826	PSG3	-5.29	0	0.02

Shown are differentially expressed genes enriched for AUD cells over non-AUD cells, where the adjusted p value was 0.05 or lower.